

SPECIAL SYMPOSIUM ISSUE OF LENZINGER BERICHTE
„ADVANCES IN WOOD CHEMISTRY“ –
OPENING ADDRESS

H. Harms

Lenzing AG, A – 4860 Lenzing, Austria

This special issue of *Lenzinger Berichte* encompasses selected contributions to the symposium „Advances in Wood Chemistry“ which was held at the University of Agricultural Sciences in Vienna on May 31, 1999. As the research director of Lenzing AG, I am very pleased to have the opportunity to present an opening address to this journal volume of *Lenzinger Berichte*.

The International Symposium „Advances in Wood Chemistry“ had been planned as a special opportunity to advance scientific efforts in the field of wood and cellulose chemistry, to present new research activities and discuss novel scientific ideas, but also, on the occasion of his 70th birthday, as a celebration of Prof. Dr. Josef S. Gratzl, a well-known and important figure in this field who has been influencing wood chemistry by his scientific contributions for a long time.

The Symposium was organized by the new Christian-Doppler Laboratory for “Pulp Reactivity” at the Institute of Chemistry of the University of Agricultural Sciences in Vienna as its introduction to the scientific world and was financially supported by the Austrian Ministry of Science and Transport (BMWV), the Lenzing AG and the österreichische Bundesforste AG, besides several minor industrial, commercial and private contributors. According to newsprint releases and the unanimous judgement of the participants, the symposium „Advances in Wood Chemistry“ ranked among other top wood chemistry congresses with about 150 registered participants from 15 countries.

Joe Gratzl to whom the symposium was dedicated is the only one of the fathers of Austrian wood chemistry who is still active. Although most of his work was done in the USA

at the North Carolina State University, Raleigh, Prof. Gratzl’s academic career started at the Vienna University at a time when Austria still had a high reputation in this field. It was with the retirement of Prof. Karl Kratzl at Vienna and that of Prof. Kratky and Prof. Schurz at Graz, that almost all R&D activities at Austrian universities in the field of wood chemistry have unfortunately died down, despite the importance of the cellulose industry for the Austrian economy. At the same time, more and more of the related industries have also stopped most of their own R&D activities.

“Knowledge” in Research and Development.

The topic discussed with the biggest emphasis and concern in recent meetings of Research Directors of major European companies, is „knowledge management“ in the field of R&D in today’s business environment. Everybody agrees that knowledge is a key asset of a company, even though it seems very difficult to be managed. This might be taken as an entry to the following thoughts.

First, „knowledge“ has to be generated, and it is obvious that it represents much more than just „data“ or „information“. The biggest data bases and the best information will not lead to decisions or actions unless they are understood and transformed into applicable knowledge. Only R&D persons „who know“ can contribute to this process by finding solutions for current problems, by generating new and better products, optimized processes, thereby significantly contributing to business success.

Second, efficient knowledge management must therefore always care about renewal of knowledge by generating knowledgeable persons and about preventing their loss. Old-fashioned terms, such as „tradition within a

group“ and „continuity“ are preconditions for an efficient renewal of knowledge. This is a very difficult task for a medium-sized company in today’s business environment. For us in Lenzing it was, among others, Prof. Joe Gratzl who as a consultant for many years helped to bridge the gap and to maintain a certain minimum amount of research activities in the field of cellulose chemistry over the last couple of years. That is why, not too long ago, we could start over to dig out the potential which lies in improving the processes and the quality of our dissolving pulp. Only recently we realized again, how much can be done by taking benefit from the integration of pulp and fiber manufacturing in one manufacturing site like Lenzing: it offers an enormous potential for optimization. But we realized also, how little in fact we know about our most important raw material.

Lenzing’s strategies to manage the new thrust in its R&D activities.

1) We try to maintain and enlarge our basis of competence by participating in co-operative projects and by selling R&D services to those in our industry who already have given up their own R&D. By carrying out projects for other parties we get them to share the costs for developing and maintaining our expensive methods and sophisticated pilot plants. In addition, we participate in a process of cross-fertilization between different industries and come across new ways to think about our own core business.

Lenzing has an exceptionally large scope of industrial activities relating to cellulose, starting from the conversion of wood into pulp and various fine chemicals, producing cellulose derivatives, cellulose solutions, and finally various manmade cellulosic products. We are therefore in a good position to offer partners and customers a singularly attractive and unusually large field of expertise.

- *We are producing dissolving pulps in both, a magnesium bisulphite and a prehydrolysis kraft mill. The „Visbatch“ process was developed in our laboratories and then implemented in 1995 with the start-up of Bacell, our new 120.000 tpa prehydrolysis kraft mill in Brazil. All R&D work was done*

with 10 liter pilot reactors originally developed for our sulphite process in Austria. The successful up-scaling is a proof of the quality and sophistication of this equipment.

- *Lenzing was the first company world-wide who introduced Totally Chlorine Free (TCF) Bleaching for their dissolving pulps. Already in the late eighties we developed and implemented such the process for our beech pulp in our bisulphite mill here in Austria. We also managed later a TCF process for Eucalyptus dissolving pulps for our kraft mill in Brazil which was already implemented at the start-up of this plant. One of the key elements of this process was our own, patented medium consistency reactor.*
- *We are one of the very few pulp producers who started concentrating on a recovery of substances other than cellulose from wood. In order to cope with steadily tightening environmental regulations in Austria we were compelled to find solutions to generate additional income from our raw material. We started this process by extracting acetic acid and furfural from the vapor condensates of the spent cooking liquor. Just recently, this focus has led us into a co-operation with a Finnish partner who is separating xylose from our spent liquor after installing a 60 million US\$ facility next to our plant. As a consequence of a systematic study of our process we have been able to increase the xylose concentration from originally below 10 to presently above 15%. Everybody who is familiar with separation processes can imagine the commercial implications of this improvement.*
- *Given the challenges of our new Bacell process it is to our own surprise that the quality of the pulp can be developed towards high-grade applications, such as cellulose acetate or cellulose ethers. Suddenly our need for the characterization of pulps was not only confined to the traditional viscose area and to the NMMO process, but we had to gain new experience with lab methods for those other applications and processes.*
- *Last but not least we developed our own Lyocell Technology and implemented a*

commercial plant for the production of manmade cellulosic fiber in Heiligenkreuz, Austria. The direct route to dissolve pulp in an organic solvent without prior derivatization presents many new challenges and a lot of additional needs to characterize cellulosic substrates. But it offers also an enormous scope for other products based on that cellulose solution.

Partners cooperating with us in their R&D projects or contracting our services are very often in completely different businesses, but have similar upstream processes. Several companies from the pulp and paper industry are among our customers. Our cooperation with UCB, the leading manufacturer of cellophane, is just one example for a partnership in which we are working on the development of a new cellulosic film on the basis of our Lyocell process.

2) The second strategy deals with improving the general situation for research in the field of cellulose and wood chemistry in our public research institutions here in Austria. As mentioned above, almost all chemical R&D activities at our universities in the field of wood chemistry have come to an end. This neglect is all the more inexplicable when the major economic significance of the sector is taken into account. The amount of foreign exchange earned from wood and its downstream products is number one in Austria – even bigger than tourism! Once more almost 90% of this amount results from chemical processing of wood: pulp, paper, paperboard, and more than 15% solely from Lenzing's textile fibers and their downstream products.

A discussion on "sustainable industries based on renewable resources" has been going on in Austria for the last several years. For some inexplicable reasons, however, wood has been mentioned very little in this context. In contrast, peripheral economic subjects with only limited developmental potential even in the long term, such as hemp, linseed oil, etc., have attracted a disproportionately great amount of public and governmental attention and support. And if wood is mentioned at all, the focus has been placed either on its combustion as a replacement of petrochemical fuels in the context with the

Kyoto Targets or on its use as a construction material.

It was highly alarming when we realized that the Austrian infrastructure of R&D in the whole field of wood chemistry has virtually broken down. The implications for Lenzing are much more serious than meaning just a lack of support of our own projects. Lenzing AG, which uses 95% of the industrial beech wood harvested in Austria for its products, altogether depends on a well-functioning domestic wood industry for its survival. And we surely know from our own corporate experience that the most important factor for the sustainability of our industry is a continuous improvement of our efficiency by innovation in our processes and products.

New ways to advance Austrian research activities in wood chemistry.

As it is clear that no commercial enterprise of Lenzing's size can finance the required long-term and basic research on its own, we had to find ways for a continuous and high-quality support of our in-house innovation process. So we started activities to implant cellulose chemistry again at one of the Austrian universities. This resulted finally in a partnership with the University of Agricultural Sciences Vienna (Universität für Bodenkultur Wien – BOKU) and in founding the „Christian-Doppler-Laboratory for Pulp Reactivity“ (Christian-Doppler-Labor für Zellstoffreaktivität). Its presentation to the scientific world in the symposium was another reason for celebration today. In this context, I would like to repeat my sincere thanks to Rektor März and Professor Kögerler for their active support, and to Professor Kosma for all his efforts to establish the laboratory and to start off the research activities so promptly; without them the laboratory could never have come into existence. With the CD lab, wood and cellulose chemistry has finally become a subject for R&D at an Austrian university again. The importance of this first step for the whole value chain can also be seen from the active participation of the Österreichische Bundesforste AG, the biggest Austrian forest estate, as a partner in this laboratory.

Scientific work at the CD lab has started at an incredible pace and even results with clear practical applications - most important for the industrial partners - have started to flow. In recent decades, progress in polymer chemistry was mainly achieved in the field of fully synthetic polymers. It now appears that cellulose chemistry can benefit from this progress and is able to generate results rather quickly in a manner also aimed at actual applications. An increasing academic interest in cellulose can be observed and a network of different groups at several universities in Austria is developing around the CD lab. A couple of students have started work for their diploma or their Ph.D. theses and we are already looking forward to the innovative contributions of scientists and students from the Universität für Bodenkultur also as future employees and cooperation partners of Lenzing.

Future prospects.

Although initial progress has been made, it soon becomes clear that a second step is needed for the industry in Austria. Apart from cellulose chemistry – most important to producers and users of dissolving pulp like Lenzing – also a focus on other topics of wood chemistry is urgently needed in Austria. Subjects like wood cooking, wood components isolation and utilization, wood surface reactions, such as activation, gluing and derivatization to name but a few, and wood composites formation are not sufficiently covered. Also in this field the traditions at our universities have been more or less discontinued and will have to be revived. Given the widespread need for renewal, particularly at the majority of older sulfite mills in the Austrian pulp and paper business, also industry appears ready very soon to head in a new direction that will involve new cellulose production processes.

I would like to conclude with a summary of what seems to be a turning point for the importance of cellulose and wood chemistry altogether. The industry dealing with cellulose is facing a new situation with undreamed technological potentials coming suddenly within grasp. The importance of wood as a renewable

raw material is becoming increasingly important.

- For more than a decade, the industry has been focusing on resolving its environmental protection problems and creating self-contained systems. This process has now been brought to a successful conclusion.
- The competitiveness of the pulping industry in Europe in relation to producers in more favored climates can be greatly improved by expanding the material utilization of other wood constituents.
- We are about to take a quantum leap forward in the utilization of cellulosic substrates thanks to the new direct dissolution process which was established for the first time on a large commercial scale.
- The industry is experiencing a renaissance in existing cellulosic products. There are ample chances for a veritable surge in development of new cellulosic products for many different applications.
- Cellulosic products are already now of great ecological significance. Increased material utilization of wood as a renewable resource has extended the natural CO₂ cycle and significantly lightened the burden on the environment in several respects. The use of fossil materials and fuels has been reduced significantly together with the amount of CO₂ released into the atmosphere; biodegradability enables a reduction in the waste disposal in landfills and incinerators.

These facts emphasize once more the importance of active research in cellulose and wood chemistry. The various cooperations and R&D activities of Lenzing as well as the institutionalization of the Christian-Doppler laboratory mark a forceful beginning in the long process of re-establishing a wood chemistry research program in Austria. The symposium “Advances in Wood Chemistry” demonstrates exemplary that this approach has found wide acceptance, also in the international scientific community.

THE INDIVIDUAL STRUCTURES OF NATIVE CELLULOSES

R. H. Atalla

USDA Forest Service, Forest Products Laboratory
Madison, Wisconsin 53705, USA

Our understanding of the diversity of native celluloses has been limited by the fact that studies of their structures have sought to establish ideal crystal lattice forms for the native state. Departures from ideal structures in the native state are viewed as defects in the ideal lattice. In most instances real celluloses have been regarded as departing from the ideal structures primarily with respect to the degree of disorder. The disorder is considered as imparting an amorphous character to part of the cellulose and methods are sought to quantify the "amorphous" fraction. In contrast, recent developments in structural characterization, based primarily on the use of spectroscopic methods, have revealed that native celluloses are species specific composites of two forms of cellulose, I_{α} and I_{β} . They appear to possess the same secondary structure but distinctly different tertiary structures. Their aggregation appears to reflect an inherent tendency of the cellulose molecules to self-assemble into fibrils at a hierarchy of levels. This is most clearly revealed through observations of the biogenesis of cellulose in model systems incorporating cultures of *Acetobacter xylinum*.

The unique character of celluloses from particular species suggests that the intimate

blending of the two forms of cellulose is regulated during biogenesis. Furthermore, the uniqueness of particular native structures appears to emerge at the nanoscale level (2 to 10nm), a level that is not well detected or characterized by traditional methods for the investigation of structure. This report describes efforts to characterize the nature of native celluloses and their states of aggregation beyond simply categorizing their degree of order and in a manner that may allow more comprehensive systematization of the diversity of the native structures. It will examine the degrees to which information based on different methods of structural characterization can be complementary. Particular attention will be given to the balance of information derived from spectroscopic methods, including solid state ^{13}C NMR, IR and Raman spectroscopy, and information derived from diffractometric methods, including x-ray and electron diffraction. The report will also include consideration of the far wider category of celluloses which, in their native states, are intimately blended with other polysaccharides and with lignin and are even more diverse with respect to their patterns of aggregation.

Introduction

The diversity of the structures of native celluloses is important because, perhaps more than any other natural substrate, the susceptibility of cellulose to chemical reagents or to enzyme action is as much a function of its state of aggregation as it is of its primary structure. And the state of aggregation of each native cellulose seems to be specific to the species within which it is formed. This has not been generally recognized, in part, because of the tendency of studies of cellulose

structure to view cellulose within the conceptual framework of polymer science without adequate attention to its biological character. Thus, studies of structure often seek to establish an ideal crystal lattice for native cellulose and to regard all real celluloses as departing from this ideal form primarily with respect to the degree of disorder. The disorder is then regarded as imparting an amorphous character to some of the cellulose and methods are sought to quantify the "amorphous" fraction.

In contrast, recent studies have shown that all celluloses that are relatively pure in their native states are composites of two distinct forms that are intimately blended in a manner and in proportions that are unique to the species producing them. The far wider category of celluloses that, in their native states, are intimately blended with other polysaccharides and with lignin, are even more diverse with respect to their patterns of aggregation. This report will discuss efforts to characterize the nature of native celluloses and their states of aggregation in a manner that may allow more comprehensive investigations of the nature of the interaction between the cellulosic substrates and the chemical and biological systems that act upon them. One intent of the discussion is to make the case that, particularly in the context of biological studies, there is a need for a significant shift in the manner in which cellulose is viewed. In particular, it is no longer adequate to regard it simply as the β -1,4-linked polymer of anhydroglucose and to apply to it most of the usual principles and methods of polymer science. While these are helpful in many contexts, the traditional principles of polymer science do not begin to capture the distinctive features of the molecule which are derived from its biological origin.

In this report we first address the issues that complicate characterization of the structure of cellulose. We then review recent developments concerning our understanding of structure in native celluloses. Information developed from spectroscopic investigations that have been undertaken in recent decades is presented first. The patterns of self-assembly of native cellulose are then considered on the basis of observations of its biogenesis in model systems incorporating cultures of *Acetobacter xylinum*, the cellulose producing bacterium. Finally, future directions are considered briefly.

Background

The view of cellulose presented here is not unlike that of Cross and Bevan, who wrote "*The root idea of crystallography is identical invariability; the root idea of the world of living matter is essential individual variation*" [1]. Their comments were motivated by the first proposals of crystallinity in cellulose based on

observations of its birefringence fully a decade before the first x-ray diffraction patterns had been recorded.

In recognition of the important biological functions of cellulose, there is a need to reclaim it from the field of polymer science and to recognize that it is a unique biological molecule with many distinctive properties that are key to its role in biological processes. Over the past 100 years much of the research on cellulose has been undertaken in relation to its utilization in industrial processes. It is in this context that many of the paradigms of polymer science were first developed, though they were extended considerably in relation to synthetic polymers. The perspective these methods represent, however, is not adequate to the native celluloses. The majority of crystallizable synthetic polymers, as well as cellulose regenerated from solution, can be viewed in terms of heterogeneous combinations of separate domains that are amorphous or crystalline, depending on the past history of the sample. For native celluloses, in contrast, it is increasingly obvious that they must be regarded as self-assembling naturally occurring substances, and that the self-assembly occurs at a hierarchy of levels that cannot be understood in terms of the simplistic notions of crystallization and separate phases, both of which are rooted in the classical thermodynamics of macroscopic systems.

When considering the structures of native celluloses we will distinguish two categories of native forms. The first category, the *Pure Celluloses*, includes the celluloses that occur in relatively pure form in their native state and which can be isolated using relatively mild procedures that do not alter the state of aggregation to any significant degree. Such celluloses have been the subject of most structural studies. Examples would be cotton, bacterial cellulose and some of the algal celluloses. The second category, the *Complex Celluloses*, which includes the vast majority of naturally occurring forms, consists of the celluloses that are an integral part of the complex architecture of higher plant cell walls. In the vast majority of such plants, the celluloses are intimately blended with the other cell wall constituents. The celluloses in this second category undergo significant changes in their state of aggregation during traditional isolation procedures [2]. However, these changes have not

been well recognized in most instances. One of the major challenges yet to be overcome in future studies is the definition and characterization of the native state of such celluloses prior to the application of isolation procedures that, in most instances, are severe and disruptive of structure.

Until recently, it has generally been assumed that the cell wall structure in higher plants can be represented as a two phase system, one consisting of the microfibrils of pure cellulose, the other a blend of all of the other constituents [3]. It is implicit in this view that the cellulose from such cell walls can be isolated by removing the other components, leaving behind the cellulose in a condition that approximates its native state. Furthermore, it is also generally assumed that the microfibrils, both in their native state and after isolation, are not unlike those that occur in the pure native celluloses. There are now reasons to reassess the assumptions, and the reassessments are at two levels [4]. The first follows from observations that it is not possible to remove the other cell wall constituents without altering the cellulose at the microfibrillar level. The second follows from evidence that raises questions concerning validity of the two phase model.

Much of the discussion of the pure celluloses has concentrated on secondary and tertiary structure at the level of the unit cell (with characteristic dimensions of the order of 1 nm), and on the equivalence or non-equivalence of different monomeric or dimeric units within the unit cell [4]. What are more relevant to the species-specific character of native celluloses, however, are the implications of organization at the level next above that of the unit cell; for native celluloses that level is the most elementary of fibrillar structures. And it is at this level that departures from the organization of an ideal lattice first manifest themselves. They are most clearly obvious in the curvature and twisting that is seen in most electron micrographic images of native celluloses. The key point is that because they represent departures from an ideal lattice they influence the results of all measurements that are sensitive to lattice order. Measurements carried out on a substance with an ideal lattice would result in diffraction patterns that are very sharp and spectral lines that are very narrow. Departures from such a lattice result in broadening of both diffraction and spectral measurements, and such broadening is frequently used in efforts to quantify

order in materials or arrive at measures of the degrees of their crystallinity. Such measurements have also been adopted in attempts to quantify the degree of order in cellulosic samples and they have been used to explore correlations between order in the cellulosic substrates and their susceptibility to chemical reagents or enzymatic action. The difficulty with this approach is that the traditional interpretations of broadening in diffractometric patterns or spectral lines have been in terms of the occurrence of domains of *homogeneously disordered* matter. While assumptions that such domains occur are reasonably valid approximations in the case of most synthetic polymeric materials, and even for regenerated cellulose, they are at best very questionable in the instance of native celluloses.

The reality is that most native celluloses are not disordered but rather highly organized in a hierarchy of structures that are defined at different scales of observation of the native tissue within which the cellulose occurs. The most elementary level beyond the unit cell is the microfibril, with characteristic lateral dimensions of 4 to 6 nm, and with longitudinal dimensions considerably in excess of 10 nm. With the exception of selected algal and tunicate celluloses, which can have microfibrils with lateral dimensions of the order of 20 nm, all native celluloses depart from the ideal lattice at the level of the microfibril. These departures represent features that are unique to a particular native cellulose, and are the primary basis for species specificity of structure.

The curvature and the twisting of the fibrils necessarily result in departures from ideal lattice order. In order to characterize these departures it is useful to consider the different levels of structure in cellulose. The primary structure has been well established for some time, of course, and is no longer in question. The secondary level of structure, that is, the conformation, reflects the internal organization of individual monomeric units within a molecule. The tertiary level then is concerned with the arrangements of the molecules relative to each other in a particular aggregated form. In much of the literature on cellulose structure the distinctions between primary, secondary, and tertiary levels are not considered because specification of the coordinates of the atoms within a unit cell implicitly defines all three levels of structure. The recent findings mentioned above are based on spectroscopic observations,

and in their interpretation the distinctions between primary, secondary and tertiary levels of structure is important. The distinction between the different levels of structure is also likely to be helpful in future studies of the interactions of cellulose with any agents of chemical transformation. The ability to distinguish between secondary and tertiary structures and to characterize them separately opens up the possibility of more precise interpretation of the results of observations. For example, mechanistic analyses of effects that are related to steric and conformational differences may be attributable to variability in secondary structures, while those that arise from differences in accessibility may be more directly related to tertiary structure.

Recent developments

Spectroscopic studies. The characterization of structure by spectroscopic methods has progressed along two lines recently. Raman spectral studies revealed that there is greater diversity in the secondary structures of celluloses than previously recognized on the basis of diffractometric investigations. They also suggested that adjacent anhydroglucose units in the chain are not symmetrically equivalent and that the basic repeat unit of structure must be recognized as anhydrocellobiose. But perhaps of broader significance was the finding, on the basis of solid state ^{13}C NMR investigations, that native celluloses are composites of two distinct forms and that the organization of the composite structures is distinctive of the particular species or tissue within which the cellulose is produced.

It is beyond the scope of this report to review the Raman spectral findings in full; a brief overview, however, is helpful. The first key finding was that the crystallographic models propounded in the 1970s for cellulose could not rationalize the differences between the spectra of native celluloses (form I) and those of regenerated or mercerized celluloses (form II). The interpretation of the spectral observations included investigations of the vibrational spectra, both infrared and Raman, of many model systems. When the spectra of the celluloses were evaluated in this context it became clear that structures described as twofold helical conformations of the chains represented approximations of the true

structures but they ignored some of the key differences detected from the spectral information. Although the departures from twofold helical organization were small, they were found to be at the heart of the distinctive features of the structures of many celluloses. In summary, the conclusions were that the adjacent anhydroglucose units in a cellulose chain are nonequivalent and that the nonequivalences take different forms in celluloses I and II. In cellulose II, they are centered at the glycosidic linkages, while in native celluloses the departures from equivalence are somewhat less at the glycosidic linkages but greater at the primary alcohol group at C6 [5].

The inadequacy of crystallographic models brought out by the Raman spectral studies were also encountered in the solid state ^{13}C NMR studies of the celluloses. The earliest of the NMR studies focused on the diverse forms of cellulose and attempted to resolve the question of nonequivalences among successive anhydroglucose units in the cellulose chain. It soon emerged, however, that the solid state ^{13}C NMR spectra revealed evidence of a structural diversity among native celluloses that had only been hinted at by earlier results [6, 7]. The diversity is well illustrated by the spectra shown in Figure 1, which includes the solid state ^{13}C NMR spectra of a variety of native celluloses, and one sample of cellulose I that had been regenerated from phosphoric acid solution at elevated temperatures [6, 7]. The spectra show a number of complex multiplet resonances associated with carbons that are chemically equivalent. The assignments of the resonances are well established [8]. Beginning at the downfield side, they are: C1 between 104 and 108 ppm; C4 with sharp resonances between 88 and 92 ppm, and broad components ranging down to about 83 ppm; a cluster assigned to C2, C3, and C5 in the range between 70 and 80 ppm; the resonances below 70 ppm are associated with C6.

After investigation of alternative interpretations of the diversity of the spectra of the different native celluloses, the possibility of composite structures was explored. It was found that the spectra in Figure 1 can be resolved into linear combinations of spectra corresponding to two forms of cellulose I; these have been designated I_α and I_β to distinguish them from earlier efforts to categorize the diversity of native celluloses. The spectra of these two forms are shown in Figure 2.

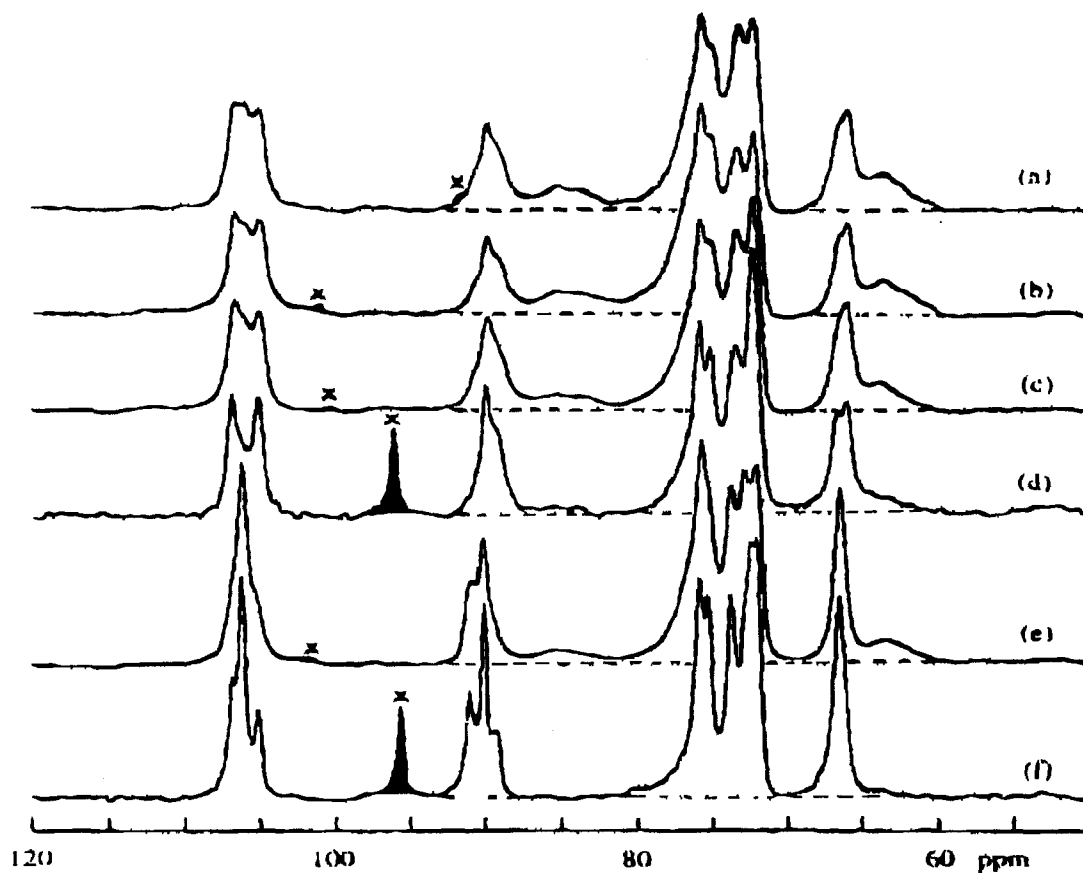


Figure 1. The solid state ^{13}C NMR spectra of a number of cellulose I samples: (a) ramie; (b) cotton; (c) hydrocellulose from cotton linters; (d) a low DP regenerated cellulose I; (e) *Acetobacter xylinum* cellulose; (f) *Valonia Ventricosa* cellulose. The (x) marks the first spinning side band of linear polyethylene, which was added as a chemical shift reference. Adapted from [7].

After investigation of a wide variety of pure native celluloses, a number of patterns emerged. First, it was clear that all of the celluloses from plant sources are blends or composites of the two forms of cellulose and that the particular blend is specific to the species and tissue from which the cellulose is isolated. The features distinguishing spectra of a particular cellulose include the relative proportions of the I_α and I_β forms and the degree of resolution of the resonances associated with each of the carbon atoms. Next, it was noted that among the pure celluloses from higher plants the I_β form always appears to be dominant. In contrast, the bacterial celluloses as well as all the algal celluloses of high crystallinity are predominantly of the I_α form. Finally, it was obvious that the spectra recorded from samples that had been shown to be highly ordered on the basis of diffractometry exhibit the sharpest resonances in the multiplets and have the smallest shoulders associated with resonances of C4 and C6.

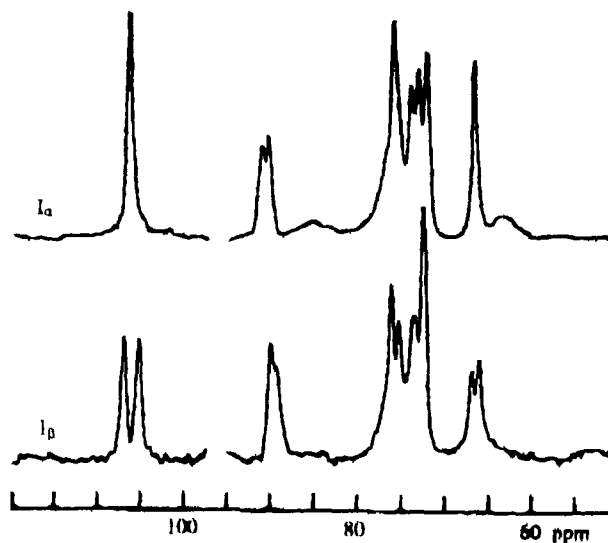


Figure 2. Solid state ^{13}C NMR spectra of: (a) the I_α form; (b) the I_β form. The spectra were generated from linear combinations of spectra (d) and (e) in Figure 1. Discontinuities in the spectra occur where the spinning side bands of polyethylene would have occurred [7].

The differences between the I_α and I_β forms have been explored using two approaches. Electron diffractometric studies have indicated that the I_α form has a triclinic unit cell with one chain per unit cell and with nonequivalent anhydroglucose units. They also suggested that the I_β form has a monoclinic cell of space group $P2_1$ with two chains per unit cell and the twofold screw axis symmetry coincident with the chains, requiring that adjacent anhydroglucose units be symmetrically equivalent [9]. The other line of inquiry has been based on vibrational spectroscopy including both infrared [10] and Raman spectral measurements [11]. Both sets of spectral measurements point to similar secondary structures in the two forms but with distinctly different hydrogen bonding patterns. These findings are illustrated in Figure 3, which shows the Raman spectra of *Valonia*, an algal cellulose, which is predominantly of the I_α forms, and *Halocynthia*, a tunicate cellulose, which is predominantly of the I_β form. Their comparison is particularly useful because the lateral dimensions of their fibrils are both of the order of 20 nm, and they, therefore, allow the generation of spectra of

equal resolution. It is clear from the comparison that the spectra are essentially identical in the low frequency region, which is most sensitive to secondary structure. In the OH stretching region, in contrast, there are significant differences between the band structure for the two forms. The indication here is that the secondary structures of the two forms are the same but the tertiary structures are different. This finding is in sharp contrast to the conclusions derived from the diffractometric data. Another important observation with respect to the Raman spectra is that there is no evidence of correlation field splitting in either of the spectra; such splitting is expected in the spectra of polymeric systems that have more than one chain per unit cell. This observation is not consistent with the interpretation of the diffractometric data that ascribes a two chain unit cell to the I_β form. Thus the results of the infrared and Raman spectral studies appear to be at variance with those of the diffractometric observations. It is clear that the nature of the differences between the I_α and I_β forms is not fully understood at the present time.

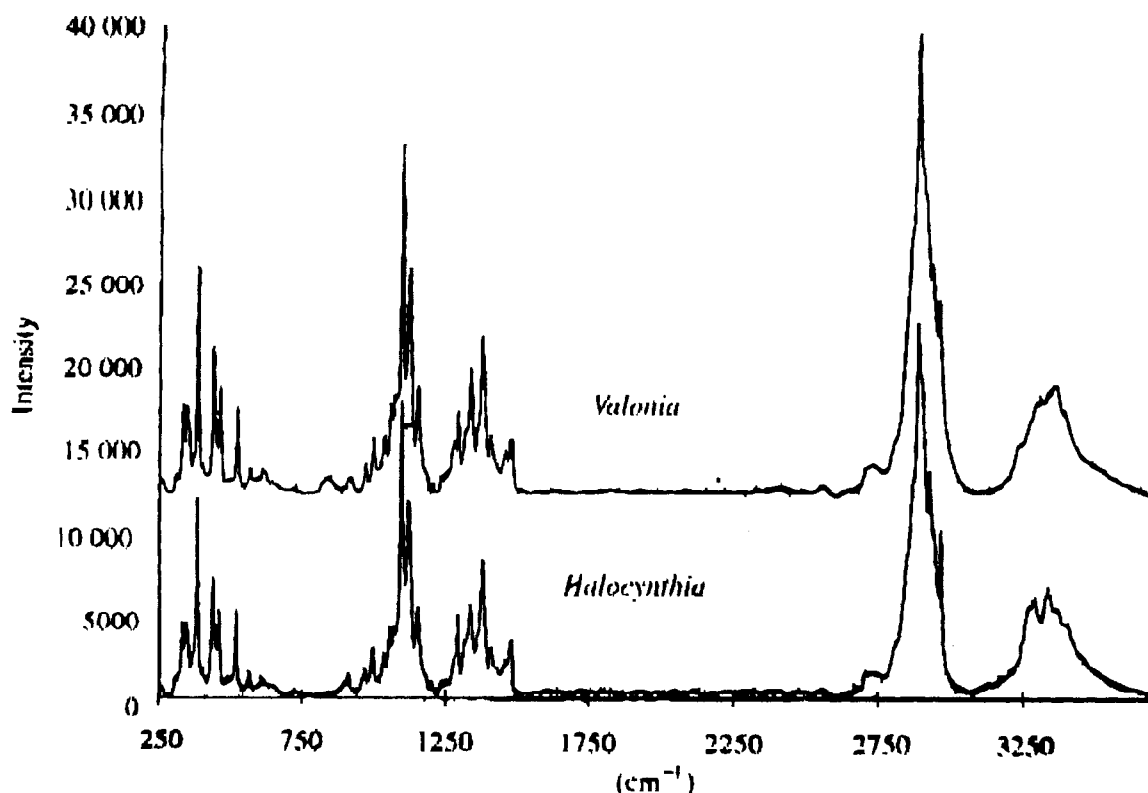


Figure 3. Comparison of the Raman spectra of I_α rich *Valonia* cellulose and I_β rich *Halocynthia* cellulose. Note the near identity of the spectra in the region below 1500 cm^{-1} and in the region between 2700 and 3000 cm^{-1} (C-H stretching). This is in contrast to the clear difference in the O-H stretching region above 3000 cm^{-1} [11].

Model System. A number of important advances with respect to understanding native celluloses have resulted from studies *Acetobacter xylinum* and the celluloses it can produce. Two aspects will be reviewed briefly. The first is the hierarchic assembly of native celluloses. The second is the regulation of cellulose aggregation by hemicelluloses.

It was noted earlier that native celluloses must be regarded as self assembling biological molecules that are organized hierarchically. This

is obvious from examination of the microfibrillar structure of bacterial celluloses produced under different conditions that can perturb the process of assembly at the different levels. The most common form of the cellulose produced is shown in Figure 4, which depicts the fibrils emerging from bacterial cells under normal conditions of culture. The individual fibrils are of the order of 6 nm in width and they have the form of a ribbon with a regular twist to it [12]. The twist was recently shown to be right handed [13].

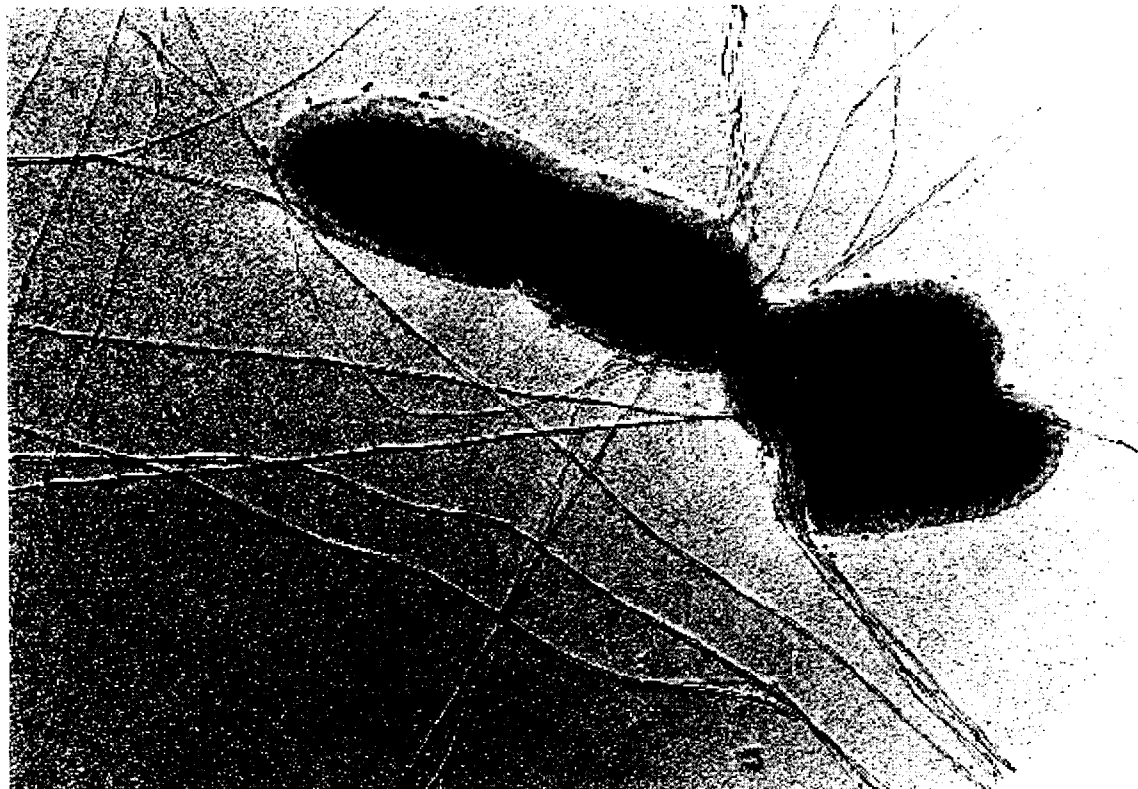


Figure 4. Several normal ribbons of cellulose synthesized by *Acetobacter xylinum*. Twists occur at several points, and in some regions smaller fibrillar subunits are visible. Adapted from [12] courtesy of Dr. C. Haigler.

Figures 5 and 6 show ribbons that have experienced two different levels of perturbation. In Figure 5, the cellulose produced by *Acetobacter xylinum* was cultured in a medium containing carboxymethylcellulose (CMC). It clearly has resulted in some reduction of the coherence of order within the ribbons, as the micrograph reveals evidence of substructures that appear to be fibrillar and that are braided together as they might be in a rope. This points to the capacity of molecules similar to cellulose to associate with it and to limit the degree of self assembly.

Greater limitation on self assembly is revealed in Figure 6, which shows the effects of an agent that can associate with the cellulose even

more strongly than the CMC. The sample shown in Figure 6 resulted from culture in a medium containing the fluorescent brightening agent (FBA) calcofluor, followed by dilute acid washing to remove the FBA. The presence of the FBA results in the formation of a broad non-crystalline band of cellulose that is perpendicular to the cell axis. The micrograph shows that the most elementary of substructures can aggregate into individual fibrils after the acid wash, but they cannot self-assemble further to form a ribbon structure similar to those shown in Figure 4. The fibrils are of the order of 1.5 nm in lateral dimension and correspond to the assemblies of cellulose molecules that emerge from individual

assembly complexes on the plasma membrane.

If it is assumed that the patterns of aggregation displayed by the ribbons of cellulose formed by *Acetobacter xylinum* reflect the inherent self assembly characteristics of the cellulose molecule, it would follow that the most basic building blocks are the 1.5 nm fibrils emerging from a single assembly complex. These then would assemble with similar fibrils emerging from adjacent complexes. In the absence of agents capable of associating with the

nascent cellulose this would result in the normal ribbons shown in Figure 4. If the pattern of self assembly is an inherent characteristic of the cellulose molecule in its nascent state, it can be anticipated that the same influences would prevail during the formation of cellulose in higher plants, and that the basic building blocks would have similar characteristics. This is in fact what has been observed in much of the electron microscopic examination of celluloses from higher plants.

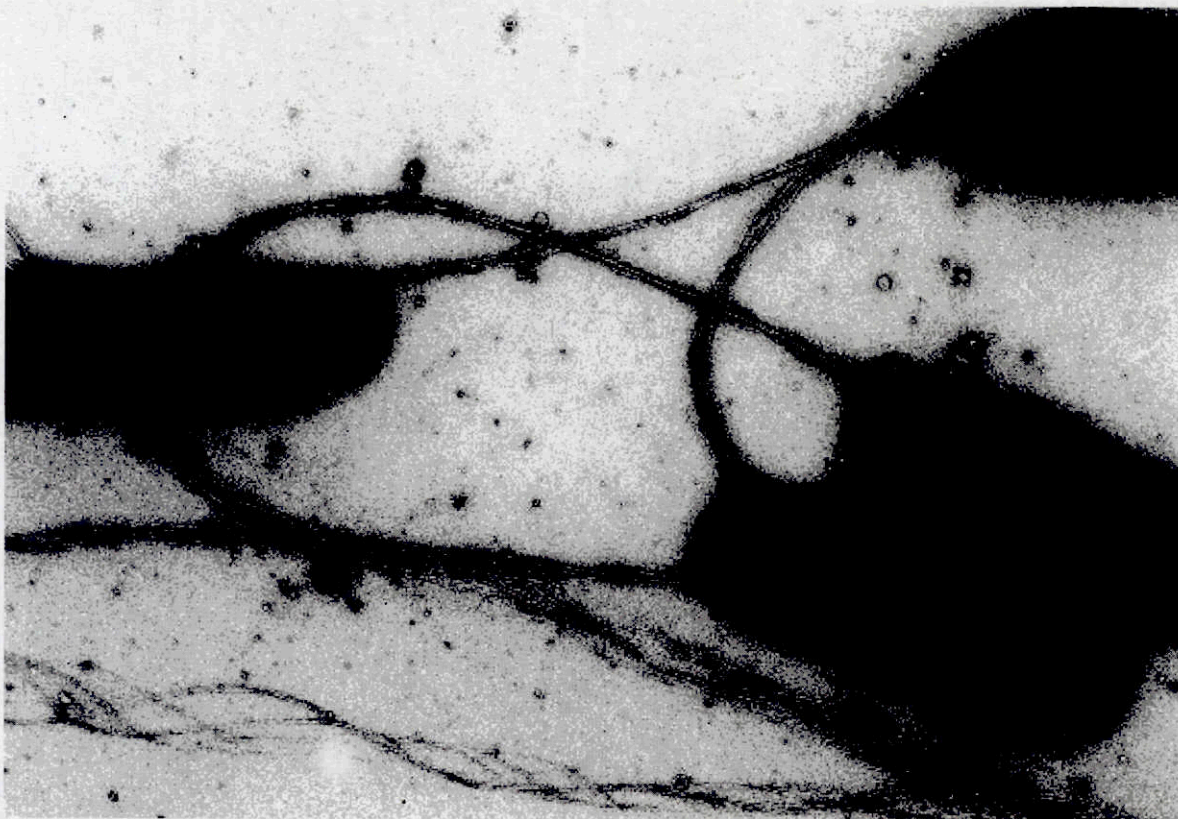


Figure 5. *Acetobacter xylinum* cellulose: substructures of the normal ribbon remain separate when synthesized in the presence of corboxymethyl cellulose. They may lie closer together, thereby resembling normal ribbons, but close inspection shows separated or sometimes highly splayed subunits. Adapted from [12] courtesy of Dr. C. Haigler.

In studies of the *Acetobacter xylinum* model system cited above, the modifying agents were added to the culture medium. In higher plants, in contrast, it is expected that during the formation of the cell wall matrix many agents will be present that can interact with cellulose to modify its assembly. The possible effects of matrix components were investigated in studies of the *Acetobacter xylinum* system where different hemicelluloses were added to the cultures at relatively low levels [14, 15, 16]. It was observed that the hemicelluloses are indeed incorporated into the structures of the celluloses and that each of the hemicelluloses elicited a

different pattern of modification of the cellulose produced in its presence. Furthermore, the changes induced by the presence of the hemicelluloses resulted in aggregation of the celluloses in a manner similar to that of higher plants. In particular, the solid state ^{13}C NMR spectra revealed a predominance of the I_β form as a result of the influence of the hemicelluloses. It can be anticipated on this basis that the patterns of self-assembly and the final tertiary structures of the native celluloses of higher plants are likely to be as diverse as the plants within which they are formed.

On the basis of the observations of the model systems it may be concluded that the celluloses in the category defined as pure celluloses are formed in environments where the other cell wall components cannot associate with the nascent cellulose sufficiently to modify its tertiary structures, while the complex celluloses are formed in cell wall matrices that include

constituents that can modify the tertiary structure. A clearer definition of the diversity of the tertiary structures is essential to advancing our understanding of the species specificity of native celluloses. Further elaboration of the diversity of native celluloses is beyond the scope of this report; the author has addressed many aspects in greater detail elsewhere [4].



Figure 6. *Acetobacter xylinum* cellulose: a helix of microfibrils formed by gentle washing of the FBA dye from extended sheets formed in its presence. The microfibrils contain cellulose I crystallites with smaller dimension than controls. All of these microfibrils would have been part of one normal ribbon. Adapted from [12] courtesy of Dr. C. Haigler.

Future directions

One of the most significant conclusions that can be derived from the spectral studies is that the secondary and tertiary structures of native celluloses are, at a minimum, species and tissue specific. This requires that discussions of the entry of cellulose into biological processes begin to factor this reality into the analyses of data related to processes that can be influenced by the states of aggregation of the cellulose. The effort to characterize the species specific aspects of the variability of the structures of native celluloses is in its early infancy. As noted above, until recently it had seemed adequate to pursue the details of an ideal lattice structure. With the

development of spectroscopic methods to complement the diffractometric methods there is now available a broader foundation upon which to base explorations of the species and tissue specificity of cellulosic structures.

A better characterization of the basis for species specificity is important for advancing understanding both with respect to the processes of biogenesis of cellulose as well as with respect to the processes at the heart of its disassembly by microorganisms. The relevance in regard to the latter field of study is highlighted by recent observations that certain microorganisms capable of cellulolytic action release different proportions of the isozymes of a particular cellulase when cultured on different cellulosic

substrates [17, 18]. Clearly the action of the microorganisms must involve an induction process that includes a yet unknown mechanism whereby the nature of the tertiary structure of the cellulosic substrate is communicated to the site for regulation of the expression of the cellulases. Explorations of the nature of this feedback mechanism will facilitate advancing a better understanding of the cellulolytic action of microorganisms at the same time as it adds insight into the basis of species specificity of secondary and tertiary structure in celluloses.

Acknowledgements

The author's work in this area has benefited from many collaborations all of which cannot be acknowledged in the space available. The work in the area of solid state ^{13}C NMR spectroscopy has been in collaboration with Dr. D. L. VanderHart, NIST. The micrographs were kindly provided by Dr. C. H. Haigler, Texas Tech University, and the Raman spectra were acquired by Dr. U. P. Agarwal, USDA Forest Service, and Dr. J. M. Hackney, University of Wisconsin. The work has been supported by the USDA Forest Service and the Division of Energy Biosciences of the Office of Science of the US Department of Energy. All are gratefully acknowledged.

References

- [1] Cross, C.F.; Bevan, E.J. *Researches on Cellulose (III)*. Longmans, Green & Co.: London, 1912.
- [2] Atalla, R.H.; Whitmore, J. *J. Polym. Sci., Polym. Lett.* **1978**, *16*, 601.
- [3] Preston, R.D. *The Physical Biology of Plant Cell Walls*. Chapman and Hall: London, 1974.
- [4] Atalla, R.H. in: *Comprehensive Natural Products Chemistry*, ed. B. M. Pinto, 1999, vol. 3, Chapter 16, pp. 529-598.
- [5] Atalla, R.H. In: *The Structures of Cellulose*, ed. R.H. Atalla, *ACS Symp. Ser.* **1987**, *340*, 1.
- [6] Atalla, R.H.; VanderHart, D.L. *Science* **1984**, *223*, 283.
- [7] VanderHart D.L.; Atalla, R.H. *Macromolecules* **1984**, *17*, 1465.
- [8] Gast, J.C.; Atalla, R.H.; McKelvey, R.D. *Carbohydr. Res.* **1980**, *84*, 137.
- [9] Sugiyama, J.; Okano, T.; Yamamoto, H.; Horii, F. *Macromolecules* **1990**, *23*, 3196.
- [10] Sugiyama, J.; Vuong, R.; Chanzy, H. *Macromolecules* **1991**, *24*, 4168.
- [11] Atalla, R.H.; Agarwal, U.P.; Hackney, J.M.; Isogai, A. to be published.
- [12] Haigler, C.H. In: *Biosynthesis and Biodegradation of Cellulose*, eds. C.H. Haigler and P.J. Weimer, Marcel Dekker: New York, 1991, p. 99.
- [13] Hirai, A.; Tsuji, M.; Horii, F. *Sen'i Gakkaishi* **1998**, *54*, 506.
- [14] Uhlin, K.I.; Atalla, R.H.; Thompson, N.S. *Cellulose* **1995**, *2*, 129.
- [15] Atalla, R.H.; Hackney, J.M.; Uhlin, K.I.; Thompson, N.S. *Int. J. Biol. Macromol.* **1993**, *15*, 109.
- [16] Hackney, J. M.; Atalla, R.H.; VanderHart, D.L. *Int. J. Biol. Macromol.* **1994**, *16*, 215.
- [17] Vallim, M. A.; Janse, B.J.H.; Gaskell, J.; Pizzirani-Kleiner, A.A.; Cullen, D. *Appl. Environ. Microbiol.* **1998**, *64*, 1924.
- [18] Cullen, D.; Atalla, R.H., unpublished results.

SUPERMOLECULAR STRUCTURE OF CELLULOSIC MATERIALS BY FOURIER TRANSFORM INFRARED SPECTROSCOPY (FT-IR) CALIBRATED BY WAXS AND ^{13}C NMR

T. Baldinger, J. Moosbauer, H. Sixta

Lenzing AG, A-4860 Lenzing, Austria

Fourier Transform Infrared Spectroscopy (FT-IR) was applied to cellulosic substrates for measuring both lattice types and lattice transitions (cellulose I and II) and for quantitative determination of crystallinity. Calibration was done by X-ray scattering (WAXS) and ^{13}C NMR.

For cellulose I / II transition both KBr-transmission and DRIFT measurements are applicable, the variation of bands at 1370 cm^{-1} or 898 cm^{-1} agrees very well with both WAXS and ^{13}C -NMR data. The evaluation of the OH

region after deconvolution gives satisfactory results as well.

Provided the sample handling is performed most carefully, the correlation with WAXS-data is good for both cellulose I and II in the case of crystallinity, the correlation with ^{13}C NMR data is good for cellulose I, but less satisfactory for cellulose II.

Keywords: cellulose structure, cellulose I / II, FT-IR, crystallinity

Introduction

The ratio of crystalline / amorphous regions in cellulosic substrates is an important parameter, correlated e.g. with reactivity and accessibility of pulps and mechanical properties of cellulosic fibers. Also the knowledge about the type of crystal lattice (cellulose I, II, ...), see Figure 1, and the ease of transformability is an important information about processability of pulps and fibers.

Usually such properties are measured by wide angle x-ray spectroscopy (WAXS) and solid state ^{13}C -NMR, both complex and costly methods because of expensive equipment and necessity of well trained and experienced operating personal. The infrared spectrum of cellulosic material also contains a lot of information on molecular regions which are expected to be influenced by the degree and type of order in their chemical environment and thus can be used to obtain similar information (Figure 2) [1] – [7].

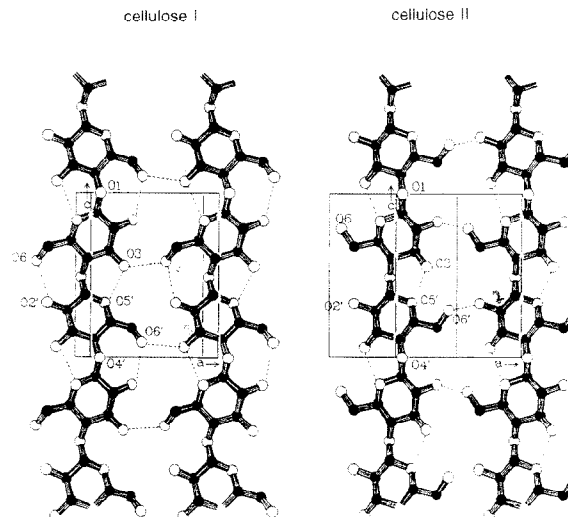


Figure 1. Configuration of cellulosic chains and unit cells for cellulose I and cellulose II, and H bridges:

| | <i>Cellulose I:</i> | <i>Cellulose II:</i> |
|---------------------|------------------------|------------------------|
| Intramolecular | O3-H...O5' | O3-H...O5' |
| H bridges: | O2'-H...O6 | |
| Intermolecular | O6'-H... O3 | O6'-H... O2 |
| H bridge: | | |
| Exocyclic OH-group: | <i>tg</i> conformation | <i>gt</i> conformation |

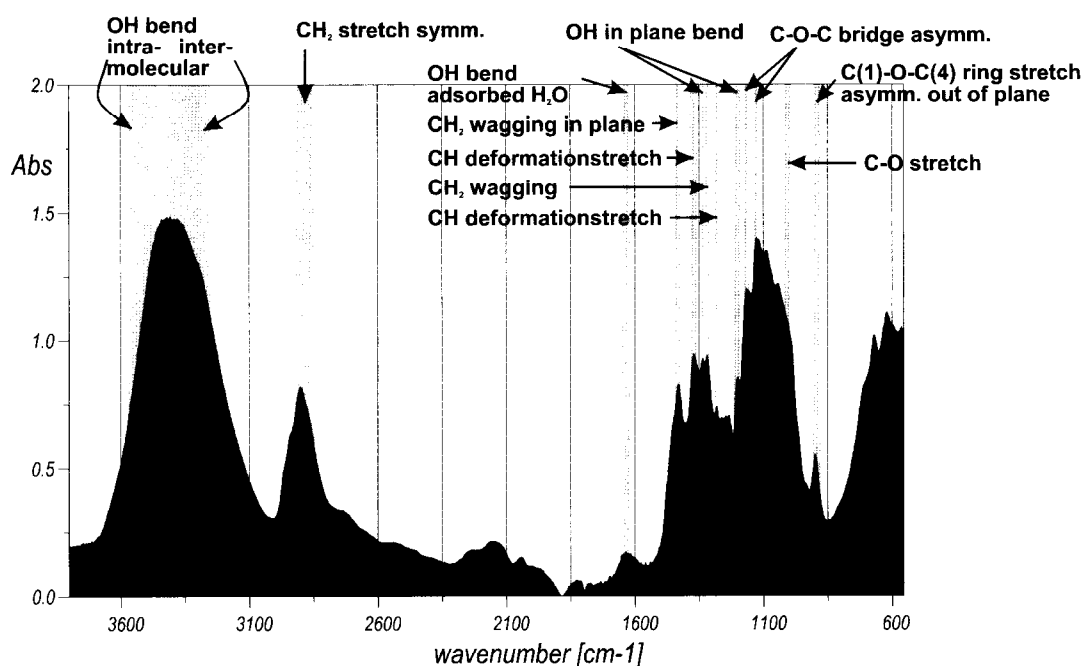


Figure 2. Infrared Spectrum of Cellulose.

Experimental

All FT-IR experiments were carried out on a Bruker IFS 66 Spectrometer. Reference measurements (WAXS: Siemens D5000 and ^{13}C NMR: Varian Unity 400) were done at the Fraunhofer Institut für Angewandte Polymerforschung, Berlin Teltow.

Parameters tested. FT-IR sampling and spectra acquisition: cutting, grinding, drying of samples, KBr transmission measurements and DRIFT measurements; spectral manipulations: baseline correction, normalization, derivative spectra, and deconvolution; evaluation: band height, band area, band frequencies, band intensities, band ratios for most bands suggested in literature, with the ratios of band areas generally giving the best results.

Samples. To cover a range of crystallinities as wide as possible, a set of 8 cellulose-I samples and 6 cellulose-II samples was fully characterized by the reference methods. Cellulose I: LAG BKZO3 (amorphous), Avicell PH 101 (partly amorphous), LAG BKZO3, Bacell pulp, Avicell PH 101, Cotton Linters Temming 010, bacterial cellulose, cotton linters (HCl hydrolyzed). Cellulose II: LAG Lyocell fiber (amorphous), LAG SZS fiber, LAG ZS fiber, LAG Modal fiber, LAG Lyocell fiber, Polynosic fiber.

Results and Discussion

For the cellulose I / II transition both KBr-transmission and DRIFT measurements are applicable. The bands at 1370 cm^{-1} or 898 cm^{-1} (as ratios with either 670 cm^{-1} or 2900 cm^{-1} as the reference band) give very good results in agreement with both WAXS and ^{13}C NMR data. Also the evaluation of the OH region (bands around 2720 , 3278 , 3344 , 3422 , and 3450 cm^{-1} with 2900 cm^{-1} as reference band) after deconvolution showed satisfactory results (Figures 3 and 4).

For the determination of crystallinity (Figure 5) the sample handling has to be performed most carefully (no mechanical cutting or grinding), KBr transmission spectra (only baseline corrected, no derivative!) give far better results than DRIFT. The type of crystal lattice should be known, each lattice type needs a different calibration. In contrast to [3], we found the ratio of intensities at $1370/2900\text{ cm}^{-1}$ to depend on the modification. For both cellulose I and II the correlation with WAXS data is good, the correlation with ^{13}C NMR data is good for cellulose I, but less satisfactory for cellulose II.

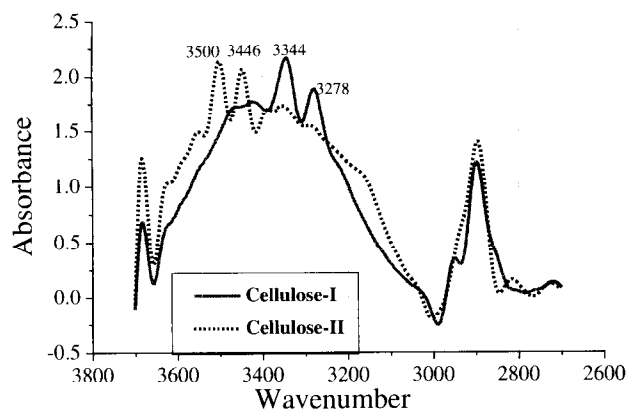


Figure 3. OH region after deconvolution.

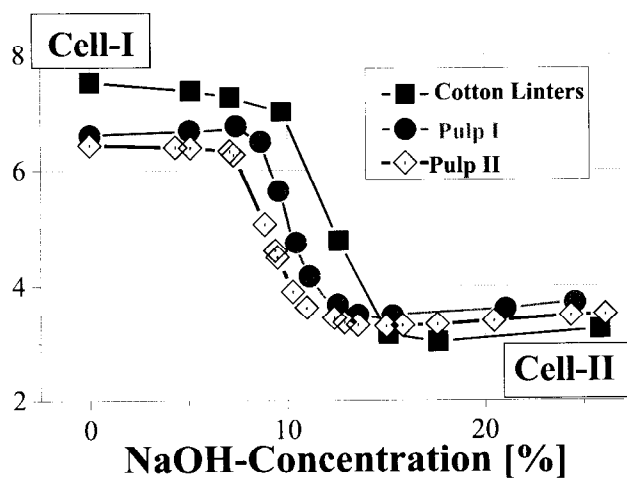


Figure 4. Transition cellulose I – cellulose II for cotton linters and two industrial pulp grades by NaOH treatment at different concentrations.

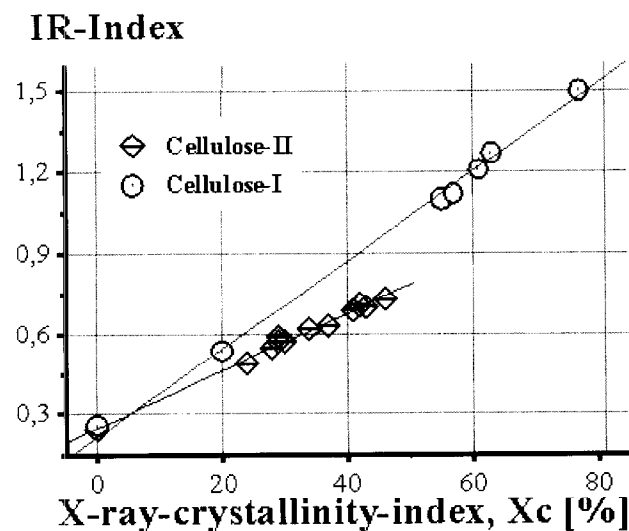


Figure 5. Calibration of cellulose crystallinity FT-IR vs. WAXS.

Conclusion

Evaluation and correlation of IR spectra from various samples fully characterized by WAXS and ^{13}C NMR provide algorithms to obtain information on type and transformability of crystal lattice (cellulose I, II, ...) and crystallinity of unknown samples.

Methods for a practical use could be established and were applied successfully. The set of reference samples is continuously increased by control samples used for validation of the established methods.

References

- [1] O'Connor, R.T.; DuPré, E.F.; McCall, E.R. *Text. Res. J.* **1958**, *28*, 382.
- [2] O'Connor, R.T.; DuPré, E.F.; McCall, E.R. *Text. Res. J.* **1958**, *28*, 542.
- [3] Nelson, M.L.; O'Connor, R.T. *J. Appl. Polymer Sci.* **1964**, *8*, 1311.
- [4] Fengel, D.; Jakob, H.; Strobl, C. *Holzforschung* **1995**, *49*, 505.
- [5] Evans, R.; Newman, R.H.; Roick, U.; Suckling, I.D.; Wallis, A.F.A. *Holzforschung* **1995**, *49*, 498.
- [6] Schultz, T.P.; McGinnis, G.D.; Bertran, M.S. *J. Wood Chem. Technol.* **1985**, *5* (4), 543.
- [7] Hulleman, S.H.D.; van Hazendonk, J.M.; van Damm, J.E.G. *Carbohydr. Res.* **1994**, *261*, 163.

SLIGHT CARBOXYMETHYLATION OF CELLULOSE

J. Borsa,^a I. Rácz,^b S. K. Obendorf,^c G. Bodor^a

^a Technical University of Budapest, Budapest, Müegyetem rkp. 3, H-1111, Hungary

^b Bay Zoltán Institute for Materials Science and Technology,
Budapest, Fehérvári u. 130, H-1116 Hungary

^c Cornell University, Ithaca, New York 14853-4401, USA

Cellulose having only 5–10 carboxymethyl groups per 100 monomer units has fibrous character while its properties differ from those of the original fiber. The high accessibility of slightly carboxymethylated cotton cellulose was found to be advantageous in textile finishing.

The aim of our work was a systematic study of the connection between the reaction parameters and the fiber properties in order to get a more convincing explanation for the contradictory data, and to find possible utilizations of the modified fiber. It has generally been believed that a higher DS is connected with a more disordered structure and, consequently, with high accessibility. Our results suggested that there was no close

correlation between DS and accessibility, moreover, the accessibility of the modified fiber could be even less than that of the untreated one, due to the dissolution of the most accessible molecules. A linear correlation was found between the surface of the fiber, characterized by iodine sorption, and the volume of the pores accessible for water (water retention).

Fabric manufactured by a technology chosen according to the reaction parameter study has a high sorption capacity for pesticides as well, and can be used as protective clothes.

Keywords: carboxymethyl cellulose, low degree of substitution, accessibility, textile finishing, protective cloth

Introduction

Partially carboxymethylated cellulose (CMC) at low degree of substitution ($DS < 0.2$) retains its fibrous character while many of its properties differ from those of the original fibre: more significant anionic character, higher accessibility, and hydroxyl reactivity is the usual outcome of the modification. These characteristics vary in wide ranges depending on carboxymethylation parameters. According to the laboratory experiments published [1-5], modified cellulose can be used in different textile finishing processes and in further modifications.

Choosing methods for the manufacturing of partially carboxymethylated cellulose fibers has crucial importance. Properties of the product are very sensitive to many factors. Statistical methods help to study the main factors influencing the characteristics of the modified celluloses and to find their applications in traditional and new technologies.

The aim of this paper is to give a summary of the results of a systematic study of slightly carboxymethylated cotton cellulose.

Experimental

Carboxymethylation. Bleached cotton fabric of 108 g/m^2 from Goldberger Textile Printing Factory (Hungary) was soaked in a $10 \text{ cm}^3/\text{dm}^3$ acetic acid solution for 5 min at 50°C , then was washed with tap water and neutralized with distilled water. The fabric was then dried at room temperature. Solutions of sodium hydroxide and monochloroacetic acid were mixed and cooled. This solution was used 20 min after mixing. Cotton fabric was padded by mixed solution with two dips (each for 1 min) at room temperature. Fabric sealed in a polyethylene foil was put into an oven thermostated at 70°C , which is the optimum temperature of the reaction [6-8], for

different time periods. The cloth was washed by tap water, soaked with hydrochloride acid solution (8cm^3 conc. HCl / dm^3) for 60 min and neutralized by distilled water. Part of the treated fabric was air dried at room temperature; the rest was left in distilled water.

Three factors (concentrations of reagents and period of time) were varied while temperature of reaction, dipping, washing, and drying conditions were held constant. The concentration range of the NaOH solution was 3-5 mol/kg chosen according to region of its sorption maximum [9]. The molar ratio of sodium hydroxide and monochloroacetic acid was between 1.5 and 7.6. A 5×5 Latin square with one replicate was used as an experimental design ($5^{3-1}=25$ factor level combinations for the 3 factors). The experimental conditions are shown in Table 1.

Table 1. Experimental Conditions for Factorial Design.

| Independent Var. | Level | | | | | Interval of Var. |
|-------------------------------|-------|------|------|------|------|------------------|
| | -2 | -1 | 0 | 1 | 2 | |
| c_{MCAA} [mol/kg] | 0.66 | 1.00 | 1.33 | 1.66 | 2.00 | 0.33 |
| c_{NaOH} [mol/kg] | 3.0 | 3.5 | 4.0 | 4.5 | 5.0 | 0.5 |
| time t [min] | 20 | 40 | 60 | 80 | 100 | 20 |

Degree of substitution (carboxyl content). The value of carboxyl content (C_{carb} mmol/mol), as a sum of original carboxyl content of the fabric ($C_{\text{carb}}=3$ mmol/mol) and of the degree of substitution, was determined by zinc cation sorption from zinc acetate solution [10].

Crystal structure, disorder. Ratios of crystallites (cell I and cell II) and amorphous material (A) were measured by the X-ray diffraction method (Müller Mikro 111, $\text{CuK}\alpha$ radiation, $2\Theta = 5-35^\circ$). The diffractograms were analysed by a Du Pont 310 Curve Resolver.

Specific area. Measurements of iodine sorption capacities (S_p) of samples [11] were used to determine the specific areas (SA) being accessible for water, according to the linear correlation between these two quantities found by Brederick [12]: $\text{SA} [\text{m}^2/\text{g}] = 1.72 S_1 + 130$.

Volume of pores. Water retention values (WRV) measured by centrifugal hydroextraction [13] just after carboxymethylation without intermediate drying were used for the determination of pore volumes (PV) applying Brederick's result [12] on the equality of WRV and PV measured by solute exclusion.

Modeling of layered clothing system. 5×5 cm fabrics were tacked together with sewing thread. The layered systems were contaminated by C^{14} labeled methyl parathion solution. After two days, the fabrics were separated and the amount of pesticide in each layer was measured by radiotracer analysis [14].

Results and Discussion

Degree of substitution (carboxyl content). Figure 1. [15] Using the Stepwise Variable Selection procedure of STATGRAPH [16], the following second order polynomials were obtained as a functional dependence between the carboxyl content (C_{carb}) and the independent variables (C_{MCAA} , C_{NaOH} and t).

$$C_{\text{carb}} = 91.077 + 16.115x_1 + 7.796x_2 + 4.870x_3 - 3.666x_2^2 + 3.277x_1x_3$$

were considered, where $x_1 \rightarrow C_{\text{MCAA}}$, $x_2 \rightarrow C_{\text{NaOH}}$, $x_3 \rightarrow t$ are the coded level of factors.

1. Concentrations: Slopes of surfaces along the concentration of monochloroacetic acid are higher than along the alkali concentration. It is very important from the industrial technology point of view that the concentration of the costlier reagents seems to be the leading factor among parameters investigated.

2. Concentrations and time: At very low concentrations, the carboxyl content does not depend on the reaction time. Two process of opposite effects are supposed to coexist during carboxymethylation: a) carboxyl contents of samples increase by substitution, and b) carboxyl contents of samples decrease by washing off of highly substituted (highly accessible) fractions by the reaction medium. At higher alkali concentrations and longer periods of time the effect of dissolution can overwhelm the result of the reaction.

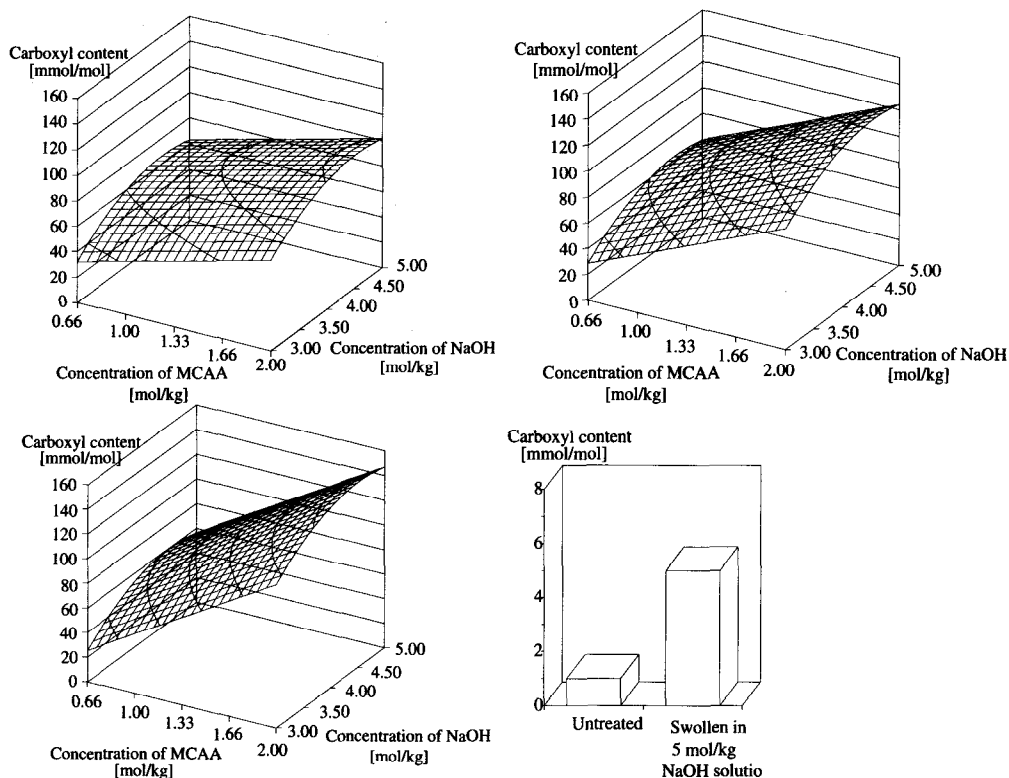


Figure 1. Carboxyl content of carboxymethylated cotton as a function of reagent concentrations and time (carboxymethylated for 20, 60 and 100 min, respectively).

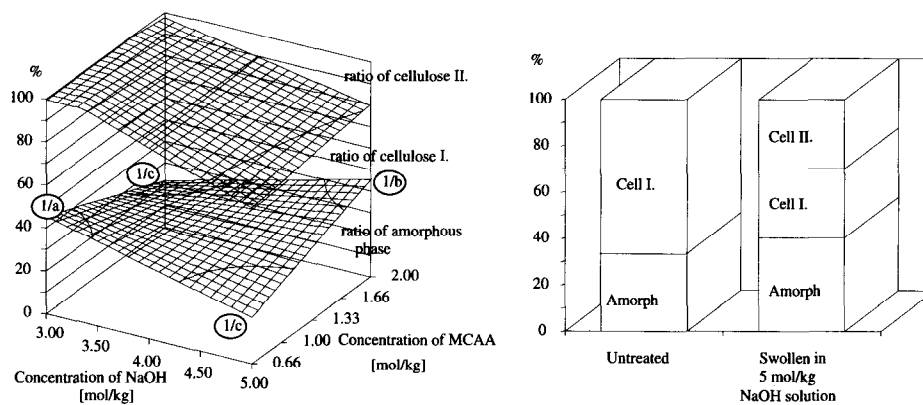


Figure 2. Crystal structure of carboxymethylated cotton as a function of reagent concentrations.

Crystal structure, disorder. Figure 2. [17]
Polynomials (see notations above):

$$\text{Cell I.} = 86.04 + 3.16x_1 - 8.18x_2$$

$$\text{Cell II.} = 7.16 - 2.12x_1 + 4.04x_2$$

$$A = 33.44 + 2.97x_1x_2$$

1. Concentrations: a) Samples carboxymethylated at the lowest concentrations and swollen in 5 mol/kg NaOH solution, respectively, have nearly the same degree of disorder (mark 1/a). b) Unexpectedly, only the same disorder is obtained at high concentrations of reagents (mark 1/b). c) In certain regions of

the investigated interval the disorder is decreasing by increasing reagent concentrations (mark 1/c). It is a proof of dissolution of highly substituted, most accessible fractions (see carboxyl content No 2b). All data of disorders should be considered as results of two coexisting processes, namely chemical reaction and dissolution. d) The crystal lattice change from Cellulose I to Cellulose II depends almost exclusively on the alkali concentration.

2. Time: The ratios of Cell I, Cell II and amorphous phase do not depend on the reaction time in the investigated interval.

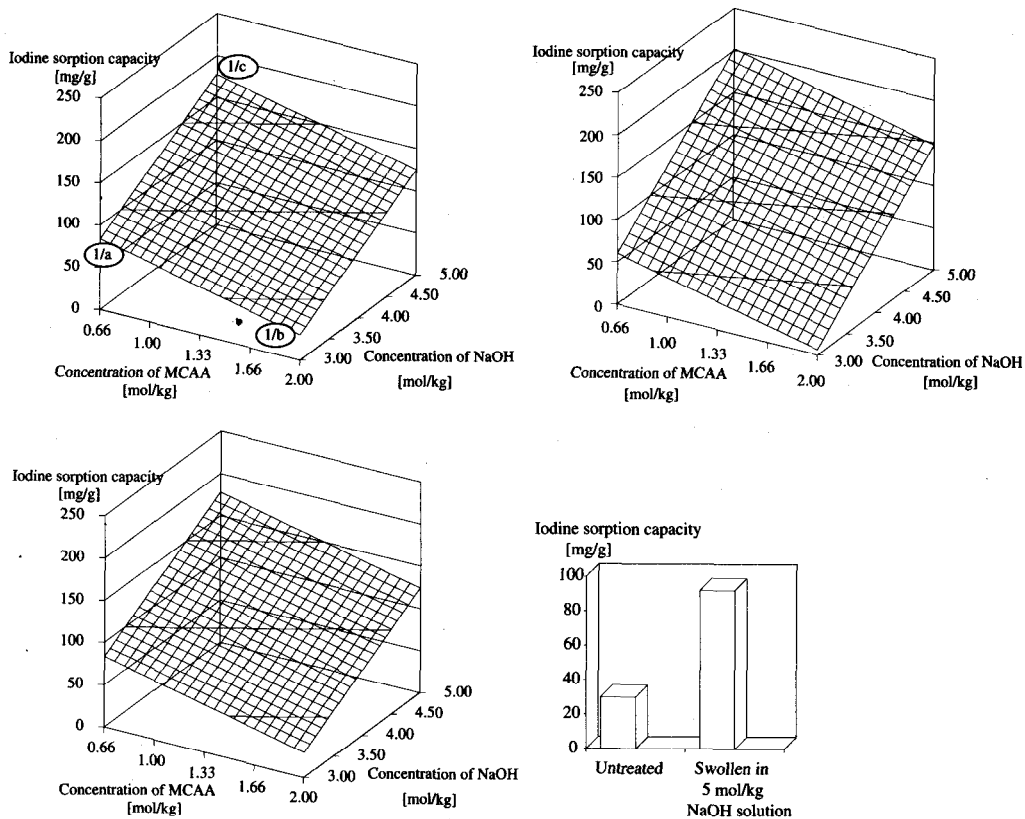


Figure 3. Specific area (iodine sorption capacity) of carboxymethylated cotton as a function of reagent concentrations and time (carboxymethylated for 20, 60 and 100 min, respectively).

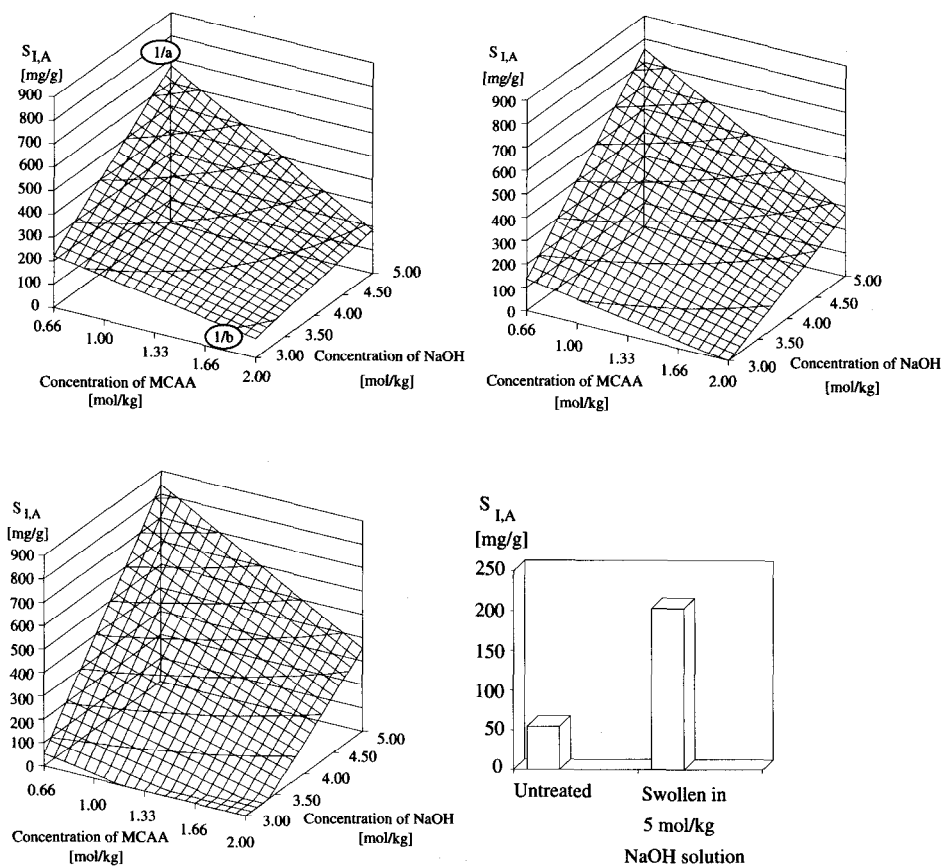


Figure 4. Disorder of the amorphous fraction (iodine sorption capacity) of carboxymethylated cotton as a function of reagent concentrations and time (carboxymethylated for 20, 60 and 100 min, respectively).

Specific area: Figure 3. [17] Values of iodine sorption [mg/g] are well known numbers for textile chemists, that is why these data are presented. Polynomials (see notations above):

$$S_1 = 103.7876 - 13.37108x_1 + 35.3852x_2 + 5.89674x_2x_3$$

1. Concentration: The specific area of carboxymethylated samples varies in a very wide interval. Its values can be significantly lower or higher than that of samples swollen in 5 mol/kg NaOH solution. A) Analogous to the disorder data, iodine sorption capacity is increased by carboxymethylation, even at the lowest reagent concentrations, nearly to the same extent than by swelling in 5 mol/kg NaOH solution (mark 1/a). b) The minimum values of iodine sorption are at the high acid and low alkali concentrations where the disorder measured by X-ray diffraction (see Crystal Structure No 1c) is also very small (mark 1/b). c) The largest specific area was obtained at the highest alkali and lowest acid concentrations (mark 1/c). Bearing in mind the low ratio of amorphous fraction in this part of the investigated interval (see Crystal Structure No 1c) it must be supposed that this amorphous material is very disordered, its accessibility is extremely high.

2. Time: Reaction time has no significant effect on the iodine sorption.

Disorder of amorphous fraction. (Figure 4). [17] Iodine sorption of cellulose samples is a sum of sorptions on amorphous material and on crystallites. The maximum value of the latter one, according to Schwertassek [18], is 18 mg/g. Sorption on amorphous fraction can be calculated from the equation:

$$S_1 = \frac{C}{100} S_{1,C} + \frac{A}{100} S_{1,A}$$

where S_1 : iodine sorption measured on the sample [mg/g]; C: ratio of crystallites measured by X-ray diffraction [mass %]; A: ratio of amorphous material measured by X-ray diffraction [mass %]; $S_{1,C}$: iodine sorption on crystallites, 18 mg/g; $S_{1,A}$: iodine sorption on amorphous material - to be calculated [mg/g].

Polynomials (see notations above):

$$S_{1,A} = 290.1256 - 78.332x_1 + 111.3758x_2 - 21.8072x_1x_2 + 21.0837x_2x_3$$

1. Concentrations: Analogous to the specific area's data, the degree of disorder

calculated from the iodine sorption capacity of the amorphous fraction varies over a very wide interval. Its values can be higher or lower than that of samples swollen in 5 mol/kg NaOH solution. Both the most disordered (mark 1/a) and the less disordered (mark 1/b) amorphous fractions are at those parts of the investigated concentration interval where the dissolution of highly accessible molecules is dominating (see Crystal Structure 1c). High concentration of alkali makes less ordered amorphous material (mark 1/a). Amorphous phases of cellulose carboxymethylated at high acid and low alkali concentrations are less disordered than that of the untreated cotton (mark 1/b). These facts represent the crucial importance of carboxymethylation technology.

2. Time: The difference between the maximum and minimum values of disorder increases as a function of time.

Volume of pores. Figure 5. [19] Polynomials (see notations above):

$$WRV = 68.2476 - 2.2436x_1 + 8.9936x_2 + 1.724x_3 + 1.3149x_1x_2$$

The WRV was increased to 73% by swelling in 5 mol/kg NaOH. Application of monochloroacetic acid of practically any concentration together with alkali of *this* concentration improved the WRV to a larger extent than alkali did alone. As can be seen from the polynomial equation and from Figure 5, the concentration of alkali is the dominant factor in the reaction while influences of acid concentration and time are much smaller.

A linear correlation was found between the surface of the fiber characterized by iodine sorption, and the volume of pores accessible for water (water retention), Figure 6.

$WRV[\%] = 44 + 0.255 S_1 [\text{mg/g}] \quad r^2 = 0.897$
The value of alkali swollen samples is included in this correlation.

Modeling of layered clothing systems. Figure 7. [14] The tests were carried out on fabric found to be the most accessible among the samples (*e.g.*, treated by 5 mol/kg NaOH, 0.66 mol/kg MCAA solution for 20 minutes). Untreated and alkali swollen samples were used for control.

Due to high accessibility about 30-45% more pesticide was trapped by carboxymethylated outer layer than by the control fabrics.

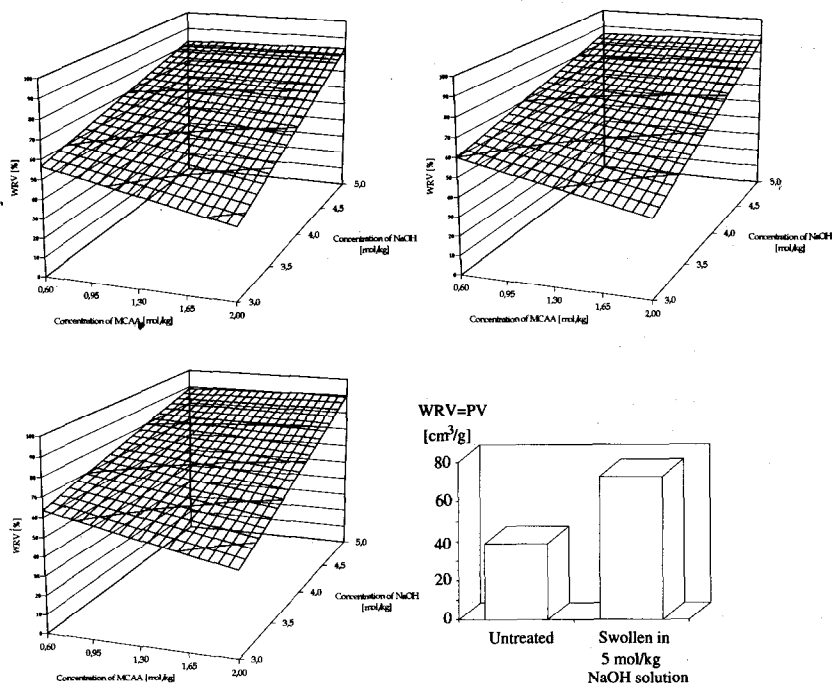


Figure 5. Volume of pores (water retention value) of carboxymethylated cotton as a function of reagent concentrations and time (carboxymethylated for 20, 60 and 100 min, respectively).

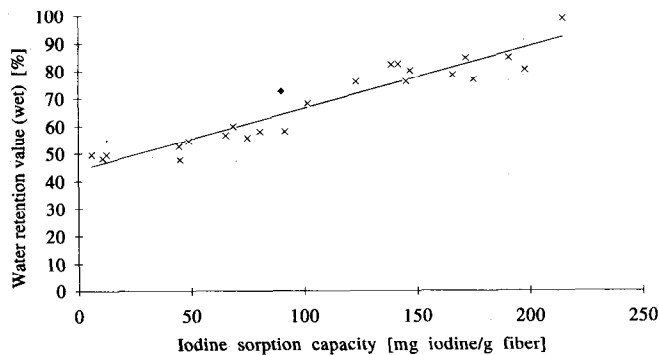
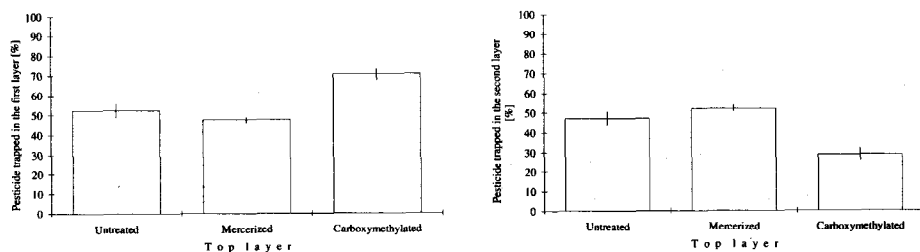
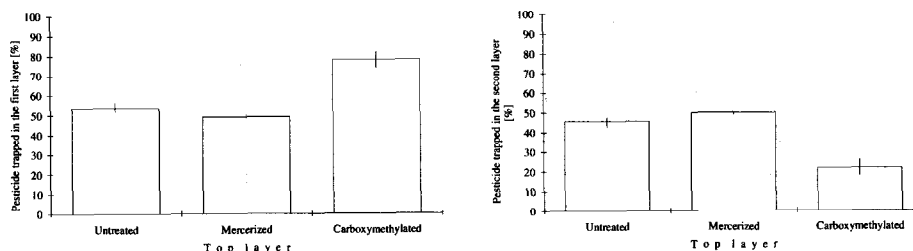


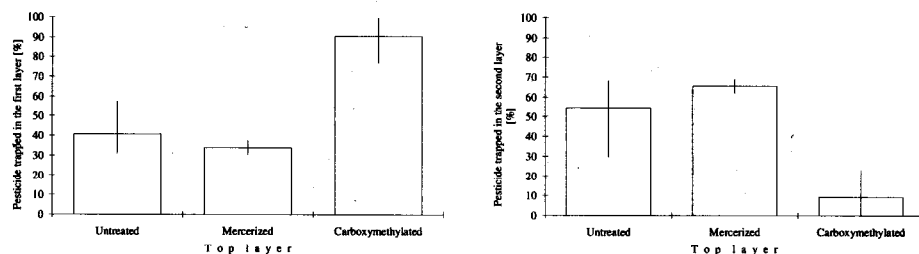
Figure 6. Correlation between the water retention value (WRV) and the iodine sorption capacity.
◆ swollen in NaOH



a) Second Layer: Untreated



b) Second Layer: Mercerized



c) Second Layer:
Carboxymethylated

Figure 7. Pesticide retention and transfer in layered clothing systems.

Conclusion

Reaction parameters have crucial importance especially from the point of view of the properties of the product. Cotton fabrics carboxymethylated by a proper technology might be advantageous in crease resistant and soil release finishes. Textiles with improved soil release parameters can be used as protective clothes for personnel involved in handling and application of pesticides. Cellulose of high accessibility can be successfully utilized as protective cloth for agricultural workers.

Acknowledgements

Special thanks are due to Dr. A. Deák for some help in the mathematical evaluation of the results. Partial support by the Hungarian National Scientific Research Fund (OTKA T 022173) and the Joint US-Hungarian Fund (JF-321/93) are gratefully acknowledged.

References

- [1] Hebeish, A.; El-Rafie, M.H.; El-Aref, A.T.; Khalil, M.I.; Abd El-Thalouth, I.; El-Khasouti, M.; Kamel, M.M. *J. Appl. Polym. Sci.* **1982**, *21*, 3703.
- [2] Jansen, E. German Patent 332 203, 1918.
- [3] Obendorf, S.K.; Ravichandran, V.; Sagan, R.; Borsa, J. 2nd International Symposium on the Performance of Protective Clothing, Tampa, Florida, USA, 1987.
- [4] Obendorf, S.K.; Sagan Kasunick, R.; Ravichandran, V.; Borsa, J.; Coffmann, W. *Arch. Environ. Contam. Toxicol.* **1991**, *21*, 10
- [5] Perrier, D.M.; Benerito, R. R. *J. Appl. Polym. Sci.* **1973**, *17*, 3375.
- [6] Daul, G.C.; Reinhardt, R.M.; Reid, J.D. *Textile Res. J.* **1952**, *22*, 787.
- [7] Dkhariyal, C.D.; Zhigach, K.F., Malinina, A.I.; Timokhin, I.M.; Finkel'stein, M.Z. *Zhur. priklad. khim.* **1964**, *37*, 1099.
- [8] Xiquan, L.; Tingzhu, Q.; Shaoqui, Q. *Acta Polymerica* **1990**, *41*, 220.
- [9] Zeronian, S.H. Intracrystalline Swelling of Cellulose, in: Cellulose Chemistry and Its Application, eds. Nevell, T. P.; Zeronian, S.H., J. Wiley: New York, 1985, pp. 161.
- [10] Doering, H. *Das Papier* **1956**, *10*, 140.
- [11] Nelson, M.L.; Rouselle, M.A.; Cangerni, S.I.; Trouard, P. *Text. Res. J.* **1970**, *40*, 872.
- [12] Bredereck, K.; Blüher, A.; Hoffmann-Frey, A. *Das Papier* **1990**, *44*, 648.
- [13] Scallan, A. M.; Carles, J. E. *Svensk Papperstidning* **1972**, *75*, 699.
- [14] Rácz, I.; Obendorf, S. K.; Borsa, J. *Text. Res. J.* **1998**, *68*, 69.
- [15] Rácz, I.; Deák, A.; Borsa, J. *Text. Res. J.* **1995**, *65*, 348.
- [16] STATGRAPHICS 5.0, Educational Institution Ed., Statistical Graphics Corp., 1991.
- [17] Rácz, I.; Borsa, J.; Bodor, G. *J. Appl. Polym. Sci.* **1996**, *62*, 2015.
- [18] Schwertassek, K. *Faserforschung und Textilberichte* **1952**, *3*, 251.
- [19] Rácz, I.; Borsa, J. *Cellulose* **1997**, *4*, 293.

COMPARISON OF LIGHT-INDUCED AND HEAT-INDUCED YELLOWING OF PULP

K. Fischer, M. Beyer

Dresden University of Technology
Institute of Wood and Plant Chemistry
Piennner Str. 23, D - 01737 Tharandt, Germany

The mechanisms and main factors of light- and heat-induced yellowing of lignocellulosics and pulps are compared. In mechanical pulps, irradiation by sunlight or related sources causes irreversible changes preferentially in the lignin part, leading to changes of the molecular weight of lignin and to the formation of lignin-carbohydrate complexes. Radical intermediates are formed during the exposure to light. An increased content of carbonyl groups indicates photooxidation. Singlet oxygen ($^1\text{O}_2$) was detected at the surface of mechanical pulps. It reacts with double bonds and aromatic structures causing the formation of chromophores. Regions exist in the pulps which are not accessible to molecular oxygen. Contrary to this, bleached chemical pulps, especially those bleached with TCF sequences,

show an enhanced tendency to heat-induced yellowing. The yellowing is reinforced in the presence of heavy metal ions and carboxyl groups that cause low pH values. A humid atmosphere accelerates the yellowing. This suggests that heat-induced yellowing is mainly caused by hydrolysis, dehydration and condensation reactions. During heating, the relatively short fragments of carbohydrates formed during oxidative bleaching stages undergo rearrangements to form various furan derivatives, the polymerization of which generates most of the chromophores.

Keywords: yellowing, chromophores, singlet oxygen, oxidation, mechanisms

Introduction

What caused the authors of this paper to deal with both light-induced and heat-induced yellowing of pulps in a joint presentation? Since the types of energy initiating these discoloration processes are quite different, the reactions leading to chromophores by light or heat are supposedly rather different. And so should be the reaction products. The main reason for such a general discussion of both types of yellowing is the new generation of paper materials which has started to conquer the paper market within the past few years. For recent years, bleached mechanical pulps have been obtaining a growing importance in the manufacture of fine paper products. In such materials they are used in blends with ECF- or TCF-bleached chemical pulps. In the future, the content of high-yield pulps in fine papers is intended to be increased further. However, their high lignin content

causes photo-yellowing. On the other hand, chemical pulps are susceptible to heat-induced discoloration. These problems confine the usage of such paper. The investigations presented here will give an overview of the main processes of both types of yellowing which, from our point of view, could be a basis of the development of combined countermeasures against discoloration of lignin-containing high-quality paper products.

Materials and methods

Pulps. For the investigations of light-induced yellowing, thermomechanical or chemo-thermomechanical pulps from spruce were used. Heat-induced yellowing was carried out with chlorine-free bleached spruce sulfite pulps. The bleaching sequence was (OP)A(EOP)ZPP with varying concentrations of ozone and peroxide.

Milled wood lignin (MWL). For irradiation experiments, lignin was dissolved in 90% acetic acid or tetrahydrofuran (THF). This solution was poured on glass plates. The irradiation took place after evaporation of the solvent. In some cases, filter paper was impregnated with this solution.

Detection of singlet oxygen. 1g of mechanical pulp was disintegrated and suspended in 300 ml methanol containing 0.001M of 2-methyl furan or cholesterol serving as probe of singlet oxygen formation. This suspension was irradiated in a photoreactor equipped with a halogen lamp. During irradiation, air was purged through the reactor. The concentration changes of the probes were measured by GC.

GPC analysis of MWL. Gel permeation chromatography was performed on Eurogel columns (1000, 500, 50 Å; KNAUER) with UV/VIS detection. The solvent was THF.

SEC chromatography of cellulose. Prior to measurement, the cellulose samples were nitrated. The chromatographic separation was carried out on polystyrene – divinylbenzene gel columns (100, 10⁴, 10⁶ Å). The solvent was THF. For further experimental details, cf. ref. [1 – 5].

Results and discussion

Light-induced yellowing of high yield pulps.

Chemical changes of lignin. Irradiation with sunlight or even ambient light causes yellowing of lignin-containing pulps. The effect of the light depends on its wavelength; in some cases, especially in the visible short-wave range, slight photobleaching was observed [6]. However, after longer times of exposure to light, the paper materials underwent yellowing. The elemental analysis of lignins before and after irradiation with a source simulating the sunlight spectrum showed significant changes in their chemical compositions (Figure 1).

The lignin isolated from irradiated TMP or CTMP pulps had a lower carbon to oxygen ratio, it contained less methoxyl groups but an increased amount of carbonyl and carboxyl groups (Table 1). This indicates that irradiation of pulps leads to a significant oxidation of lignin structures.

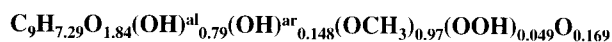
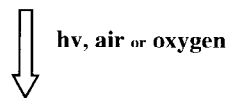
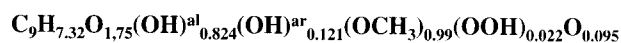


Figure 1. Light-induced changes of the elemental composition and hydroxyl and methoxyl content of milled wood lignin.

Table 1. Content of functional groups in milled wood lignin isolated from spruce TMP.

| | Non-irradiated | Irradiated |
|----------------------|----------------|------------|
| Carbonyl content, w% | 1.40 | 2.43 |
| Carboxyl content, w% | 0.64 | 0.92 |

Molecular mass distribution of lignin. The investigation of the molecular weight distribution of the lignins shows a remarkable decomposition of the high molecular mass fractions (Figure 2). However, at short irradiation times up to 30 min, the lignin undergoes a shift to higher molecular masses even in the presence of air, whereas further exposure to light leads to the destruction of the large polymer fractions (cf. [5]). The irradiation leads also to the formation of new covalent bonds between lignin and carbohydrates [7].

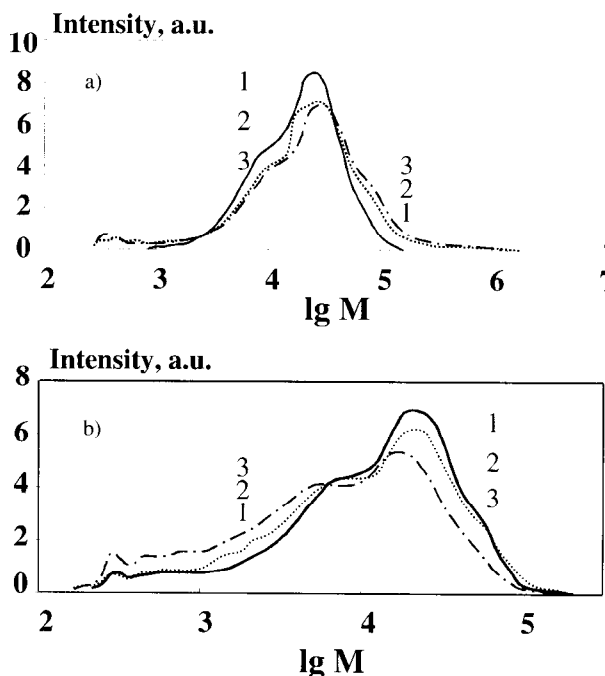


Figure 2. Molecular weight distribution of lignin isolated from TMP before and after irradiation. Irradiation times: a) 1: 0 min; 2: 15 min; 3: 30 min; b) 1: 45 min; 2: 90 min; 3: 135 min. 1 —; 2; 3 - - - -.

The application of room-temperature phosphorescence spectroscopy at different oxygen concentrations showed that in pulps, which had not been exposed to light, regions exist which are not accessible to oxygen (Figure 3). In such a case, a residual phosphorescence remains under ambient conditions. During irradiation, these regions become smaller or disappear completely.

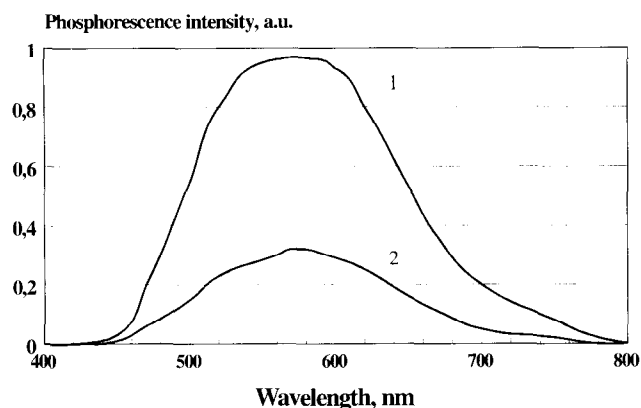


Figure 3. Room-temperature phosphorescence spectra of TMP at different oxygen concentrations. 1. Oxygen partial pressure $5 \cdot 10^{-3}$ Torr. 2. Ambient conditions. Delay time approx. 1 μ s.

Hence, in these sites photoirradiation is not accompanied by oxidative processes. Therefore, irradiated lignin which forms radical intermediates can enlarge its molecular mass by recombination reactions or form bonds to cellulose. In this case, photoyellowing is rather weak.

Longer irradiation leads to a deeper penetration of oxygen into the pulp, giving rise to oxidative decomposition of the lignin. These facts show that the role of molecular oxygen is that of a mobile, highly reactive partner of the lignin in a rigid, glassy polymeric medium. However, the triplet oxygen ground state has rather low activity. The phosphorescence measurements showed that triplet states of photo-irradiated lignin are quenched by oxygen (Figure 4). This quenching process forms singlet oxygen, which is an excellent oxidizing agent able to react with a large number of different structures (phenolic OH, double bonds, C-H acidic groups). An average amount of 10^{-11} mol/L of $^1\text{O}_2$ at the fiber surface was detected by the irradiation of pulp suspensions in the presence of different dyes. Its concentration inside the fibers could be even higher.

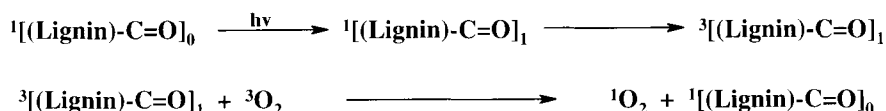


Figure 4. Quenching of triplet excited lignin units leading to the formation of singlet oxygen.

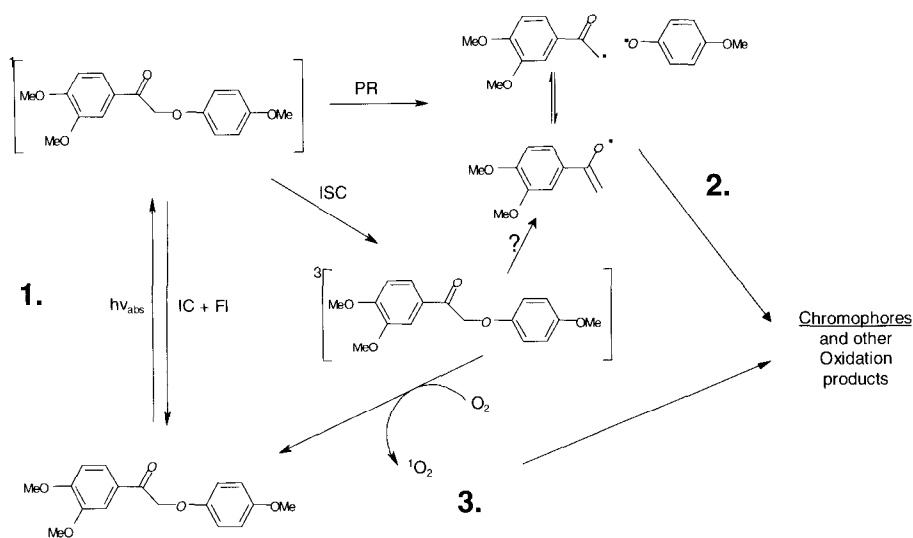


Figure 5. Schematic outline of photo-induced reactions of a lignin model compound. 1. Absorption of a photon; 2. Chromophore formation by reactions of phenoxyl radicals; 3. Chromophore formation by oxidation with singlet oxygen. PR: direct photoreaction; ISC: intersystem crossing – the transition pathway to excited triplet states; IC: internal conversion – the radiationless channel to deactivate the excited singlet state; FL: fluorescence – deactivation of the excited state by emission of light.

Investigations showed that the initial act of the photo-yellowing process after absorption of a photon by a lignin unit is the fast homolytic cleavage of α - and β -aryl ether bonds directly from the singlet-excited state [8a,b]. This reaction gives free phenoxy radicals. These radicals are oxidized to quinones which are assumed to be one of the main sources of chromophores. Most effective light-absorbing structures are those containing a carbonyl group in α -position to double bonds. The quinones are one of these light absorbing systems. As is evident from lignin analysis, new carbonyl groups are formed during irradiation. The result is a reinforced light absorption which in turn leads to an intensive light-induced oxidation. Hence, photo-yellowing is a never-ending story driven by a feed-back mechanism, the reaction rate of which becomes slower only when the amount of oxidizable matter is exhausted. The main steps of the yellowing mechanism are demonstrated by the reaction of a lignin model compound (Figure 5). Light absorption leads to singlet excited lignin structures which form phenoxy radicals by a fast homolytic cleavage process (1.). These radicals can recombine or react with oxygen. In the latter case chromophores are formed (2.). Part of the excited singlet states are transformed to long-lived triplet states which transfer their excitation energy to molecular oxygen (3.). Singlet oxygen is formed

which reacts with double bonds and C-H acidic structures. Intermediate peroxides undergo decomposition and carbonyl and carboxyl groups are formed as a part of chromophores.

Heat induced yellowing of TCF-bleached chemical pulps.

In contrast to photoyellowing of high-yield pulps, bleached chemical pulps, especially those that were bleached with TCF sequences, show an enhanced tendency to heat-induced yellowing. As was shown recently, strong yellowing is observed in pulps with high concentrations of heavy metal ions and carboxyl groups that cause low pH values [4].

Molecular weight distribution of carbohydrates.

The molecular weight distribution of different pulps was measured prior to and after heating. At 130°C, the molecular weight increases temporarily within about to 30 min, whereas a prolonged heating leads to an increased formation of cellulose with shorter chains. Higher temperatures lead to the decrease of the average molecular mass at comparable heating times. At least two competing thermal processes effect the changes in the molecular weight distribution of carbohydrates during heating (Figure 6).

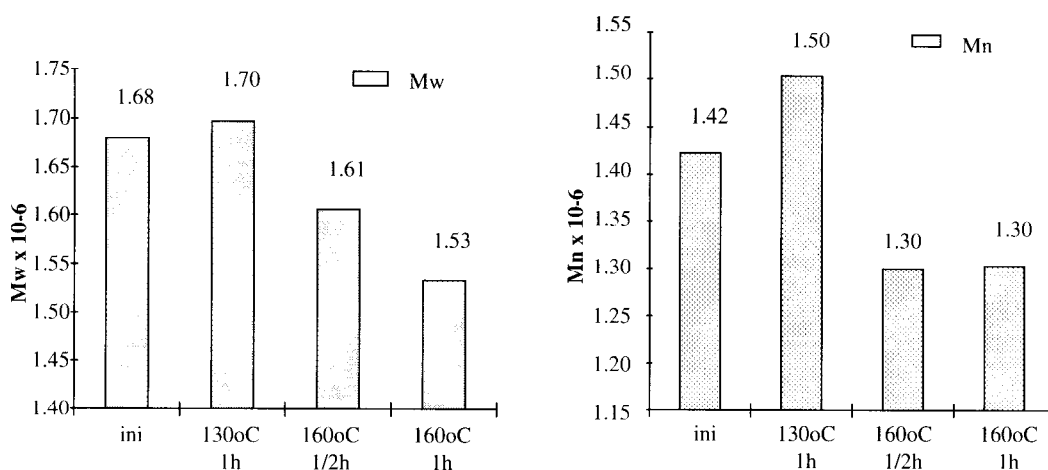


Figure 6. Average mol. weights of an EOP P bleached pulp before and after thermal treatment under various conditions.

Light scattering experiments showed branching or crosslinking of the carbohydrate molecules. The branching probability was found to be the highest at rather short carbohydrate chains. In addition, branching was stronger at an

(OP)A(EOP)ZP bleached pulp than at an incompletely bleached (OP)A(EOP) pulp [9]. These facts suggest that oxidative damage of the carbohydrate chains due to bleaching has a favorable effect on branching reactions. As was

shown recently, higher oxidative damage leads also to a stronger yellowing [10]. Hence, an interrelation between branching and color formation must be supposed. The investigated chromophores contained a high amount of furan oligomers. They are suggested to be the main constituents of color-forming substances. These compounds are formed by polymerization of different furyl derivatives.

Prerequisites to chromophore formation. According to [11], carboxyl groups in C1/C6 position of the glucose ring are a crucial

prerequisite to color formation. Keto groups at C2/C3 also contribute to discoloration, whereas aldehyde groups have a slight effect only. The carbonyl groups are then oxidized to carboxyl groups. In addition, the carbonyls serve as prerequisites to bond cleavage due to peeling-like reactions which occur in alkaline bleaching stages. The role of the molecular weights of the carbohydrates in combination with their functional groups in heat-induced yellowing suggests an easier oxidation of small carbohydrate units.

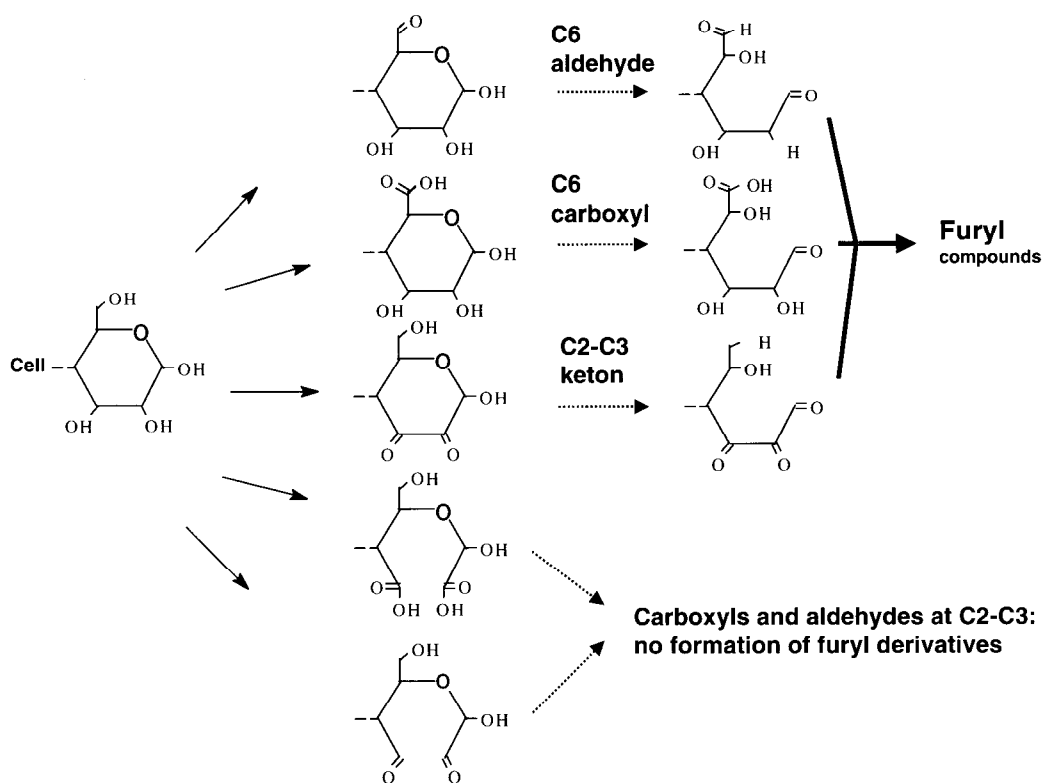


Figure 7. Influence of the positions of functional groups on the ability to form furans.

The formation of chromophores is therefore favored in pulps which fulfill the following requirements:

- a high content of short-chain carbohydrate molecules;
 - high concentrations of carboxyl groups attached to these small molecules;
 - carboxyl groups attached to preferred positions.
- Furan derivatives are formed from carbohydrate rings by H^+ -catalyzed reactions occurring *via* ring opening. Therefore, carboxyl groups cause the ring to open more readily. The subsequent closure to a furan ring is only possible if the C2-C3 bond remains undamaged. Both facts explain the role of the position occupied by the functional groups (Figure 7).

Furthermore, it was observed that each pulp investigated had its optimum pH at which it was most stable against yellowing. This optimum lies at a pH about 6-7. However, the optimum of this pH depends on the bleaching conditions under which the pulp was produced (Figure 8).

This behavior can also be explained having in mind the conditions of chromophore formation and the role of functional groups discussed above. At low pH, fast formation of furans can be expected, whereas under alkaline conditions oxidation occurs leading to further decomposition of carbohydrate chains. Formation of aromatic rings as suggested in [12] is also possible under these conditions.

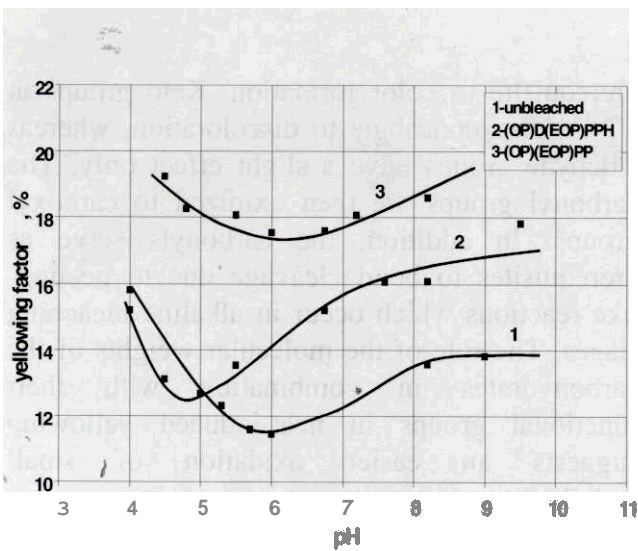


Figure 8. Plot of the yellowing of differently bleached vs. pH (130°C, 6h).

Hydrolyzable matter and heat-induced yellowing. Different methods were examined to remove those parts of the carbohydrates that contribute to heat-induced yellowing to a high extent. Partial hydrolysis in dilute acids revealed that yellowing is the stronger the higher the content of hydrolyzable matter of a pulp (Tab. 2). A similar effect was obtained by an enzymatic treatment with xylanase. Unfortunately, xylanase treatment caused an additional decrease of the DP of the cellulose suggesting considerable cellulase activity of this enzyme.

Table 2. Yellowing of industrial kraft pulps and changes occurring during hydrolytic treatment. (YF: $\Delta R/R_0 \cdot 100$).

| | Acidic hydrolysis, 2N HCl, 3h, 95°C | | Enzym. hydrolysis, 1% xylanase, pH 4.5, 3h, 35°C | |
|-------------------------|----------------------------------------|-----------|--------------------------------------------------------|-----------|
| | m loss, % | YF, 150°C | Delta DP | YF, 130°C |
| Hardwood ECF | 13.0 | 8.4 | 160 | 2.2 |
| Mix. hard- wood, TCF | 14.1 | 5.4 | 65 | 0.9 |
| Hardwood, TCF | 24.1 | 10.3 | 199 | 5.1 |
| Eucalyptus, TCF | 20.1 | 6.5 | 112 | 2.1 |
| Softwood, TCF | 6.4 | 4.9 | 11 | 2.2 |
| Softwood, TCF | 10.3 | 6.3 | | |
| Hardwood | - | 8.7 | 194 | 5.6 |

In addition, it is evident from these experiments that the hydrolysed part contains the major proportion of the overall carboxyl groups. Their removal leads to more stable pulps. Alkaline extraction turned out to be an alternative to remove short-chain carbohydrates by dissolving them. It causes also a stabilization of the cellulose.

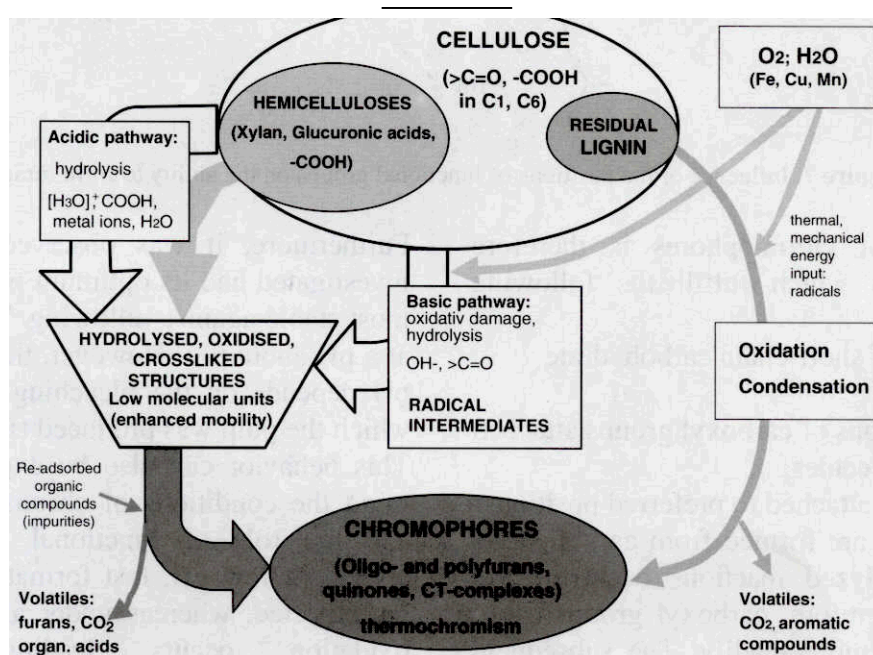


Figure 9. Schematic diagram of the pathways, boundary conditions, reactive intermediates and reaction products of heat-induced yellowing of bleached chemical pulps.

Mechanism of heat-induced yellowing. The schematic diagram (Fig. 9) presents the main factors, the boundary conditions and pathways of heat-induced yellowing. It shows the role of the pulp components and the most important intermediates occurring in the discoloration processes. The carbohydrates are pre-oxidized in bleaching and in the primary steps of heating. Oxidized structures are easily cleaved as a result of hydrolytic processes. The products of hydrolysis are converted to furan derivatives which then polymerize to give colored substances. Lignin, if present in sufficient amounts, is directly oxidized to chromophores. The oxidation reactions of both carbohydrates and lignin are catalyzed by heavy metal ions.

Acknowledgement

These studies have been carried out with financial support from the European Commission, specific RTD program Agriculture and Fisheries (FAIR), CT95-0312: „Heat-induced Yellowing – a Secondary Phenomenon of TCF-bleaching“ as well as from Deutsche Forschungsgemeinschaft (Fi-476).

References

- [1] Beyer, M. The luminescence of lignin-containing pulps – A comparison with the fluorescence of model compounds in several media. *J. Photochem. Photobiol. A: Chem.* **1993**, *76*, 217 – 224.
- [2] Beyer, M.; Bäurich, C.; Fischer, K. Mechanismen der licht- und wärme-induzierten Vergilbung von Faserstoffen. *Das Papier* **1995**, *10A*, V8 – V 14.
- [3] Fischer, K.; Beyer, M.; Koch, H. Photo-Induced Yellowing of High-Yield Pulps. *Holzforschung* **1995**, *49*, 203 – 210.
- [4] Beyer, M.; Lind, A.; Koch, H.; Fischer, K. Heat-induced yellowing of TCF-bleached pulps – Mechanistic Aspects and factors that influence the process. *J. Pulp and Paper Science* **1999**, *25*, 47 - 51.
- [5] Koch, H.; Hübner, K.; Fischer, K. The influence of light on the molecular mass of lignin. *J. Wood Chem. Technol.* **1994**, *14*, 339 – 349.
- [6] Forsskåhl, I.; Janson, J. Irradiation of mechanical pulps with monochromatic light at selected wavelengths. *Proc. 6th ISWPC*, 1991, 255 - 263.
- [7] Heller, V. Die Bildung von Lignin-Kohlenhydrat-Komplexen während der lichtinduzierten Vergilbung von Lignocellulosen. PhD thesis. Dresden University of Technology, Tharandt, 1997.
- [8] a) Schmidt; J.A. *et al.* Photodegradation of the lignin model α -guaiacoxycetoveratrone, unusual effects of solvent, oxygen, and singlet state participation. *Can. J. Chem.* **1991**, *69*, 104 – 107; b) Palm, W.U.; Dreeskamp, H.; Bonas-Laurent, H.; Castellan, A. The photochemistry of α -phenoxyacetophenones investigated by flash-CIDNP spectroscopy. *Ber. Bunsenges. Phys. Chem.* **1992**, *96*, 50 – 61.
- [9] Beyer, M.; Heller, V.; Koch, H.; Fischer, K. Structural Aspects of the Heat-induced Yellowing of TCF-Pulps. *Proc. 10th ISWPC*, Yokohama 1999, 452 – 456.
- [10] Forsskåhl, I.; Tylli, H.; Olkkonen, C. Participation of carbohydrate-derived chromophores in the yellowing of high-yield and TCF pulps. *Proc. 9th ISWPC*, Montreal, 1997, vol.1, K 3-1 – K 3-4.
- [11] De La Chapelle, V.; Chirat, C.; Lachenal, D. International Pulping and Bleaching Conference, Helsinki, June 1 – 5, 1998, *Proc.*, vol. 2, p. 587.
- [12] Forsskåhl, I.; Popoff, Theander, O. Reactions of D-xylose and D-glucose in alkaline, aqueous solutions. *Carbohydr. Res.* **1976**, *48*, 13 – 21.

LIGNIN ANALYSIS IN *ARABIDOPSIS THALIANA* USING THE PHOTOMETER-MICROSCOPE MPM800

W. Gindl,^a M.-T. Hauser,^b R. Wimmer^a

^aUniversity of Agricultural Sciences Vienna, Institute of Botany,
Gregor Mendel Strasse 33, A-1180 Wien, Austria

^bUniversity of Agricultural Sciences Vienna, Center of Applied Genetics

Lignin as a major component in plant cell walls is an important quality factor in numerous industrial processes. Especially ongoing breeding programs are trying to alter lignin and, therefore, reliable and high-resolution analysis methods for lignin are essential. In this paper, we report data on the applicability of UV microscopy for the analysis of lignin composition in xylem cell walls of *Arabidopsis thaliana* (Schmalwand, thale cress) stems. The lignin composition was determined in different parts of the xylem cell

walls by measuring the absorbance at wavelengths of 235 to 400 nm. The resulting spectra indicate considerable variability of lignin content and composition between the middle lamellae, the secondary wall of vessels and fibers. UV microscopy has proven to be highly useful for quantitative lignin analysis in *Arabidopsis* xylem tissues.

Keywords: *Arabidopsis thaliana*, lignin, UV microscopy

Introduction

Lignification is a final step in cell wall formation and influences a variety of physico-chemical properties. In the pulp and paper industry, lignin content of feedstock is an important quality factor as it is inversely related to energy consumption during chemo-thermomechanical pulping. Also, in biochemical conversion of lignocellulosic feedstock to ethanol, costs and types of feedstock pretreatment are strongly influenced by lignin content and composition [1]. Lignin is rich in energy with an energy content similar to that of coal. Lignin is an important co-product in ethanol production from biomass which is used to produce heat required in the production process [2]. In ongoing breeding programs geneticists are trying to unravel the processes that control lignification in plants with the goal to alter lignin in plant tissues. Therefore, quantitative and reliable methods of lignin analysis in plant cell walls are essential for this type of research. Conventionally, histochemical analyses using specific dyes have been applied for a qualitative assessment of lignin distribution and composition in plant material [3,4,5].

Quantitative assays such as Fourier Transformed Infrared Spectroscopy (FTIR) and classical wet-chemistry methods (*e. g.*, Klason) provide gross values of lignin contents of plant tissue [6]. When information about the distribution and concentration of lignin on a cellular level is required, UV microscopy is the most suitable method. Lignin analysis in woody tissues using UV microscopy is a well established technique [7,8] which was used to measure mature cell walls of xylem cells of flowering stems of *Arabidopsis thaliana* (Figure 1). This plant is widely known among molecular and developmental geneticists as a model plant to study the fundamental processes of plant morphogenesis and cell differentiation. The availability of different ecotypes adapted to various environments and geographic locations allows to determine the genetics behind lignin variability among these different genotypes [9]. Hence, the main purpose of this investigation was to assess the applicability of UV microscopy to *Arabidopsis thaliana* and to compare the resulting absorbance spectra to the ones obtained from cell walls of tree stems.

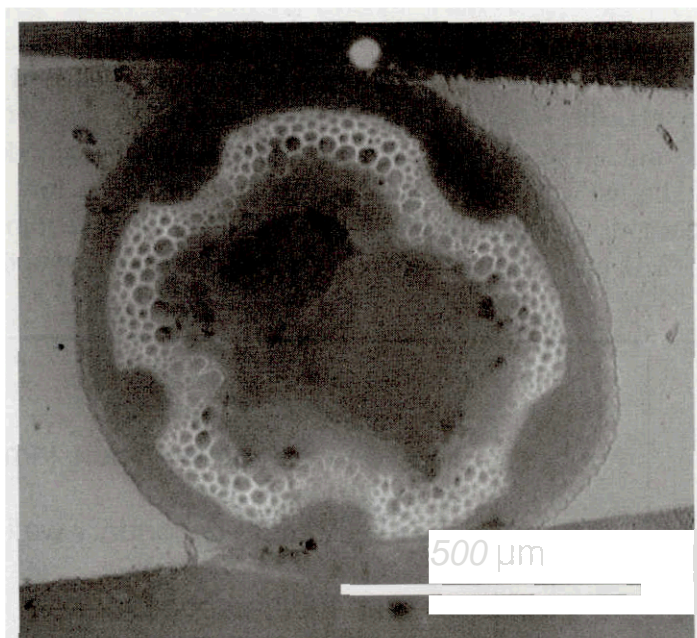


Figure 1. Incident light fluorescence photograph of a stem cross section of *Arabidopsis thaliana*. Lignified cells are visible due to their bright fluorescence.

Material and Methods

Three pieces, 10 mm in length, were cut from the basal part of the stem of a flowering *Arabidopsis thaliana* (Schmalwand), ecotype Columbia plant. After dehydration in a graded ethanol-acetone series, the samples were embedded in Spurr's resin [10].

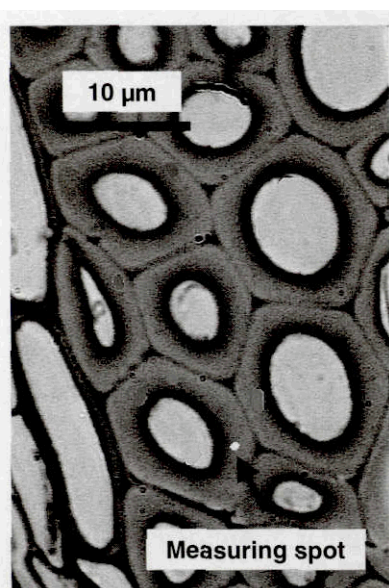


Figure 2 Transmitted-light photograph of a stem cross section of *Arabidopsis thaliana*. The circular measuring spot (diameter = 0.5 μm) is positioned in the centre of the secondary wall of a thick-walled fibre.

Cross sections, 1 μm thick, were prepared on an ultramicrotome equipped with a diamond knife. UV absorbance of the secondary walls of xylem vessels and fibers as well as the middle lamella in the corner between adjacent fibers were determined using a Zeiss MPM-800 spectrophotometer-microscope. To ensure accurate positioning at a magnification of 1000, a circular measuring spot of 0.5 μm in diameter was chosen (Figure 2). Consequently, a monochromator bandwidth of 5 nm had to be selected to ensure a sufficient level of light intensity for the photomultiplier. Spectra were recorded from 235 to 400 nm in 1 nm steps.

Results and Discussion

Spectra from ten measurements were averaged, the mean curves are displayed in Figure 3. Similar to published wood-lignin spectra [11, 12], our results show maximum absorbance at the shortest wavelengths, local minima around 260 nm and local maxima around 280 nm. Towards the visible part of the spectrum, the absorbance approaches zero. The highest local maximum of absorbance was found in the cell corner middle lamella region at 280 nm, indicating a high concentration of guaiacyl lignin, which has its absorbance maximum at 280

nm [11]. With regard to secondary cell walls, fibers absorb at their maximum (at 278.5 nm) only half as much as vessels, the latter having their maximum at 280 nm. The maximum absorbance shift towards shorter wavelengths in fibers indicates the presence of syringyl lignin, which absorbs highest at 270 nm. The ratio of

guaiacyl : syringyl in *Arabidopsis thaliana* is about 77 : 23 [4], and as a conclusion drawn from our analysis, most of the syringyl lignin can be found in the secondary walls of the fibers. This pattern, *i.e.*, a low guaiacyl : syringyl ratio in fiber tissue as compared to vessels, is also encountered in hardwood [13, 14, 15, 16].

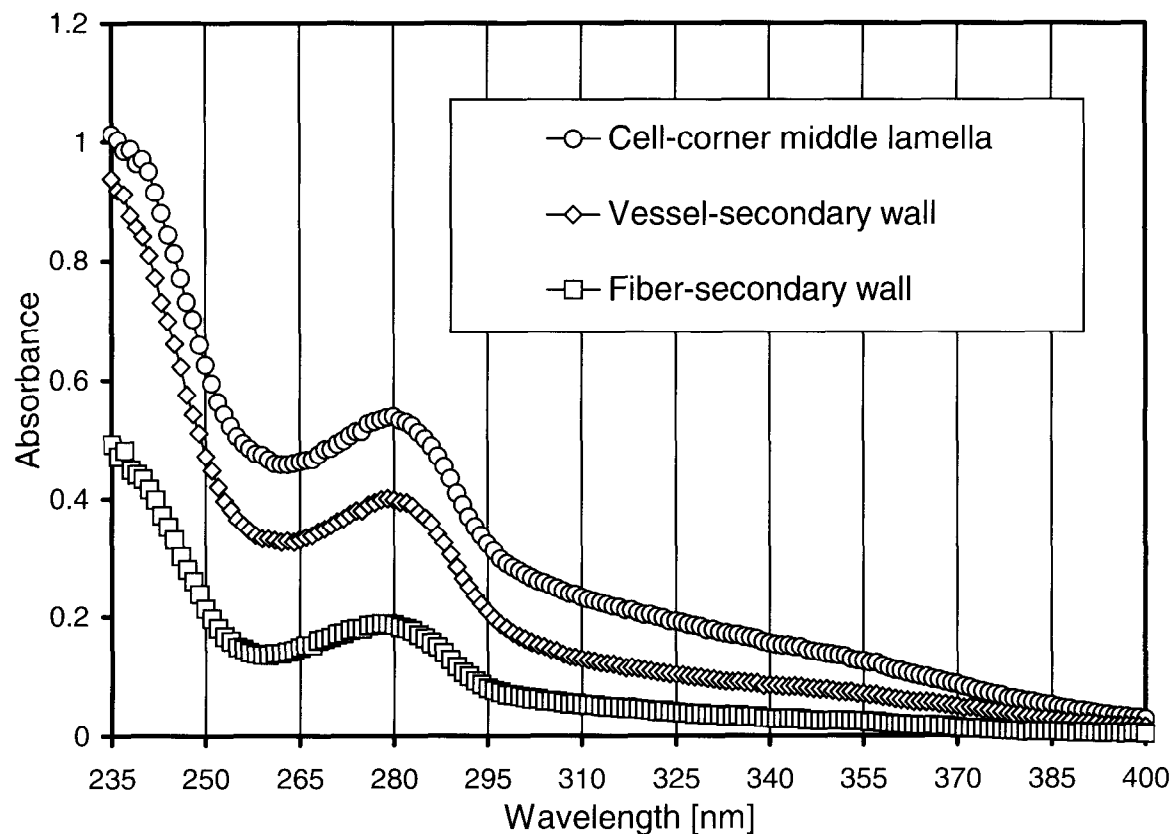


Figure 3. Absorbance spectra of different morphological regions in lignified tissue of *Arabidopsis*.

Conclusions

It is shown, that UV microscopy detects variations in lignin content and composition at a subcellular level in *Arabidopsis thaliana*. In future, this method will be applied to detect possible variations of lignin composition during stem development and in different *Arabidopsis thaliana* ecotypes and the closely related species *Arabis lyrata*. These analyses will provide important data for the basic understanding of the developmental and genetic regulation of lignin biosynthesis and deposition.

References

- [1] Tuskan, G.A.; West, D.; Bradshaw, H.D.; Neale, D.; Sewell, M.; Wheeler, N.; Megraw, B.; Jech, K.; Wiselogle, A.; Evans, R.; Elam, C.; Davis, M.; Dinus, R. Two high-throughput techniques for determining wood properties as part of a molecular genetics analysis of loblolly pine and hybrid poplar. *Applied Biochem. Biotech.* **1999**, 77-79, 1.

- [2] McLaughlin, S.B.; Samson, R.; Bransby, D.; Wiselogel, A. Evaluating physical, chemical, and energetic properties of perennial grasses as biofuels. In: Bioenergy 1996: Partnerships to develop and apply biomass technologies. *Proceedings, Seventh national bioenergy conference, Nashville, Sept. 15-29, 1996*, p.1-8.
- [3] Gerlach, D. Botanische Mikrotechnik. Thieme: Stuttgart, 1984, pp. 311.
- [4] Dharmawadhana, D.P.; Ellis, B.E.; Carlson, J.E. Characterization of vascular lignification in *Arabidopsis thaliana*. *Can. J. Bot.* **1992**, *70*, 2238.
- [5] Turner, S.R.; Somerville, C.R. Collapsed xylem phenotype of *Arabidopsis* identifies mutants deficient in cellulose deposition in the secondary wall. *Plant Cell* **1997**, *9*, 689.
- [6] Dence, C.W. The Determination of Lignin. In: Lin, S.Y. and Dence, C.W. *Methods in Lignin Chemistry*. Springer Series in Wood Science, 1992, pp. 33.
- [7] Scott, J.A.N.; Procter, A.R.; Fergus, B.L.; Goring, D.A.I. The application of ultraviolet microscopy to the distribution of lignin in wood. Description and validity of the technique. *Wood Sci. Technol.* **1969**, *3*, 73.
- [8] Fukazawa, K. Ultraviolet Microscopy. In: Lin, S.Y. and Dence, C.W. *Methods in Lignin Chemistry*. Springer Series in Wood Science, 1992, pp. 110.
- [9] Campbell, M.M.; Sederoff, R.R. Variation in lignin content and composition. *Plant Physiol.* **1996**, *110*, 3.
- [10] Spurr, A.R. A low viscosity embedding medium for electron microscopy. *Ultrastructure Res.* **1969**, *26*, 31.
- [11] Fengel, D.; Wegener, G.; Wood: Chemistry, Ultrastructure, Reactions. DeGruyter: Berlin, 1989, pp. 613.
- [12] Whiting, P.; Goring, D.A.I. Chemical characterisation of tissue fractions from the middle lamella and secondary wall of black spruce tracheids. *Wood Sci. Technol.* **1982**, *16*, 261.
- [13] Fergus, B.J.; Goring, D.A.I. The distribution of lignin in birch wood as determined by ultraviolet microscopy. *Holzforschung* **1970**, *24*, 118.
- [14] Fergus, B.J., Goring, D.A.I. The location of guaiacyl and syringyl lignins in birch xylem tissue. *Holzforschung* **1970**, *24*, 113.
- [15] Musha, Y.; Goring, D.A.I. Distribution of syringyl and guaiacyl moieties in hardwoods as indicated by ultraviolet microscopy. *Wood Sci. Technol.* **1975**, *9*, 45.
- [16] Takabe, K.; Miyauchi, S.; Tsunoda, R.; Fukazawa, K. Distribution of guaiacyl and syringyl lignins in Japanese beech (*Fagus crenata*): Variation within an annual ring. *IAWA Bull n.s.* **1992**, *13*, 105.

MONOSULFITE SPLITTING - AN IMPORTANT PART OF THE SECONDARY RECOVERY SYSTEM OF THE MAGNESIUM BASE ACID BISULFITE COOKING PROCESS

G. Götzinger, A. Schrittwieser and R. Mühlbacher

Lenzing AG, A-4860 Lenzing, Austria

The drying and splitting behavior of magnesium monosulfite for the technical raw material being encountered at the SO₂ recovery plant of Lenzing AG was studied in simple laboratory experiments. Small samples containing either little amounts of free water in excess to the trihydrate, or being almost completely pre-dried, were thermally treated in an electrically heated quartz tube. The solids were kept stationary in a ceramic crucible and heated to predetermined temperatures for technical relevant times under controlled gaseous environments. The remaining water content and the sulfate formation, respectively, depending on process conditions were studied by simple wet

chemistry. A comparison with literature data showed that sulfate formation in the drying step of the technical raw material was in the same range as for pure dehydrated monosulfite. It was concluded that thermal disproportionation is the major source of sulfate in the drying step. The critical temperature range for disproportionation is 300 to 650 °C. While air has to be carefully avoided in the splitting process, this is of less importance for the drying step. Dilution of the evolved SO₂ gas during splitting seems to be recommendable.

Keywords: chemical recovery, magnesium monosulfite, thermal treatment, sulfate formation

Introduction

Already in 1993 Lenzing AG switched its pulping process from calcium base to magnesium base [1] due to environmental and economical reasons. This allowed the recovery of the cooking chemicals SO₂ and MgO, and it was a prime target to maximize the degree of recovery since then. However, because the secondary recovery (consisting of combustion of spent liquor and recombination of SO₂ and MgO to recovered raw cooking liquor) yields a solution with a ratio of 2SO₂/MgO which is close to unity and because the primary recovery (*i.e.*, cooking liquor tanks taking up digester relief gas) yields only limited free SO₂, it is necessary to feed (liquid) SO₂ to the digester. Hence, in order to keep a stable mass balance one has to accept equivalent losses of chemicals. As a result, free SO₂ in the cooking process was steadily lowered during the last decades. Since the advent of a process that splits monosulfite [2, 3] in its components (SO₂ being liquified and recycled to the digester), it was

possible to further minimize chemical losses and to increase the amount of free SO₂ in the digester. After the production-scale plant went into full operation in 1998, it turned out, however, that efficiency was limited by a rather high rate of sulfate formation. As a first step, the reasons of sulfate formation had to be established in lab trials for the case of the technical raw material being encountered at Lenzing. Since the big scale process is divided into a drying and splitting step we studied the removal of water on one hand and the evolution of SO₂ on the other hand in relation to sulfate formation for the technically most important process parameters and compared to the literature [4, 5].

Experimental

Samples taken for lab experiments were obtained in their crude, technical state from the recovery plant of Lenzing (sample points were set after the absorption system and before, respectively after, the drying stage of the monosulfite splitting

process). The samples taken for drying experiments contained 19.6% MgO, 0.9% CaO, 27.1% SO₂, 4.9% SO₃ and 47.5% H₂O (actually the undetermined remainder). The samples taken for splitting experiments contained 34.5% MgO, 2.1% CaO, 49.1% SO₂, 4.8% SO₃ and 9.5% H₂O (again the undetermined rest). Approximately 2 grams of samples were put into a ceramic crucible and introduced into the electrically pre-heated quartz tube of approx. 35 mm opening. A gaseous stream (0.2 l/min of nitrogen containing less than 5 vpm H₂O and less than 3 vpm oxygen, ambient air or H₂O vapor and in the case of splitting experiments occasionally 5 or 20vol% SO₂ in nitrogen) was maintained throughout the complete experiment. All thermal treatments were performed at atmospheric pressure. Steam as drying medium was prepared by heating deionized water to boiling temperature at atmospheric pressure. After treating the sample at constant temperature for predetermined times the crucible was moved to the cold part of the tube and cooled down to room temperature. Analysis before and after thermal treatments were performed by simple wet chemistry: MgO and CaO were determined by complexometry, SO₂ by oxidimetry with chloramine as the reagent, and SO₃ by gravimetry as BaSO₄, the undetermined rest was usually regarded as H₂O. All experiments were run in duplicate.

Results and Discussion

Since the technical drying process uses steam for directly heating the monosulfite and a certain amount of leakage is unavoidable, it was of crucial importance to get an idea about the significance of the water vapor content in the gas and to learn something about the direct oxidation of monosulfite by air. Figure 1 compares the remaining water content and sulfate formation after heating the samples to 250 °C for 60 minutes with nitrogen, air and steam as the drying atmosphere.

Clearly, nitrogen showed the best drying efficiency while the action of steam resulted almost only in the removal of free water and insignificant removal of crystal water. At the same time, application of air did not increase sulfate formation drastically (being calculated as percentage of original SO₂ which is converted

into sulfate). Thus, when using steam one is tempted to increase temperature in order to maintain sufficient drying extent. The influence of temperature on the extent of drying and sulfate formation was therefore studied at two hours retention time using nitrogen as the drying agent. While it is clearly visible in Figure 2 that the remaining amount of crystal water is somewhat reduced by increasing the temperature from 200 to 300 °C, it is also apparent that sulfate formation is increased to an unacceptable level at 300 °C.

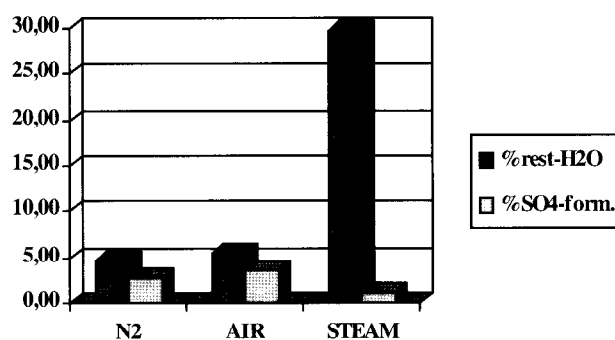


Figure 1. Water content and sulfate formation after heating monosulfite at 250 °C for 60 minutes with nitrogen, air or water vapor as the drying medium.

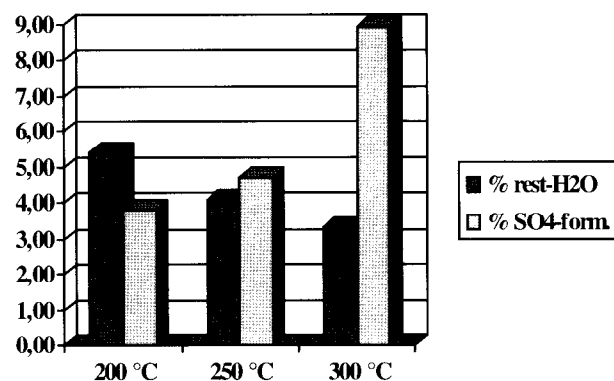


Figure 2. Water content and sulfate formation upon heating monosulfite at 200, 250 and 300 °C for 120 minutes in a stream of nitrogen.

It is well-known [6] that splitting of sulfite is favorable for the magnesium salt as compared to calcium. Nevertheless, sulfate formation by disproportionation of sulfite and direct oxidation by air is still an important side reaction for magnesium. This holds especially true for impure substances [5]. Therefore, we performed a series of splitting experiments applying increasing temperatures and different gaseous environments. As apparent from Figure 3, sulfate formation

decreased with increasing temperatures. The values are in good agreement with those for the pure substances according to Ketov and Pechkovskii [5]. As expected, splitting experiments in a current of air resulted in a pronounced formation of sulfate. The extent of sulfate formation seems to exceed the one for the pure substance reported in [5], and it was practically constant despite an increase of 100 °C. It is also in accordance with the statements in [5] that sulfate formation was drastically increased (even at elevated temperatures of 650 and 750 °C) when SO₂ gas was applied during thermal treatment. The result is largely independent on whether 5 or 20 vol% SO₂ was used.

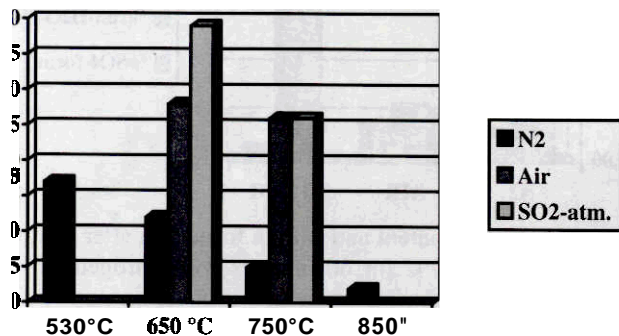


Figure 3. Percentage of sulfate formation upon heating monosulfite to different temperatures for 60 minutes in different gaseous environments.

Conclusion

The experimental data show that sulfate formation by disproportionation is the most important side reaction in thermal treatment of magnesium monosulfite. While air has to be carefully avoided in the splitting process, this is of less importance for the drying step. It is of primary importance to avoid a temperature range of 300 to 650 °C in order to minimize sulfate formation. Dilution of the evolving SO₂ gas during the splitting step seems to be recommendable.

References

- [1] Hornke, R. *Papier* **1966**, *19*, 86.
- [2] Apel, W. *et al.*, *Austrian patent* AT 347236.
- [3] Künstner, W.; Wolschner, B. *Papier* **11**, 529.
- [4] Rammelsberg, C. *Pogg. Ann.* **1845**, *67*, 250.
- [5] Ketov, A. N.; Pechkovskii, V.V. *Zhur. Org. Khim.* **1959**, *4*, 172.
- [6] Schwitzgebel, K.; Lowell, P.S. *Environmental Sci. Technol.* **1973**, *13*, 1157.

NEW POLYMERS BASED ON CELLULOSE

T. Heinze, M. Vieira, U. Heinze

Institute of Organic Chemistry and Macromolecular Chemistry,
Friedrich Schiller University of Jena, Humboldtstrasse 10, D-07743 Jena, Germany

Novel regioselectively functionalized cellulose derivatives were synthesized using protective group technique and selective oxidation of primary hydroxyl groups. Carboxymethyl cellulose, methyl cellulose and cellulose sulfate with a functionalization at O-2 and 3 were prepared via 6-O-(4-monomethoxy) triphenylmethyl and 6-O-thexyldimethylsilyl cellulose, respectively. The subsequent oxidation was

carried out with NaBr/NaClO mediated with TEMPO. The molecular structure of the new polymers was revealed by means of NMR spectroscopy.

Keywords: regioselective functionalization, 2,3-O-substituted celluloses, selective oxidation, 6-carboxycellulose derivatives, NMR

Introduction

Chemical modification reactions continue to provide a dominant route towards cellulose utilization in polymer-based materials. Especially products with a controlled pre-set functionalization pattern should possess new and useful properties [1,2]. They are important in basic investigations to study for instance structure and interactions in solution and the formation of well-defined supramolecular assemblies. Moreover, studying regioselective functionalization will result in a better knowledge about reaction mechanisms and the control of processing and end-use properties. However, the synthesis of cellulose derivatives of structural uniformity is still a problem. In the course of our studies on polysaccharides, an important goal of a basic research program is the evolution of synthesis pathways due to their potential of regioselectivity. This includes of course the development of appropriate analytical tools.

In the present paper we report about the preparation of new ionic cellulose polymers obtained by using a protecting group technique as well as a selective oxidation procedure.

Materials and Methods

Cellulose powder (AVICEL PH 101, DP_{Cuoxam} 280) and spruce sulfite pulp (DP_{Cuoxam} 650, FLUKA) was used. 6-O-(4-monomethoxy) triphenylmethyl ("trityl") cellulose was synthesized under homogeneous reaction conditions in *N,N*-dimethylacetamide (DMA)/LiCl according to ref. [3]. The DS_{Trityl} values were determined by elemental analysis (see Table 1). The carboxymethylation of 6-mono-O-(4-monomethoxy)trityl cellulose and subsequent detritylation according to ref. [7] gives 2,3-O-carboxymethyl cellulose of a DS_{CMC} of 1.20. The 6-mono-O-thexyldimethylsilyl cellulose of a DS_{Silyl} of 1.04 was prepared in ammonia-saturated *N*-methylpyrrolidone. Subsequent methylation and desilylation was carried out as described in ref. [9,10] yielding 2,3-O-methyl cellulose (DS_{Methyl} 1.80).

Sulfation of 6-mono-O-(4-monomethoxy) triphenylmethyl "trityl" cellulose. In a typical example, 6 g (14 mmol) of 6-mono-O-(4-monomethoxy)trityl cellulose (DS_{Trityl} = 0.98) was dissolved in 150 ml dimethyl sulfoxide (DMSO). 8.9 g (56 mmol, 2 mol/mol unmodified hydroxyl group) of SO_3 /pyridine complex was added at room temperature and stirring was continued for 4.5 h at room temperature. The polymer was

precipitated in 500 ml of methanol and neutralized with ethanolic sodium hydroxide solution. The product was washed with ethanol and dried in vacuum at 50°C. The product is soluble in DMSO and in water acetone mixtures (v/v = 9/1). FTIR (KBr): 1251 cm⁻¹ (ν SO₂) and the characteristic signals of the triphenylmethyl moiety.

Cellulose-2,3-sulfate. 2 g of 6-mono-*O*-(4-monomethoxy)trityl cellulose-2,3-sulfate was suspended in 250 ml of methanol and 12 ml of concentrated HCl was added. The mixture was stirred for 16 h at room temperature and filtrated. The product was suspended in water and neutralized with aqueous NaOH yielding a solution. After precipitation into ethanol, the product was dried in vacuum (0.1 Torr) at 50°C. ¹³C NMR (D₂O): δ 60.2 (C-6), 73.0-75.3 (C-2, 3, 5), 78.1-79.2 (C-4 and C-4''), 80.2 (C-2'), 82.3 (C-3'), 100.3 (C-1), 102.4 (C-1''), see Figure 2. Conditions and results of a variety of sulfating reactions of 6-*O*-(4-monomethoxy)trityl cellulose carried out according to this procedure are summarized in Table 1.

Oxidation of primary hydroxyl groups of cellulose derivatives, typical example. 1.0 g (5.3 mmol) of 2,3-*O*-methyl cellulose (DS=1.80), 7.5 mg (0.045 mmol) of 2,2,6,6-tetramethyl-1-piperidinyloxy radical (TEMPO) and 50 mg (0.48 mmol) of NaBr were dissolved in 50 ml of distilled water with stirring. A solution with a pH value of 5.0 results. The mixture was kept in an ice bath at about 1°C, and aqueous sodium hypochlorite solution (13%, w/v) was added dropwise until a pH of 10.8 was obtained. The pH value of the system was monitored. When the pH dropped below 10.8, sodium hypochlorite was added. After complete consumption of 11.0 ml of sodium hypochlorite solution the clear system obtained was precipitated in ethanol, filtered, washed with ethanol/water (v/v = 8/2) and dried in vacuum at 50°C. FTIR (KBr): 3387 (ν OH), 2891 (ν CH), 1607 and 1406 (ν COONa) 1034 (ν COC) cm⁻¹. ¹³C NMR (D₂O): δ 58.6, 60.1 (CH₃ and C-6), 73.4-76.8 (C-2, 3 and 5), 82.4-82.8 (C-4, C-4''), 101.8 (C-1''), 174.5 (COONa).

Reaction conditions and results of oxidation reactions of regioselectively functionalized cellulose derivatives carried out according to this procedure are summarized in Table 2.

Measurements. ¹³C NMR spectra were acquired on a Bruker DRX 400 spectrometer in DMSO-d₆ or D₂O at 25°C. The number of scans was around 6000. FTIR spectra were recorded on a Nicolet Impact 400 spectrometer using KBr pellets. The sodium content was analyzed with a flame photometer, type Flapho 41.

Results and discussion

The synthesis paths studied in this work is depicted in Figure 1. In order to selectively modify the primary hydroxyl groups of cellulose, two different protecting groups were used. On one hand, tritylation, a well-known and common method of 6-*O* protection of polysaccharides [3-7], was carried out under homogeneous reaction condition in *N,N*-dimethylacetamide (DMA)/LiCl using 4-monomethoxytriphenylchloromethane [3]. By this effective procedure a 6-*O*-(4-monomethoxy)triphenylmethyl ("trityl") cellulose (**1-3**) of high regioselectivity was obtained. On the other hand, the possibility to protect polysaccharides with bulky trialkylsilyl moieties was studied recently in detail [8-10]. The silylation of cellulose with thexyldimethylchloro-silane under heterogeneous reaction conditions in ammonia-saturated *N*-methylpyrrolidone at -15°C yields 6-*O*-thexyldimethylsilylcellulose (**4**) with a DS_{Silyl} of 1.04 and a complete reaction at *O*-6.

Synthesis of 2,3-*O*-functionalized products via 6-*O*-(4-monomethoxy)trityl cellulose. Due to the stability of 4-monomethoxytrityl groups under alkaline conditions we were able to prepare 2,3-*O*-carboxymethyl cellulose. The 6-*O*-(4-monomethoxy)trityl cellulose was dissolved in dimethyl sulfoxide (DMSO) and activated by solid NaOH powder.

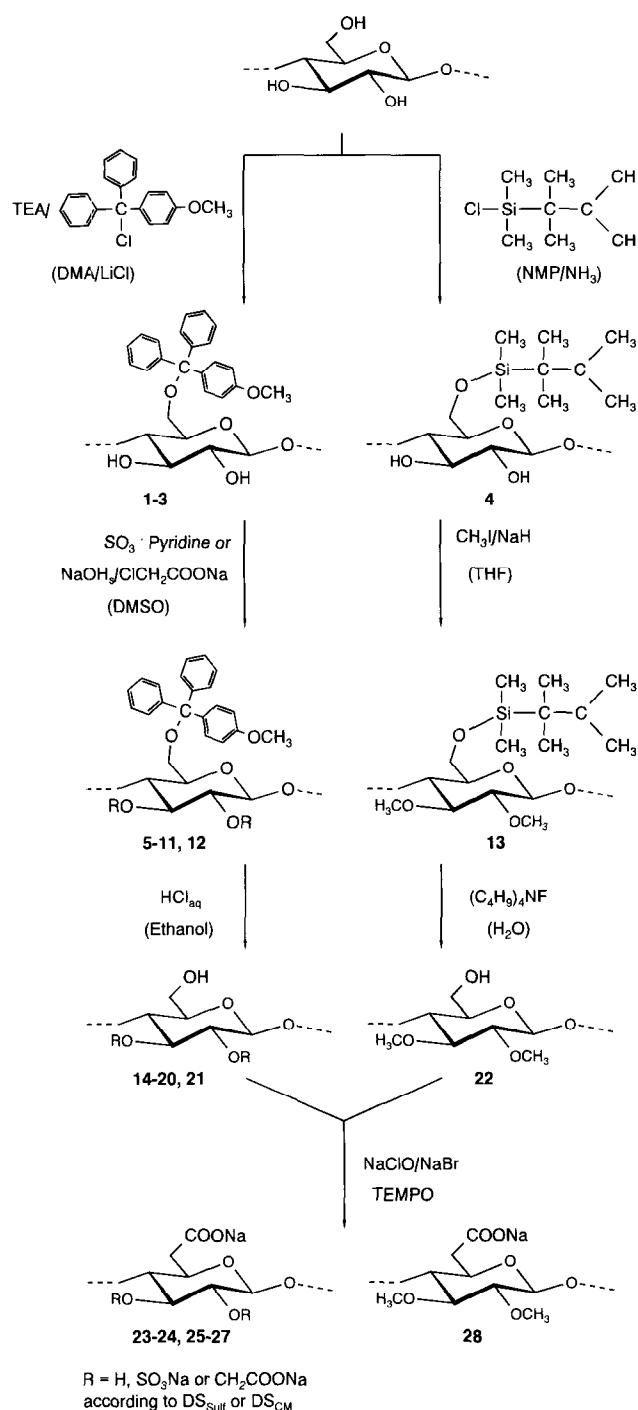


Figure 1. Synthesis paths for regioselective functionalization of cellulose.

The conversion with mono-chloroacetate and subsequent detritylation with HCl afforded the 2,3-*O*-CMC (**12, 21**) as described in detail in ref. [7, 11]. However, no information about sulfation of 6-*O*-(4-monomethoxy)trityl cellulose were available up to now.

The sulfation of the 6-*O* protected samples **1-3** was carried out homogeneously in DMSO using SO₃-pyridine complex as sulfating agent at room

temperature (Tab. 1). After a reaction time of 2 to 4.5 h, the products were precipitated in methanol and neutralized with ethanolic NaOH solution in order to transfer the free acid form of the sulfuric acid half esters into the sodium salt form. This is very important to prevent an acid degradation of the polymer chain as well as an undesired acidic detritylation. The products obtained are very hygroscopic yielding rubber like materials by attracting water. The 6-*O*-(4-monomethoxy)trityl cellulose sulfates (sodium salt) are soluble in DMSO and mixtures of water/acetone (v/v = 9/1). They possess surface active properties.

The FTIR spectra of these polymers **5-11** show the characteristic absorptions of the sulfuric acid half esters. Peaks are visible at 1251 cm⁻¹ (νSO₂) and 810 cm⁻¹ (νSO), however the last one is mixed with the signal of the C-H vibration of the aromatics (δCH). The typical peaks of the trityl moieties at 3028 and 1608 cm⁻¹ (νCH and CC) are also found in the spectra.

By exposing the 6-*O*-(4-monomethoxy)trityl cellulose-2,3-sulfate to controlled acidic conditions the trityl group can be completely removed yielding a pure cellulose-2,3-sulfate. In the FTIR spectra of the detritylated products the signals in the aromatic region disappear. The DS_{Sulfate} values were determined by means of elemental analysis. It was found that during the detritylation a partial removal of sulfuric acid half ester groups occurs as well (Tab. 1).

The ¹³C NMR spectra of the cellulose sulfates recorded in D₂O show the characteristic signals of the carbon atoms of the modified AGU in the range between 60.2 and 102.6 ppm. From the spectra it may be concluded that no sulfation of the primary hydroxyl groups took place if the DS_{Trityl} is 0.98 (samples **8-11**). There is a peak for the C-6 bearing a OH group at δ = 60.2 ppm only. On the other hand, the peaks at δ = 80.5 (C-2_S) and 81.3 (C-3_S) indicate the exclusive reaction at these positions (Figure 2).

Synthesis of regioselectively functionalized products via 6-mono-O-thexyldimethylsilyl cellulose. Due to their high regioselectivity, the bulky trialkylsilyl cellulose represents valuable and versatile reactive intermediates for subsequent regioselective reactions. The silyl function can be used as an activating group as

well as an protecting group. For example, the reaction with SO_3 proceeds via insertion of SO_3 into the Si-O bond. Consequently, this polymer is not suitable for the preparation of cellulose-2,3-sulfates. However, methylation of 6-*O*-thexyldimethylsilyl cellulose with methyl iodide

in the presence of NaH occurred at the free OH-groups only (13). Treatment with tetrabutylammonium fluoride to remove the thexyldimethylsilyl afforded pure 2,3-di-*O*-methyl cellulose (22).

Table 1. Results of the sulfation of 6-*O*-(4-monomethoxy)trityl cellulose (MMTC) with 2 mol sulfating agent per mol unmodified hydroxyl group (in dimethyl sulfoxide at room temperature).

| MMTC | | Reaction conditions | | MMTC sulfate | | | Cellulose sulfate | | |
|------|-----------------------------------|----------------------|----------|--------------|-------|------------------------------------|-------------------|-------|------------------------------------|
| No. | DS _{Trityl} ^a | Sulfating agent | Time (h) | No. | S (%) | DS _{Sulfate} ^a | No. | S (%) | DS _{Sulfate} ^a |
| 1 | 0.60 | SO ₃ -DMF | 2.5 | 5 | 7.55 | 0.93 | 14 | 5.37 | 0.32 |
| 2 | 0.83 | SO ₃ -Py | 2.0 | 6 | - | - | 15 | 5.91 | 0.37 |
| 2 | 0.83 | SO ₃ -Py | 2.5 | 7 | - | - | 16 | 6.75 | 0.44 |
| 3 | 0.98 | SO ₃ -Py | 2.0 | 8 | - | - | 17 | 4.92 | 0.30 |
| 3 | 0.98 | SO ₃ -DMF | 2.5 | 9 | 9.30 | 1.80 | 18 | 8.22 | 0.57 |
| 3 | 0.98 | SO ₃ -Py | 2.5 | 10 | - | - | 19 | 9.59 | 0.70 |
| 3 | 0.98 | SO ₃ -Py | 4.5 | 11 | - | - | 20 | 12.00 | 0.99 |

a) DS, Degree of substitution calculated on basis of elemental analysis

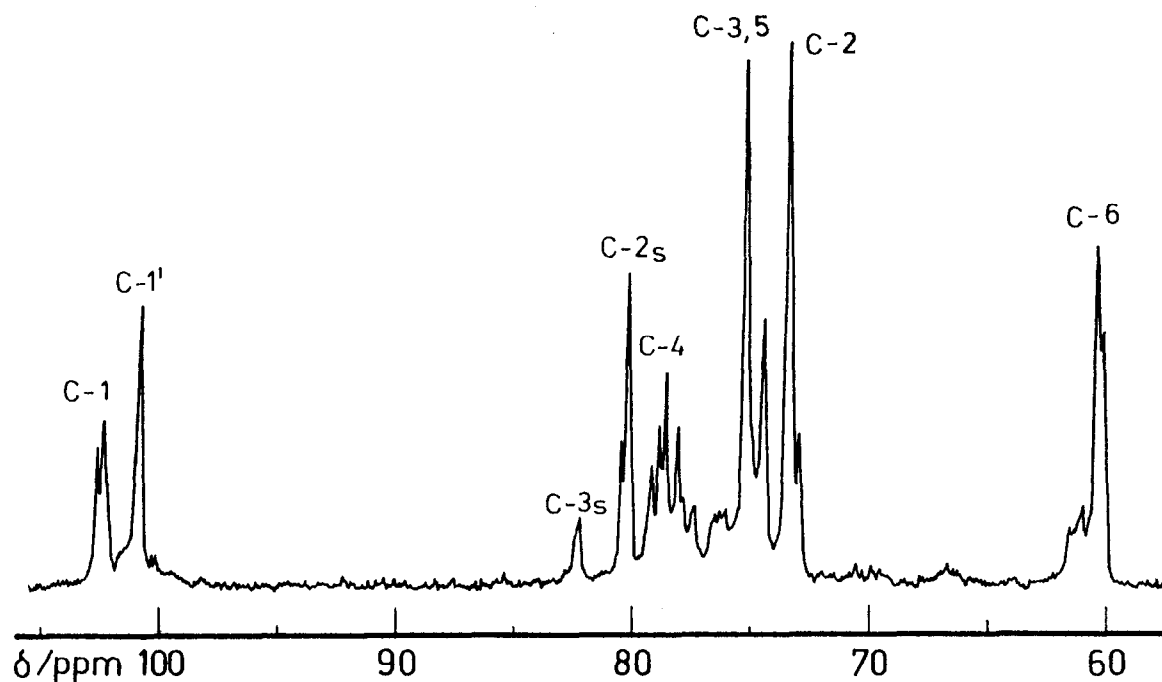


Figure 2. ¹³C-NMR spectrum of cellulose-2,3-sulfate 20.

Oxidation of 2,3-O-functionalized cellulose derivatives. Recently, de Nooy *et al.* succeeded in the selective oxidation of water-soluble polysaccharides like starch, inulin, and pullulan [12, 13]. The oxidation is carried out in water homogeneously and is mediated by 2,2,6,6-

tetramethyl-1-piperidinyloxy radical (TEMPO) using hypobromite as the oxidizing agent and NaOH to control the pH value of the reaction medium. The oxidation method was applied to cellulose as well [14]. The cellulose has to be strongly activated by mercerization prior to

oxidation. In our own work, the oxidation of water-soluble hydroxyethyl cellulose was investigated. It was found that the adjustment of the pH-value is very important for both a selective oxidation and low chain degradation [15]. It is worth mentioning that the pH-value can be adjusted by the oxidation agent NaClO itself, *i.e.*, the additional use of aqueous NaOH is not necessary.

Table 2. Conditions and results of the oxidation of cellulose derivatives.

| Starting polymer | | Molar ratio ^b | Rxn. time (min) | Oxidized polymer | | |
|------------------|-------------------|--------------------------|-----------------|------------------|-----------------|-----|
| No. | Type ^a | | | No. | DO ^c | |
| 21 | CMC | 1.2 | 5 | 10 | 23 | 0.8 |
| 21 | CMC | 1.2 | 5 | 30 | 24 | 1.0 |
| 13 | CS | 0.3 | 5 | 25 | 25 | 0.9 |
| 15 | CS | 0.4 ^d | 5 | 20 | 26 | 0.8 |
| 18 | CS | 0.7 | 5 | 10 | 27 | 0.5 |
| 22 | MC | 1.8 | 10 | 40 | 28 | 1.0 |

a) MC, 2,3-*O*-methyl cellulose; CMC, 2,3-*O*-carboxymethyl cellulose; CS, cellulose-2,3-sulfate; DS, degree of substitution

b) NaClO / AGU (Anhydroglucose unit) [mol/mol]

c) Degree of oxidation (DO) calculated from sodium content determined by means of flame photometry

d) Partially functionalized at the 6 position (DS 0.2)

For the oxidation of regioselectively 2,3-functionalized cellulose derivatives (see Fig. 1), the polymers **15**, **18**, **21**, and **22** were dissolved in water containing a catalytic amount of TEMPO and NaBr. Aqueous sodium hypochlorite solution was added maintaining a constant pH value of 10.8 (Tab. 2.). The ¹³C-NMR spectra of the isolated products show, compared to the starting polymers, new peaks at about $\delta = 175$ ppm indicating the transformation of the CH₂OH to a COONa group (Figure 3).

The aqueous solution of the oxidized polymers show lower viscosity values compared to the starting materials. This might be a consequence of the introduction of carboxyl groups and probably a result of depolymerization as a side reaction. Preliminary GPC measurements show that only a low chain degradation occurs under the oxidation conditions applied. However, additional studies have to be carried out due to the known problems of the determination of the molecular mass of cellulose derivatives by means of GPC.

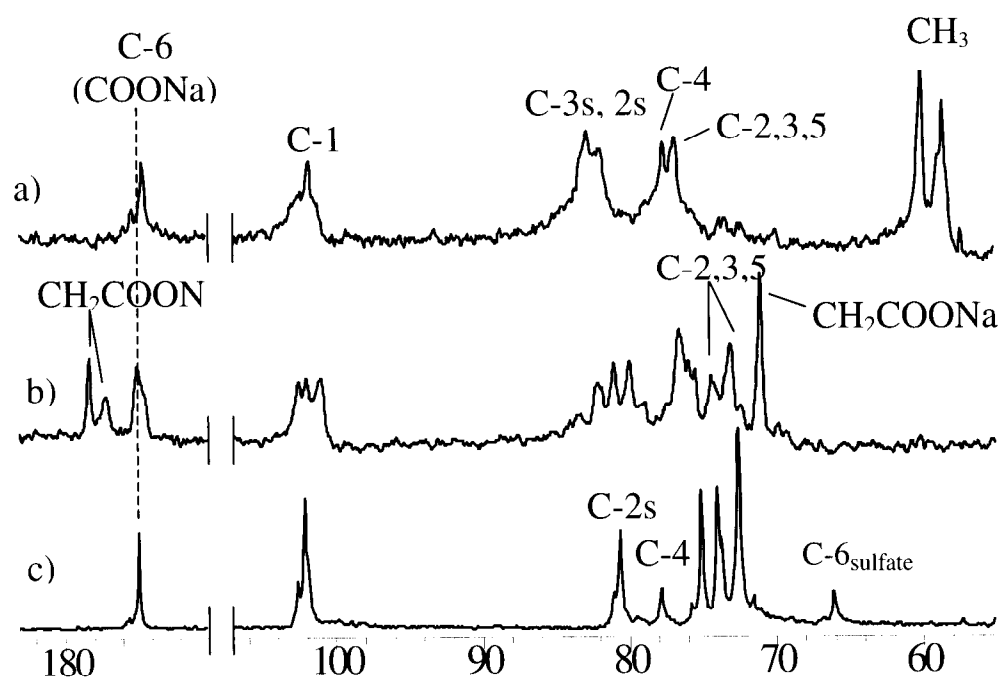


Figure 3. ¹³C-NMR spectra of a) 6-carboxy-2,3-*O*-methyl cellulose with degree of oxidation (DO) = 1.0 and degree of substitution (DS) = 1.8, b) 6-carboxy-2,3-*O*-carboxymethyl cellulose, DO = 1.0, DS = 1.2 and c) 6-carboxy-cellulose sulfate, DO = 0.8 and DS = 0.4 (partially sulfated at position 6)

Conclusions

The synthesis paths studied represent interesting routes to new polymers based on cellulose. The products obtained by a protecting group technique and a selective oxidation possess a very uniform distribution of the functional groups. The molecular structure was evaluated in detail by means of ^{13}C -NMR spectroscopy. The properties of the new polymers (behavior in solution, interaction with cations, gel and simplex formation) are under investigation.

References

- [1] Klemm, D.; Stein, A.; Heinze, T.; Philipp, B.; Wagenknecht, W. *Polymeric Materials Encyclopedia: Synthesis, Properties and Applications*, ed. Salamone, J.C., CRC Press, Inc.: Boca Raton, USA, 1996, 1043.
- [2] Heinze, T. *Macromol. Chem. Phys.* **1998**, *199*, 2341.
- [3] Camacho Gomez, J.A.; Eler, U.; Klemm, D. *Macromol. Chem. Phys.* **1996**, *197*, 953.
- [4] Harkness, B.R.; Gray, D.G. *Macromolecules* **1991**, *24*, 173.
- [5] Harkness, B.R.; Gray, D.G. *Macromolecules* **1991**, *24*, 1800.
- [6] Kondo, T.; Gray, D.G. *Carbohydr. Res.* **1991**, *220*, 173.
- [7] Heinze, T.; Röttig, K.; Nehls, I. *Macromol. Rapid Commun.* **1994**, *15*, 311.
- [8] Klemm, D.; Stein, A. *J. Macromol. Sci.-Pure Appl. Chem.* **1995**, *A32*, 899.
- [9] Koschella, A.; Klemm, D. *Macromol. Symp.* **1997**, *120*, 115.
- [10] Stein, A.; Klemm, D. *Papier* **1989**, *43*, 653.
- [11] Heinze, U.; Heinze, T.; Klemm, D. *Macromol. Chem. Phys.* **1999**, *200*, 896.
- [12] de Nooy, A.E.J.; Besemer, A.C., van Bekkum, H. *Recl. Trav. Chim. Pays-Bas* **1994**, *113*, 165.
- [13] de Nooy, A.E.J.; Besemer, A.C., van Bekkum, H. *Carbohydr. Res.* **1995**, *269*, 89.
- [14] Isogai, A.; Kato, Y. *Cellulose* **1998**; *5*, 153.
- [15] Vieira, M.; Liebert, T.; Heinze, T. *Proceedings, Cellucon'98 conference "Pulp and Papermaking—Fiber and Surface Properties and of other aspects of cellulose technology"*, Turku/Abo, Finland, in press.

NEW WATER SOLUBLE POLYSACCHARIDE CROSSLINKERS: SYNTHESIS, VISCOMETRIC STUDIES ABOUT THE CROSSLINKING REACTION AND CHARACTERIZATION OF CROSSLINKED PRODUCTS

B. Heublein,^a G. Kühne,^a U. Heinze,^b T. Heinze,^a D. Klemm,^a

A. Nechwatal,^b M. Nicolai,^b K.-P. Mieß ^b

^a Institute of Organic Chemistry and Macromolecular Chemistry, Friedrich Schiller University of Jena, Humboldtstrasse 10, D-07743 Jena, Germany

^b TITK e.V., Breitscheidstrasse 97, D-07407 Rudolstadt-Schwarza, Germany

The synthesis of new crosslinking agents based on divinyl sulfone is described. The crosslinking efficiency was determined by rheological measurements starting from aqueous solutions of hydroxyethyl cellulose. Moreover, the new agents can be used to

reduce the fibrillability of Lyocell fibers as a result of the crosslinking reaction.

Keywords: divinyl sulfone derivatives, crosslinking, rheology, Lyocell fibers

Introduction

Besides its growing impact on the chemical fiber market, the amine oxide process, employing a melt of *N*-methyl-morpholine-*N*-oxide (NMMNO) as solvent for cellulose, is both a stimulus to research in cellulose structure formation from solution and a catalyst in getting people from fundamental and applied research together for joint effort [1]. It is well known that cellulosic fibers of the „Lyocell“ type, *i.e.*, fibers spun from cellulose-NMMNO solutions, are provided with extraordinary clothing-physiological properties. However, they may possess a high wet fibrillation tendency which is undesired for textiles with good wash and wear properties [2].

There are different approaches for reducing the fibrillation tendency. On one hand, the variation in the spinning technology and, on the other, chemical modifications of the cellulosic fibers by crosslinking may be appropriate to improve the fiber quality. Crosslinking agents reinforce among other things the linkage between the crystalline ranges and hence the dimensional stability, which can result in a reduced wet abrasion tendency. Numerous crosslinking

agents, as for instance triacryloyl-hexahydro-1,3,5-triazine and *N,N'*-methylene-bisacrylamide, have been used [3]. Moreover, polyfunctional reactive dyestuff can also influence the fibrillability of NMMNO fibers [4, 5].

In our studies water soluble precursors of divinyl sulfone (DVS) derivatives with various spacers between the reactive vinyl moieties were synthesized and the influence of the molecular structure of these crosslinkers on the wet abrasion tendency of the treated cellulose fibers using wet abrasion number was investigated [6]. For characterization of the crosslinking efficiency, hydroxyethyl cellulose (HEC) was used as a model compound and the crosslinking reaction was evaluated by means of small-amplitude oscillatory measurements [7].

Materials and methods

Syntheses of the crosslinkers [8]. 1,6-bis(2-hydroxyethyl sulfanyl)-hexane (typical example for preparation of a crosslinker with aliphatic spacer groups). A solution of 0.5 mol of 2-mercaptoethanol and 0.25 mol of 1,6-bis-bromohexane in 50 ml ethanol was refluxed

under inert conditions, and 0.5 mol of KOH in 200 ml ethanol/water (50:1) was added within one hour. After two hours reaction time with stirring and cooling down to room temperature, the potassium bromide was filtered off, the filtrate was concentrated, washed with chloroform and dried over sodium sulfate. Yield: 74%, Fp = 102-105 °C. ¹H-NMR (DMSO-d₆): δ 3.8-3.2 (hydroxyethyl), 3.1-1.4 (hexane).

1,2-bis(2-hydroxyethylsulfanyl)-benzene ("aromatic crosslinker"). To a stirred solution of 0.038 mol of benzene-1,2-dithiol in 25 ml of aqueous NaOH (10%, w/v) 0.078 mol of 2-chloroethanol was added and stirred under reflux for 3 h. After cooling to room temperature, 15 ml of acetic acid ethylester was added, the organic phase was separated and concentrated under vacuum. Fp = 84-86 °C. ¹H-NMR (DMSO-d₆): δ 7.4-7.2 (aromatics), 4.98-3.0 (hydroxyethyl). For details of the synthesis procedure see ref. [6].

The oxidation of sulfanyl functions to sulfonyl groups with H₂O₂ and the sulfation of the hydroxyl groups with SO₃-DMF complex was carried out as described in ref. [7] yielding the corresponding disodium bissulfatoethyl sulfonyl derivatives.

Rheological measurements. To a solution of divinyl sulfone derivatives (4×10^{-5} mol/2 ml), dissolved in water at 50 °C for 30 minutes under stirring, 1.5×10^{-4} mol of hydroxyethyl cellulose (HEC; medium viscous) was added and cooled to room temperature. After addition of 0.16 ml of 10% (w/v) aqueous sodium hydroxide, the solution was transferred to the cone-plate system of the rheometer.

The crosslinking reaction of hydroxyethyl cellulose with an appropriate divinyl sulfone derivative under alkaline conditions at 25 °C was monitored by determination the storage (G') and the loss (G'') modulus as well as the complex viscosity (η^*) at a fixed frequency of 2.15 Hz and a deformation of 0.02 as a function of time. The reaction time was monitored from lye addition for 30 minutes.

An accurate temperature control (within ± 0.1 °C) was achieved with a Haake F6-C25 thermostat. A Haake controlled-stress rheometer (Rheo Stress 150) with air bearing was used to perform small-amplitude oscillatory measurements, using a cone-plate geometry (C60/1 Ti).

The reaction of the crosslinkers with Lyocell fibers according to the Foulard procedure (so-called Kalt-Klotz-Verweil-Verfahren) and the characterization of the obtained fibers by loop, elongation and tenacity strength were carried out as described in detail in ref. [9,10] and according to standard methods (DIN 53816). The wet abrasion number z_n was determined by stressing the fiber on a rotating hollow shaft until the fiber breaks.

The ¹H and ¹³C NMR spectra of synthesized crosslinkers were recorded on AC 200 and WP 200 SY spectrometers (Bruker).

The sulfur content of the fibers was determined by an elemental analyzer CHNS-936 (LECO).

Results and discussion

Lyocell fibers are characterized by extraordinary textile properties but also by a special fibrillation propensity caused by reduced cohesion of the fibrils in the water swollen state. It is known that the crease recovery and wash and wear properties of cellulose fibers and fabrics can be improved by crosslinking with divinyl sulfone [11, 12].

Synthesis of new crosslinkers containing divinyl sulfone moieties. As shown in Figure 1, in our study new water soluble precursors of divinyl sulfone derivatives with aliphatic (-CH₂-, -C₂H₄-, -C₆H₁₂-) and aromatic (*ortho*- and *meta*-substituted) spacers were synthesized. For improving the water solubility, the precursors were converted into the corresponding disodium bissulfatoethylsulfonyl derivatives (Table 1).

Addition of alkali to an aqueous solution of the disodium bissulfatoethyl sulfonyl derivatives leads to the formation of vinyl sulfone groups which react according to the well known Michael addition with activated hydroxyl functions of cellulose, *e.g.*, forming stable crosslinks (see Figure 2).

By means of rheological measurements using hydroxyethyl cellulose as a water-soluble polymer it was revealed that the change of the elastic and viscous behavior may be used to evaluate the crosslinking efficiency of the new vinyl sulfone derivatives. A typical curve for a gel-like polymer established by crosslinking of hydroxyethyl cellulose with compound **I**, **II** or

III demonstrating the evolution of the storage modulus (G') and the loss modulus (G'') at constant frequency as a function of time is shown in Figure 3. The beginning of the crosslinking process is dominated by a viscous behavior of the system ($G'' > G'$). After a short reaction time (80 s in case of derivative **II**) the elastic behavior dominates ($G' \gg G''$). Both moduli increase as a result of the growing junction zones density. However, the increase of the storage modulus is

more sharp. Moreover, the slope of G' in dependence on the reaction time is much higher for aliphatic spacer groups of the DVS derivatives with increasing chain length, *i.e.*, hexyl > ethyl > methyl. Within a reaction time of up to 30 minutes, the values of G' have a great variation covering about two orders of magnitude, whereas that of G'' was distinctly lower than one order.

Table 1. Characterization of divinyl sulfone derivatives with various spacers (X-CH₂-CH₂-SO₂-(spacer)-SO₂-CH₂-CH₂-X).

| No. Spacer | X = OH m. p. (°C) | X = SO ₃ Na | | -SO ₂ CH=CH ₂ | |
|---------------------------------------------------|----------------------|------------------------|-----------------|-------------------------------------|-----------------------|
| | | MW (g/mol) | WS ^a | MW (g/mol) | distance ^b |
| I CH ₂ | 83 | 436 | ++ | 196 | C(1)...C(7) 0.615 |
| II (CH ₂) ₂ | 114-115 | 450 | + | 210 | C(1)...C(8) 0.681 |
| III (CH ₂) ₆ | 102-105 | 506 | ++ | 226 | C(1)...C(12) 1.025 |
| IV <i>o</i> -C ₆ H ₅ | 106-108 | 498 | ++ | 258 | C(1)...C(8) 0.672 |
| V <i>m</i> -C ₆ H ₅ | 108-110 | 498 | ++ | 258 | C(1)...C(9) 0.849 |

^a Water solubility: soluble in + hot and ++ cold water

^b Distance in nm between the divinyl sulfone moieties calculated by *Cosmos* [13]; divinyl sulfone C(1)...C(5), 0.373 nm

In contrast to these findings, in case of DVS derivatives with aromatic spacer groups (**IV** and **V**, Table 1) a significantly steeper rise of the storage modulus can be observed (Figure 4). Besides this, no G' - G'' cross-over is measurable because of an extremely fast crosslinking reaction as compared to the samples described above. That means that the very short period of viscous behavior is due to the described preparation conditions and cannot be detected further by oscillatory measurements. After a rapid increase of G' up to about 300 Pas the storage modulus keeps increasing slightly. It can be assumed that mainly within 150 s the formation of crosslinks takes place. In dependence on a drop of accessibility of reaction sites of HEC the crosslinking with the aromatic divinyl sulfone derivatives occurs then significantly slower. The graphical course of the complex viscosity (η^*) is similar to that of G' (Figure 5). This result can be traced back to the significant differences of G' and G'' values ($G' \gg G''$). Because of that, the complex viscosity ($\eta^* = G'^2 + G''^2/\omega^{1/2}$) is predominantly influenced by elastic behavior of the crosslinked polymers.

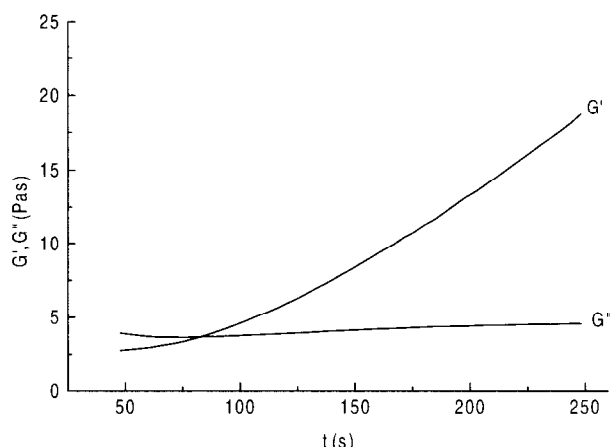


Figure 3. Storage (G') and loss (G'') moduli of hydroxyethyl cellulose crosslinked with disodium bisulfatoethylsulfonyl derivative (ethyl-spacer group) as a function of time.

However, no significant deviation in the crosslinking efficiency between the two DVS derivatives with aromatic spacer groups could be observed. The elastic behavior is independent of the position of the vinyl sulfone groups within the aromatic ring (ortho or meta).

The reaction of the crosslinkers with Lyocell fibers using the Foulard procedure leads to fibers of a reduced fibrillability as indicated by a high wet abrasion number (z_n). Besides this reduction of fibrillability, other fiber properties like tenacity, loop and elongation strength decrease in

dependence on the concentration of DVS. The textile-physical parameters of Lyocell fibers crosslinked with DVS and with different bissulfatoethyl sulfonyl derivatives are summarized in Table 2. It is worth to mention that the crosslinkers with aromatic spacer groups exert a slightly stronger influence onto z_n than aliphatic ones. In comparison to the very significant differences in elastic behavior of HEC crosslinked starting from a homogeneous solution, the results of crosslinking Lyocell fibers under heterogeneous conditions indicate that the degree of crosslinking depends, besides structural and solubility reasons, also on the affinity of the crosslinking agent to the fibers.

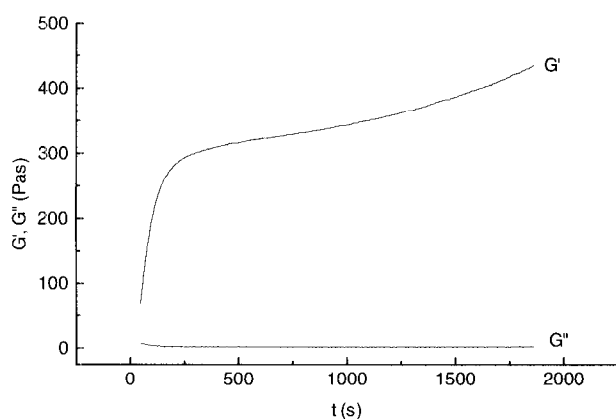


Figure 4. Storage (G') and loss (G'') moduli of hydroxyethyl cellulose crosslinked with disodium bissulfatoethyl sulfonyl derivative with a *m*-phenylene spacer group in dependence on crosslinking time.

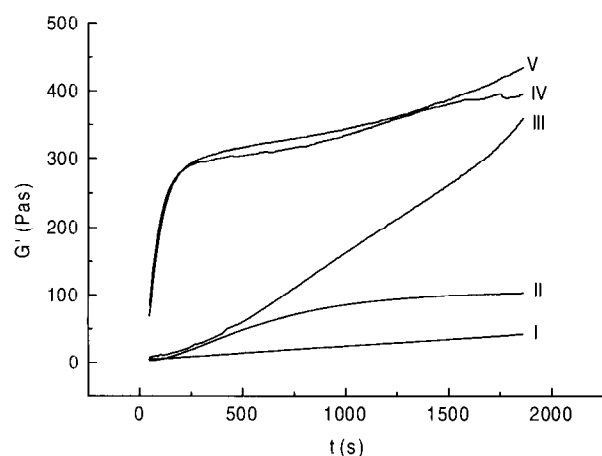


Figure 5. Storage modulus (G') of hydroxyethyl cellulose crosslinked with divinyl sulfone derivatives I-V (see Table 1) as a function of reaction time.

Table 2. Fiber parameters of Lyocell crosslinked with divinyl sulfone (DVS) and different bissulfatoethyl sulfonyl derivatives (crosslinker 20 g/l; 2 ml 4 % (w/v) aq. NaOH; 40 g/l Na_2SO_4 ; duration time 18 h at 22 °C).

| Cross-linker | Wet abrasion no. z_n | Tensile strength (cN/tex) | Loop strength (cN/tex) | Elong. strength (%) |
|------------------|------------------------|---------------------------|------------------------|---------------------|
| w/o | 20-40 | 36-40 | 14 | 12-14 |
| DVS ^a | 408 | 35.1 | 10.6 | 10.0 |
| I | 107 | 35.2 | 10.7 | 11.6 |
| II | 159 | 37.7 | 13.1 | 14.2 |
| III | 84 | 35.8 | 12.4 | 12.3 |
| IV | 240 | 34.1 | 11.5 | 10.5 |
| (1,2) | | | | |
| V (1,3) | > 386 | 31.1 | 8.7 | 9.2 |

^a Concentration 10 g/l

Conclusions

New water soluble disodium bissulfatoethylsulfonyl derivatives with aliphatic ($-\text{CH}_2-$, $-\text{C}_2\text{H}_4-$, $-\text{C}_6\text{H}_{12}-$) and aromatic (*ortho*- and *meta*-substituted) spacers were synthesized which crosslink hydroxyl groups containing polymers (*e.g.*, hydroxyethyl cellulose and cellulose fibers) under alkaline conditions *via* formation of the corresponding reactive divinyl sulfone derivatives. The influence of the molecular structure of the crosslinker on the efficiency of crosslinking reaction was investigated by means of small-amplitude oscillatory measurements. The slope of storage modulus (G') of hydroxyethyl cellulose crosslinked with aliphatic disodium bissulfatoethylsulfonyl derivatives increased dependent on the chain length of the spacer (methyl < ethyl < hexyl). In case of aromatic spacer moieties a significant steeper rise of storage modulus and no $G'-G''$ cross-over can be observed. It is likely that this behavior is caused preferably by electronic factors, since only minor differences exist between aliphatic and aromatic spacer group distances.

The textile-physical properties of Lyocell fibers are improved by the treatment with the disodium bissulfatoethyl sulfonyl derivatives. The fibrillability is reduced while other fiber properties remain almost unchanged.

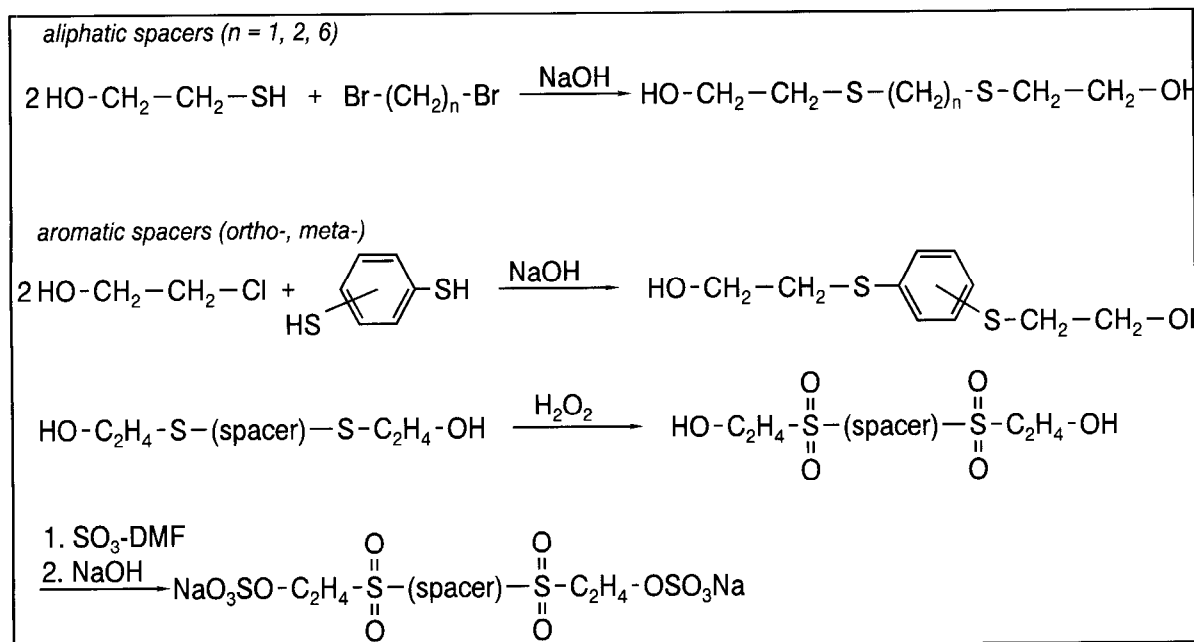


Figure 1. Synthesis of water soluble precursors of divinyl sulfone derivatives.

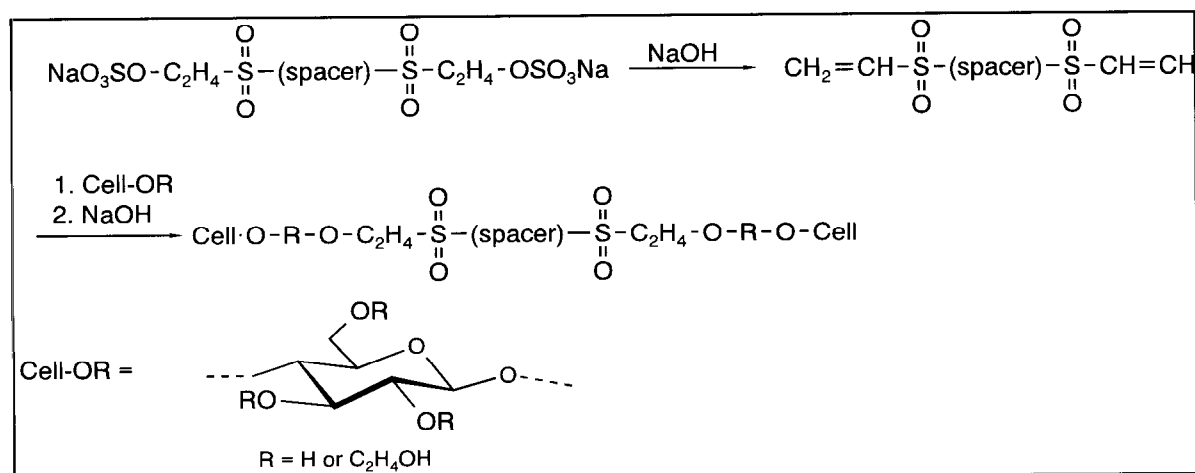


Figure 2. Reaction of vinyl sulfone derivatives with cellulose.

References

- [1] Couley, M.; Smith, S. *Lenzinger Ber.* **1996**, 75, 51.
- [2] Lyocell-Fasern-Faserstoff-Tabellen, acc. to P.A. Koch, *Melliand Textilber.* **1997**, 78, 575.
- [3] Valk, G.; Schliefer, K.; Klippel, F. *Melliand Textilber.* **1970**, 51(6), 714.
- [4] Nicolai, M.; Nechwatal, A.; Mieck, K.P. *Text. Res. J.* **1996**, 66, 191.
- [5] Bredereck, K.; Schulz, F.; Ottenbach, A. *Melliand Textilber.* **1997**, 78, 703.
- [6] Nicolai, M.; Nechwatal, A.; Mieck, K.P. *Angew. Makromol. Chem.* **1998**, 256, 21.
- [7] a) Oppermann, W. *Das Papier* **1995**, 49, 765.
- b) Anbergen, U.; Oppermann, W. *Polymer* **1990**, 31, 1854.
- [8] Nicolai, M.; Nechwatal, A.; Mieck, K.P.; Heublein, B.; Kühne, G.; Klemm, D. *Angew. Makromol. Chem.*, in press.
- [9] Lutringer, J.P.; Trikas, A. *Textilveredlung* **1990**, 25, 311.
- [10] Mieck, K.P.; Nicolai, M.; Nechwatal, A. *Chem. Fibres Int.* **1995**, 45, 44.
- [11] a) Farbwerke Hoechst, DAS 1080261. b) US Rubber Co., A. Pat. 252 4399. c) Amer. Visc. Corp., A. Pat. 2753388.
- [12] Rowland, S. P.; Braunan, M. A. F. *J. Appl. Polym. Sci.* **1990**, 14, 1854.
- [13] Sternberg, U. Computer-Simulation von Molekülspektren "COSMOS", Friedrich Schiller University of Jena.

DETERMINATION OF LIGNIN DEGRADATION COMPOUNDS IN DIFFERENT WOOD DIGESTION SOLUTIONS BY CAPILLARY ELECTROPHORESIS

T. Javor,^a W. Buchberger,^a I. Tancos^b

^aDepartment of Analytical Chemistry, Johannes-Kepler-University Linz
Altenbergerstrasse 69, A-4040 Linz, Austria

^bInstitute of Chemical Technology of Organic Materials, Johannes-Kepler-University Linz
A-4040 Linz, Austria

This work presents the investigation of various capillary electrophoretic techniques for the separation of low-molecular-weight phenolic and neutral lignin degradation products. A successful CE mode was micellar electrokinetic chromatography (MEKC) with carrier electrolytes containing micelle-forming reagents, such as sodium dodecylsulfate. Important phenolic and neutral lignin degradation compounds could be separated by MEKC after acidification of the liquors and extraction of the compounds with dichloromethane. The influence of electrolyte composition, pH, amount of organic solvent, temperature and voltage have been investigated to determine the best

separation conditions. In addition, microemulsion electrokinetic chromatography (MEEKC) was investigated as an alternative to MEKC. It is a CE technique in which analytes interact with moving oil droplets present in a microemulsion electrolyte system. Both MEKC and MEEKC allowed the investigation of different wood digestion procedures and differences in lignin degradation products from different kinds of wood (eucalyptus, beech, scotch pine and acacia).

Keywords: capillary electrophoresis; lignin degradation; wood digestion

Introduction

During the production of paper from wood, lignin is undesirable in the final product due to color, hydrophobicity, and poor mechanical properties. Therefore, lignin has to be removed in the process of wood digestion without degrading the cellulosic structure. There are different methods in use for degrading the lignin polymer: the kraft process (digestion solution: NaOH and NaS), the sulfite process (digestion solution: acidic sulfite), the soda process (digestion solution: NaOH), the quatum process [1] (digestion solution: tetramethylammonium hydroxide), and some others.

The degradation of lignin during the pulping process leads to various monomeric phenolic compounds as well as to a range of neutral products. In the pulping process, lignin is simply a waste product. On the other hand, lignin and its

degradation products may be a potential source for raw materials in the chemical industry. For this reason, the availability of modern and efficient analytical methods for lignin digestion solutions is of major importance. Data obtained from such analytical work would also contribute to clarifying reaction mechanisms of different digestion procedures.

The analysis of wood digestion solutions is a challenging task due to the complexity of the sample. Recently, some investigations have been reported to employ capillary electrophoresis (CE) for this purpose [2-4], but these investigations have not yet included all of the lignin degradation products eventually important in real samples. Therefore, further development of CE methods seems necessary.

Among different CE techniques available, micellar electrokinetic capillary chromatography (MEKC) is nowadays the preferred method for

simultaneous separation of mixtures of charged and uncharged solutes [5-7]. It is a CE technique which uses a micellar solution as the carrier electrolyte. MEKC allows the separation of electrically neutral analytes because it is not only based on electrophoretic principles, but also on chromatographic interactions with a micellar pseudostationary phase. Sodium dodecylsulfate (SDS) and various other surfactants can be employed as micelle-forming agents.

Alternatively, microemulsion electrokinetic chromatography (MEEKC) has recently become an interesting approach to the separation of neutral analytes. This CE technique is based on microemulsions used as pseudostationary phase in the carrier electrolyte, for a review see [8,9].

The aim of the present work was the development of MEKC and MEEKC methods for the characterization of different wood digestion procedures (including the use of different kinds of wood).

Experimental

A HP^{3D} CE instrument in combination with a diode array detector was used for capillary electrophoretic investigations. The separations were carried out in fused silica capillaries with a total length of 64.5 cm, a length of 56 cm to the detector and an inner diameter of 50 μm . To improve sensitivity, "bubble cell" capillaries were employed. Injection was done in the hydrodynamic mode.

Carrier electrolytes for MEKC consisted of 20mM sodium tetraborate buffer containing 10-50mM sodium dodecylsulfate (SDS) and 0-20vol.% methanol and were adjusted to a pH of 7.5-10.5 with 0.1 N H₃PO₄ or 0.1 N NaOH.

Microemulsions were prepared according to the method of Terabe *et al.* [10] by mixing a microemulsion-forming organic solvent such as n-hexane, cyclohexane, n-octane, n-heptane or 1-butylchloride (0.81 %, w/w), SDS (1.66 %, w/w), n-butanol (6.61 %, w/w) and 20 mM sodium tetraborate buffer (90.29 %, w/w). The pH was adjusted to 7.0 - 9.4.

Sample preparation was accomplished by delignification of different kinds of wood at 170°C with NaOH and/or tetramethylammonium hydroxide; the resulting liquors were acidified

and extracted with dichloromethane; the extracts were dried, re-dissolved in 0.1 N NaOH and filled up to a volume of 10 ml. The sample solutions were passed through 0.45 μm filters, diluted 1:10 with water and injected into the CE instrument without further pretreatment. Standards were prepared in water / 0.1 N NaOH (v/v=98:2).

Results and discussion

In the present work, the separation was optimized for 15 analytes listed in Table 1. These compounds were considered to be significant model substances for lignin degradation products.

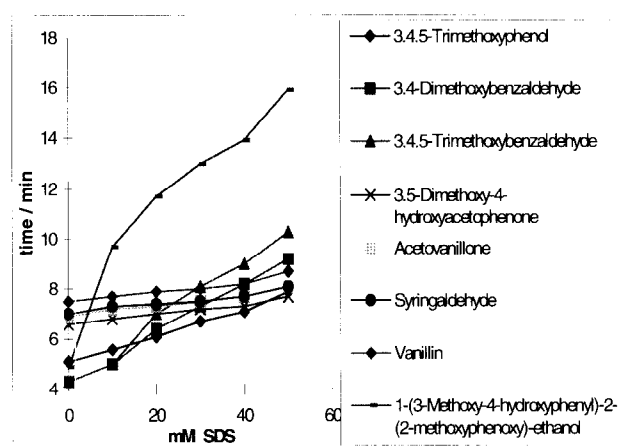
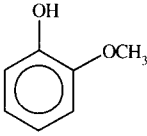
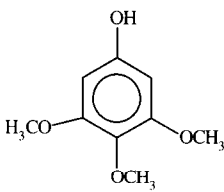
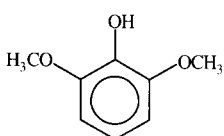
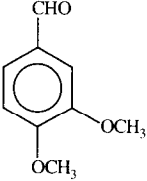
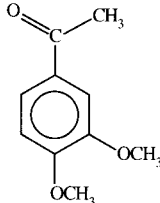
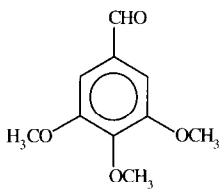
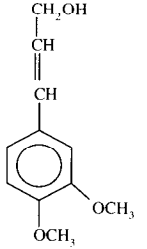
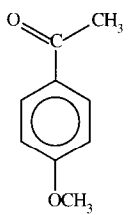
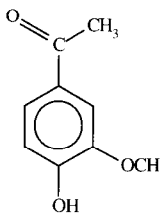
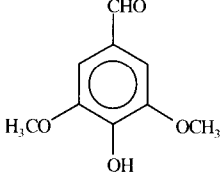
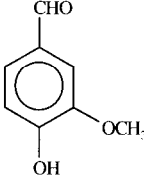

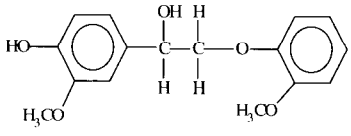
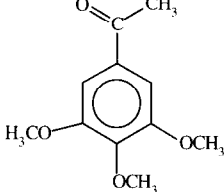
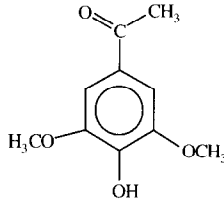


Figure 1. Influence of the SDS concentration in the carrier electrolyte on migration times. Carrier electrolyte: 20 mM sodium tetraborate / SDS (0-50 mM), pH 9.4.

Optimization of separation selectivity in MEKC is possible by variation of type and concentration of the micelle-forming surfactant in the carrier electrolyte and by addition of organic solvents. Within this work, mixtures of 20 mM sodium tetraborate containing varying amounts of SDS (10-50 mM) and methanol (0-20 % v/v) were employed, see Figure 1.

The most favourable results were obtained at a concentration of 50 mM of SDS (higher concentrations were not used to avoid excessively high currents). A fine-tuning of the separation selectivity is possible by addition of organic modifiers to the carrier electrolyte, although this may result in longer analysis times due to the reduction of the electroosmotic flow (Figure 2).

Table 1. Lignin degradation products investigated within this work.

| | | |
|-------------------------------------------------------------------------------------|-------------------------------------------------------------------------------------|---------------------------------------------------------------------------------------|
|  |  |  |
| 2-Methoxyphenol | 3,4,5-Trimethoxyphenol | 2,6-Dimethoxyphenol |
|  |  |  |
| 3,4-Dimethoxybenzaldehyde | 3,4-Dimethoxyacetophenone | 3,4,5-Trimethoxybenzaldehyde |
|  |  |  |
| 3-(3,4-Dimethoxyphenyl)-2-propen-1-ol | 4-Methoxyacetophenone | 4-Hydroxy-3-methoxyacetophenone (Acetovanillone) |
|  |  |  |
| 3,5-Dimethoxy-4-hydroxybenzaldehyde (Syringaldehyde) | 4-Hydroxy-3-methoxybenzaldehyde (Vanillin) | 4-Hydroxybenzaldehyde |
|  |  |  |
| 1-(3-Methoxy-4-hydroxyphenyl)-2-(2-methoxyphenoxy)ethanol | 3,4,5-Trimethoxyacetophenone | 3,5-Dimethoxy-4-hydroxyacetophenone |

Best overall resolution of all analytes could be achieved with a carrier electrolyte consisting of a mixture of 20 % (v/v) methanol and 80 % (v/v) 20 mM borate / 50 mM SDS. The signal was linear in a range from 2-70 mg/l, with a detection limit of 0.29-0.60 mg/l.

Unfortunately, under these conditions 3,4,5-trimethoxyphenol and 2-methoxyphenol

comigrate. Therefore, samples containing this two analytes have to be run a second time in a carrier electrolyte of 20 mM sodium tetraborate / 50 mM SDS without methanol which allows a sufficient separation of 3,4,5-trimethoxyphenol and 2-methoxyphenol (although the other analytes are poorly resolved). A typical separation of a standard mixture is shown in

Figure 3. The optimized separation system allowed the analysis of solutions obtained from different wood digestion procedures (soda and quatam) and the investigation of differences in the pattern of lignin degradation products during use of different kinds of wood (eucalyptus, beech, scotch pine and acacia). Typical MEKC electropherograms of degradation products of lignin in acacia and scotch pine with 1.2 M TMAH as digestion medium are shown in Fig. 4.

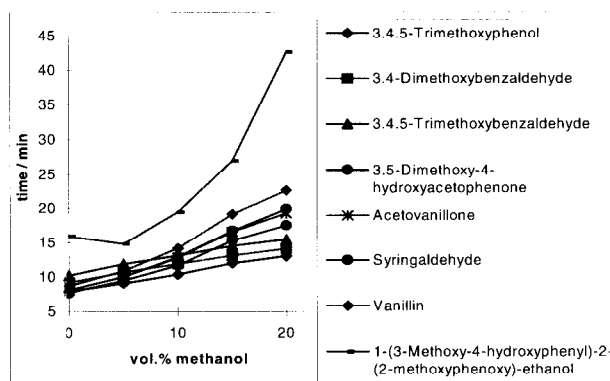


Figure 2. Effect of organic modifier in the carrier electrolyte on migration times. Carrier electrolyte: 20 mM sodium tetraborate containing 50 mM SDS (pH 9.4) / MeOH (0-20 % v/v).

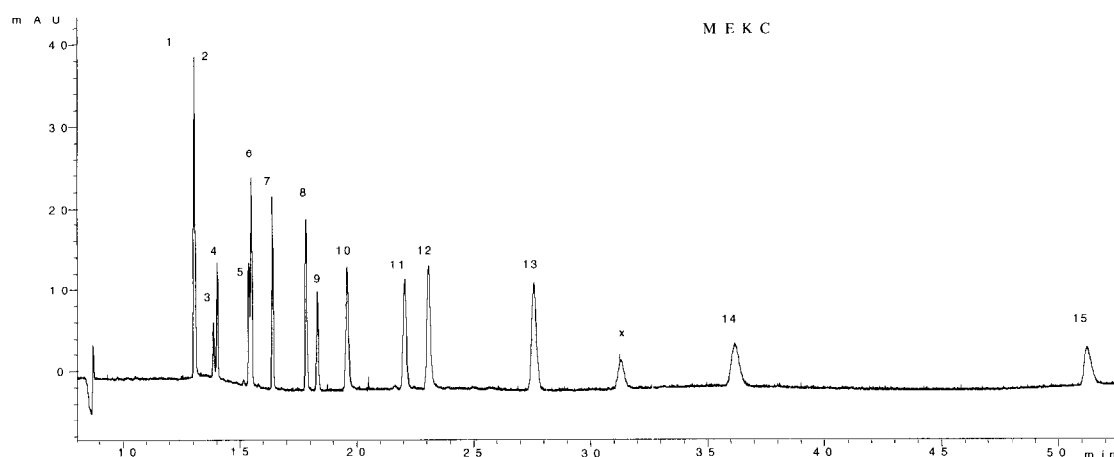


Figure 3. MEKC separation of lignin degradation products under optimized conditions. Carrier electrolyte: 20 mM sodium tetraborate containing 50 mM SDS (pH 9.4) / MeOH (80:20 v/v); UV detection at 214 nm; voltage: +30 kV; temperature: 20°C; injection: 10 s, 35 mbar. Peaks: 1=2-methoxyphenol, 2=3,4,5-trimethoxyphenol, 3=2,6-dimethoxyphenol, 4=3,4-dimethoxybenzaldehyde, 5=3,4-dimethoxyacetophenone, 6=3,4,5-trimethoxybenzaldehyde, 7=3,4,5-trimethoxyacetophenone, 8=3-(3,4-dimethoxyphenyl)-2-propen-1-ol, 9=4-methoxyacetophenone, 10=3,5-dimethoxy-4-hydroxyacetophenone, 11=acetovanillone, 12=syringaldehyde, 13=vanillin, x=impurity, 14=4-hydroxybenzaldehyde, 15=1-(3-methoxy-4-hydroxyphenyl)-2-(2-methoxyphenoxy)-ethanol.

From the data in Table 2 it can be seen that different kinds of wood have different ratios of S (syringyl type) and G (guaiacyl type) compounds. Besides, 4-hydroxybenzaldehyde was found only in the acacia sample but not in the beach or eucalyptus sample.

The aim of this work was not only to compare the different kinds of wood but also to analyze solutions from different digestion procedures. Figure 5 shows once again an acacia sample, but this time digested in 1.2 M NaOH. A comparison with Figure 4 demonstrates minor differences in the concentrations of the degradation products.

Besides MEKC, MEEKC can be widely applied to a range of compounds with varying charge and hydrophobicity including neutral compounds.

Therefore, it appeared interesting to do a direct comparison of this technique with MEKC.

Composition of the background electrolytes for MEEKC was the same in all cases within the present work (i.e., 0.81 % (w/w) organic modifier, 1.66 % (w/w) SDS, 6.61 % (w/w) n-butanol and 90.29 % (w/w) 20 mM sodium tetraborate) and differed only in the nature of the organic modifier. n-Heptane, n-hexane, n-octane, cyclohexane and 1-butylchloride were investigated as the microemulsion-forming solvents. The most critical pair of analytes in the MEEKC separation was acetovanillone and syringaldehyde which comigrated in all of the carrier electrolytes mentioned above. Emulsions with n-hexane and n-octane turned out to be less stable, so that they were excluded from

additional investigations. n-Heptane looked most promising for further optimization with respect to the pH; a complete separation of all analytes was

finally achieved by adjusting the borate electrolyte to pH 9.2. The separation under optimized conditions is shown in Figure 6.

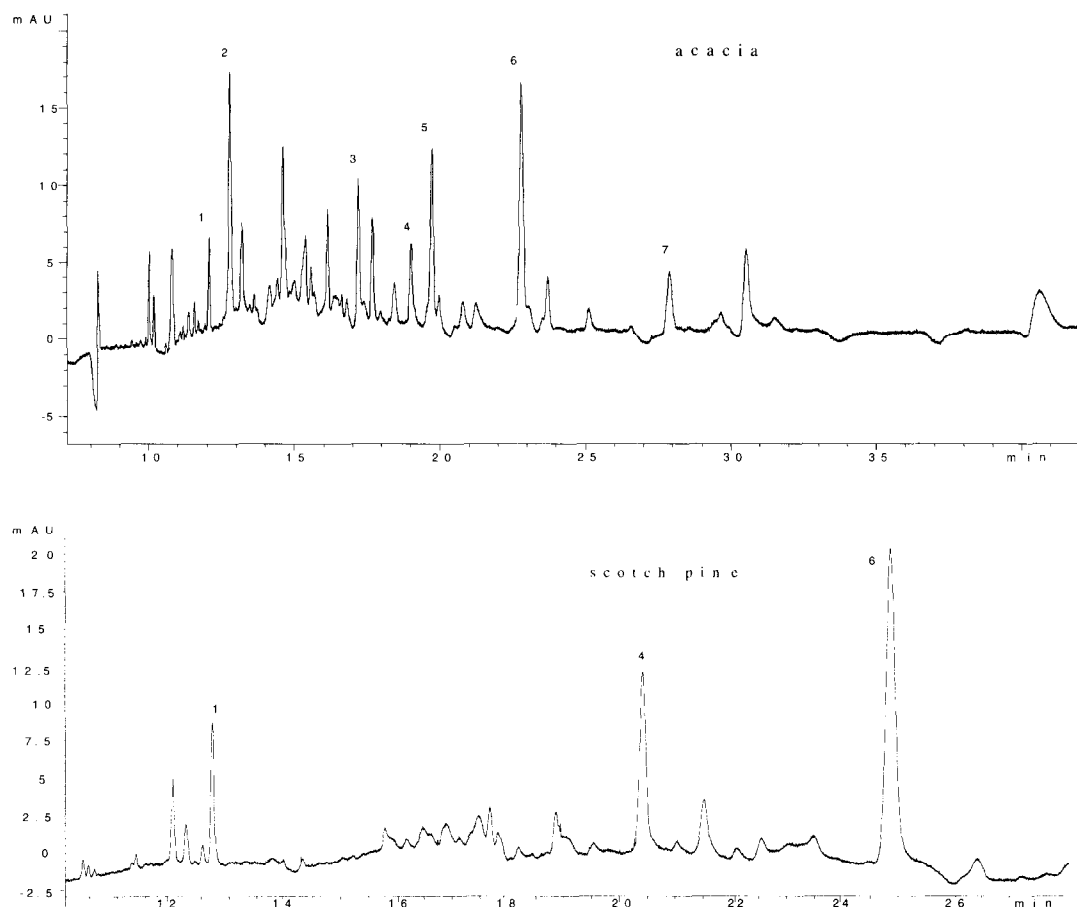


Figure 4. MEKC electropherograms of lignin digestion solutions from different kinds of wood. Carrier electrolyte: 20 mM sodium tetraborate - 50 mM SDS / methanol (80:20 v/v); UV detection at 214 nm; voltage: +30 kV; temperature: 20°C; injection: 10 s, 35 mbar. Peaks: 1=2-methoxyphenol, 2=2,6-dimethoxyphenol, 3=3,5-dimethoxy-4-hydroxyacetophenone, 4=acetovanillone, 5=syringaldehyde, 6= vanillin, 7=4-hydroxybenzaldehyde.

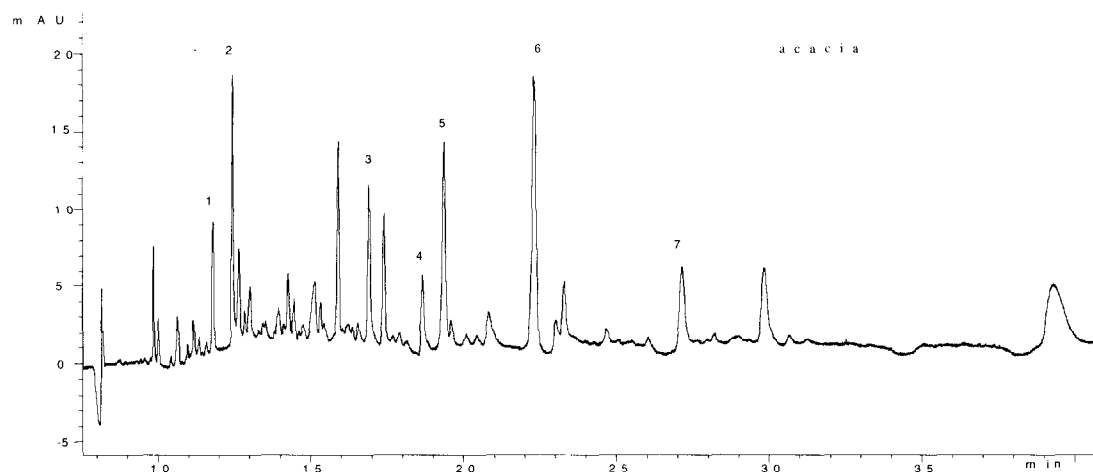


Figure 5. MEKC electropherogram of reaction products of lignin in acacia (digestion solution 1.2 M NaOH). Carrier electrolyte: 20 mM sodium tetraborate - 50 mM SDS / methanol (80:20 v/v); UV detection at 214 nm; voltage: +30 kV; temperature: 20°C; injection: 10 s, 35 mbar. Peaks: 1=2-methoxyphenol, 2=2,6-dimethoxyphenol, 3=3,5-dimethoxy-4-hydroxyacetophenone, 4=acetovanillone, 5=syringaldehyde, 6=vanillin, 7=4-hydroxybenzaldehyde.

Table 2: Different ratios of S (syringyl type) and G (guaiacyl type) compounds in different kinds of wood.

| Type of wood | D / A ^a | S / V ^b | S / G ^c |
|--------------|--------------------|--------------------|--------------------|
| Beach | 4.60 | 1.62 | 2.30 |
| Eukalyptus | 4.53 | 2.40 | 3.05 |
| Acacia | 1.76 | 0.78 | 1.01 |
| Beach | 3.12 | 1.81 | 2.19 |
| Eukalyptus | 5.83 | 2.64 | 3.51 |
| Acacia | 2.01 | 0.84 | 1.17 |

^a 3,4-Dimethoxy-4-hydroxyacetophenone / acetovanillone

^b Syringaldehyde / vanillin

^c \sum Syringyltype / \sum Guaiacyltype

The migration order in MEKC and MEEKC is somewhat different as can be seen by comparison of Figures 3 and 6. An advantage of MEEKC was the fact that the separation could be carried within 15 min, whereas analysis times in MEKC were around 50 min.

Conclusions

It could be demonstrated that capillary electrophoresis with carrier electrolytes containing micelles or microemulsions as pseudostationary phases is well suited for establishing patterns of lignin degradation products. Such patterns are useful for characterisation of different digestion procedures and / or different types of wood. They also enable the estimation of the different ratios of S (syringyltype) and G (guaiacyltype) compounds. A comparison of the electropherograms from MEKC and MEEKC indicates that for the present application the MEEKC method yields superior results with respect to analysis time, separation efficiency and resolution. A drawback of MEEKC may be the somewhat limited stability of the microemulsion depending on the kind of organic solvent used.

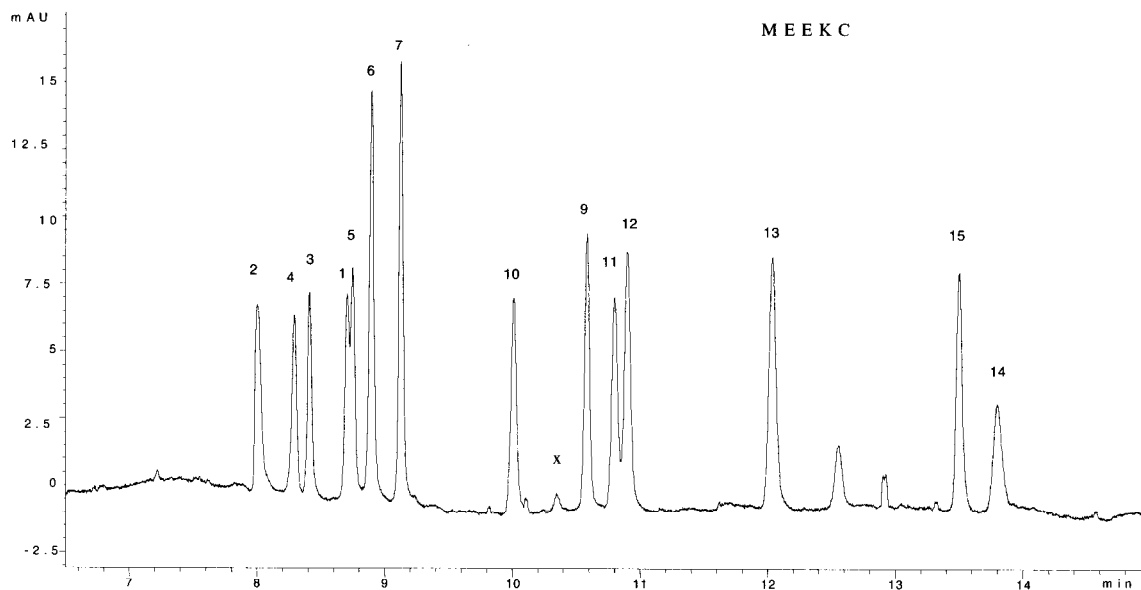


Figure 6. MEEKC separation of lignin degradation products under optimized conditions. Carrier electrolyte: 20 mM sodium tetraborate (90.92 % w/w) pH 9.2, 1.66 % (w/w) SDS, 0.91 % (w/w) n-heptane and 6.61 % (w/w) 1-butanol; UV detection at 214 nm; voltage: +30 kV; temperature: 20°C; injection: 3 s, 35 mbar. Peak assignment: see Figure 3.

References

- [1] Tanzcos, I.; Schmidt, H. *Patent* AT 403703 B, 1998.
- [2] Masselter, S.; Zeman, A.; Bobleter, O. *Chromatographia* **1995**, *40*, 51.
- [3] Volgger, D.; Zeman, A.; Bonn, G. *J. High Resol. Chromatogr.* **1998**, *21*, 3.
- [4] Maman, O.; Marseille, F.; Guillet, B.; Disnar, J.; Morin, P. *J. Chromatogr. A* **1996**, *755*, 89.
- [5] Terabe, S.; Otsuka, K.; Ando, T. *Anal. Chem.* **1985**, *57*, 834.
- [6] Terabe, S.; Otsuka, K.; Ichikawa, K.; Tsuchiya, A.; Ando, T. *Anal. Chem.* **1984**, *56*, 111.
- [7] Nishi, H.; Terabe, S. *J. Chromatogr. A* **1996**, *735*, 3.
- [8] Altria, K.D. *J. Chromatogr. A* **1999**, *844*, 371.
- [9] Altria, K.D. *Chromatographia* **1999**, *49*, 457.
- [10] Terabe, S.; Matsubara, N.; Ishihama, Y.; Okada, Y. *J. Chromatogr.* **1992**, *608*, 23.

NEW GLYCOSIDES OF LIGNIN

D. Joniak,^a M. Poláková,^a B. Košíková,^a V. Demianová^b

^a Institute of Chemistry, Slovak Academy of Sciences, 842 38 Bratislava, Slovakia

^b Faculty of Chemical Technology, Slovak Technical University, 812 37 Bratislava, Slovakia

New biodegradable surface active agents were prepared by glycosidation of prehydrolysis lignin with the D-glucose using anhydrous ferric chloride as the catalyst which afforded polymeric alkyl, benzyl and aryl glucoside derivatives of lignin. Moreover, a series of novel lignin-based surface active agents was obtained by subsequent oxidation of the primary alcohol groups of D-glucose

into carboxyl groups by 2,2,6,6-tetramethyl-1-piperidine oxoammonium ions with sodium hypochlorite and sodium bromide in an aqueous alkaline solution at pH 11.

Keywords: glycosylation, lignin-glucoside, lignin-glucosiduronic acid, surface tension

Introduction

Lignin sulfonate has long been used as surface-active agent. The application of other industrial lignins as surfactants requires modifications to improve their water solubilization. Lignin, co-product of a prehydrolysis stage of kraft beechwood pulping representing low molecular sulfur-free lignin, was found to be useful for the preparation of composite polypropylene films [1] and dispersing agents [2]. Surface active agents based on carbohydrates were first patented in 1930. Industrial applications were found mainly for sucrose and some alditol esters and owing to their higher water solubility ethoxy derivatives. [3]. Glycosidic type surfactants C₆-C₁₂-alkyl-β-D-glucopyranosides. have been prepared by the Koenigs-Knorr reaction [4].

Ferrieres [5] described O-glycosylation of long chain alcohols with totally unprotected neutral carbohydrates, performed in heterogenous media and promoted by anhydrous ferric chloride, which afforded alkyl D-glycosides in high yields. Application of this method for the synthesis of several alkyl, aryl and benzyl α-D-glucosides as well as their β-anomers was described in our previous paper [6].

The objective of the present paper is the preparation new biodegradable surface active agents by glycosidation of prehydrolysis lignin with D-glucose according to Ferries [5] and subsequent oxidation of the primary alcoholic group of D-glucose into carboxyl groups in the prepared lignin derivatives.

Materials and Methods

Lignin samples. The sulfur-free preparation of average molecular weight 1900 was obtained by fractionation of hardwood prehydrolysate (170° C). It contained 19.1 % OCH₃ and 0.15 % ash.

Glycosidation procedure. To a suspension of D-glucose (3.6 g) in dry 1,4-dioxane (50 mL) at room temperature were added 3 g of appropriate lignin and, by small portions (9.72 g) of anhydrous FeCl₃. After 24 h at room temperature and removal of the solvent, the residue was partitioned between n-butanol and 5 % aqueous HCl. The organic layer was washed with acidic water solution, and the aqueous layers thus obtained were extracted with n-butanol (3x20 mL). The combined organic extracts were concentrated under reduced pressure.

Oxidation procedure. The lignin sample after glycosidation (1 g) was suspended in 200 mL of water containing 2,2,6,6-tetramethyl-1-piperidine

oxoammonium salt (50 mg), 1.6 g of sodium bromide and 95 ml of 5.0% (w/v) sodium hypochlorite solution and stirred for 2 h. The pH was adjusted to 10-11 and kept constant with 0.5 M NaOH. The majority of the reaction was conducted at $0^\circ \pm 2^\circ \text{C}$. When the oxidation was finished (about 2 h), the reaction was quenched by adding 96% EtOH (10 mL), followed by neutralization with 4 M HCl. The oxidized glucose derivative of lignin was isolated by dialysis and subsequently lyophilization.

Analytical methods. The glucose content was determined by GLC analysis of neutral sugars as alditol trifluoroacetates. The amount of the glucuronic acid produced by oxidation of the primary alcohol groups to carboxylate groups was obtained by measuring the amount of sodium hydroxide that was required to maintain the pH at 11. The uronic acid content of the final oxidized lignin sample was determined according to the Dische carbazole method [7] after acid hydrolysis of the oxidized lignin-glycosidic sample.

Infrared spectra were measured on a NICOLET Magna-IR 750 with DTGS detector and OMNIC 3.2 software. The samples were pressed into KBr

pellets with sample/KBr ratio of 2/200 mg. 128 scans at a resolution of 4 cm^{-1} were averaged.

Surface tension measurements were performed using tensiometer by Lecompte du Nouy, based on the ring method carried out at 25°C .

Results and discussion

Recently, Ferriers *et. al.* [3] revealed a new type of *O*-glycosylation of long chain alcohols (n-octyl, n-decyl, n-dodecyl, 10'-undecenyl) with totally unprotected uronic acids and neutral carbohydrates, performed in heterogenous media and promoted by anhydrous ferric chloride, which afforded alkyl D-glycofuranosid uronic acids and alkyl D-glycofuranosides, respectively, in high yields. These alkyl glycofuranosides are becoming increasingly important as surfactants [8] or liquid crystals [9] and can be obtained through a convenient one-pot synthesis. By application of this method on the lignin model monomeric compounds, alkyl and aryl α and β -D glucofuranosides as well as glucopyranosides were prepared. [4]

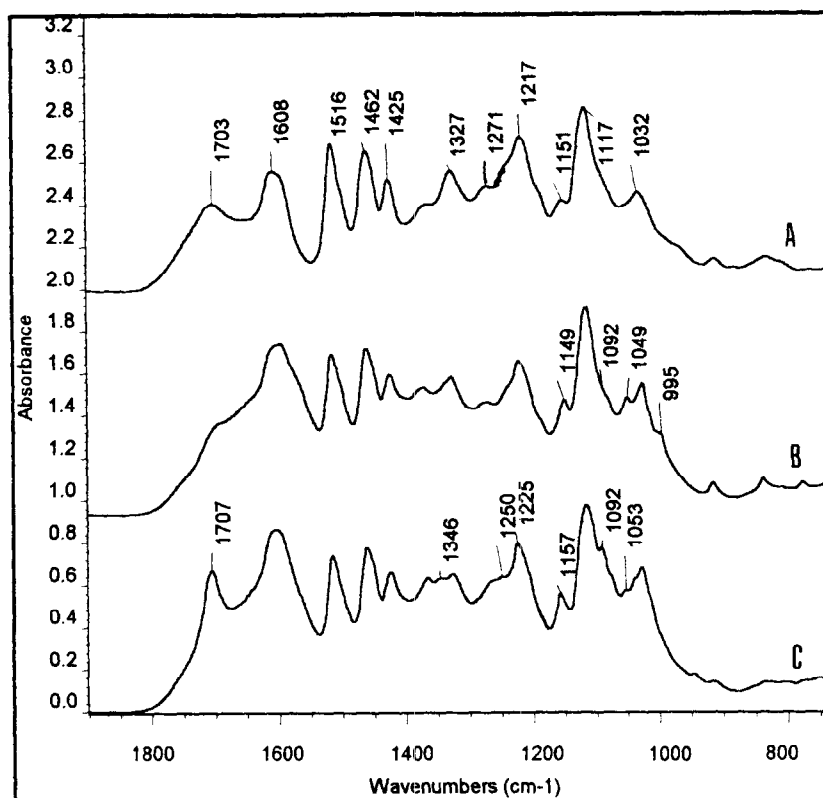


Figure 1. FTIR spectra of the prehydrolysis lignin (A), glycoside lignin (B) and glycosiduronic acid lignin (C).

Glycosidation of prehydrolysis lignin with D-glucose in heterogeneous media (1,4-dioxane) using anhydrous ferric chloride as a catalyst afforded new polymeric glucoside of lignin containing approximately 4.2 % of D-glucose. The prepared lignin derivatives were examined by IR spectroscopy (Fig. 1). The presence of bound D-glucose is evident from the new absorption bands at 995 and 1092 cm^{-1} corresponding to

C-O and C-C stretching vibrations and at 1160 cm^{-1} assigned to C-O-C antisymmetric stretching vibrations [10].

Based on our previous results with lignin model compounds, it can be suggested that the reaction product of lignin with D-glucose contains predominantly lignin-glycosidic linkages as illustrated in Figure 2.

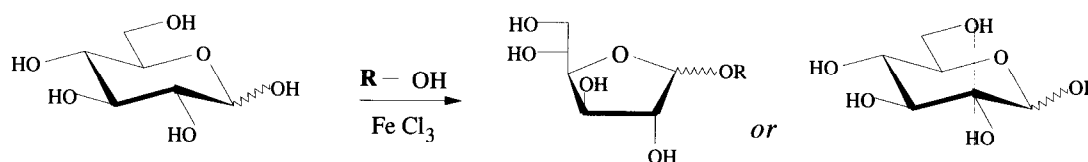


Figure 2. R = lignin.

In addition, the lignin-glucuronosiduronic acid was obtained by subsequent specific oxidation of the primary alcoholic group of D-glucose to carboxyl groups in the prepared glucoside of lignin with 2,2,6,6-tetramethyl-1-piperidine oxoammonium ion with sodium hypochlorite and sodium bromide in an aqueous alkaline solution at pH 11, according to de Nooy [11], and Chang [12]. The new lignin-glycosiduronic acid derivate, prepared this way contains approx. 3.9% of D-glucuronic acid. Under these conditions, other hydroxyl groups of glucose and as well as aliphatic alcohols are resistant towards oxidation (13).

The IR spectrum of this lignin derivative (Fig 1 C) shows that the carboxyl group of glucuronic acid contributes to the increase in intensity in the non-conjugated lignin carbonyl region (1707 cm^{-1}). Moreover, the new band at 1235 cm^{-1} corresponding to carboxyl vibration was revealed. This observation indicates the transformation of $-\text{CH}_2-$ into COOH groups [10].

The conversion of lignin-glucosides into glucuronic acid lignin derivatives is shown in Figure 3.

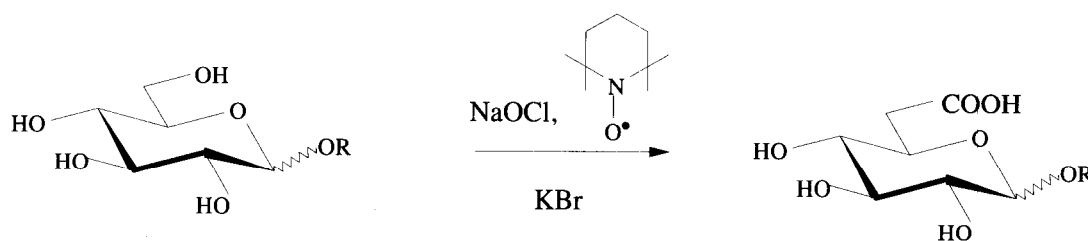


Figure 3. R = lignin.

An important property of surfactants is their positive adsorption in the water-air phase boundary, the result of which is the decrease of the surface tension of water. Both new sulfur-free lignin derivatives were tested from the viewpoint of their surface activity tension. The values determined, as illustrated in Figure 4, indicate that both types of modifications increase the surface activity of prehydrolysis lignin significantly due to its high hydrophilicity.

It can be assumed that the activity of surfactants depends upon the presence of different types of polar hydroxyl and carboxyl groups. The glycosiduronic acid derivative of lignin contains both hydroxyl and carboxyl groups which increase its hydrophilicity. Therefore, this derivative exhibits high solubility in water and also shows the highest surface activity.

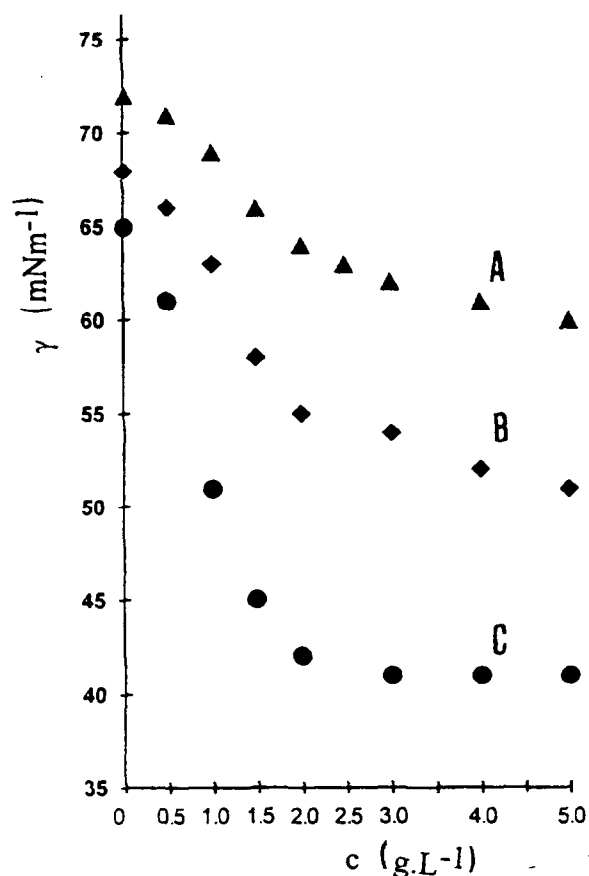


Figure 4. Plots of surface tension vs. concentration of the prehydrolysis lignin (A), glycoside lignin (B) and glycosiduronic acid lignin (C).

Conclusion

Based on the obtained results, it can be concluded that glycosidation represents a rapid and simple method for increasing solubility and surface activity of lignin. This effect is more significant after subsequent oxidation of primary alcoholic groups of glucose present in the prepared lignin-glycoside. The surface properties of the new D-glycoside and D-glycosiduronic acid derivatives of beech wood prehydrolysis lignin showed that the chemical modification used yielded sulfur-free, modified biopolymers which exhibit properties of biodegradable polymeric surfactants.

Acknowledgment

We are grateful to the Slovak Grant Agency (project 2/506098) for financial support.

References

- [1] Košíková, B.; Demianová, V.; Kacuráková M. Sulfur-Free Lignin as Composites of Polypropylene Films. *J. Appl. Polym. Sci.* **1993**, *47*, 1065.
- [2] Demianová, V.; Košíková, B. and Hodúl, P. New lignin derivatives as dispersants for disperse dyes. *Fibers and Textiles* **1995**, *2* (4), 152.
- [3] Shick, M.J. *Nonionic Surfactants*, Marcel Decker M: New York, 1967, p. 608.
- [4] Blacej, A.; Hodul, P.; Markušovská, E.; Novák, L.; Paulovic, M.; Vyskocil, I. *Tenzidy*, Alfa: Bratislava, 1977, p. 98.
- [5] Ferrieres, V.; Bertho, J.N.; Plusquellec, D. A convenient synthesis of alkyl D-glucosiduronic acids and alkyl D-glucosides from unprotected carbohydrates. *Carbohydr. Res.* **1998**, *311*, 25.
- [6] Joniak, D.; Poláková, M.; Landge, A.B. *Ind. J. Chem.* **1999**, in press.
- [7] Dische, Z. Color Reactions of hexuronic acids. *Methods Carbohydr. Chem.* **1962**, *1*, 497.
- [8] de Nijs, S.M.P.; Maat, T.L.; Kieboom, A.P.G. *Recl. Trav. Chim. Pays-Bas* **1990**, *109*, 429; and references cited therein.
- [9] Jeffrey, G.; Wingert, L.M. *Liq. Crystals* **1992**, *12*, 179; and references cited therein.
- [10] Harrington, K.J.; Higgins, H.G.; Michell, A.J. Infrared Spectra of *Eucalyptus regnans* F. Muell. and *Pinus radiata* D. Don. *Holzforschung* **1964**, *18*, 108.
- [11] de Nooy, A.E.J.; Besemer, A.C.; van Bekkum, H. Highly selective nitroxyl radical-mediated oxidation of primary alcohol groups in water-soluble glucans. *Carbohydr. Res.* **1995**, *269*, 89.
- [12] Chang, P.S.; Robyt, J.F. Oxidation of primary alcohol groups of naturally occurring polysaccharides with 2,2,6,6-tetramethyl-1-piperidine oxoammonium ion. *J. Carbohydrate Chem.* **1996**, *15* (7), 819.
- [13] Siedlecka, R.; Skaryewski, J.; Mlochowski, J. Selective oxidation of primary hydroxy groups in primary-secondary diols. *Tetrahedron Lett.* **1990**, *15*, 2177.

BIOTRANSFORMATION OF LIGNIN BIOPOLYMERS BY YEAST MICROORGANISMS

B. Košíková, E. Sláviková

Institute of Chemistry, Slovak Academy of Sciences,
Dúbravská cesta 9, 842 38 Bratislava, Slovakia

Due to a lack of information about the interaction of yeasts with lignin biopolymers, the effect of lignin derived from organosolv pulping on the growth of the yeast species *Sporobolomyces roseus*, *Rhodotorula rubra*, and *Bullera alba*, isolated from natural microflora, was examined. The production of biomass was significantly increased in the presence of oxidized lignin preparations. In this study, a relationship between surface tension of lignin preparations and growth of the yeasts tested was revealed. GPC analysis and ^{13}C NMR spectroscopy was applied for the characterization of lignin fractions

isolated from culture media by extraction with organic solvents. The structural changes of lignin biopolymer caused by the yeasts indicate demeth(ox)ylation and degradation of aromatic rings, similar to that observed with lignin-degrading hyphal fungi. The observed structural changes confirm a biotransformation of the lignin by *Sp. roseus*, in particular when lignin was the only source of carbon.

Keywords: organosolv lignin, biotransformation, ^{13}C NMR, yeasts

Introduction

Previously, it has been described that yeasts can utilize monomeric phenolic compounds [1]. In spite of this, there is no information about the interaction of yeasts with lignin macromolecules. The intention of this work is to examine the effect of lignin on the growth of *Sporobolomyces roseus*, *Rhodotorula rubra*, and *Bullera alba* species isolated from aqueous environment. Generally, these yeast species are widely distributed in the different sources [2], e. g., soil, plant and wood leaves, wood pulp as well as waste water where simple carbon sources are present in low concentration.

Material and Methods

Lignin samples. Organosolv spent liquor was derived from methanol-based organosolv pulping of beech wood (methanol-water 1:1, 190 °C, 50 min). NaOH, at the concentration of 18 % was added for the second stage (165 °C, 1 h).

Organosolv lignin was recovered by acidification of the combined spent liquors after evaporation of methanol. Oxidation of the sample was performed by bubbling oxygen through the aqueous alkaline solution at 100 °C for 8 h [3].

Cultivation and yeast microorganisms. The yeast strains *Bullera alba* (CCY 12-1-4), *Rhodotorula rubra* (CCY 20-7-25), and *Sporobolomyces roseus* (CCY 19-6-6) were obtained from the Culture Collection of Yeasts (Institute of Chemistry, Slovak Academy of Sciences, Bratislava) and maintained on malt agar slants at 5 °C. They were cultured in a medium containing 6.7 g YNB (Difco), and lignin samples (3 g) in the presence or absence of glucose (20 g) per litre of solution in distilled water. The pH was adjusted to 6.5. The medium was sterilized by autoclaving at 121 °C for 15 min. The strains were cultivated in flasks (500 ml) containing 250 ml of medium. 4 ml of suspension (10^6 cells per ml) was used for inoculation. Incubation proceeded on rotary shakers at 2.7 Hz and 28 °C for 16 d. The growth of yeasts was determined

based on the nitrogen content in the dry solid product separated by centrifugation of the cultivation medium. In the case of *Sp. roseus*, the lignin sample was recovered from the sediment by extraction with acetone and evaporation to dryness (yield 30 %).

GPC analysis. The prepared lignin derivatives were analysed by gel permeation chromatography on a Sephadex LH 60 column (53x0.8 cm) using

a mixture of dioxane and water containing 0.005 M aqueous NaOH and 0.001 M LiCl (7:3) as the eluent [4].

¹³C NMR spectra of the acetylated lignin samples were recorded in CDCl₃ on a Bruker AM-300 spectrometer operating at 75.47 MHz in the inverse gated decoupling mode. The pulse delay was 10 s, the total number of scans ranged from 10000 to 20000.

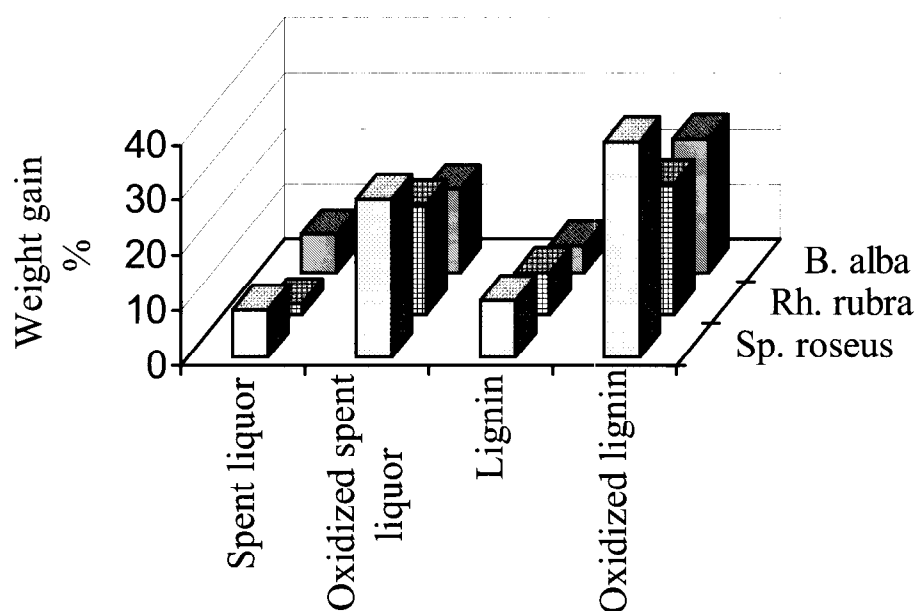


Figure 1. Growth of some yeast species in the presence of lignin biopolymers (mass gain, %).

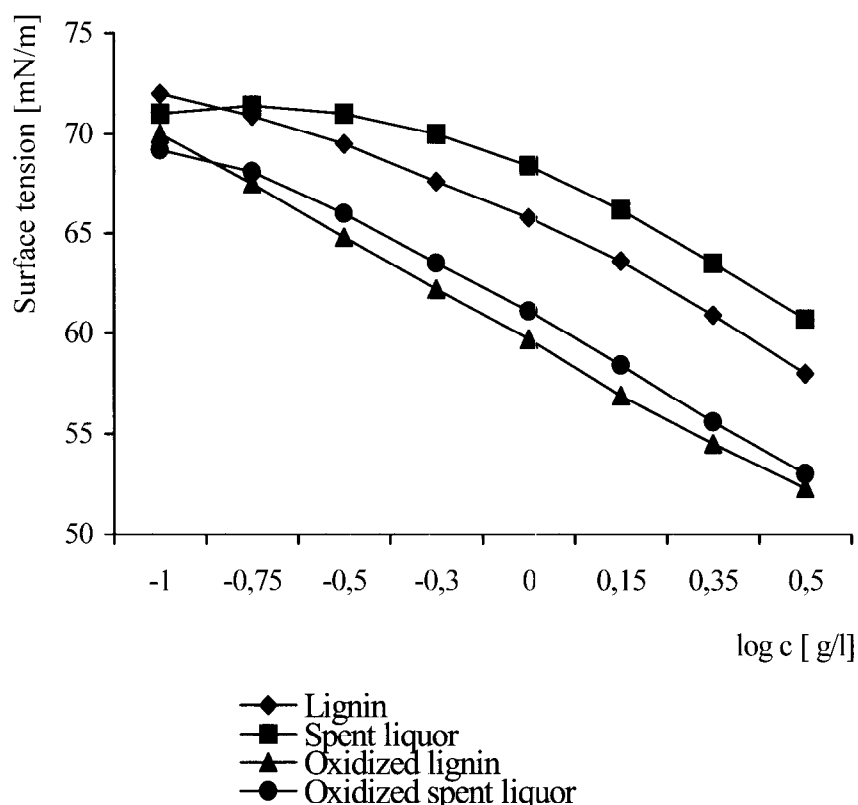


Figure 2. Plots of surface tension vs. log [concentration of lignin preparations].

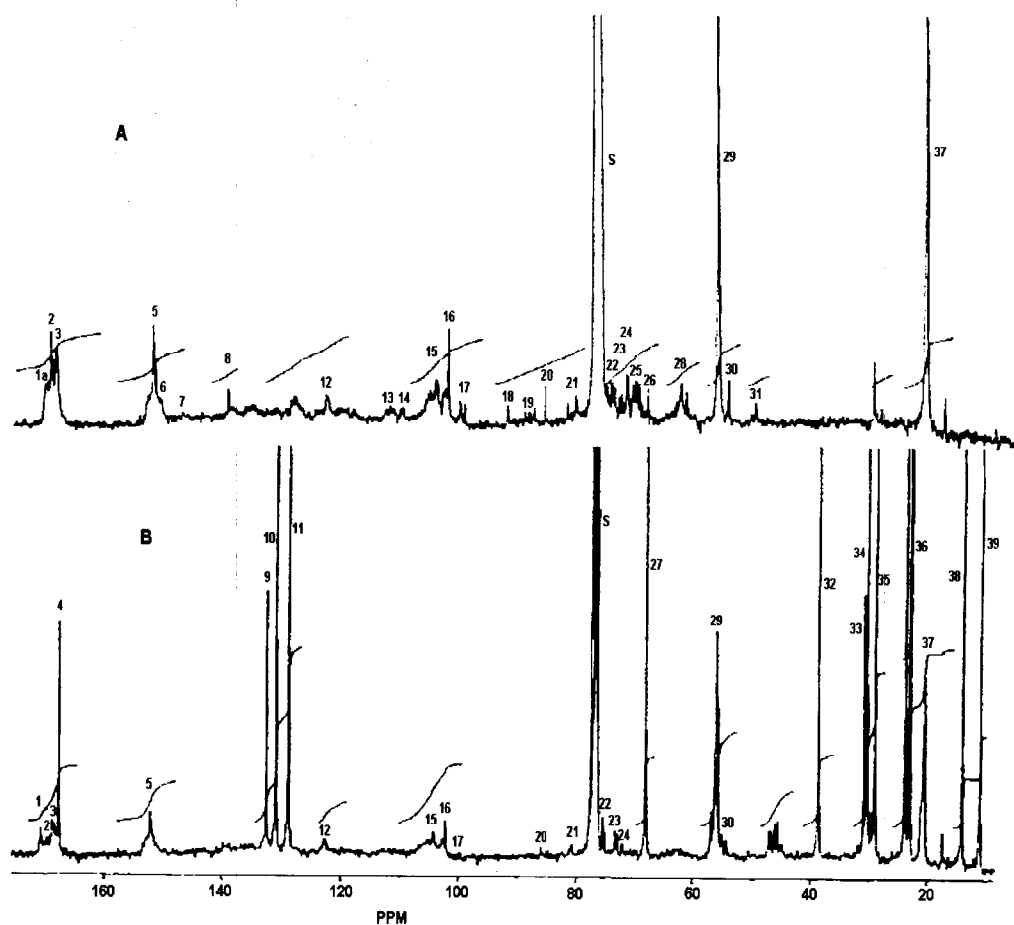


Figure 3. ^{13}C NMR spectra of a lignin sample before (A) and after cultivation with *Sp. Roseus* in the presence of glucose (B). Solvent: CDCl_3 .

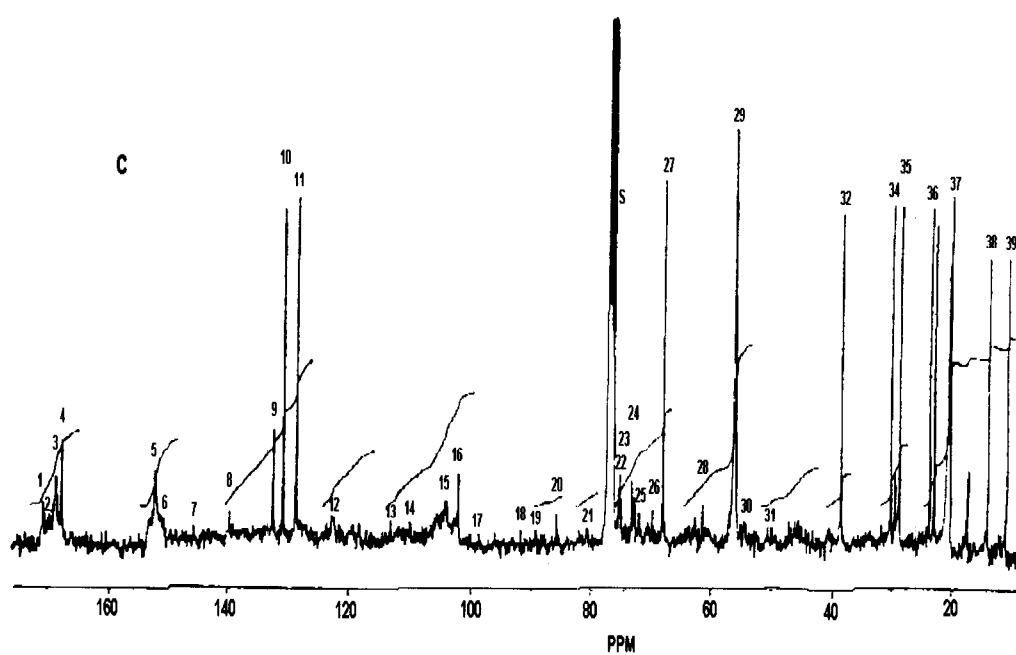


Figure 4. ^{13}C NMR spectrum of lignin sample after cultivation with *Sp. roseus* in the absence of glucose. Solvent: CDCl_3 .

Results and Discussion

The effect of spent liquor as well as of isolated lignin, derived from organosolv pulping of beechwood before and after oxidation, on the growth of *Sp. roseus*, *Rh. rubra*, and *B. alba* was examined. As follows from the results summarized in Figure 1, the lignin samples have a different influence on the growth of the yeast strains used. The biomass formation was most significant in the case of *Sp. roseus*, particularly if the lignin samples were oxidized. The observed differences in the efficiency of the samples could be explained by their different surface characteristics because surfactants decrease the interfacial tension and increase interfacial area of the cells [5] (Figure 2). The ability of *Sp. roseus* to transform organosolv lignin in the presence and/or absence of glucose in the cultivation medium was studied by ^{13}C NMR spectroscopy.

A comparison of the ^{13}C NMR spectra of a lignin sample before (Figure 3A) and after treatment with *Sp. roseus* (Figure 3B) shows a decrease of the original aromatic and methoxy signals 5, 6 and 29 as well as the appearance of new prominent resonances 4, 9, 10, 11, 27, 32-36. Based on literature data [6-8], in the yeast-treated lignin fractions the most significant signal at 67.8

ppm corresponds to $-\text{OCH}_2-$ carbon of Alkyl- $\text{OCH}_2\text{-COOH}$ and is caused by $\text{C}_\alpha\text{-C}_\beta$ cleavage. This alkoxyacetic acid indicates the transformation of the native C-4 into a methylene carbon by ring cleavage in β -arylether substructures which are still linked to the polymer. The new signals 9, 10, 11 were assigned to C_α and C_β in $\text{Ar-CH=CH-CH}_2\text{OH}$ structures. The signal 4 at 167.2 ppm belongs to aromatic carboxylic structures. More obvious new signals between 34 and 22 ppm indicate methylene carbons of saturated n-alkyl groups. The attack of *Sporobolomyces roseus* on lignin macromolecule follows similar patterns as described for partial degradation by known ligninolytic organisms, such as *Phanerochaete chrysosporium*. The observed structural changes of the lignin tested confirm its biochemical transformation due to the action of *Sp. roseus*. This effect was more intense if the cultivation was carried out in the absence of glucose (Figure 4). As to low differences in the molecular weight of the lignin biopolymer before and after treatment with *Sp. roseus* (Fig. 5), it can be concluded that the structural transformation of lignin macromolecules was not accompanied by a significant degradation.

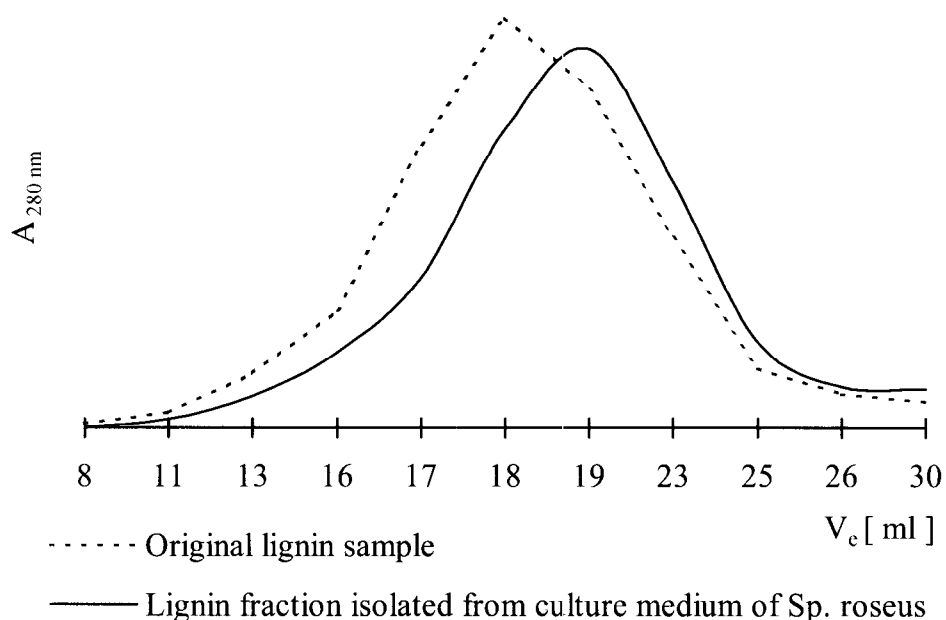


Figure 5. The effect of *Sp. roseus* on the molecular weight of lignin biopolymer.

Acknowledgement

This work was supported by grants from VEGA No 2/5060/98 and No 2/4145/98.

References

- [1] Middelhoven, W.J.; Koorevaar, M.; Schuur, G. Degradation of benzene compounds by yeasts in acidic soils. *Plant & Soil* **1992**, *145*, 37.
- [2] Kreger-van Rij N.J.W. *The Yeasts: a Taxonomic Study*. Elsevier Science Publishers: Amsterdam, 1984.
- [3] Kratzl, K.; Schaefer, W.; Claus, P.; Gratzl J.; Schilling P. Oxidation of ¹⁴C-labeled phenols (lignin models) with oxygen in aqueous alkaline solution. *Monatsh. Chem.* **1967**, *98*, 891.
- [4] Košíková, B.; Mlynár, J.; Joniak, D. Effect of lignin derivatives on the macromolecular properties of lignin in NSSC cooking. *Holzforschung* **1990**, *44*, 47.
- [5] Erickson, L. E.; Nakahara, T. Growth in culture with two liquid phases. Hydrocarbon uptake transport. *Proc. Biochem.* **1975**, *10* (5), 9.
- [6] Chua, M.G.S.; Chen, C.L.; Chang, H.M. ¹³C NMR Spectroscopic study of spruce lignin degraded by *Phanerochaete chrysosporium* I. New structures. *Holzforschung* **1982**, *36*, 165.
- [7] Haider, K.; Kern, H.W.; Ernst, L. Intermediate steps of microbial lignin degradation as elucidated by ¹³C NMR spectroscopy of specifically ¹³C-enriched DHP-lignins. *Holzforschung* **1985**, *39*, 23.
- [8] Nimz, H.H.; Robert, D.; Faix, O.; Nembr, M. Carbon ¹³ NMR spectra of lignins, 8 Structural differences between lignins of hardwoods, softwoods, grasses and compression wood. *Holzforschung* **1981**, *35*, 16.

IRRADIATION OF DISSOLVING PULP BY ELECTRON BEAMS

G. Kraft, N. Schelosky

Lenzing AG, A - 4860 Lenzing, Austria

Different dissolving pulps were treated by electron beams. The dose-DP relation was investigated by different accelerators. The parameters of the *Sakurada* equation differ from pulp to pulp.

As a result of our examinations the DP distribution inside a mini bale shows a great inhomogeneity of the viscosity. The strongest degradation was observed at the edge positions of single pulp sheets in a penetration depth of 30 sheets. The uniformity of the DP distribution, measured by GPC in LiCl/DMAc, of the alkali cellulose (AC) before xanthation was compared to conventional AC for different pulps. In all these examinations no significant differences between pre-aged and irradiated pulp was observed.

The phase transition from cellulose I to cellulose II depending on temperature and steeping lye concentration, measured by FT-IR-spectroscopy, takes place in the same range of NaOH-concentration for irradiated and untreated pulp samples.

The influence of CS₂, cellulose content, and alkali ratio (AR) was examined using hemicellulose-free steeping lye in order to check the influence of irradiation on viscose quality. In case of irradiated pulp the steeping lye concentration was 16%. In these trials the

viscosity of AC before xanthation was the same for both types of pulp. In a wide range of CS₂ input (36% to 26% calculated on α -cellulose) and AR from 0.60 down to 0.47 no difference between the irradiated samples and the conventional pre-aged pulp was observed. Increasing the cellulose content up to 15.7% (relative to standard), no benefit was observed by using irradiated pulp. Only in case of a drastic reduction of the input chemicals down to 22% CS₂ and AR 0.5 the irradiated pulp gives a better viscose quality than the reference pulp under the same conditions. The same trials performed in the 2kg lab plant did not show any statistical difference between irradiated and conventional pre-aged pulp.

Regarding the fibre quality there was no difference between irradiated and conventional pre-aged pulp samples in terms of elongation and tenacity. The fibres from the irradiated pulp showed a higher degree of yellowing. The formation of H₂S was not increased according to by-product analyses.

The frequently published results of drastically better viscose quality by using irradiated pulp could not be confirmed in our study.

Keywords: viscose, irradiation, electron beam

Introduction

There has been some correspondence among several research groups claiming that irradiation of dissolving pulps prior to viscose production could be beneficial in several ways:

- the caustic requirement for steeping will be reduced because the conversion to the cellulose II state could be achieved at a remarkably lower caustic soda concentration;
- the degree of polymerization can be easily adjusted and, thus, the aging step after alkalization could be omitted;

- the xanthation will occur with substantially reduced carbon disulfide input and, because of a higher reactivity of pulp degradation, still give a viscose with good filterability;

- less CS₂-derived byproduct formation will result in a reduced H₂S-formation.

The objective of this study was the evaluation of the potential of electron treatment of dissolving pulps with a special focus on the feasibility of a drastic reduction of CS₂ and NaOH charges in the case of Solucell dissolving pulp.

Economical considerations. The price of irradiated pulp is composed of high costs of both investment and operation, the latter one mainly depending on expenses for electric power. From this point of view, the irradiation of pulp would become an economically interesting innovation only if it is possible to carry out the viscose process with drastically reduced input chemicals (22% CS₂, AR: 0.5) without any impairment of the fiber quality.

Experimental

For the experiments at lab plant and pilot plant, 50 sheets (isostack) of Solucell 450 were irradiated at STUDER AG with a 10MeV Rhodotron TT300 accelerator built by IBA.

The viscose quality was evaluated by PVC and KWP filter value (constant pressure) and particle

count. The viscose was also characterized by rheological investigations and analysis of byproducts, see Table 1 and Figure 1.

No optimization of spinning conditions was done for these experiments.

Table 1. Viscose composition for the experiments at lab plant and pilot plant.

| Plant | CS ₂ (%) | AR | Cell conc. |
|-------|---------------------|-------|---------------------|
| Lab | 36 | 0.6 | Standard |
| Lab | 32 | 0.6 | Standard |
| Lab | 28 | 0.55 | Standard |
| Lab | 26 | 0.5 | Standard |
| Lab | 22 | 0.5 | Standard |
| Lab | 28 | 0.55 | Standard + 15.6% |
| Lab | 28 | 0.475 | Standard + 15.6% |
| Pilot | 22 | 0.5 | Standard |

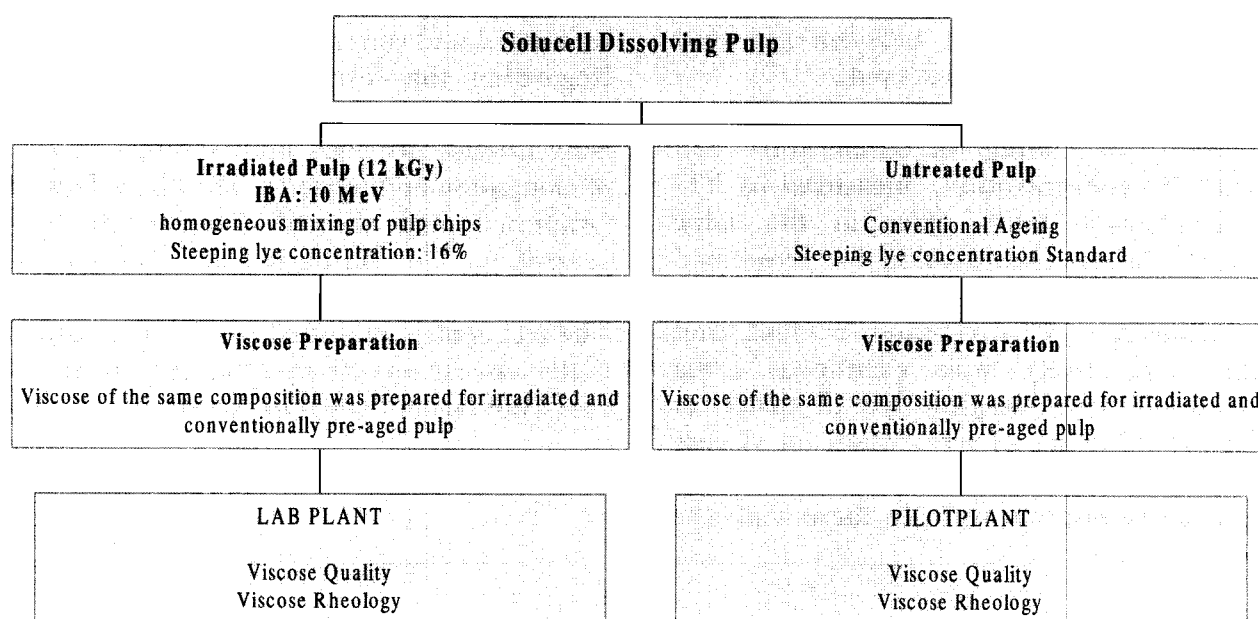


Figure 1. Experimental setup.

Results and Discussion

Homogeneity. To check the homogeneity of pulp irradiation within one mini bale (50 sheets), samples were taken from three different positions (edge, middle, center position) within one sheet of every 10th layer. The intrinsic viscosities of these samples were examined (Figure 2).

The homogeneity of irradiation within one mini bale and across the sheet area turned out to be rather poor.

To get a good average sample for the tests in the lab and pilot plant, the sheets were divided into squares of 6 x 6 cm, which were very well mixed. Pressing of irradiated pulp turned out to be difficult.

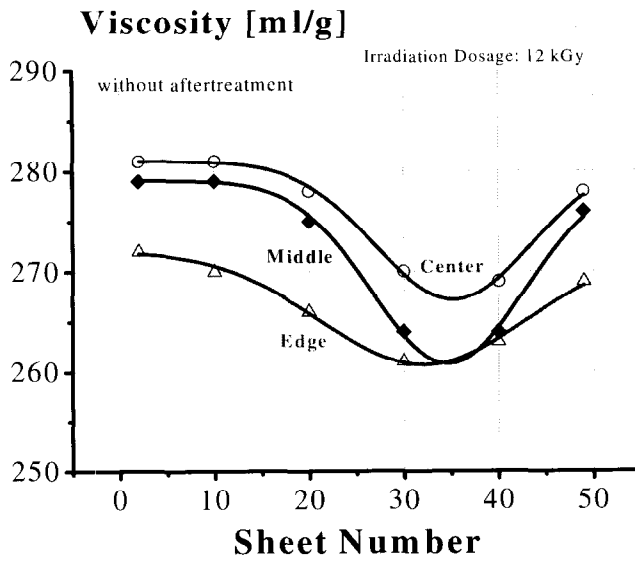


Figure 2. Intrinsic viscosity distribution within one mini balt: homogeneity of irradiation at a dosage of 12 kGy.

In case of irradiated pulp the hemicellulose concentration in press lye was higher than in the conventional process (2.25 g/l versus 1.48 g/l).

Ball fall of viscose. As published, the ball fall of viscose made from irradiated pulp should be lower than that of viscose made from conventionally pre-aged pulp. Thus, it should be possible to increase the production capacity by using a higher content of irradiated cellulose under retention of the same ball fall of the viscose as before. However, only at high cellulose content (115.6% of standard) and very low alkali content a lower ball fall seemed to result from the use of irradiated pulp (Figure 3). There is no benefit in ball fall by using irradiated pulp.

Polydispersity of AC. No difference regarding polydispersity between aging and electron beam treatment could be observed in the respective viscosity range (Figure 4).

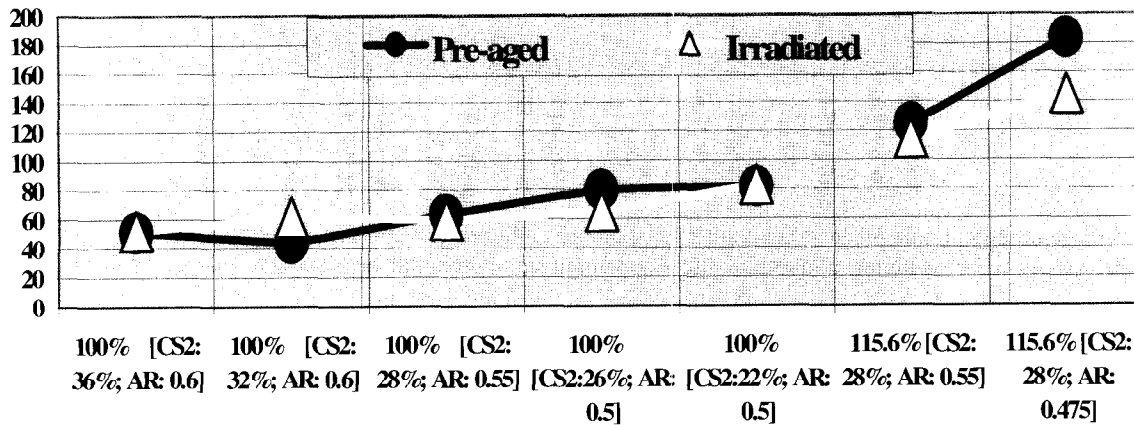


Figure 3. Ball fall of various compositions of viscose prepared from irradiated and pre-aged pulp; lab-plant trials. Ball fall corrected to target cellulose concentration.

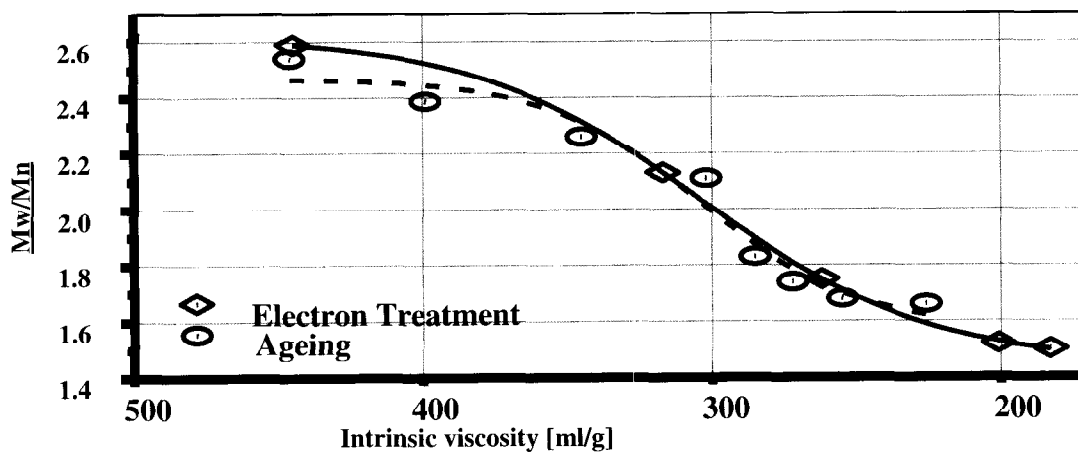


Figure 4. Polydispersity vs. intrinsic viscosity of AC.

Phase transition Cellulose I - Cellulose II. The phase transition takes place in the same range of NaOH concentration for irradiated and untreated pulp samples.

Rheology of Viscose Spinning Dope. Under standard conditions, irradiated pulp yields rheologically worse viscose than reference pulp. Under conditions of CS₂ reduction and increase in cellulose, irradiated pulp yields rheologically better viscose than reference pulp. Irradiated pulp seems to have a lower tendency of forming

networks under extreme conditions (CS₂ reduction, increase in cellulose) than reference pulp. It has a higher potential for savings from this point of view.

Viscose from irradiated pulp under saving conditions is rheologically worse than one from reference pulp under standard conditions.

Quality of viscose. The often published results of drastically better viscose quality by using irradiated pulp could not be confirmed in our study of Solucell 450.

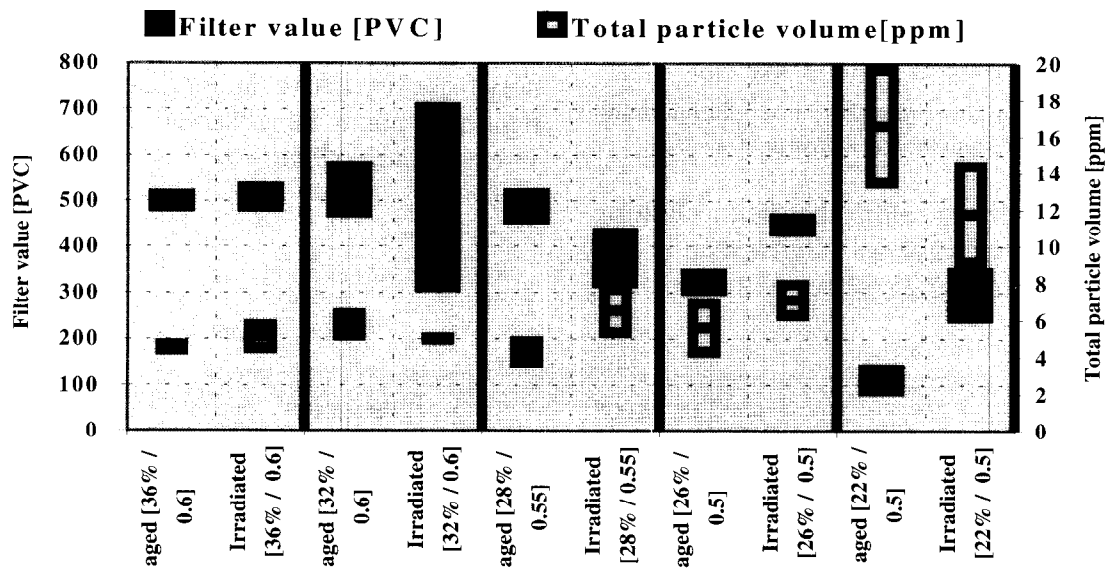


Figure 5. Viscose quality. Trials made at lab plant with standard cellulose concentration (average +/- 95,4% conf. interval). Filter value (higher is better) and total particle content at standard cellulose content in viscose [CS₂%/AR].

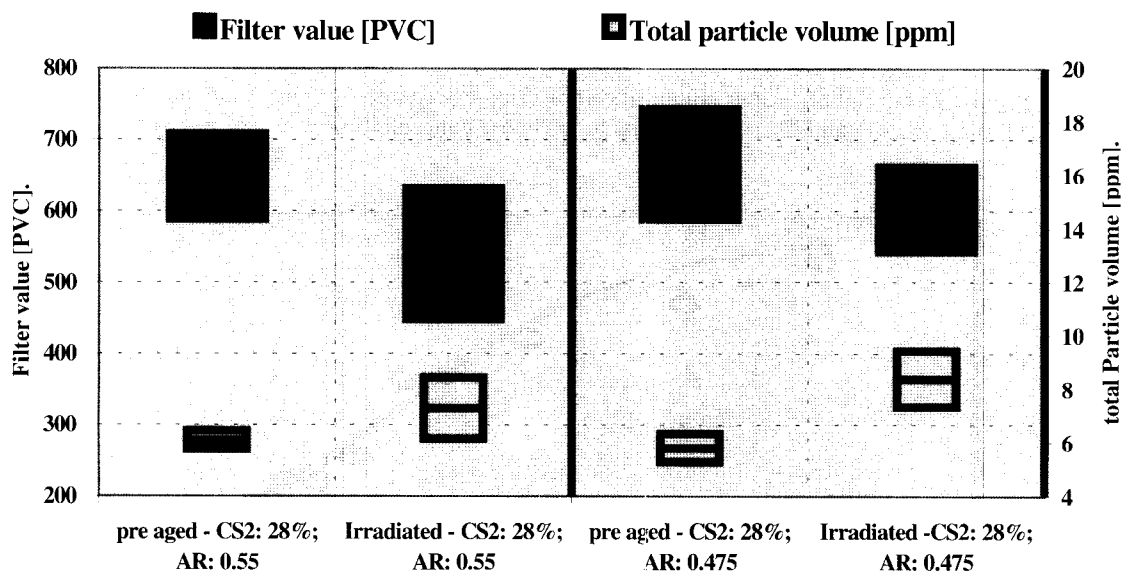


Figure 6. Viscose quality. Trials made at lab plant with standard cellulose concentration (average +/- 95,4% conf. interval). Filter value (higher is better) and total particle content at 15.6% higher cellulose content in viscose [CS₂%/AR].

In a wide range of CS₂ input (36% to 26% calculated on α -cellulose) and AR from 0.60 down to 0.47 no significant difference in viscose quality between the irradiated samples and the conventionally pre-aged pulp was observed. Upon increase of the cellulose content up to 115.7% of standard, no benefit was observed by using irradiated pulp. Only in case of a drastic reduction of the input chemicals down to 22% CS₂ and AR 0.5 the irradiated pulp gave a better viscose quality than the reference pulp under the same conditions (Figures 5 and 6). The same trials performed at the 2kg pilot plant did not show any statistical difference between irradiated and conventionally pre-aged pulp (Table 2).

Byproducts. There seems to be a slight tendency to lower trithiocarbonate formation in the viscose made from the irradiated pulp.

Fibre properties. Viscose of reduced CS₂ content showed good spinning properties, the spinning conditions were not optimized. Tenacity and elongation were not significantly influenced by the use of irradiated pulp, the tendency is slightly better for aged pulp.

Tenacity and elongation were significantly impaired by the reduction of CS₂ charge using standard spinning conditions (Figure 7).

Brightness and yellowing of fibres were negatively influenced by both the use of irradiated pulp and the reduction of CS₂ charge (Figure 8).

Table 2. Results of trials at a pilot plant [average/range].

| | conventional | | irradiated | |
|------------------------------|--------------|------------|------------|-----------|
| CS ₂ [%] | Std. | 22 | Std. | 22 |
| Alkali ratio | Std. | 0.5 | Std. | 0.5 |
| unfiltered viscose | | | | |
| Filter value, PVC | 452 /25 | 252 /167 | 393 /156 | 335 /103 |
| Filter value, KWP | 77 /44 | 230 /230 | 117/69 | 123 /39 |
| Total particle volume [ppm] | 12.4 /7.8 | 28.3 /40.0 | 18.6 /17.1 | 22.1 /3.2 |
| Time for filtration, min. | 43 | 78 | 60 | 70 |
| viscose spinning dope | | | | |
| Filter value, PVC | 528 /186 | 233 /121 | 528 /34 | 439 /32 |
| Filter value, KWP | 26 /12 | 47 /16 | 40 /15 | 43 /45 |
| Total particle volume [ppm] | 1.2 /0.6 | 2.5 /1.8 | 1.4 /0.5 | 1.3 /0.3 |
| Ball fall [sec] | 49 | 83 | 60 | 93 |
| Ripening ind., °H | 14.7 | 6.5 | 15.9 | 7.8 |

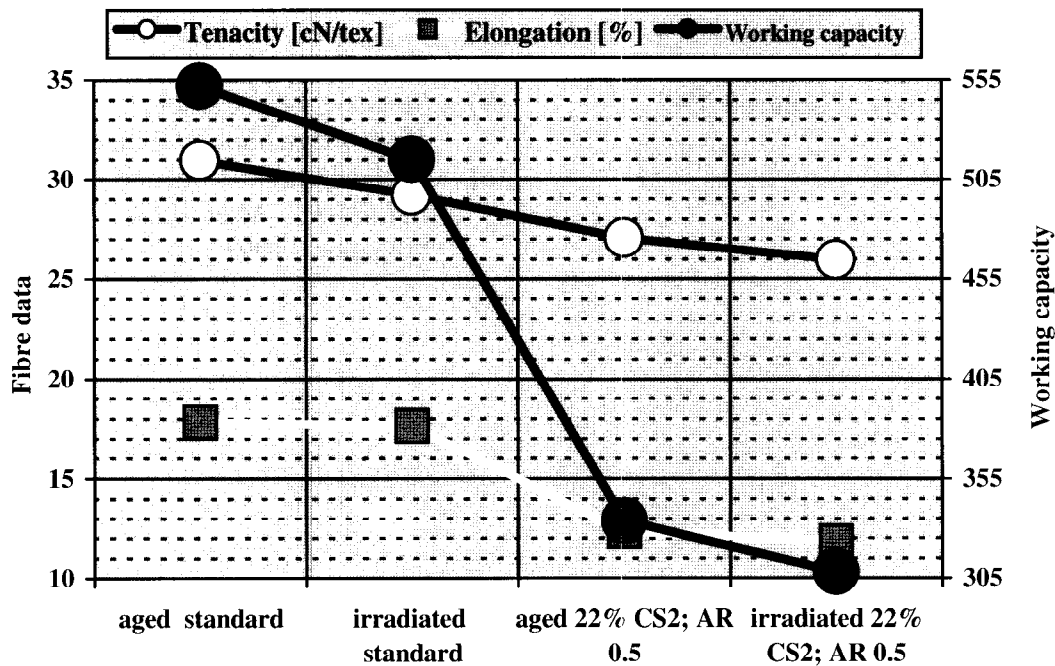


Figure 7. Tenacity and elongation of fibers at standard spinning conditions (pilot plant trials).

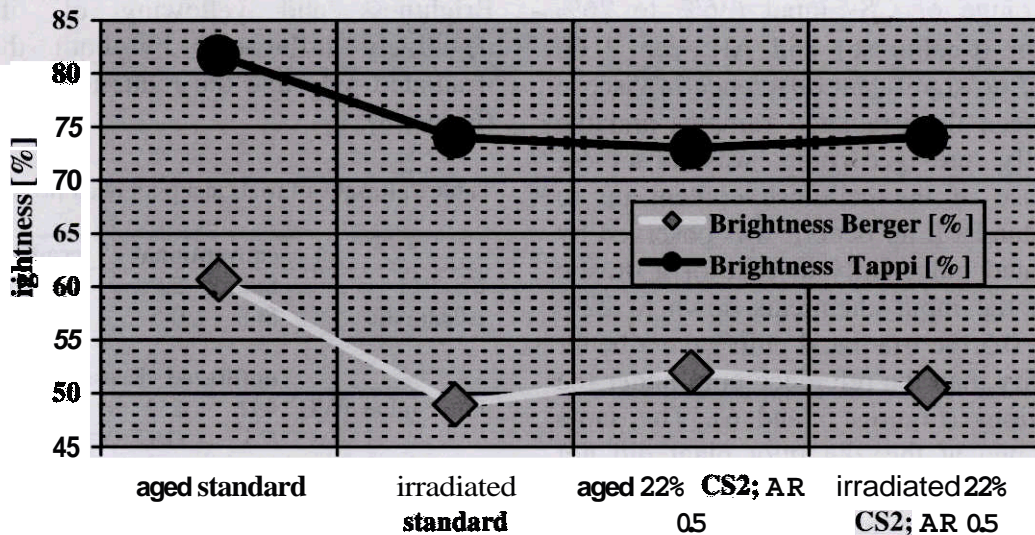


Figure 8. Brightness of unbleached fibers at standard spinning conditions (pilot plant trials).

Conclusion

Electron beam treatment of pulp slightly improves viscose filterability at a very low level of CS₂ charge (lab plant).

However, this improvement is not large enough to justify the additional costs of electron beam treatment. The higher hemicellulose content in the steeping lye and the enhanced yellowing of the fibers are further arguments against electron beam treatment of dissolving pulp.

The often published results of drastically better viscose quality by using irradiated pulp could not be confirmed in our study of Solucell 450.

References

- [1] Fischer, K.; Goldberg, W.; Wilke, M. *Lenz. Ber.* **1985**, *59*, 32.
- [2] Rajagopal, S. *et al.* "Enhancement of Cellulose Reactivity in Viscose Production Using Electron Processing Technology" *Viscose Chemistry Seminar*; Stockholm, 1994.
- [3] Rajagopal, S. *PETAS Seminar*, Hamburg, 1995.
- [4] Rajagopal, S. *Cellulosic Man-Made Fibre Summit*, Singapore, 1997.
- [5] Stavtsov, A.; Cassel, A. *Cellulosic Man-Made Fibre Summit*, Singapore, 1997.
- [6] Schleicher, H.; Bornmeister, B.; Voges, M. *Cellulosic Man-Made Fibre Summit*, Singapore, 1997.

FUNCTIONALIZATION OF CELLULOSE

U. Mais, S. Knaus, W. H. Binder, H. Gruber

Institute of Chemical Technology of Organic Materials
Vienna University of Technology, Getreidemarkt 9/162, A - 1060 Vienna, Austria

Cellulose tosylates, synthesized by homogeneous tosylation in DMA/LiCl, were reacted with cysteamine, methylamine and dimethylamine yielding amino functionalized celluloses up to a DS of 1. By grafting of 2-methyl-1,3-oxazoline onto the cellulose tosylates and subsequent quenching with diethylamine graft copolymers with up to 7 N-

acetyleneimine units per anhydroglucose unit were obtained. All products were characterized by elemental analysis, IR and ^{13}C CP/MAS NMR spectroscopy.

Keywords: cellulose derivatives, aminodeoxy-cellulose, cellulose-graft-poly(N-acetyleneimine), ^{13}C CP/MAS NMR spectroscopy

Introduction

In recent years cellulose, an abundant carbohydrate of commercial and biological importance, has attracted increasing interest as biomaterial for biomedical applications. Especially derivatives with amino functionalities have become very attractive. Recently, Klemm *et al.* [1,2] investigated cellulose derivatives obtained by reaction of cellulose *p*-toluene sulfonic acid esters (tosylates) with diamino compounds as building blocks of supramolecular architectures.

McCormick *et al.* first synthesized tosylated cellulose homogeneously in dimethylacetamide (DMA)/ LiCl, a good solvent system for cellulose [3]. Klemm *et al.* reported the homogeneous synthesis of tosylcelluloses with degrees of substitution (DS) from 0.4 up to 2.3 with different cellulosic materials [3]. These uniformly substituted tosylates with controllable DS showed improved solubility properties, and were used for nucleophilic substitution reactions [4,6].

In this contribution, we present two different approaches to cellulose derivatives with amino groups. Homogeneously synthesized cellulose *p*-toluenesulfonates were used as intermediates for nucleophilic displacement reactions with amines and as initiators for grafting 2-methyl-1,3-oxazoline onto cellulose [7], with subsequent end functionalization of poly(N-acyl-ethyleneimines)

side chains by quenching with amines. The products were characterized by elemental analysis, IR-spectroscopy and ^{13}C CP/MAS solid state NMR spectroscopy in order to verify the chemical structures of the amino-functionalized celluloses.

Experimental

Materials. As starting material for the substitution reactions cellulose tosylates were synthesized homogeneously in the system DMA/LiCl according to Rahn *et al.* [3] using a highly degraded cellulose with an average degree of polymerization (DP) of 225.

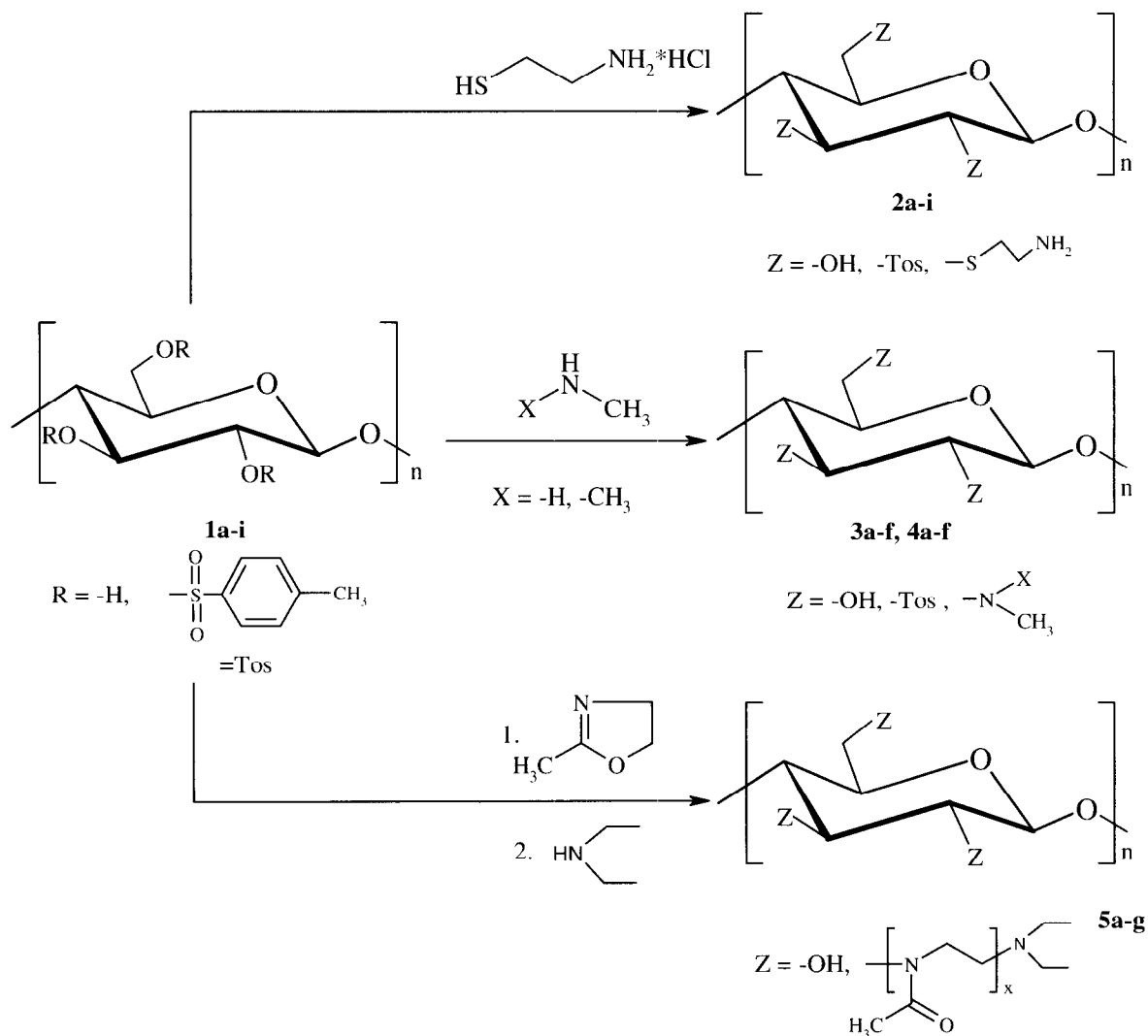
General procedures for the synthesis of cysteaminodeoxycellulose, methyl- and dimethylaminodeoxycellulose and cellulose-graft-poly(N-acetyleneimine) (Scheme 1) are given below.

Reaction of tosylcellulose with 2-aminoethanethiol. At room temperature potassium *tert*-butoxide was added to a mixture of toluene and *tert*-butyl alcohol (1:1) under nitrogen atmosphere. After dissolution 2-aminoethanethiol hydrochloride (cysteamine hydrochloride) was added and refluxed for 3 h under stirring until the mixture became slightly turbid. Then, over an interval of 1.5 h, cellulose tosylate was added in small portions and refluxed under stirring for 24 h (molar ratio potassium

tert.-butoxide: cysteamine hydrochloride: cellulose tosylate = 8.4: 5: 1). For products of tosylcellulose with DS < 1.3, the precipitate, obtained after cooling to room temperature, was first washed with distilled water, then treated with an aqueous solution of potassium hydroxide (25%), and washed again extensively with

distilled water. Finally, the product was washed with acetone and dried at 50°C under vacuum.

To isolate products from tosylcellulose with initial DS_{Tos} > 1.3, the reaction mixture was poured into diethyl ether and the precipitate was suspended in water and isolated after dialysis (up to 3d).



Scheme 1. Synthesis of aminodeoxycelluloses and cellulose -graft-poly(N-acetyleneimine).

Nucleophilic substitution of tosylcellulose with amines. An aqueous solution of methylamine or dimethylamine, respectively, was added dropwise to a solution of tosylcellulose in DMA (molar ratio tosylcellulose: amine = 1:30). The reaction mixture was heated to 50°C for 24 h. During the reaction the homogeneous mixture became partly heterogeneous. After cooling to room temperature, the brownish solution was poured into 2-propanol, washed with an excess

of water to remove the remaining salts and dried at 50°C under vacuum.

Grafting of 2-methyl-1,3-oxazoline onto cellulose. Freshly distilled benzonitrile was added to cellulose tosylate and placed in a reaction tube under argon atmosphere. The tube was sealed and the mixture stirred at 50°C. 2-Methyl-1,3-oxazoline was injected into the sealed tube with an injection needle and the mixture was then heated to 90°C. After stirring for 2 days the tube was opened and the content

was poured into a solution of diethylamine and benzonitrile (3:1) and stirred for 24h. The resulting mixture was then poured into diethyl ether to complete precipitation. The graft copolymer was separated from polyoxazoline homopolymer by extraction with water. After filtration the insoluble fraction consisting of graft copolymer was dried under vacuum at 50°C. All fractions were weighed and analyzed by elemental analysis.

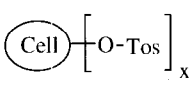
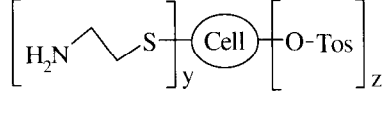
Measurements. Elemental analysis was carried out by means of an EA 1108 CHNS-O analyzer from Carlo Erba. The FTIR spectra were recorded on a Biorad FTS 135 using KBr pellets. ¹³C CP/MAS NMR spectroscopy was measured on a Bruker Avance DRX 400 spectrometer operating with a 4mm probe head at a frequency of 100.62 MHz. The samples were filled into zirconia rotors which were spun at 5000 Hz. The spectra were acquired in the cross polarisation mode using contact times of 3ms and high power dipolar decoupling to reduce line broadening. In some cases cpseltics was used to suppress spinning side band effects. The puls repetition time was 3s, 1000 to 5000 scans were accumulated.

Results and Discussion

Reaction of tosylcellulose with 2-cysteamine. By reaction of tosylcelluloses with a DS from 0.2 to 1.8 with cysteamine under heterogeneous conditions yellowish, insoluble products (**2a-2i**) were obtained (Scheme 1). The DS values as calculated from elemental analysis, and the yields are summarized in Table 1.

A complete substitution of the tosyl moieties was achieved up to a DS_{Tos} of 0.8 (**2a-2e**). The DS of cysteamine groups was generally slightly lower than the starting DS_{Tos}, probably due to partial hydrolysis of tosyl moieties. With higher DS_{Tos} values the tosyl moiety still could be removed completely, but nucleophilic substitution only took place to a maximum DS of 1 due to hydrolysis as side reaction (**2f-2i**). **2g-2i**, obtained by reaction of tosylcelluloses with DS_{Tos} > 1.32, were isolated after dialysis in very low yields.

Table 1. Reaction of cellulose tosylates with cysteamine.

| Cellulose tosylate | | Cysteaminodeoxycellulose | | | |
|-----------------------------------------------------------------------------------|------------------|-------------------------------------------------------------------------------------|------------------|------------------|----------------------|
|  | |  | | | |
| sample | x ⁽¹⁾ | sample | y ⁽²⁾ | z ⁽³⁾ | Yield ⁽⁴⁾ |
| 1a | 0.2 | 2a | 0.01 | 0.01 | 70 |
| 1b | 0.44 | 2b | 0.27 | 0.11 | 77 |
| 1c | 0.58 | 2c | 0.54 | 0.02 | 77 |
| 1d | 0.73 | 2d | 0.43 | 0.06 | 72 |
| 1e | 0.8 | 2e | 0.76 | 0 | 75 |
| 1f | 1.21 | 2f | 0.77 | 0.02 | 64 |
| 1g | 1.32 | 2g | 0.96 | 0.06 | -(⁵) |
| 1h | 1.7 | 2h | 0.99 | 0.08 | -(⁵) |
| 1i | 1.81 | 2i | 1.02 | 0.04 | -(⁵) |

⁽¹⁾ DS_{Tos} calculated from the data of sulfur analysis

⁽²⁾ DS of the remaining tosylate group after nucleophilic substitution, calculated from the data of sulfur and nitrogen analysis

⁽³⁾ DS of amino groups, calculated from the data of sulfur and nitrogen analysis

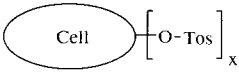
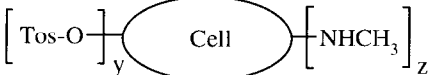
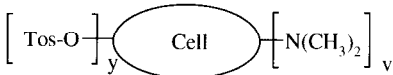
⁽⁴⁾ Yield [%]: quotient (*100) of amount of product isolated to the theoretical weight based on the composition calculated from the elemental analysis

⁽⁵⁾ products were obtained in very low yields by dialysis

Nucleophilic substitution of tosylcellulose with amines. Substitution reactions with both methylamine and dimethylamine were examined in detail with tosylcelluloses of DS 0.2-1.7 (Scheme 1). The DS_{Tos} of the starting tosylcelluloses **1a-h** and the results of the reaction with methyl- and dimethylamine are presented in Table 2.

Displacement of tosyl moieties was achieved completely with methylamine up to an initial DS_{Tos} of 0.9 (samples **3a-3d**) and with dimethylamine up to an DS of 0.6 (samples **4a-4c**). With higher DS_{Tos} values incomplete substitutions with both types of amine occurred, and the attainable maximum of amino functionalization was about DS 1 (samples **3e, 3f, 4d-4f**) (Figure 1).

Table 2. Reaction of cellulose tosylates with methylamine and dimethylamine.

| Cellulose tosylate | | Methylaminodeoxycellulose | | | Dimethylaminodeoxycellulose | | | | |
|-----------------------------------------------------------------------------------|------------------|-----------------------------------------------------------------------------------|------------------|------------------|------------------------------------------------------------------------------------|------------|------------------|------------------|--------------------------|
|  | |  | | |  | | | | |
| sample No. | x ⁽¹⁾ | sample No. | y ⁽²⁾ | z ⁽³⁾ | yield (%) ⁽⁴⁾ | sample No. | y ⁽²⁾ | v ⁽³⁾ | yield (%) ⁽⁴⁾ |
| 1a | 0.2 | 3a | 0.02 | 0.13 | 71 | 4a | 0.01 | 0.12 | 78 |
| 1b | 0.44 | 3b | 0.03 | 0.4 | 82 | 4b | 0.07 | 0.47 | 99 |
| 1c | 0.58 | 3c | 0.07 | 0.64 | 74 | 4c | 0.08 | 0.61 | 96 |
| 1e | 0.86 | 3d | 0.07 | 0.8 | 92 | 4d | 0.13 | 0.76 | 50 |
| 1f | 1.21 | 3e | 0.3 | 1.04 | 72 | 4e | 0.4 | 0.92 | 91 |
| 1h | 1.7 | 3f | 0.59 | 0.96 | 78 | 4f | 0.69 | 0.92 | 75 |

(1) DS_{Tos} calculated from the data of sulfur analysis

(2) DS of remaining tosylate groups after nucleophilic substitution, calculated from the data of sulfur and nitrogen analysis

(3) DS of amino groups, calculated from the data of sulfur and nitrogen analysis

(4) Yield: quotient (*100) of amount of product isolated to the theoretical weight based on the composition calculated from the elemental analysis

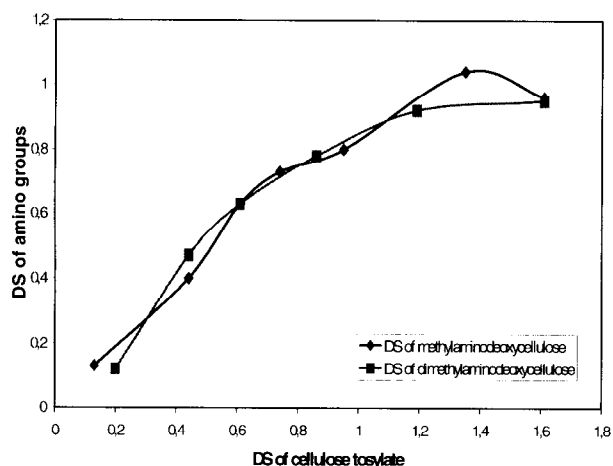


Figure 1. DS of tosylcelluloses versus DS of methyl- and dimethylamino groups

The residual tosylate remained unchanged. Considering the deviation resulting from elemental analysis data, the sum of both the DS of amino groups and the DS of remaining tosylate group correspond to the DS_{Tos} of the starting material. The results of elemental analysis could be confirmed by FTIR and ¹³C CP/MAS NMR spectroscopy. In ¹³C CP/MAS NMR spectra of tosylcellulose the tosyl resonances are clearly visible at 21.26 ppm, 130.05 ppm and 144.93, whereas in spectra of methylaminodeoxycellulose the disappearance of

these resonances together with the appearance of the methylamino moiety at 35.53 ppm can be observed (Figure 2). The products showed general poor solubility properties, but were highly swellable in water.

Grafting of 2-methyl-1,3-oxazoline onto cellulose. Cellulose tosylates with DS_{Tos} from 0.2 to 1.8 were used as initiators for the ring opening polymerization of 2-methyl-1,3-oxazolines to yield cellulose-graft-poly(N-acetyleneimine) [7]. By quenching with dimethylamine the amino functionalized products **5a**–**5g** were obtained (Scheme 1). DS_{Tos} values, molar ratios and grafting yields are summarized in Table 3.

As determined by elemental analysis, up to 7 N-acetyleneimine units could be grafted on average on one anhydroglucose unit (AGU). At DS_{Tos} values <0.4 the grafting reaction proceeded insufficiently, probably due to the heterogeneity of the reaction system. Cellulose tosylates with a DS>0.4 were sufficiently swellable in benzonitrile, leading to an increased grafting yield. FTIR spectra showed the lack of tosylate resonances and an additional adsorption band at 1649 cm⁻¹ which corresponds to C=O-resonance of the N-acetyleneimine unit (Figure 3).

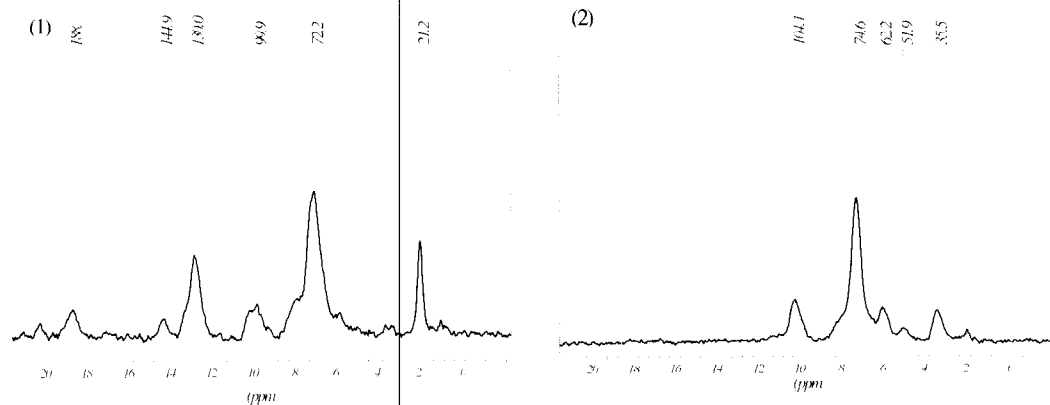


Figure 2. ^{13}C CP/MAS NMR- spectra of tosylcellulose (1) and methylaminodeoxycellulose (2).

Table 3. Grafting of 2-methyl-1,3-oxazoline (Oxaz) onto cellulose.

| Cellulose tosylate | | | Cellulose graftcopolymer | |
|--------------------|-----------|-----------------------|--------------------------|-------------------------|
| sample No. | $x^{(1)}$ | Oxaz/x ⁽²⁾ | sample No. | GP / AGU ⁽³⁾ |
| 1a | 0.2 | 50 | 5a | 0.48 |
| 1b | 0.44 | 45 | 5b | 5.28 |
| 1c | 0.58 | 50 | 5c | 4.93 |
| 1e | 0.81 | 50 | 5d | 4.06 |
| 1f | 1.21 | 30 | 5e | 5.77 |
| 1g | 1.32 | 25 | 5f | 6.98 |
| 1i | 1.81 | 20 | 5g | 2.81 |

(1) DS_{Tos} calculated from the data of sulfur analysis

(2) Molar ratio 2-methyl-1,3-oxazoline (Oxaz) per tosylate group (x)

(3) N-acetyleneimine units per remaining anhydroglucose units (AGU) based on the data of elemental analysis

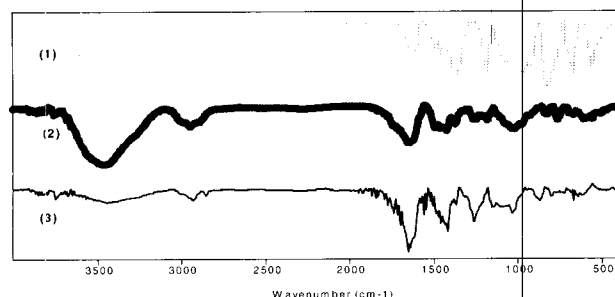


Figure 3. IR- spectra of tosylcellulose (1), cellulose-graft-poly (N-acetyleneimine) (2) and poly(N-acetyleneimine) (3).

For further characterization ^{13}C CP/MAS solid state NMR spectroscopy was applied. As shown in Figure 4 grafting is confirmed by peaks at 21.27 ppm, 46.53 ppm and 172.62 ppm. The different grafting yields, resulting from reaction with various DS_{Tos} , cause different intensity ratios of the ethyleneimine resonance *versus* the anhydroglucose resonances.

Conclusions

In contrast to reactions of tosylcellulose with cysteamine, which resulted in completely insoluble, non swelling products, reactions with dimethylamine and methylamine yielded highly swellable products in polar solvents. Up to a DS_{Tos} of 1 aminofunctionalized celluloses were obtained with high reproducibility. Grafting of 2-methyloxazolines onto tosyl celluloses with DS from 0.4 to 1.3 and subsequent quenching with diethylamine yielded amino functionalized celluloses containing up to 7 N-acetyleneimine units per AGU. Grafting yields calculated from elemental analysis data showed good correspondence to the data determined by ^{13}C CP/MAS NMR spectroscopy. These results demonstrate that homogeneously prepared cellulose tosylates with DS_{Tos} up to approx. 1 are appropriate intermediates for the synthesis of uniformly substituted amino-functionalized cellulose by nucleophilic substitution reactions as well as by grafting and end functionalization by quenching with suitable amines.

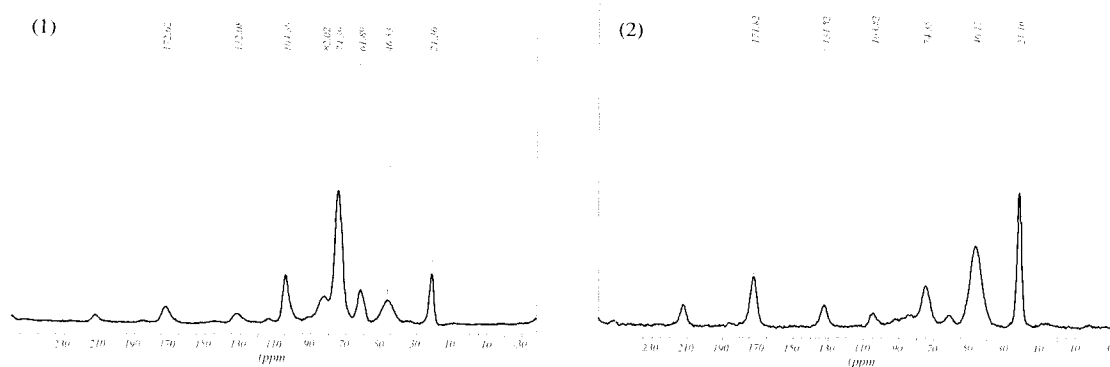


Figure 4. ^{13}C CP/MAS NMR spectra of cellulose-graft-poly(N-acetyleneimine) with $\text{DS}_{\text{Tos}}=0.2$ (**5a**) (1) and $\text{DS}_{\text{Tos}}=0.6$ (**5c**) (2).

References

1. Tiller, J.; Berlin, P.; Klemm, D. *Macromol. Chem. Phys.* **1999**, *200*, 1.
2. Berlin, P.; Tiller, J.; Klemm, D. *Papier* **1998**, *52*, 737.
3. Dawsey, T.R.; Newman, J.K.; McCormick, C.L. *Polym. Prep.* **1989**, *30*(2), 191.
4. Rahn, K.; Diamantoglou, M.; Klemm, D.; Berghmans, H.; Heinze, T. *Angew. Makromol. Chem.* **1996**, *238*, 143.
5. Heinze, T.; Rahn, K. *Papier* **1996**, *50*, 721.
6. Heinze, T.; Rahn, K. *Macromol. Symp.* **1997**, *120*, 103.
7. Kobayashi, S.; Kaku, M.; Saegusa, T. *Macromolecules* **1988**, *21*, 1921.

SIMULATION OF LENZING'S CHEMICAL RECOVERY SYSTEM

R. Mühlbacher

Lenzing AG, A-4860 Lenzing, Austria

Using the simulation software ASPEN-PLUS [1] the Lenzing Chemical Recovery System [2], a complex chemical recovery system of an acid magnesium bisulfite pulp cooking process, was modeled. It was possible for the first time to describe the solid-liquid-vapor equilibrium during the preparation of Lenzing's cooking liquor, dependent on temperature, pressure and concentration of inorganic compounds by means of computer-aided process simulation. After a time-consuming phase of model testing and model

verification, the process model has been used in Lenzing for many important applications, such as process optimization etc., and helped to save costs by replacing expensive mill trials by cheap virtual mill trials on the PC. One interesting example of application, the influence of cooking conditions on the chemical recovery efficiency, is discussed.

Keywords: computer-aided process simulation, ASPEN-PLUS, chemical recovery system, acid magnesium bisulfite pulp cooking process

Introduction

Within the last years, computer-aided process simulation (CAPS) has proved to be an indispensable tool in many fields of the chemical industry. The rapid improvement of hardware and software allows the use of highly sophisticated models concerning thermodynamics, chemistry and physics, and the access to extensive physical property data banks. Only these conditions make it feasible to model the complex processes in the chemical industry. Nowadays, process optimization and process design are the main fields of application of CAPS.

Strict environmental regulations and challenging competition force the pulp and paper industry to complex interdependent process cycles which soon lead the one-dimensional human ratio to its limits. In many cases CAPS is supportive.

The use of wood as a natural product combined with complex electrolyte cocktails, so-called cooking liquors, has made it impossible to model the cooking process or chemical recovery of pulp mills by means of CAPS so far. Using the simulation software ASPEN-PLUS [1] on one hand and investing all available research capacity on the other hand, the pulp-R&D-team of the

Lenzing AG succeeded in developing a process model of Lenzing's chemical recovery system.

Results and Discussion

Similar to other recovery processes of magnesium sulfite pulp mills, thin liquor coming from the digester is evaporated up to 65 %-DS (thick liquor) before it is burnt in the recovery boiler. The cooking liquor is recovered from boiler flue gas, digester relief gas, and boiler ash using countercurrent absorption columns (for aqueous solution of $Mg(HSO_3)_2$) and subsequent pressure-stage fortification systems (for absorption of gaseous SO_2). The actual recovery efficiency of cooking chemicals, calculated as MgO and sulfur, is about 80% each. A block scheme of this complex cycle process is displayed in Figure 1.

More than 100 blocks, such as reactors, mixers, separators, tanks, columns etc., were connected by material streams to a complex flow chart to model this recovery process (Figure 2). By reconnecting sources and/or destinations of streams on the Graphical User Interface (GUI) of ASPEN-PLUS it is easy to simulate different modes of operation.

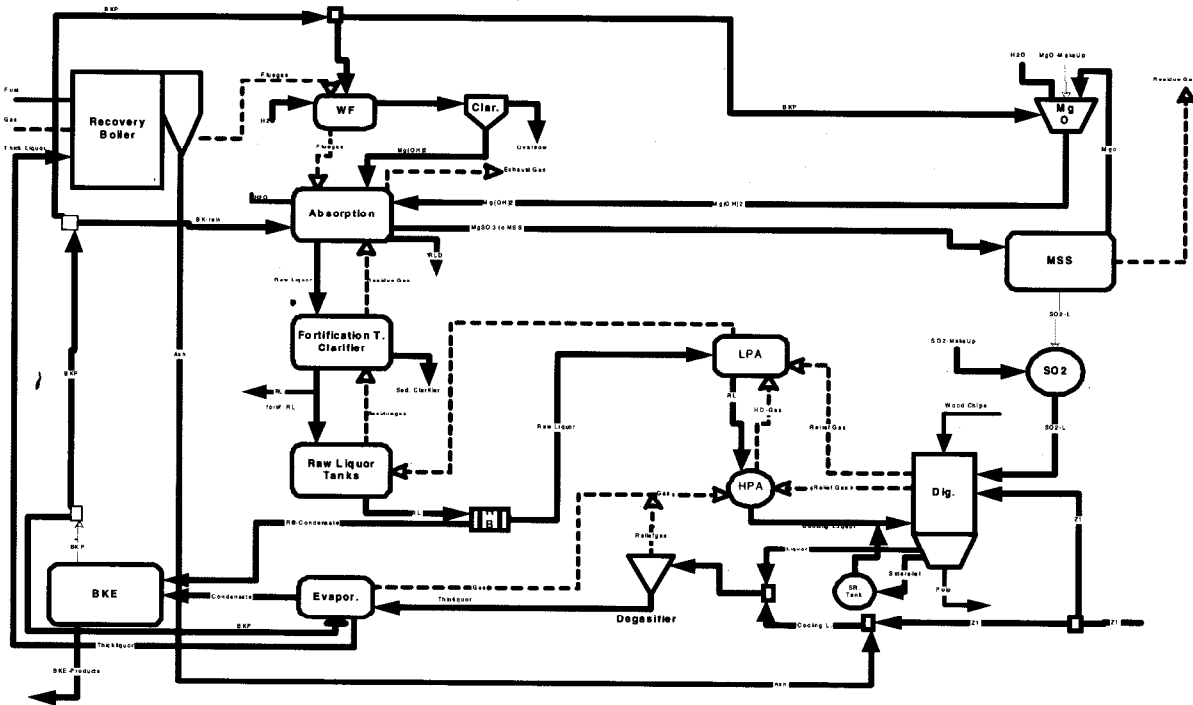


Figure 1. Lenzing's Chemical Recovery System.

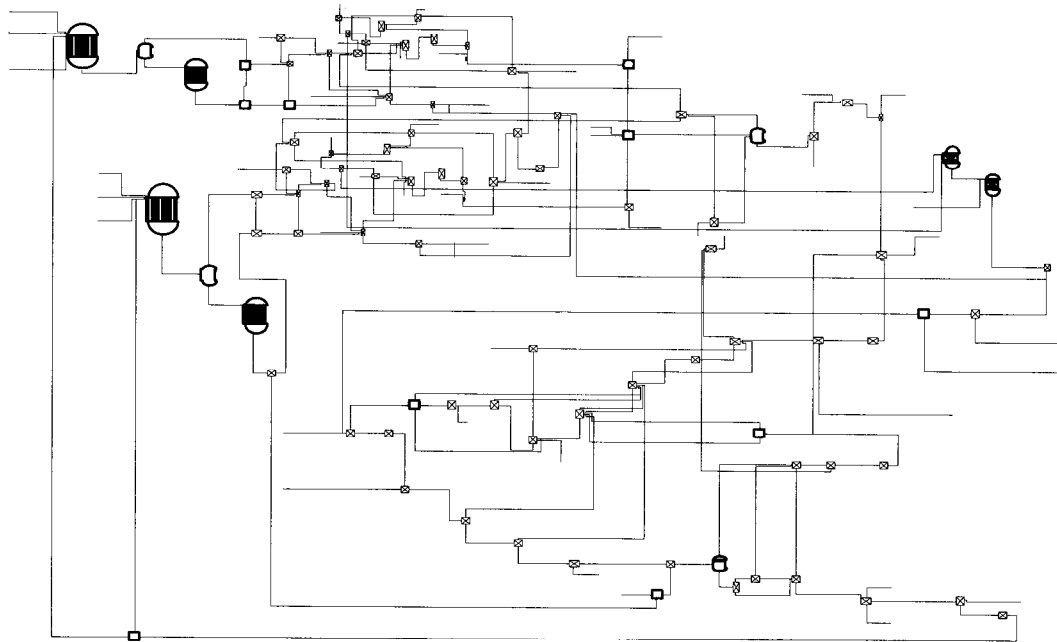


Figure 2. ASPEN-PLUS flow sheet.

While developing this process model a main problem was the investigation of solid-vapor-liquid equilibria (SVLE) inside the absorption columns which form the main part of flue gas purification system. ASPEN-PLUS contains a high performance electrolyte module based on the well known NRTL model (non random two liquid) [3] to calculate thermodynamic properties

of many interesting aqueous electrolyte systems. Unfortunately, due to missing property parameters within the Aspen databanks, it was not possible to describe the complex three-phase behavior of aqueous electrolyte systems consisting of $\text{Mg}(\text{HSO}_3)_2$, MgSO_3 , MgSO_4 and SO_2 .

Based on literature data [4, 5] the missing solubility parameters for $\text{MgSO}_3 \cdot 3\text{H}_2\text{O}$ and $\text{MgSO}_3 \cdot 6\text{H}_2\text{O}$ could be implemented in ASPEN-PLUS in cooperation with AspenTech. The ideal solubility behavior of MgSO_3 in water according to literature data is shown in Figure 3.

For the first time it was possible to describe the SVLEs during the preparation of Lenzing's raw liquor in multiple stage absorption towers

depending on system temperature, system pressure, pH, amount and concentration of chemical components (ions and gases) by means of CAPS. Only the correct simulation of this three-phase behavior allows a proper calculation of process-stream compositions of raw or cooking liquor streams, for instance, and the modeling of important phase separating units, such as clarifying tanks.

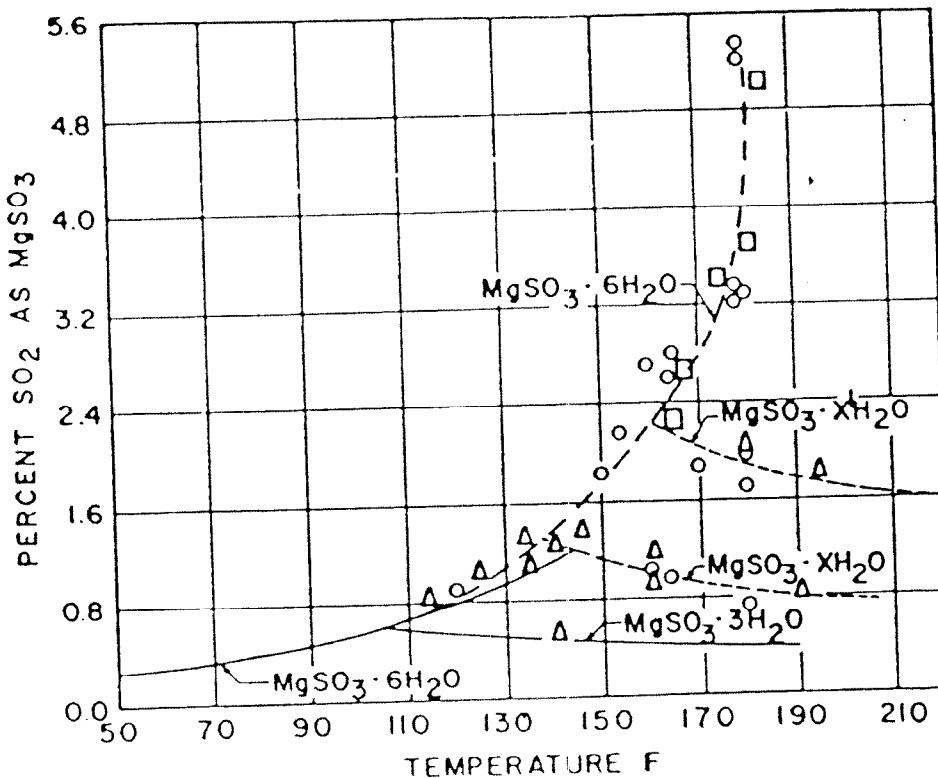


Figure 3. Solubility of MgSO_3 in water [5].

This new part of the recovery model was connected to the remaining process model which had been finished in a simplified way beforehand. After adjusting and verifying the recovery model by comparing real process data to simulation results, it has been successfully used in Lenzing for many important applications to improve the efficiency of the recovery, or to replace expensive mill trials by cheap virtual mill trials on the PC.

A very interesting question is for instance the influence of different cooking conditions, such as cooking temperature or the concentration of free- SO_2 and total- SO_2 of cooking liquor, on the efficiency of chemical recovery. The consumption of makeup chemicals can be used to evaluate the recovery efficiency in this case.

Calculating so-called „Sensitivity Analyses“ the concentration of total- SO_2 and free- SO_2 in the cooking liquor was varied at constant cooking temperatures. The corresponding consumption of makeup chemicals were simulated and stored as result tables.

The following charts (*cf.* Figures 4 and 5) show these results of process simulation. The numbers inside the charts represent the multiplier of normal makeup chemical consumption. Increasing the concentration of free- SO_2 and/or total- SO_2 cause(s) increasing amounts of makeup chemicals to be consumed. In other words, higher concentrations of free- SO_2 and/or total- SO_2 in the cooking liquor lead to lower recovery efficiencies due to larger losses in cooking chemicals.

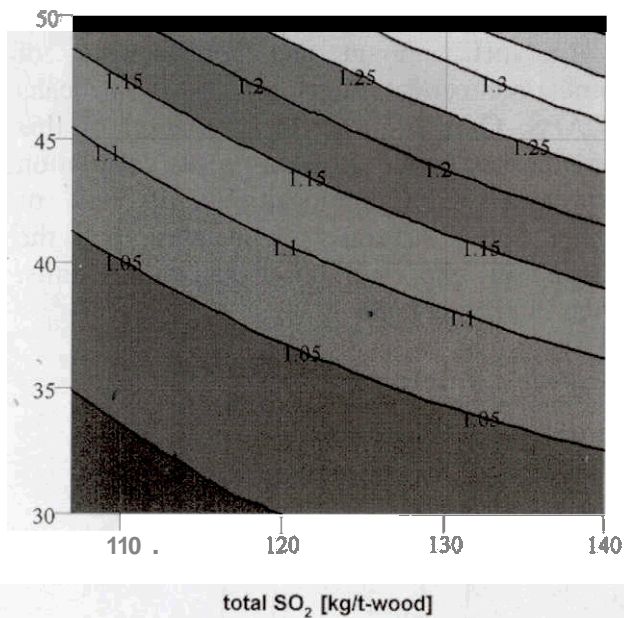


Figure 4. Consumption of makeup-SO₂ during cooking liquor preparation (free SO₂ [%] vs. total SO₂ [kg/t wood]).

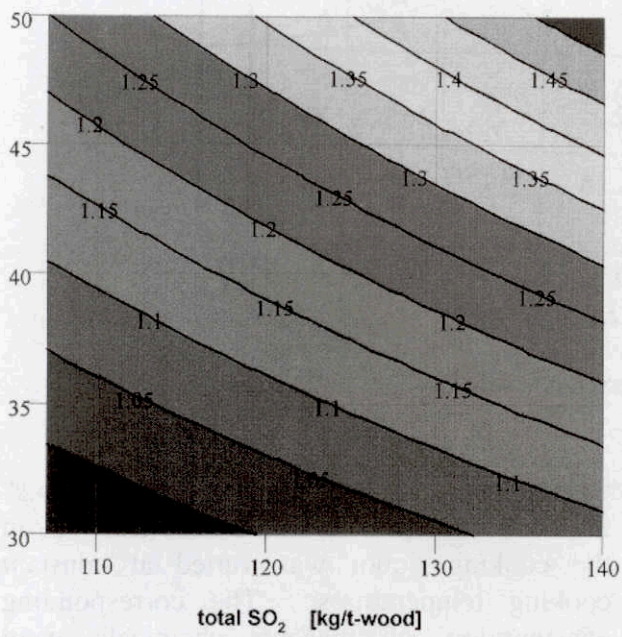


Figure 5. Consumption of makeup-MgO during cooking liquor preparation (free SO₂ [%] vs. total SO₂ [kg/t wood]).

Conclusions

A process model of a complex chemical recovery system of an acid magnesium bisulfite pulp cooking process was developed by means of the simulation software ASPEN-PLUS. For the first time it was possible to describe the three-phase behavior (SLVE) of process streams during the cooking liquor preparation. Although

it is a simplified computer model of a very complex process cycle it has been successfully applied in Lenzing many times to improve the efficiency of the recovery.

Acknowledgements

The author would like to express his gratitude to DI Juan-Carlos **Mani** (Manager, Business Support, AspenTech) for his support concerning the implementation of property data of MgSO₃ into the ASPEN-PLUS environment, to Dr. Gerhard Göttinger (R&D, Lenzing AG) for his scientific assistance and to Univ.-Doz. Dr. Herbert Sixta (Manager of Pulp Research Department, R&D, Lenzing AG) for his patience and mental support during the long developmental phase of the process model.

References

- [1] Aspen Plus, Version 9.3; AspenTech Inc., Cambridge, Massachusetts, USA.
- [2] Ingruber, O.V.; Kocurek, M.J.; Wong, A. Pulp and Paper **Manufacture**, Vol. 4 - Sulfite. Science & Technology, 3rd ed., Joint Textbook Committee of the Pulp and Paper Industry, TAPPI, 1985, pp. 281.
- [3] Chen, C.C.; Britt, H.I.; Boston, J.F.; Evans, L.B. *AICHE Journal* 1982, 28, 588.
- [4] Hagiwara, H. *Bull. Inst. Phys. Chem. Research* 1933, 12, 976.
- [5] Markant, H.P. et al., *Tappi* 1965, 48, 648.

DEMANDS ON MODERN PULPING PROCESSES

R. Patt, O. Kordsachia

Institute for Wood Chemistry, Leuschnerstr. 91
D - 21031 Hamburg, Germany

1. Introduction

Despite increasing paper and board consumption figures, chemical pulp production is stagnating and pulp prices are on a level which do not cover production costs. Increasing fiber demand is supplied by recycled fibers, the utilization of which has increased between 1990 and 1996 by almost 50 %. Today, the share of recycled fibers in the total fiber furnish for paper and board production is very close to the chemical pulp input. It can be predicted that this tendency will continue. In countries like Germany more than 60 % of all fibers used for paper and board production are recycled ones. About 80 % of all paper and board products can be recovered, but 20 % is not recoverable consisting of hygienic papers, long-living fiber products like books and non-recoverable materials, *e. g.*, decor papers. The actual recovery rate in Germany and Austria is around 70 %, and it is an open question as to how far the gap between 70 % and 80 % can be closed. From the actual development in waste paper processing and the quality needs for production of different paper and board qualities, it can be concluded that the maximum utilization rate may be about 70 %. But between the actual utilization rate of roughly 45 % and the maximum there is still a big gap which will be at least partly closed in the years to come (Fig. 1). It can be expected that pulp prices will be depressed as long as waste paper utilization rates are increasing. Growing secondary fiber utilization rates have an impact on the quality demand for virgin fibers and on their recyclability. Virgin fibers should be as strong as possible in order to substitute the poor strength properties of secondary fibers, and they should maintain their papermaking properties in the recovery cycle as far as possible.

Strong fibers require alkaline pulping conditions which provide a more intact fiber with a more homogeneous DP distribution in the different cell wall layers.

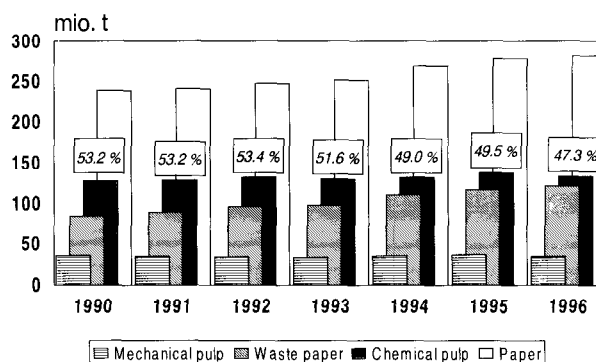


Figure 1. Share of different fibers used for paper and board manufacture [1].

The demands on modern alkaline pulping processes are listed in Table 1.

Table 1. Demands on modern alkaline pulping processes.

- Suitability for a wide spectrum of raw materials
- High pulp yield
- High pulp strength
- High process flexibility yielding different pulp types
- Good bleachability with chlorine free components
- Effective and simple recovery system
- No odor emission
- Closed mill
- Reasonable production costs
- Proven technology
- Good fiber recyclability

We will try to find out to what extent existing pulping processes are able to meet these demands and what has to be done in future to reach these targets.

2. Demands on pulping

Table 2 shows a summary on existing and potential pulping processes.

Table 2. Alkaline pulping processes.

| | |
|-----|-------------------------------------------------------------------------------------------------------------------------------------------------------------------------------------------------------------------------------------------------------------------------------------------------------------------------------------------------------------------------------|
| 1. | <i>Modified kraft pulping</i> |
| 1.1 | By chemical modification: <ul style="list-style-type: none"> - Polysulfide - AQ (anthraquinone) - Polysulfide / AQ |
| 1.2 | Variations of sulfidity and alkali profile during the cook by modification of the cooking procedure: <ul style="list-style-type: none"> - Modified continuous cooking (MCC) - Extended modified continuous cooking (EMCC) - Isothermal cooking (ITC) - Super-Batch - Rapid Displacement Heating (RDH) - Enerbatch |
| 1.3 | Combinations of above modifications |
| 2. | <i>Modified soda pulping</i> |
| 2.1 | Soda/AQ |
| 2.2 | Soda/AQ/methanol |
| 3. | <i>Modified sulfite pulping</i> |
| 3.1 | Neutral sulfite/AQ |
| 3.2 | Alkaline sulfite/AQ |
| 3.3 | ASAM |
| 3.4 | Two stage processes <ul style="list-style-type: none"> neutral - alkaline/AQ neutral - alkaline/AQ/methanol |

Modifications of the kraft pulping process include all the well-known continuous and batch processes which try to realize the principles of extended delignification or modified cooking [2]:

- levelled out alkali profile throughout the cook,
- high sulfidity in the beginning,
- low concentration of dissolved organics, in particular in the final phase of the cook,
- low temperature.

Chemical modifications of the kraft process which are in industrial use refer to the application of anthraquinone or polysulfide or both. In modern kraft pulping these additives are charged in modified processes following the principles of extended delignification.

Soda/AQ pulping can be successfully applied to annual plants and hardwoods. The resulting pulps have lower yield and strength properties compared to kraft pulps. These processes can not be regarded as a convincing alternative to kraft and modern alkaline sulfite pulping.

Soda/AQ/methanol liquors are able to pulp softwoods as well. However, the first industrial installation of this process failed. We tried to improve the process by optimization of some of its parameters. The pulp properties of these modified organosolv cooks were very close to conventional kraft and the yield was higher. This process shows no convincing advantages when compared with the actual state of modified kraft and alkaline sulfite pulping development [3].

The chemical modifications of alkaline sulfite processes include the addition of AQ and AQ in combination with methanol, and 2-stage-processes working mainly under alkaline conditions, which of course could be improved by additives like anthraquinone and methanol in one or the other stage. All these processes and their modifications are able to pulp any generally appropriated raw material.

2.1 Kraft pulping

Recent developments in kraft pulping improve the selectivity of this process and enhance pulp yield which was the most serious disadvantage in softwood kraft pulping. This was achieved by combination of the principles of extended delignification and addition of anthraquinone and/or polysulfide [4]. But in industrial practice it is difficult to realize all principles of extended delignification in the same cook, because this would require not only different concentrations of chemicals in different cooking phases, but also varying sodium / sulphur ratios during cooking. This ratio can only be varied within small limits in current mills. The chemical recovery does not separate sodium and sulphur compounds. The integration of bleach alkali into the recovery cycle would intensify this problem. Different approaches have been undertaken to provide flexible Na/S ratios for cooking and generating bleach alkali. A summary of these options is presented by Herschmiller [2].

Compared to sulfite pulps, softwood kraft pulps have lower yields due to increased glucomannan

dissolution. This can be overcome by different means. Olm *et al.* (1998) performed spruce/pine kraft ITC cooks and applied different process variations [4]. Addition of 2 % of elemental sulphur in a standard ITC cook increased the pulp yield from 46.5 % to 48.5 % at a kappa number of 24. The glucomannan content of the pulp increased from 8.5 to 11.2 %. The application of both, polysulfide and AQ, resulted in a synergistic yield effect. The pulp yield at kappa number 24 increased to 49.9 %, and the glucomannan content reached 12 %. The highest yield (51.8 %) was achieved by green liquor / H₂S pretreatment followed by a standard cook. In this trial the glucomannan content of the pulp was 16 %.

The authors found a strong correlation between pulp yield and strength. Increased yield resulted in 10 % tensile and about 15 % tear strength reduction which can be attributed to the lower number of load-bearing fibers in the paper sheet. The yield gain of the modified ITC cooks could at least be partly preserved in bleaching. The strength differences of bleached polysulfide and standard ITC pulps change a little bit. In comparison with unbleached pulps the difference in tensile strength is reduced, whereas the difference in tear strength is increased.

2.2 Alkaline sulfite pulping

The knowledge of the action of anthraquinone in alkaline pulping processes offers a chance to use catalyzed alkaline sulfite processes for the production of bleachable pulp grades. Pulp yield is better than in conventional kraft pulping, but when softwoods are used as raw material, delignification is limited to a kappa number around 40. On the other hand, the bleachability of these pulps is better [5]. Some authors claim that the strength of AS-AQ pulps is equivalent or even superior to kraft, but other results show that these pulps have some deficiencies in particular in tear strength [6, 7]. The limited final delignification and the rather complicated recovery systems for alkaline sulfite processes were the main reasons for the diminishing interest in these processes. Current developments in multiphase cooking, pulp bleaching and chemical recovery could be a basis for a renewed interest in these processes.

Alkaline sulfite pulping was also the basis for the development of ASAM pulping. The presence of methanol in the alkaline sulfite/AQ-system provides a highly selective final delignification yielding low kappa number pulps with high viscosity and consequently high strength. ASAM delignification proceeds in a very smooth way, preserving in particular the wood cellulose. We found that during softwood ASAM delignification only few cellulose losses occur when delignification exceeds kappa number 25 [8]. Table 3 shows the carbohydrate composition of ASAM pine pulp at different kappa numbers. The hemicellulose content of these pulps is similar to that of standard kraft pulps, but ASAM pulps have a much higher yield. This demonstrates that the high yield of ASAM pulps can be attributed to the stability of the cellulose in this pulping process.

Table 3. Carbohydrate composition of pine ASAM pulps at different kappa number.

| Kappa no. | Cellulose (%) | Glucomannan (%) | Xylan (%) |
|-----------|---------------|-----------------|-----------|
| 33.1 | 84.9 | 9.1 | 5.8 |
| 27.5 | 85.6 | 8.5 | 5.7 |
| 22.0 | 86.1 | 8.3 | 5.7 |
| 19.5 | 86.7 | 7.6 | 5.7 |

Table 4. Spruce/pine ITC-PS/AQ kraft (4) versus spruce and pine ASAM pulps.

| Pulp | Kappa # | Viscosity, ml/g | Total yield, % on wood |
|--------------|---------|-----------------|------------------------|
| Standard ITC | 23.8 | 1200 | 46.5 |
| ITC-PS | 24.5 | 1190 | 48.7 |
| ITC-PS/AQ | 23.6 | 1180 | 49.9 |
| Pine ASAM | 24.0 | 1340 | 50.9 |
| Spruce ASAM | 19.9 | 1321 | 49.7 |

The table shows that ASAM has a clear yield advantage. The PS/AQ supported ITC cook has about 1 % yield less than an ASAM cook. It is evident that the selective delignification in

ASAM pulping preserves carbohydrates even though the temperature in ASAM cooking is much higher than in kraft ITC. ASAM pulp viscosity at the same kappa number level is around 150 viscosity units higher. Even the low kappa number spruce ASAM pulp has an extremely good viscosity. In this cook the maximum temperature was lowered to 175 °C instead of 178 in pine ASAM cooking. The high selectivity of the ASAM process results in excellent pulp strength. Figure 2 shows the tear-

tensile plot of kraft ITC pulp from a mixture of spruce and pine and the corresponding pulps from PS and PS/AQ supported cooks [8,4]. Despite the lower kappa number the ASAM spruce pulp has a higher strength than the ITC and the modified ITC pulps. If the strength properties of the different pulp types are calculated on the same yield basis, the superiority of the ASAM pulps would be even more pronounced.

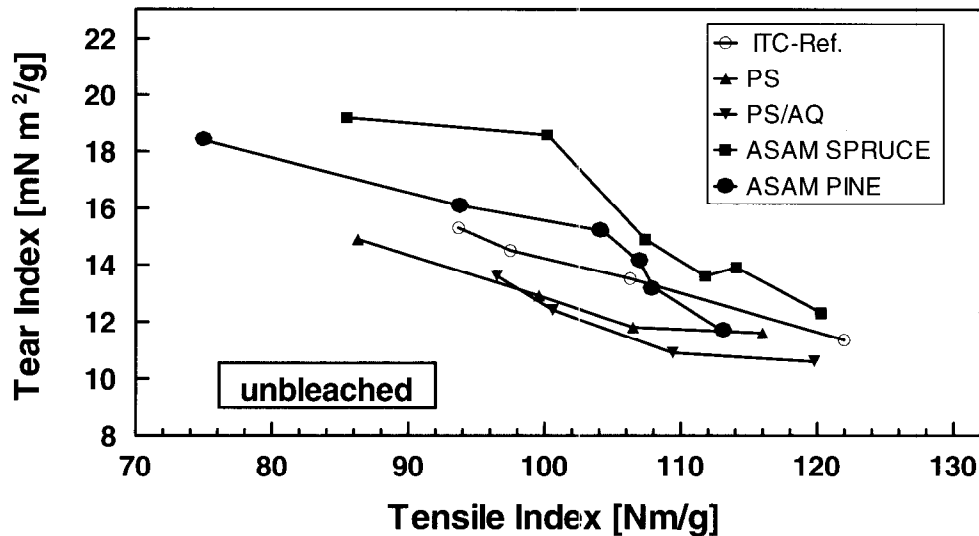


Figure 2. Tear/tensile plot of unbleached Kraft and ASAM pulps.

3. Bleaching

One of the major challenges of the pulp industry is the closure of the water cycle of a mill. This is more easily attainable when no chlorine containing compounds are used for bleaching because otherwise chlorine has to be removed from the loop. The closure of the bleach plant and moreover the closure of the total mill requires chlorine free bleaching, consequent counter-current washing and utmost similar pH and temperature conditions in different bleaching stages. Neither ECF nor actual TCF sequences using ozone are accomplishing these prerequisites in an ideal way. TCF bleaching of kraft pulp is costly and results in lower pulp strength and yield. This means that TCF bleaching has to be improved. Regarding costs and pulp properties it must be competitive with ECF bleaching and should facilitate mill closure.

We tried to improve TCF bleaching by catalyzing peroxide containing stages. This enhances delignification to a magnitude in which bleaching of kraft pulps can be performed in a short sequence applying exclusively alkaline bleaching stages [9].

Olm *et al.* performed TCF bleaching of the earlier mentioned ITC-kraft pulps. The standard kraft pulp as well as the PS-ITC pulp were bleached in a OQ(OP)AZQ(OP) sequence. For TCF bleaching of the ASAM spruce pulp we applied the same sequence and additionally an OQ(OP)_{Cat}P short sequence where a small amount of catalyst was charged in the OP stage. The results are listed in table 5.

The kraft pulps were bleached to 89 % ISO brightness and the brightness target of the ASAM pulps was 88 % ISO. Therefore, the results are not directly comparable. It is known that the bleachability of ASAM pulps is superior to kraft

[10]. The results in Table 5 show that the viscosity gain of ASAM pulps can be preserved especially when the catalyst is applied in the short sequence. The catalyst permits a very selective bleaching with reduced temperature and reaction time.

The high pulp viscosities of ASAM pulps are reflected in the pulp strength (Figure 3). In addition to the yield advantage of the ASAM pulps, they are stronger particularly at beating levels, which are used for paper production. If the strength properties of the different pulps are compared on the same yield basis, the strength advantage of ASAM pulps would be even higher.

Table 5. TCF bleaching of kraft-ITC and ASAM pulps.

| Pulp | Sequence | B. ^a | V. ^b | Y. ^c |
|--------------|-------------------------|-----------------|-----------------|-----------------|
| Kraft-ITC | OQ(OP)AZQ | 89.0 | 800 | 43.4 |
| Pine/Spruce | (OP) | | | |
| Kraft-ITC/PS | OQ(OP)AZQ | 89.0 | 830 | 45.4 |
| Pine/Spruce | (OP) | | | |
| ASAM-Spruce | OQ(OP)AZQ | 88.1 | 904 | 47.8 |
| ASAM-Spruce | OQ(OP) _{Cat} P | 87.3 | 1013 | 47.5 |

^a Brightness (% ISO)

^b Viscosity (ml/g)

^c Yield (% on wood)

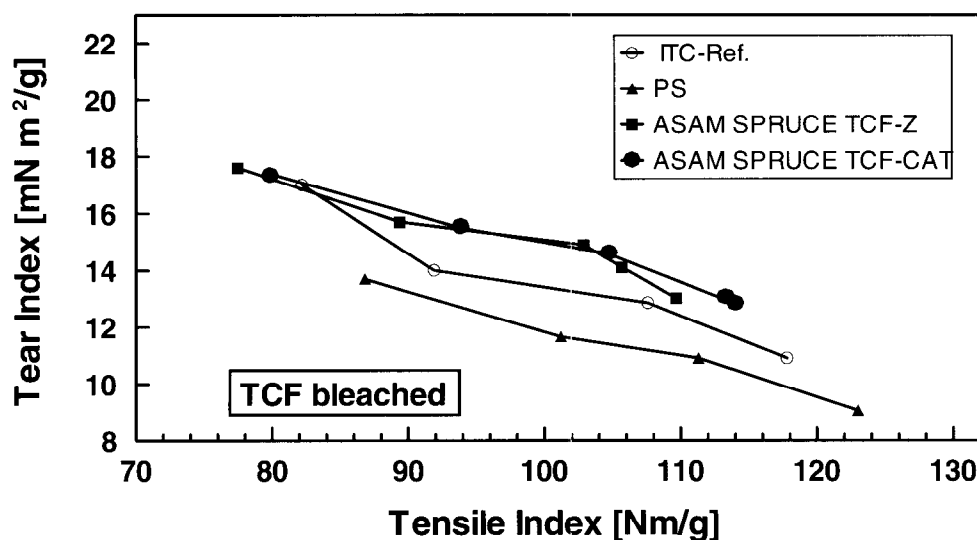


Figure 3. Tear-tensile plot of TCF bleached kraft and ASAM pulps.

4. Recovery

The application of all principles of extended kraft cooking requires a new recovery system where sulphur and sodium compounds are split into separate streams. The conversion of Na_2S to H_2S and Na_2CO_3 is complicated, and a simpler way to separate sodium and sulphur compounds would benefit kraft as well as alkaline sulfite processes. From the existing alternatives, black liquor pyrolysis or gasification seems to be the best [2]. Figure 4 shows a flow sheet of a sodium sulfide recovery system based on black liquor gasification.

Concentrated black liquor is fed into the reactor and gasified in the absence of air at temperatures

below the melting point of the sodium compounds. The organic part of the black liquor is transformed to carbon and volatile hydrocarbons. Sulphur is reacted into H_2S , and sodium into sodium carbonate. This sodium carbonate, together with the carbon, forms a powder. All other compounds leave the reactor in the gas flow. Solids have to be removed from this flow in a cyclone. In a kraft recovery unit of this type the pyrolysis gas has to be cooled and the H_2S is absorbed in a sodium carbonate solution to form sodium sulfite. The remaining hydrocarbons are burnt to generate energy. The sodium carbonate powder must be dissolved in water, and then the carbon has to be filtered off and burnt to generate energy as well.

Such a gasification system is more appropriated to recover sodium sulfite than kraft chemicals. In case of gasification of sodium sulfite black liquors, the gas stream can be directly burnt and oxidized, and the resulting SO_2 can react with

sodium carbonate to form sodium sulfite. A small part of the cleaned sodium carbonate has to be causticized to generate NaOH for cooking and bleaching. But this will not exceed 25% of the total process chemicals.

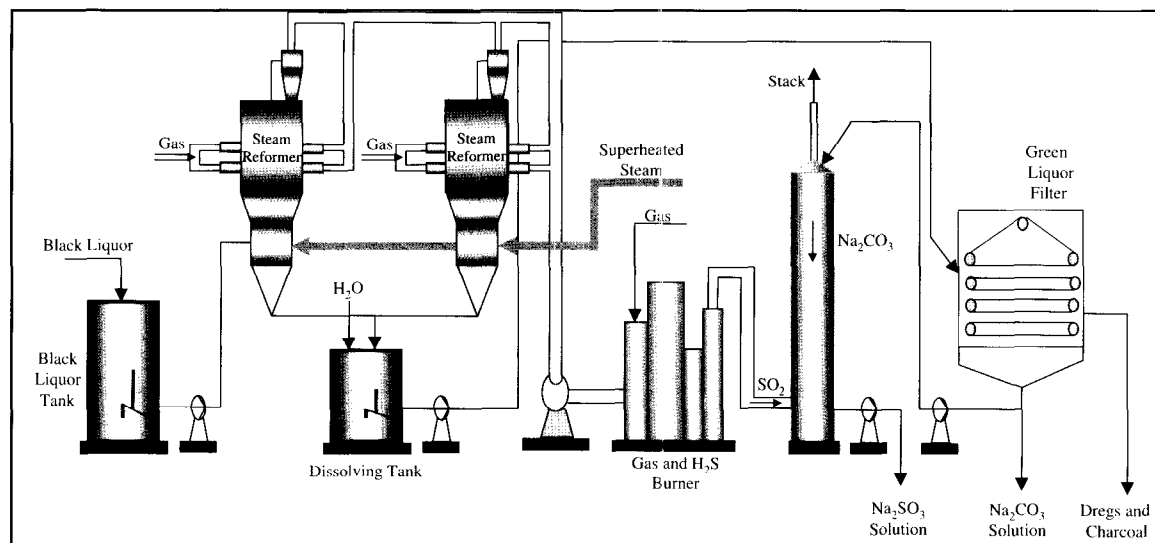


Figure 4. Simplified flow sheet of a black liquor pyrolysis process [11].

The industrial application of such a recovery system would benefit all alkaline pulping processes. Splitting of sodium and sulphur compounds renders possible the application of all principles of extended delignification in kraft pulping, and the alkali supply to alkaline TCF bleaching stages. In particular, in modified kraft cooking, the Na/S ratio can be adjusted to the needs of the different cooking phases.

Black liquor recovery would benefit the closure of the mill as well. Non-process elements (NPE) can be removed from the loop in an easier way [11]. The low gasification temperature which keeps sodium carbonate in solid form instead of forming a melt, facilitates the separation of most inorganic NPEs together with the carbon by filtering them off. By carbonation of the green liquor, the pH can be adjusted to optimize the separation efficiency for NPEs like silicon and aluminum [12].

Potassium will be recycled and does not harm cooking and bleaching reactions. Chlorine, entering the process mainly with wood, will be partly released as HCl (50%) and can be scrubbed from the gas flow by a conventional cold gas quench.

It seems that the investment as well as operating costs are lower compared to conventional furnaces. The thermal efficiency of gasification is much better than in conventional recovery systems and gasifiers can be adjusted to any mill size.

5. Conclusions

The pulping process of the future will be an alkaline one due to the better strengths properties of the resulting pulps. Modifications of the kraft process are making great progress, but the application of these modifications complicates the technical performance of the process. The best pulp quality can be produced with the ASAM process. ASAM pulps are obtained in high yield and their strength and bleachability are superior to kraft pulps. Moreover, the ASAM cooking procedure is simpler than the modified kraft pulping techniques.

Chlorine free pulp bleaching has to be improved to enhance its selectivity and reduce its costs. Corresponding developments are underway. It can be assumed that activated and catalyzed

oxygen and peroxide bleaching will overcome this problem in the near future.

All principles of modified kraft cooking can only be applied when sodium and sulphur compounds can be split in two streams in the chemical recovery system. Black liquor gasification is a promising approach reaching this goal. This would also render possible the generating of bleach alkali. The implementation of such a recovery system in industry would benefit alkaline sulfite more than kraft processes because the pyrolysis gas can directly be burnt to form SO₂ and generate energy. The removal of non-process elements from the loop can be achieved easier and only a small share of the total Na₂CO₃ stream has to be caustized.

Alkaline sulfite processes accomplish the prerequisites for a closed mill operation to a higher extent than kraft mills. Therefore, the development of alkaline sulfite multi-stage processes similar to modified kraft pulping bears a better option for further improvement of environmentally harmonized and economically favorable pulp production.

6. References

- [1] Verband Deutscher Papierfabriken. Ein Leistungsbericht der deutschen Papier- und Zellstoffindustrie. Papier 1998, VDP: Bonn, 1998.
- [2] Herschmiller, D.W. Kraft cooking with split sulfidity - a way to break the yield barrier? *Proceedings*, Tappi - Breaking the yield barrier symposium, Atlanta, 1998, 59-68.
- [3] Neumann, U.; Kordsachia, O.; Patt, R. Aufschluß von Kiefernholz im System Natronlauge / Anthrachinon / Methanol. *Papier* **1997**, 51, 573.
- [4] Olm, L.; Tormund, E.; Bergnor Gidnert, E. Possibilities to increase the pulp yield in a kraft cook of ITC-type. Tappi - Breaking the yield barrier symposium, Atlanta, 1998, 69-78.
- [5] Ojanen, E.; Tuppala, J.; Virkola, N.E. Neutral Sulfite Anthraquinone (NS-AQ) Cooking of Pine and Birch Wood Chips. *Paperi ja Puu* **1982**, 64, 453-464.
- [6] Kettunen, J.; Laine, J.E.; Yrjälä, J.; Virkola, N. E. Aspects of Strength Development in Fibers Produced by Different Pulping Methods. *Paperi ja Puu* **1982**, 64, 205-211.
- [7] Ingruber, O.V.; Allard, G.A. Alkaline Sulfite Pulping for Kraft Strength. *Pulp Paper Mag. Can.* **1973**, 74, 84-99.
- [8] Oltmann, E.; Kordsachia, O.; Patt, R. Abgrenzung der Prozessschritte zur Herstellung chlorfrei gebleichter ASAM-Zellstoffe. Teil 1: Untersuchungen zur Grenzpunktbestimmung zwischen dem Aufschluß und der chlorfreien Bleichsequenz OZEP. *Papier* **1992**, 48, 55-68.
- [9] Mielisch, H.J.; Kordsachia, O.; Patt, R.; Schubert, H.L. Novel Kraft pulp bleaching using catalyzed peroxide treatments. *Proceedings*, Tappi Intern. Pulp Bleaching Conf., Helsinki, 1998.
- [10] Teder, A.; Sjöström, K.A. Comparison of the Bleachability in TCF-Sequences for Alkaline Sulfite and Kraft Pulps. *Pulp and Paper Science* **1996**, 8, 296-300.
- [11] Rockvam, L.N.; Tenore, F. Spent Liquor Steam Reforming and Recovery. *Proceedings*, Int. Chem. Recovery Conf., Toronto, 1995.
- [12] Patt, R.; Kordsachia, O.; Schubert, H.L.; Borgards, A. System Closure Possibilities for Modern Alkaline Pulping Processes. *Papier* **1998**, 52, 10A, V1-V7.

THE EFFECT OF QUATERNARY AMMONIUM COMPOUNDS ON PULPING

A. Pfeifer, I. Tanczos, H. Schmidt

Institute of Chemical Technology of Organic Materials,
Johannes Kepler University Linz, Altenbergerstraße 69, A-4040 Linz, Austria

Recently, a new sulfur-free alkaline pulping process, called Quatam process, was developed which uses an aqueous solution of a quaternary ammonium compound, tetramethylammonium hydroxide (TMAH) as the reactive agent. Comparing the delignification results using different quaternary ammonium hydroxides shows that with increasing molecular weight of the chemicals the pulping effect decreases. TMAH seems to be the most effective by far, which can be seen in the drastic reduction of the kappa numbers. The Quatam process was

advantageously applied in the pulping of different kinds of wood types (hardwood and softwood species) and compared with soda pulping. According to the experiments, mixtures of TMAH and sodium hydroxide, depending on the mixing ratio, can be nearly as effective in delignification as the pure TMAH.

Keywords: quaternary ammonium hydroxides, tetramethylammonium hydroxide, delignification, pulping process, Quatam-process

Introduction

The conventional delignification processes (kraft and sulfite) use sulfur-containing pulping liquors. In spite of nearly closed process systems and the thorough recycling of the chemicals, these processes are connected with water and air pollution.

A few years ago, a new environmentally friendlier very effective pulping process, the Quatam-process [1] was introduced. The new pulping chemical is a quaternary ammonium base, the quaternary ammonium bases are more similar to alkali metal hydroxides than to amines. Studies with tetramethylammonium hydroxide under different pulping conditions [2, 3, 4] have shown that the Quatam process has many advantages over the conventional sulfite and kraft processes. Lower Kappa numbers and higher brightness at shorter cooking times as well as „easy-to-bleach” pulp can be obtained.

There are some studies solely relating to the swelling and dissolving of cellulose [5, 6] in quaternary ammonium hydroxides but the effect of different quaternary ammonium compounds has never been studied in delignification of

wood. Due to their highly basic character and the ability to form hydrated ion dipoles in aqueous solution, tetraalkyl- or trialkylarylammonium hydroxides were found to be good swelling agents for cellulose in a similar manner to alkali hydroxides. Tetraalkylammonium bases with a molecular weight of less than 150 are swelling agents, while those of higher molecular mass can be actual solvents for cellulose.

Recently, tetramethylammonium hydroxide is used in the pyrolysis-GC/MS analysis and also in the analysis of lignin and wood samples, too [7, 8, 9].

The aim of the present study was to examine the pulping effect of different quaternary ammonium hydroxides as well as the effectiveness of TMAH and sodium hydroxide in the pulping of different hardwood and softwood species. Experiments were also carried out with mixtures of TMAH and sodium hydroxide as pulping liquors.

Experimental

Materials. Tetramethylammonium hydroxide was donated by Inspec Fine Chemicals CFZ

Zaltbommel (Netherland) as a 25 % aqueous solution. Tetraethyl- and tetrabutylammonium hydroxides (TEAH and TBAH, 20 % aqueous solutions) and benzyltrimethylammonium hydroxide (BTAH, 40 % aqueous solution) were purchased from Merck.

Scotch pine (*Pinus Silvestris*), eucalyptus (*Eucalyptus Urugrandis*) and acacia (*Robinia Pseudoacacia*) wood chips were provided by Beloit Austria GmbH and beech wood (*Fagus Silvetica*) by Lenzing AG.

Methods. For the pulping experiments as a first step a prewetting and prehydrolysis of the wood (ca. 25 g) was carried out with water at 100 °C for 20 minutes. The dripped wood chips were placed in a 100 ml laboratory batch reactor and the necessary pulping liquor (prepared from TMAH / NaOH / TEAH / TBAH / BTAH, respectively) was added, taking into consideration the water content of the chips. The closed reactor was heated up in an oil bath reaching the desired temperature within 25 minutes and was held at a temperature of 170 °C for 60 minutes. The cooking liquor was not circulated. Finishing the reaction the black liquor was separated by filtration and the pulp was washed with distilled water (if necessary disintegrated in a mixer) and air dried.

For the characterization of the fibers the kappa-number was determined according to DIN 54 357. The ISO brightness was measured with a Perkin Elmer Lambda 14 UV/VIS spectrometer with an integrated sphere (Labsphere RSA-PE-20) according to Tappi T 452 om-92. Spectralon SRS-99-010 standard was used for calibration.

Results and Discussion

Experiments with different quaternary ammonium hydroxides. The effectiveness of tetramethylammonium hydroxide was already studied in the Quatam process [4]. According to our experiments other quaternary ammonium hydroxides, TEAH and BTAH, have also a pulping effect without significantly dissolving the cellulose (pulp yield: 49,2 %, 51,1 %, respectively). The results of the laboratory pulping cookings (Figure 1) show that with increasing chain length or molecular weight of the quaternary ammonium hydroxides, the

residual lignin content of the pulp becomes higher, and so the kappa number will increase. The same tendency was detected with TBAH.

The measured values of brightness correspond to the kappa numbers. With a higher content of residual lignin a lower degree of brightness was measured (Figure 2).

Among the tested compounds, TMAH turned out to be the best quaternary ammonium base for delignification.

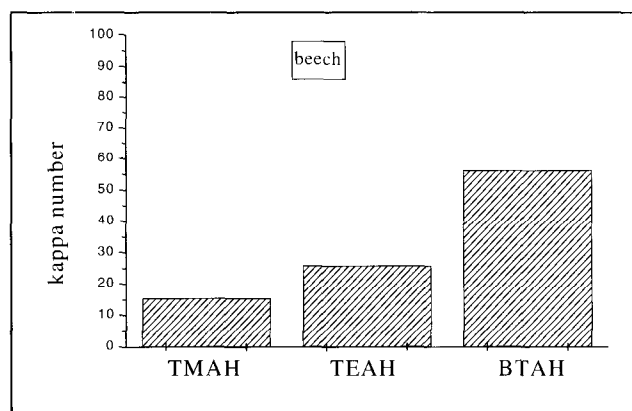


Figure 1. Effect of different quaternary ammonium bases on the kappa number in delignification of beechwood (T=170 °C, t=60 min, c=1.2 mol/l, LR=1:5).

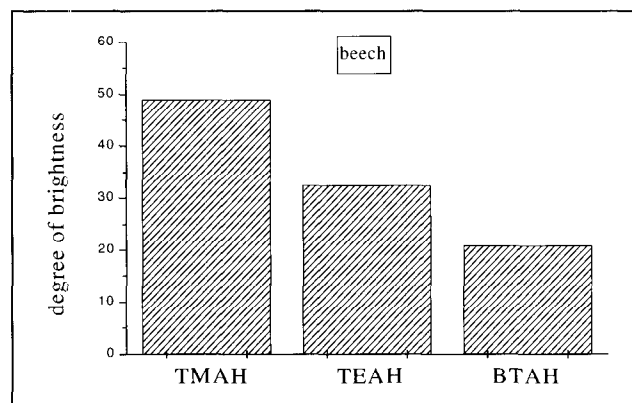


Figure 2. Effect of different quaternary ammonium bases on the brightness of pulp in delignification of beechwood. (T=170 °C, t=60 min, c=1.2 mol/l, LR=1:5).

Experiments with different kinds of wood. A set of experiments was carried out to observe the difference in the pulping effect of TMAH and NaOH depending on the type of wood. Beech, eucalyptus and acacia from the hardwoods and scotch pine as a softwood were chosen as representatives. The results are shown in Figure 3 and Figure 4. As with other processes, the delignification of softwood is more difficult than that of hardwood even at using TMAH. It means

that a higher concentration needed for a proper delignification of softwood in the Quatam process, too. But in all cases much less kappa numbers were advantageously achieved in pulping with TMAH than in pulping with NaOH. The use of TMAH results in a kappa number reduction of 30-50 % in most of the cases accompanied with a slight loss in yield of 1-2 %.

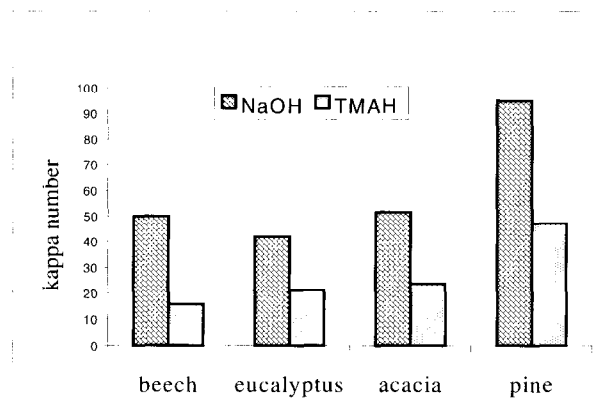


Figure 3. Kappa numbers of pulps from different kinds of wood: comparison of delignifications with TMAH and NaOH ($T=170\text{ }^{\circ}\text{C}$, $t=60\text{ min}$, $c=1.2\text{ mol/l}$, $LR=1:5$; for scotch pine $LR=1:5.5$).

In accordance with the lower kappa numbers the degree of brightness of the produced pulp was much higher in the delignification with TMAH for all kinds of the wood (Figure 4).

Experiments with mixtures of TMAH and NaOH. Investigation with mixtures of TMAH and NaOH were aimed at replacing the more expensive TMAH at least partly for the cheaper NaOH without losing the advantages provided by TMAH.

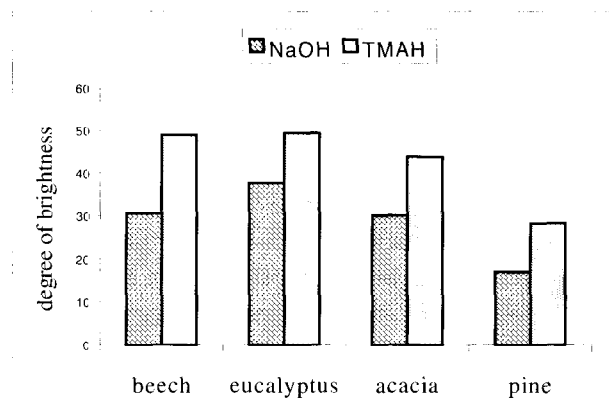


Figure 4. Brightness of pulps from different kinds of wood: comparison of delignifications with TMAH and NaOH ($T=170\text{ }^{\circ}\text{C}$, $t=60\text{ min}$, $c=1.2\text{ mol/l}$, $LR=1:5$; for scotch pine $LR=1:5.5$).

The results (Figure 5) show that the kappa number of beechwood pulp strongly depends on the composition of the pulping liquor. A mixture of 40 mol% TMAH and 60 mol% NaOH leads to a technological and economical optimum. The effect of the composition of the pulping liquor on the kappa number in softwood delignification is even more intensive (Figure 6). For softwoods a higher content of TMAH, about 60 %, is necessary to maintain the advantages of the Quatam process.

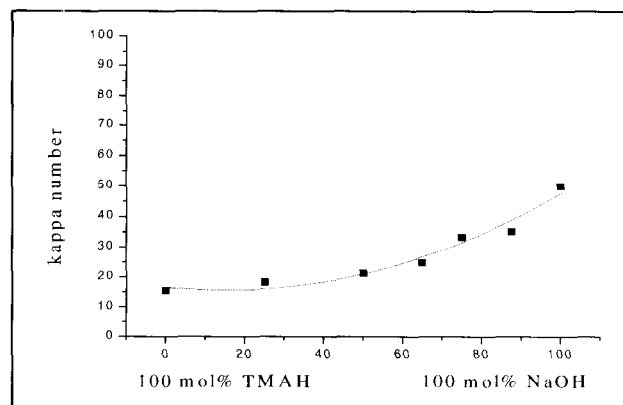


Figure 5. Kappa numbers of beechwood pulp depending on the composition of the pulping liquor ($T=170\text{ }^{\circ}\text{C}$, $t=60\text{ min}$, $c=1.2\text{ mol/l}$, $LR=1:5$).

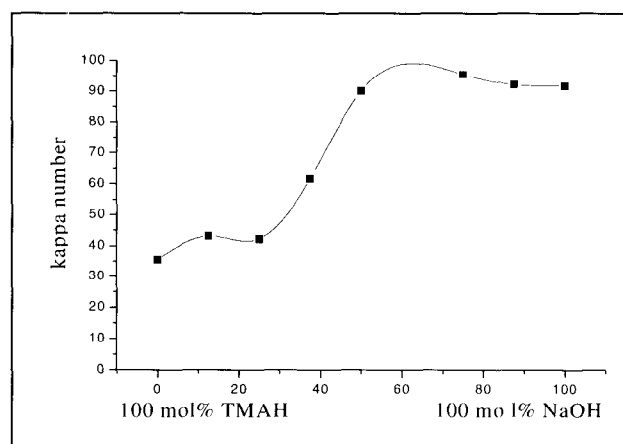


Figure 6. Kappa numbers of scotch pine pulp depending on the composition of the pulping liquor ($T=170\text{ }^{\circ}\text{C}$, $t=60\text{ min}$, $c=1.2\text{ mol/l}$, $LR=1:5$).

Conclusion

In this paper, the pulping effect of different kinds of quaternary ammonium hydroxides were compared. It is shown that among the quaternary ammonium compounds tested TMAH has the best delignification properties. It has a dramatic

effect on the kappa number reduction and offers a possibility for milder, cheaper and non-polluting bleaching.

The experiments with different kinds of wood clearly confirm that the Quatam process is equally efficient for both hardwood and softwood species, and the effectiveness of TMAH is superior to that of NaOH in producing a high quality pulp (low kappa number and high brightness) within a short cooking time and without using compounds containing sulfur. For softwood a higher chemical concentration is suggested.

According to the results on mixtures of TMAH and NaOH, there is a possibility to replace the TMAH partly by NaOH in the pulping liquor without losing its advantages and reducing the costs of the Quatam process. The critical limit is 40 mol% TMAH for hardwood and 60 mol % TMAH for softwood pulping.

Acknowledgement

We would to thank to Jan van Acquoij (Inspec Fine Chemicals CFZ Zaltbommel) for the TMAH solution.

References

- [1] Tanczos, I.; Schmidt, H. Austrian Patent, AT 403 703 B (25.06.1966).
- [2] Tanczos, I.; Putz, R.; Schmidt, H. *proceedings*, Advances in Lignocellulosics Chemistry for Ecologically Friendly Pulping and Bleaching technologies, Aveiro, 1998, p. 581.
- [3] Putz, R.; Pfeifer, A.; Tanczos, I.; Schmidt, H., *proceedings*, 10th International Symposium on Wood and Pulping Chemistry, Yokohama, 1999, vol. 2, p. 272.
- [4] Tanczos, I.; Putz, R.; Borsa, J. *proceedings*, 10th International Symposium on Wood and Pulping Chemistry, Yokohama, 1999, vol. 2, p. 288,
- [5] Krässig, H.A. Cellulose Structure: Accessibility and reactivity. Gordon and Breach Science Publishers, 1993, p. 256.
- [6] Lieser, T. *Liebigs Ann.* **1937**, 528, 276.
- [7] Challinor, J.M. *J. Anal. Appl. Pyrolysis* **1989**, 16, 323.
- [8] Hatcher, P.G.; Minard, R.D. *Org. Geochem.* **1995**, 23, 991.
- [9] Tanczos, I.; Rendl, K.; Schmidt, H. *J. Anal. Appl. Pyrolysis* **1999**, 49, 319.

HETEROLYTIC REACTIONS IN THE SYSTEM NMMO / CELLULOSE / WATER

A. Potthast, T. Rosenau, P. Kosma

Christian-Doppler Laboratory, University of Agricultural Sciences Vienna,
Muthgasse 18, A – 1190 Vienna, Austria

The occurrence of both heterolytic and homolytic reactions was demonstrated for the system *N*-methylmorpholine-*N*-oxide (NMMO) / cellulose / water applying α -tocopherol as a reporter molecule.

One major heterolytic decomposition pathway of NMMO produces formaldehyde and morpholine *via* carbenium-iminium ion intermediates. The presence of formaldehyde in solutions of cellulose in NMMO was shown by trapping formaldehyde as dimedone adduct in a two-phase system with *o*-dichlorobenzene as the inert organic solvent.

Morpholine is a degradation product of NMMO and is always present in systems containing NMMO. Formaldehyde can react

with morpholine to form transient species, *N*-methylenemorpholinium ions. The presence of this intermediate in the system cellulose / NMMO was demonstrated by trapping in a *Mannich* type reaction with 2-acetonaphthone. Both formaldehyde and *N*-methylenemorpholinium cations are highly reactive species which readily undergo further reactions with nucleophiles. These processes might contribute to the observed discoloration of the reaction mixture, and might also be responsible for the decomposition of NMMO.

Keywords: NMMO, heterolytic reactions, formaldehyde, morpholine, *Mannich* reaction

Introduction

The tertiary amine oxide *N*-methylmorpholine-*N*-oxide monohydrate (NMMO) is widely used as a solvent for cellulose in industrial fiber-making processes [1, 2, 3]. There is a considerable interest in elucidating the chemistry of side reactions and formation of byproducts in the system NMMO / water / cellulose, as these compounds promote the degradation of cellulose, cause discoloration of the resulting fibers [4], or even give rise to autocatalytic decomposition processes [5] or thermal runaway reactions [6]. However, very little is known about the underlying reactions and mechanisms.

Experimental

Materials and methods. A bleached spruce sulfite pulp and a Eucalyptus prehydrolysis kraft pulp were used as cellulose samples. NMR spectra were obtained on GE Omega and Bruker Avance instruments. MS measurements were carried out on a Jeol 50X (FAB) and a HP 5080 (EI).

Determination of the occurrence of homolytic and heterolytic decomposition reactions [7]. A 6.6 w% solution of cellulose in NMMO monohydrate was prepared by melting a mixture of both components in an inert atmosphere. After complete dissolution of the cellulose, α -tocopherol (**1**, 0.5m% relative to NMMO) was added and the mixture was vigorously mixed. The mixture was then extracted three times with *n*-hexane. The combined organic extracts were filtered through anhydrous MgSO₄ and chromatographed on acidic aluminum oxide (*Brockmann* grade I). The reaction products, spiro-dimer of α -tocopherol (**4**) and *para*-tocopheryl quinone (**2**), were eluted with *n*-hexane, α -tocopherol (**1**) as starting material was retained. After removal of the solvent *in vacuo*, the remainder was analyzed by FAB MS with *m*-nitrobenzyl alcohol as the matrix. Spectra of authentic samples of the individual components were recorded beforehand. MS (FAB+, 14 cycles, *m/z*): 429.4 (**2**, M-H₂O+H⁺), 856.8 (**4**, M⁺).

Trapping of formaldehyde [8]. A 6.6 w% solution of cellulose in NMMO monohydrate was prepared by melting a mixture of both components in an inert atmosphere. After complete dissolution of the cellulose, *o*-dichlorobenzene was added, and the mixture was vigorously agitated by means of a sufficiently powerful magnetic stirrer. Dimedone (**11**) was added in 5 portions at intervals of about 10 mins. The organic phase was separated and filtered through anhydrous MgSO₄. The organic solvent was removed by flushing with carbon dioxide. The white, solid remainder was recrystallized from ethanol to afford the pure dimedone-formaldehyde adduct **12**. Analytical data as given in the following were consistent with that of an authentic sample. ¹H NMR (CDCl₃, 300 MHz): δ 1.05 (s, 12H, CH₃), 2.30 (d (m), 8H, CH₂-CH₂), 3.17 (s, 2H, CH-CH₂-CH), 11.6 (s, broad, 2H, OH). ¹³C NMR: δ 16.1, 27.2, 29.7, 31.9, 46.1, 113.6, 189.7. MS (FAB(+), 14 cycles, matrix *m*-nitrobenzyl alcohol, *m/z*): 293.3 (MH⁺).

Trapping of carbenium-iminium ions. [8] A solution of cellulose in NMMO monohydrate was prepared as described above. After complete dissolution of the cellulose, freshly recrystallized 2-acetonaphthone (**13**) was added in 3 portions at intervals of about 2 minutes. The mixture was vigorously stirred throughout, and was subsequently extracted three times with chloroform. The combined organic extracts were filtered through anhydrous MgSO₄. *n*-Hexane was added, and the mixture was flushed with anhydrous hydrogen chloride. The resulting crystalline precipitate, the hydrochloride of β-morpholinopropionaphthone (**14**), was washed with ethyl ether and dried *in vacuo*. The free base can be obtained by treatment of the precipitate with anhydrous K₂CO₃ in chloroform. Analytical data (hydrochloride of **14**) were consistent with that of an authentic sample. ¹H NMR (CD₃CN/CDCl₃, v/v = 2:1, 300 MHz): δ 2.18 (s, b, 1H), 2.60 (t, 4H, ³J=5 Hz, N-CH₂-CH₂-O), 2.93 (t, 2H, ³J=7 Hz, CH₂), 3.46 (t, 2H, ³J=7 Hz, CH₂), 3.78 (t, 4H, ³J=5 Hz, N-CH₂-CH₂-O), 7.58-7.66 (m, 2H, ^{Ar}CH), 7.86-8.08 (m, 4H, ^{Ar}CH), 8.45 (s, 1H, ^{Ar}CH). ¹³C NMR: δ 33.7, 53.1, 53.2, 64.7, 124.4, 128.2, 128.8, 129.6, 130.1, 130.8, 131.6, 133.5, 134.2, 136.8, 198.0. MS (EI(+), 70 eV, *m/z*): 269 (M⁺).

Results and Discussion

The nature of ongoing chemical processes in a reaction system as to their homolytic or heterolytic nature can be determined by applying vitamin E (α-tocopherol, **1**) as a molecular probe. The procedure is based on the fact that α-tocopherol is oxidized both homolytically and heterolytically in a selective manner affording easily distinguishable products at comparable reaction rates: one-electron oxidation produces finally *para*-tocopheryl quinone (**2**), whereas two-electron oxidation gives the spiro-dimer of α-tocopherol (**4**) via an intermediate *ortho*-quinone methide (**3**, see Figure 1. The application of this method requires several precautions to be taken [9] if a quantitation is attempted, but it allows a rough qualitative estimation in any case.

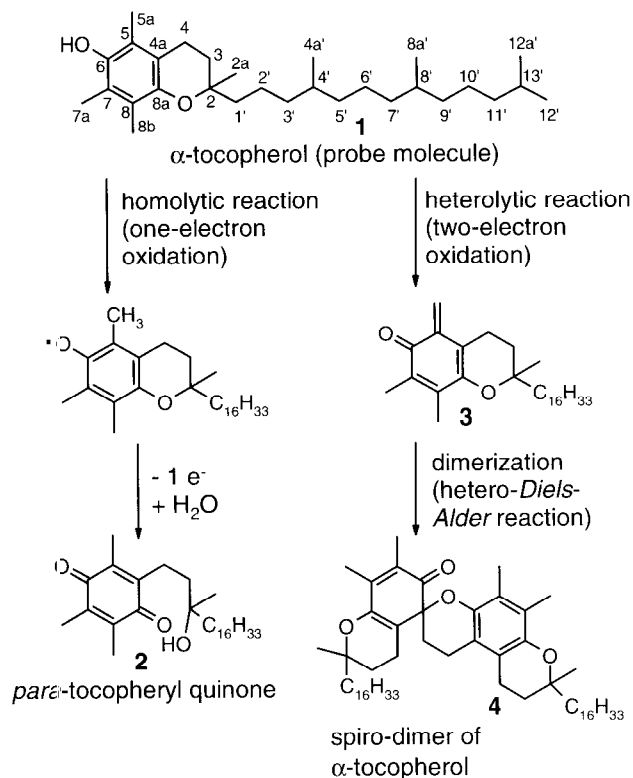


Figure 1. Determination of the occurrence of both homolytic and heterolytic processes in the system NMMO / cellulose by means of α-tocopherol as a probe molecule.

With the help of **1** as the probe molecule, the occurrence of both homolytic and heterolytic oxidation processes in the system NMMO (**5**) / cellulose / water has been determined. A comprehensive investigation and description of the side reactions thus requires to distinguish between these two general pathways; the main

heterolytic reaction mechanisms, which cause decomposition of NMMO and byproduct formation, are considered in the following.

N-Methylmorpholine (6) and morpholine (7) have been described as major byproducts during degradation reactions of NMMO [10]. It is highly important whether formaldehyde (HCHO, 8) in NMMO / cellulose solutions is present already in the reaction mixture or formed later in the spinning bath by hydrolytic reactions. Formaldehyde, as the aldehyde with the highest carbonyl reactivity, does undergo not only uncontrolled reactions with other chemical species present, but also reacts with morpholine (7) to form a carbenium-iminium ion (*N*-methylenemorpholinium cation, 10) via *N*-hydroxymethylmorpholine (9) in neutral and acidic media as shown in Figure 2. Carbenium-iminium ions, however, are capable of catalytically decomposing NMMO [5]. Thus, it is conceivable that the reactions involving 10 are a primary cause for the observed spontaneous decomposition processes in NMMO / cellulose / water systems.

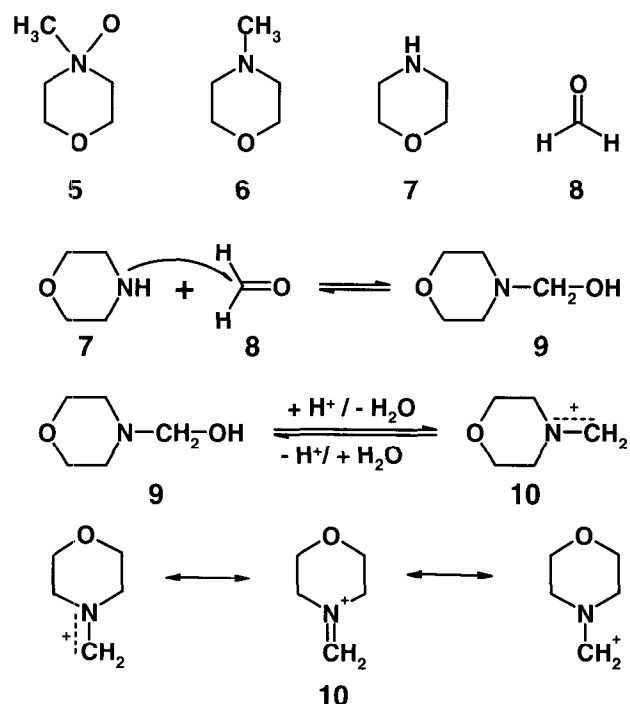


Figure 2. Species in NMMO / cellulose solutions. Formation of (methylene)morpholinium cations from morpholine and formaldehyde.

The determination of HCHO in the NMMO / water / cellulose reaction system proved to be unusually difficult. Commonly employed reactions to determine aldehydes, such as the

formation of hydrazones, semicarbazones or oximes, trapping as water-insoluble hydroxymethanesulfinic acid, or the reaction with chromotropic acid, are not suitable for the determination because the trapping reagents are either unstable under the prevailing reaction conditions, or they react with the carbohydrates present in the system. Dilution of the system with water followed by determination of formaldehyde in the resulting aqueous mixture is not a feasible approach, since determination of HCHO would not prove its presence in the NMMO / water / cellulose solution, but merely show its occurrence in the aqueous extracts. Thus, this approach cannot eliminate the possibility that the HCHO originates from a variety of hydrolytic reactions in subsequent steps. A good trapping agent for HCHO in the present case must exhibit the following characteristics:

- it must undergo a specific reaction with HCHO,
- it must react with HCHO immediately upon its formation,
- it must be sufficiently stable under the reaction conditions, and
- it must produce stable and readily separable reaction products.

As none of the conventionally used carbonyl reagents met these requirements, another approach had to be chosen.

The application of 5,5-dimethylcyclohexane-1,3-dione (dimedone, 11) in a two-phase system with *o*-dichlorobenzene as the organic phase and the cellulose / water / NMMO mixture as the "aqueous" phase finally represented a solution to this problem. Dimedone reacts with aldehydes in a well-defined reaction [11, 12]. It is insoluble in *o*-dichlorobenzene, but its reaction product with HCHO is readily soluble in this solvent, and thus readily extractable. *o*-Dichlorobenzene has a sufficiently high boiling point (180° C) and is completely inert under the reaction conditions. In addition, it does not interfere with the processes in the cellulose / water / NMMO layer in any way. By this approach the presence of HCHO in solutions of cellulose in NMMO monohydrate was unambiguously proved. Addition of dimedone into the system (0.5% relative to NMMO·H₂O) resulted in the formation of the corresponding dimedone-formaldehyde adduct 12 with a 19% yield, see Figure 3.

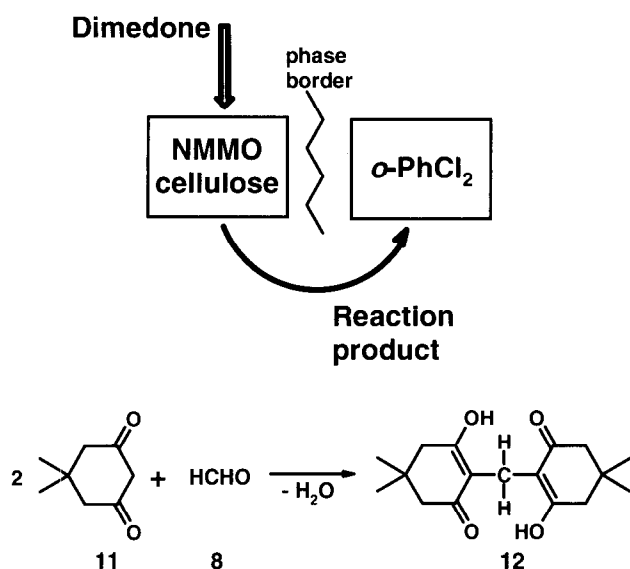


Figure 3. Experimental setup and reaction mechanism for the determination of HCHO in the system NMMO /water / cellulose.

After having established the presence of HCHO in the NMMO / water / cellulose system, the occurrence of carbenium-iminium ions, especially *N*-methylenemorpholinium cations (**10**), as the reaction products of HCHO with morpholine had to be verified. Therefore, once more a specific reaction had to be found. Trapping of carbenium-iminium ions in a *Mannich* type reaction [13], [14] proved to be a suitable approach to this task: the carbenium-iminium ion in this reaction is not formed by a separate reaction between secondary amine and HCHO, but is already present in the system and free to react with the methylene-active carbonyl compound added as the trapping reagent.

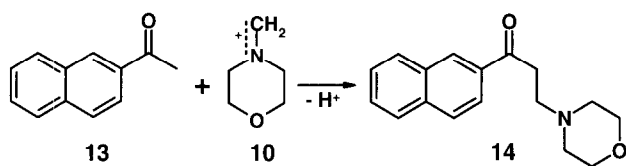


Figure 4. Reaction for the determination of *N*-methylenemorpholinium cations **10** in the system NMMO /water / cellulose.

However, the above described restrictions to the selection of a trapping reagent apply analogously. First of all, the trapping reagent must be stable under the applied reaction conditions, *i.e.*, it must tolerate temperatures about 100°C and the presence of NMMO as a relatively strong oxidant. This requirement eliminates the application of aliphatic aldehydes as trapping

reagents. In addition, the products of the reaction, usually named *Mannich* bases, must be stable and easily isolable. This turned out to be a major impediment as *Mannich* bases readily eliminate the secondary amine group to form an α,β -unsaturated carbonyl compound. After testing several arylmethylketones, we found 2-acetonaphthone (**13**) to be very suitable. With this compound as the trapping, the *in situ*-formation of the carbenium-iminium cation **10** in NMMO solutions of cellulose was unambiguously demonstrated, *cf.* Scheme 4. The product of the reaction between **13** and **10**, the corresponding *Mannich* base 3-(4-morpholino)propionaphthone (**14**), does not eliminate morpholine at temperatures below 110°C and is easily extractable into chloroform due to the lipophilic naphthene moiety. Although the yield of the reaction is very low (32% relative to **13**), the easiness in isolation of the compound and the comparison with an authentic sample allowed unambiguous identification of the compound.

Conclusion

The occurrence of both homolytic and heterolytic oxidation processes in solutions of cellulose in NMMO / water was demonstrated by means of α -tocopherol as a selective molecular probe. This result leads to the conclusion that neither a stabilization merely against homolytic processes by conventional antioxidants, nor a stabilization only against heterolytic oxidations by adding reductants is completely sufficient for NMMO / cellulose systems since both types of chemical processes are occurring simultaneously.

Formaldehyde and *N*-methylenemorpholinium cations were shown to be present *in situ* in NMMO / water / cellulose systems. Both species show a high reactivity towards CH-acidic compounds, such as carbohydrate structures present, forming chromophores that are responsible, among other condensation products, for the discoloration of the reaction mixture.

Moreover, carbenium-iminium ions are able to decompose NMMO autocatalytically. The latter reaction might become prominent if the local *in situ*-concentration of **10** increases to a degree that its consumption in other reactions cannot compensate for its production.

Acknowledgement

We thank Dr. A. Hofinger (Institute of Chemistry at the University of Agricultural Sciences Vienna) for recording the NMR spectra. We are grateful to Dr. H. Sanford (Mass Spec Facility at North Carolina State University, Raleigh, USA) for carrying out the MS experiments. We would like to thank Doz. Dr. H. Sixta and Dr. H. Firgo for inspiring discussions. The financial support by the LENZING AG, Lenzing, Austria, is gratefully acknowledged.

References

- [1] Chanzy, H. J. *Polym. Sci., Polymer Phys. Ed.* **1980**, *18*, 1137.
- [2] Chanzy, H.; Nawrot, S.; Peguy, A.; Smith, P. J. *Polymer Sci.* **1982**, *20*, 1909.
- [3] Firgo, H.; Eibl, M.; Kalt, W.; Meister, G. Internationales Symposium „Alternative Cellulose - Herstellen, Verformen, Eigenschaften“, Thüringisches Institut für Textil- und Kunststofforschung (TITK), 7.-8. Sept. 1994, Rudolstadt/Schwarza, Thüringen.
- [4] Taeger, E.; Franz, H.; Mertel, H. *Formeln, Faserstoffe, Fertigware* **1985**, *4*, 14.
- [5] Rosenau, T.; Potthast, A.; Kosma, P.; Chen, C.L.; Gratzl, J.S. *J. Org. Chem.* **1999**, *64*, 2166.
- [6] Buijtenhuis, F.A.; Abbas, M.; Witteveen, A.J. *Papier* **1986**, *40*, 615.
- [7] A detailed procedure for the use of α -tocopherol as a probe molecule is given in: Rosenau, T., Ph.D. thesis, Dresden University of Technology, Germany, 1997.
- [8] The procedure is described in more detail in: Potthast, A.; Rosenau, T.; Kosma, P.; Chen, C.L.; Gratzl, J.S. *Holzforschung* **2000**, in press.
- [9] The total amount of α -tocopherol must be rather low to avoid radical coupling. As the reaction pathways differ in aqueous, non-aqueous and water-containing media, the method has to be optimized for each reaction system. For details see: [7].
- [10] Taeger, E.; Michels, C.; Nechtawal, A. *Papier* **1991**, *12*, 784.
- [11] Hopkin, A.; Williams, E. *Organic Reagents for Organic Analysis*, 2nd ed., Chadwell Heath, 1950, pp. 61.
- [12] Cremlyn, R.J.; Osborne, A.G.; Warmsley, J.F. *Spectrochimica Acta Part A* **1996**, *52*, 1433.
- [13] Tramontini, M. *Synthesis* **1973**, 703.
- [14] Tramontini, M.; Angiolini, L. *Tetrahedron* **1990**, *46*, 1791.

LIGHT-SCATTERING STUDIES ON SOLUTIONS OF CELLULOSE IN *N,N*-DIMETHYLACETAMIDE / LITHIUM CHLORIDE

T. Röder,^{a,b} B. Morgenstern,^c O. Glatter^b

^a Christian Doppler Laboratory for Pulp Reactivity, University of Agricultural Sciences Vienna,
Muthgasse 18, A-1190 Vienna, Austria

^b Institute of Physical Chemistry, University of Graz,
Heinrichstrasse 28, A-8010 Graz, Austria

^c Institute of Physical Chemistry and Electrochemistry, Dresden University of Technology,
Mommensenstrasse 13, D-01062 Dresden, Germany

These studies are based on the solvent system *N,N*-dimethylacetamide (DMAc)/LiCl which is used, e. g., for the determination of the molecular weight distribution of cellulosic substrates by size exclusion chromatography (SEC). Results are presented on static and dynamic laser-light-scattering experiments carried out in the concentration range employed in SEC and discussed in terms of the solution state. The influence of two different methods of cellulose activation

(swelling in water and liquid ammonia followed by a solvent exchange) was investigated. Cellulose samples with high or low molecular mass were examined. In dependence on the concentrations of salt and cellulose during the dissolution process a molecular dispersion of the cellulose could be found in diluted solutions.

Keywords: cellulose, laser-light-scattering, state of solution

Introduction

In polymer chemistry size exclusion chromatography (SEC) is used to characterize various kinds of macromolecules by means of their molecular weight distribution. Since unsubstituted cellulose is soluble in only few solvent systems, cellulose derivatives are frequently synthesized which are soluble in a common solvent. However, such a derivatization reaction can falsify the results, e. g., by degradation of the cellulose molecules. On the other hand, true cellulose solvents are often multi-component systems with special properties. The dissolution of cellulose in a mixture of *N,N*-dimethylacetamide (DMAc) and LiCl has been known since 1979 [1]. DMAc alone merely causes intercrystalline swelling. The optimum concentration of LiCl is reported to be in the range between 5 and 9 wt% [2]. Activation of the cellulose is necessary before dissolution. Dependent on the salt content, on the cellulose concentration and on the pulp provenience, different architectures of cellulose

molecules, aggregates or single chains, have been found in solution [3].

Later it was found that DMAc/LiCl is a suitable eluent for the SEC analysis of cellulose. A LiCl concentration of 0.9 wt% is used. The LiCl content in the injected cellulose solution can range between 2 and 3 wt%. In the SEC column the cellulose molecules are separated according to their hydrodynamic volume which is their effective size in the solution. Larger molecules, and of course aggregates, eluate more quickly than smaller molecules [4]. A solution of single cellulose molecules is an absolute prerequisite for correct SEC measurements. The aim of our study was to investigate under which conditions molecularly dispersed cellulose solutions can be prepared.

Experimental

Materials. The cellulose samples used in this study are listed in Table 1. Degrees of polymerization (DP) were estimated by intrinsic viscosity measurements in cuen (copper

ethylenediamine complex) [5]. LiCl (p. a. grade) was dried at 200°C. DMAc (HPLC grade, water content < 0.03 %) was used without further purification.

Table 1. Cellulose samples and their degree of polymerization (DP).

| Pulp | Provenience | DP |
|------------------|--------------------------------|------|
| Avicel | micro crystalline cellulose | 285 |
| Buckeye V5 | soft wood, prehydrolysis kraft | 1360 |
| KZO ₃ | Beech magnesium bisulfite pulp | 1500 |
| viscose | normal viscose | 470 |

Cellulose activation and dissolution. Two methods were used for cellulose activation. In the case of swelling in water small pieces of pulp were dispersed in deionized water with a labor mixer. The water was then drained, and the swollen cellulose was washed twice with acetone and dried through filtration under reduced pressure. This was followed by a solvent exchange with DMAc. Aliquots of the activated pulp were added to the desired DMAc/LiCl solution (with 9 wt% or 6 wt% LiCl). By using a shaking device the dissolution process takes place at room temperature overnight. This method is described in detail in [6]. The cellulose dissolution by activation with liquid ammonia was carried out as described in [7]. The stock solutions were carefully diluted with DMAc/LiCl or pure DMAc to prepare the concentration series for the light-scattering experiments. The solutions were passed through 0.2 µm or 0.45 µm membrane filters into dust-free sample cells.

Laser-light-scattering measurements. For static measurements a SLS-2 goniometer (SLS Systemtechnik Hausen, Germany) with a 5mW He-Ne laser ($\lambda = 632.8$ nm) with a vertically polarized light beam with respect to the scattering plane was used as light source. The refractive indices of the solvents were estimated with an Atago RX-5000 digital refractometer. Viscosities were measured with a SR-5000-NF stress rheometer from Rheometric Scientific. The refractive index increments were taken from reference [8], or were interpolated. The same values were used for all pulps.

Table 2. Refractive index increment, viscosity, and refractive index of the solvents at 20°C.

| [LiCl] in DMAc, wt% | (dn/dc) (cm ³ /g) | Viscosity (cP) | Refractive index |
|---------------------|------------------------------|----------------|------------------|
| 9 | 0.055 | 10 | 1.4607 |
| 6 | 0.08 | 6.4 | 1.4522 |
| 2.6 | 0.11 | 3.4 | 1.4443 |
| 1 | 0.12 | 1.4 | 1.4365 |

Dynamic measurements were carried out using a DLS-goniometer developed by the Scattering Methods group at the University of Graz. It was equipped with an ALV-5000/E correlator and two laser-light sources – a 25mW He-Ne laser ($\lambda=632.8$ nm) and a 5W Ar-ion laser ($\lambda=514$ nm). The calculation of the size distribution of the autocorrelation function was carried out using the inverse Laplace transformation program ORT [9].

Results and discussion

Static light-scattering measurements. Two pulps – Avicel and Buckeye V5 with weight-average molecular weights of 46,000 g/mol and 220,000 g/mol, respectively – were chosen for the investigation of the solution state by means of static light-scattering. The samples were activated by the water swelling method. Two types of solutions differing in their LiCl content were measured: stock solutions containing 9 wt% or 6 wt% LiCl prepared as described in the experimental part, and so-called diluted solutions which were obtained after dilution of stock solutions with pure DMAc resulting in a LiCl content of 2.6 wt% or 1 wt%. The results were evaluated in terms of Zimm or Guinier-Zimm plots and are summarized in Table 3.

In the case of the stock solutions weight-average molecular weights M_w were obtained which were significantly larger than the M_w values measured viscosimetrically in cuen. The radii of gyration R_G were also relatively high. Both facts indicate that a certain fraction of supermolecular structures existed in the stock solutions. After dilution to 2.6 wt% or 1 wt% LiCl smaller values of M_w and R_G were obtained. However, a solution state which is characterized by the existence of only single cellulose molecules was not found.

If the initial cellulose concentration was high (e. g., 7 wt%) a very high value of M_w was obtained after dilution to 1 wt% LiCl. The cellulose was

probably not completely dissolved under these conditions as indicated by the negative second virial coefficient A_2 .

Table 3. Results of static light-scattering measurements on cellulose dissolved in DMAc/LiCl.

| Pulp | [pulp] _{stock} (wt%) | [pulp] _{meas.} (wt%) | [LiCl] _{stock} (wt%) | [LiCl] _{meas.} (wt%) | M_w (g/mol) | n_w | R_G (nm) | A_2 (mol·ml/g ²) |
|---------|----------------------------------|----------------------------------|----------------------------------|----------------------------------|---------------|-------|------------|-----------------------------------|
| Avicel | 7 | 0.9 | 8 | 1 | 1,500,000 | 31 | 139 | < 0 |
| Avicel | 3 | 1.3 | 6 | 2.6 | 258,000 | 5 | 105 | 3E-5 |
| Avicel | 3 | 0.5 | 6 | 1 | 85,000 | 2 | 56 | 6E-4 |
| Buckeye | 1 | 1 | 9 | 9 | 909,000 | 4 | 170 | 1E-5 |
| Buckeye | 1 | 0.3 | 9 | 2.6 | 300,000 | 1.5 | 61 | 1.5E-3 |
| Buckeye | 1 | 0.2 | 6 | 6 | 1,230,000 | 6 | 203 | 4E-5 |
| Buckeye | 1 | 0.4 | 6 | 2.6 | 509,000 | 2.5 | 169 | 1E-4 |

Measurements on cellulose solutions with 1 wt% LiCl prepared from stock solutions with 9 wt% LiCl and 1 wt% pulp (the solution composition is now comparable with that one used in SEC) could not be carried out due to the strong concentration dependence of the refractive index of the DMAc/LiCl solution itself [$(\delta n/\delta c)=0.316$ ml/g] [8]. Consequently, the error of the static light-scattering measurements on a concentration series with 1 wt% LiCl based on a stock concentration of 9 wt% LiCl is too large. Therefore, we carried-out dynamic light-scattering measurements to avoid this problem.

Dynamic light-scattering measurements. The quantity measured in dynamic light-scattering is the angular dependent intensity-time correlation function $g_2(q,t)$ of the coherently scattered light. Under special conditions the intensity distribution of the apparent hydrodynamic radii, R_H , can be calculated from $g_2(t)$ measured at a constant scattering-angle [9]. Due to the intensity-radius relationship $I \propto R_H^6$ a small fraction of large particles could be distinctly identified. However, true values of R_H could not be estimated because the relationship between the translational diffusion coefficient and the hydrodynamic radius was unknown for the investigated system. Nevertheless, we were able to use a simple tool to gain a qualitative information about the distribution of the size of cellulose particles in concentrated and highly diluted cellulose solutions.

Figure 1 shows the intensity time-correlation functions of solutions of Avicel in DMAc/LiCl (6 wt%) with cellulose concentrations ranging from 1 wt% to 3.5 wt%. The pulp was activated by the water swelling method. At 1 wt% Avicel

$g_2(t)$ shows a large step at a correlation time of about 0.1 ms and only a slight step between 1 and 10 ms. This corresponds to a main fraction of small particles and a very small fraction of larger particles. Amount and size of large particles increase with cellulose concentration. This is indicated by the progressive increase in the height of the second step and its shift to a longer correlation time. Furthermore, a depolarized intensity correlation function could be detected at a cellulose concentration above 3 wt%. This could be caused by the existence of anisotropic particles.

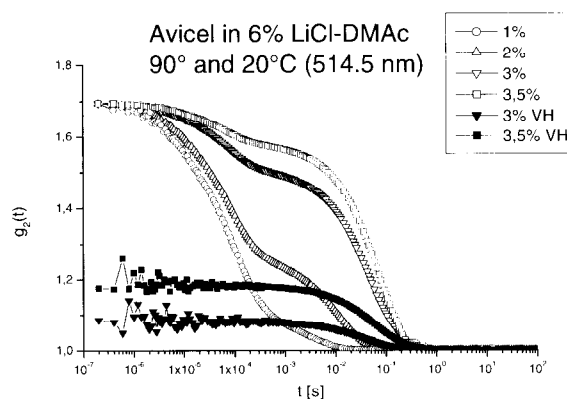


Figure 1. Autocorrelation function for Avicel in DMAc/LiCl (6 wt%).

In Figure 2 the intensity distribution of R_H in a stock solution of 1 wt% of the viscose sample at 9 wt% LiCl is depicted. There are two maxima in the distribution at an apparent R_H of <10 nm and 400 nm, where the intensity at the lower R_H is evidently higher than at the larger radius. However, the fraction of the large particles is very small because the scattering intensity is

proportional to R^6 . This observation is independent on the activation method used. In good approximation one can assume that most of the cellulose molecules exist as single chains or small aggregates.

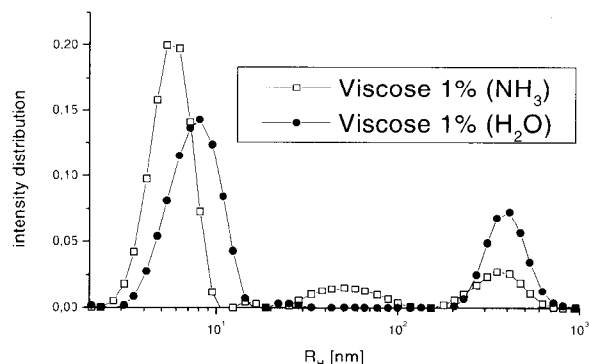


Figure 2. Intensity distribution for 1 wt% viscose in DMAc/LiCl (9 wt%).

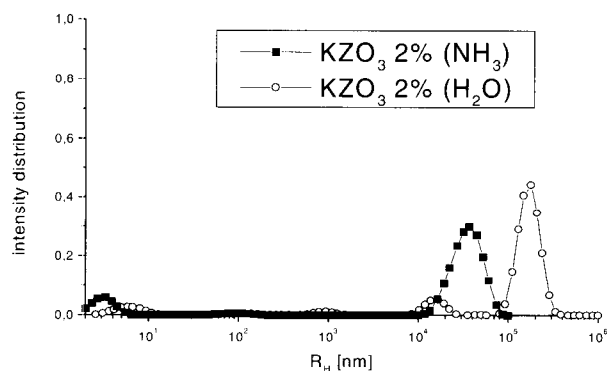


Figure 3. Intensity distribution for 2 wt% KZO₃ in DMAc/LiCl (9 wt%).

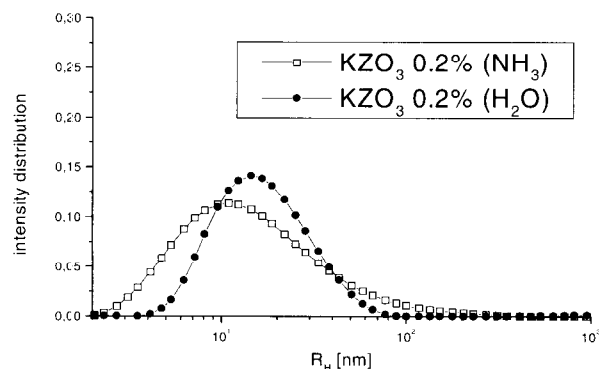


Figure 4. Intensity distribution of 0.2 wt% KZO₃ in 0.9 wt% DMAc/LiCl diluted from 2 wt% KZO₃ in 9 wt% DMAc/LiCl.

A solution with a concentration of 2 wt% cellulose (KZO₃ pulp) shows also a bimodal R_H -distribution (Figure 3). But the intensity at the large radius is many times higher than at the lower R_H . Therefore a significant fraction of large cellulose particles is present at this

concentration. These particles are associates or aggregates. Activation with liquid NH₃ favors formation of smaller supermolecular structures.

The stock solutions with 9 wt% LiCl and 1 wt%, 1.5 wt% and 2 wt% cellulose were diluted to a LiCl concentration of about 0.9 wt%. Afterwards only one maxima for the R_H distribution can be seen (Figures 4 and 5). The large particles were disintegrated. Effects attributed to the different activation methods were negligible. Nevertheless, a deviation was observed in the case of viscose fibres (Figure 6). While all the other samples form molecularly dispersed solutions at 0.9 wt% LiCl (after dilution to SEC composition) the water swollen viscose still forms supermolecular structures. For this sample an activation with liquid ammonia results in a smaller fraction of these structures.

However, in SEC measurements these different behaviors were not detectable at all [6]. During the chromatographic process the cellulose concentration diminishes to about 0.001 %. In this range the solution is molecularly dispersed.

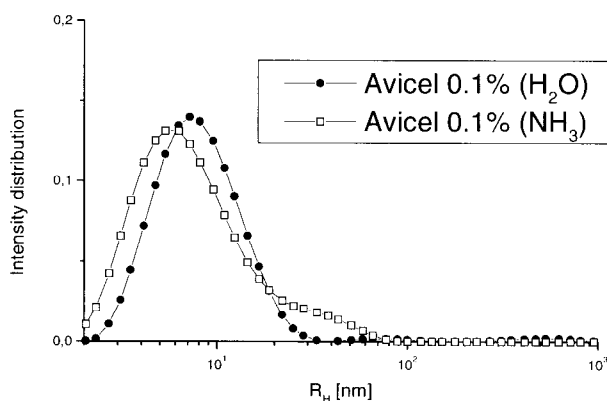


Figure 5. Intensity distribution of 0.1 wt% Avicel in 0.9 wt% DMAc/LiCl diluted from 1 wt% Avicel in 9 wt% DMAc/LiCl.

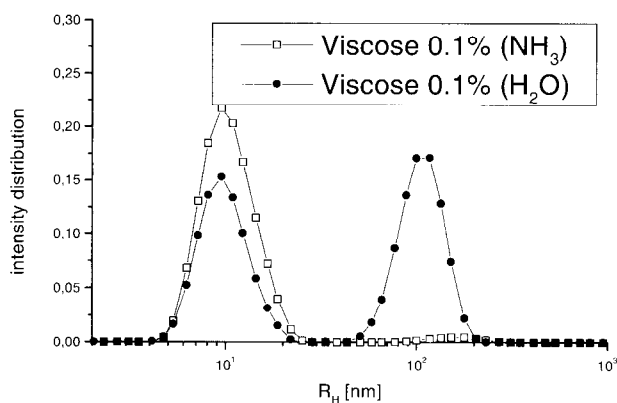


Figure 6. Intensity distribution of 0.1 wt% Viscose in 0.9 wt% DMAc/LiCl diluted from 1 wt% Viscose in 9 wt% DMAc/LiCl.

Summary

The solution state of cellulose in DMAc/LiCl solutions is influenced by the cellulose concentration, the LiCl concentration and the method used to activate the cellulose. Usually a cellulose activation by swelling in water followed by a solvent exchange is sufficient. In the case of some samples, such as viscose fibres, activation with liquid ammonia is more effective. Stock solutions with 9 wt% LiCl and a cellulose concentration > 1 wt% exhibit a bimodal distribution of the particle size. In most cases after dilution to 0.9 wt% LiCl the large particles are disintegrated, and the solutions contain almost exclusively single cellulose chains. When the stock solutions were prepared with a LiCl content of < 9 wt% the formation of large particles is favored. This behavior occurs especially when the amount of cellulose is too high depending on the DP of the cellulose. In concentrated solutions the existence of large anisotropic particles could be maintained.

Under SEC conditions truly molecularly dispersed solutions of cellulose exist in 1 wt% DMAc/LiCl.

Acknowledgements

We thank the Christian Doppler Society, Austria, and the Lenzing AG, Austria, for financial support. We are grateful to Univ.-Doz. Dr. H. Sixta (Lenzing AG) and Dr. N. Schelosky (Lenzing AG) for helpful discussions, to Mr. W. Milacher (Lenzing AG) and Mr. P. Rappold (Lenzing AG) for the preparation of stock solutions.

References

- [1] McCormick, C.L.; Lichatowich, D.K. *J. Polym. Sci., Polym. Lett. Ed.* **1979**, *17*, 479.
- [2] Dawsey, T.R.; McCormick, C.L. *J. Macromol. Sci., Rev. Macromol. Chem. Phys.* **1990**, *C30*, 405.
- [3] Terbojevich, M.; Cosani, A.; Conio, G.; Ciferri, A.; Bianchi, E. *Macromolecules* **1985**, *18*, 640.
- [4] Silva, A.A.; Laver, M.L. *TAPPI Journal* **1997**, *80*, 173.
- [5] Kocevar, F.; Pogacnik, M.; Povoden, V. *Das Papier* **1953**, *11*, 301.
- [6] Schelosky, N.; Röder, T.; Baldinger, T. *Das Papier* **1999**, *53*, in press.
- [7] Morgenstern, B.; Berger, W. *Acta Polymerica* **1993**, *44*, 100.
- [8] Fellmann, E. PhD thesis, Dresden University of Technology.
- [9] Schnablegger, H.; Glatter, O. *Applied Optics* **1991**, *30:33*, 4889.

A GENERAL METHOD FOR THE QUANTIFICATION OF NMMO AND ITS MAIN DEGRADATION PRODUCTS BY CAPILLARY ELECTROPHORESIS

T. Rosenau, A. Potthast, P. Kosma

Christian-Doppler-Laboratory, University of Agricultural Sciences Vienna,
Muthgasse 18, A – 1190 Vienna, Austria

A general analytical method based on capillary electrophoresis with indirect UV detection has been developed to separate and quantify *N*-methylmorpholine-*N*-oxide (NMMO) and its main degradation products *N*-methylmorpholine (NMM) and morpholine (M). The electrolyte is based on the two major components 4-methylbenzylamine and 2-hydroxy-2-methylpropanoic acid (hydroxy-isobutyric acid, HIBA), the latter being used to adjust the pH to a value below 3.5 which is crucial for the electrophoretic mobility and, thus, for a good detectability of the amine oxide.

The present method is widely applicable to monitor kinetics of reaction mixtures containing NMMO. NMM and M can be determined simultaneously even in a 1000fold excess of NMMO. It was employed to monitor the kinetics of NMMO reactions, such as the reaction with xylose, the degradation of cellulose and the autocatalytic decomposition induced by carbenium-iminium ions.

Keywords: *N*-methylmorpholine-*N*-oxide, capillary electrophoresis, decomposition, carbenium-iminium ions

Introduction

N-Methylmorpholine-*N*-oxide (NMMO) is used as a bulk solvent for cellulose in industrial fiber-making processes. [1] Furthermore, it is widely employed in organic synthesis for direct or transition metal-catalyzed oxidation of organic compounds. [2] Despite the obvious difference in the scale of these applications, the same byproducts, mainly *N*-methylmorpholine (NMM) and morpholine (M), are formed from NMMO in all of these processes. Naturally, there is a considerable interest in the simultaneous determination of NMMO and its degradation products from the viewpoint of both the synthetic chemist who follows reaction kinetics and the industrial chemist engaged in process control. However, no simple and generally applicable method for the simultaneous determination and quantification of NMMO, NMM and M has been reported so far. This is mainly due to inherent problems with the handling of the strong oxidant NMMO in analytical procedures and equipment. Detection by GC, for instance, is impossible due to its thermal lability and the oxidative stress imposed on the columns.

Materials and Methods

Reagents. All chemicals were obtained from commercial sources and were of the highest purity available. Ultra pure water (conductivity < 18 MΩcm⁻¹) was used in the CE measurements. A bleached spruce sulfite pulp served as cellulose sample.

Equipment. A capillary electrophoresis instrument (QE4000 by Waters Corp., Milford, MA, U.S.A.) with the following general parameters was used: capillary column 60 cm x 75 μm; indirect UV detection at 214 nm (zinc lamp). Hydrostatic sampling:

- sample time: 10s,
- run voltage: 30 kV.

Electromigration sampling:

- sample time: 10 s,
- sample voltage: 5 or 10 kV,
- run voltage: 20 kV.

Analytical method and sample preparation. The analytical procedure was optimized with a simulated sample containing NMMO, NMM and M in aqueous solution in the molar ratio 30:1:1

with the NMMO concentration being $0.5 \text{ mol} \cdot \text{l}^{-1}$. The analytical system was calibrated within the following concentration ranges: $0.005 \text{ mol} \cdot \text{l}^{-1}$ to $2.5 \text{ mol} \cdot \text{l}^{-1}$ for NMMO, $0.001 \text{ mol} \cdot \text{l}^{-1}$ to $1.0 \text{ mol} \cdot \text{l}^{-1}$ for NMM and M.

“Real-world” samples were obtained from chemically induced decomposition reactions of NMMO, one example is described below.

Electrolyte preparation. The background electrolyte was prepared by adjusting a solution of 50 mM 4-methylbenzyl amine (**1**), 50 mM 2-hydroxy-2-methylpropanoic acid (hydroxy-isobutyric acid, **2**) and 20 mM 18-crown-6 (**3**) in ultra-pure water to a pH of 3.3 ± 0.1 with additional 2-hydroxy-2-methylpropanoic acid. The electrolyte was stable for at least one week when stored at 4°C . Every 24 h the working electrolyte was replaced by a fresh electrolyte solution, with the pH value being adjusted to 3.3 beforehand, if necessary. It is not recommended to prepare the electrolyte by dilution of a concentrated stock solution, as concentrated solutions of the above electrolyte are apparently not storable over longer periods of time even at low temperatures, and apparently tend to produce decomposition products that interfere with the reproducibility of CE measurements.

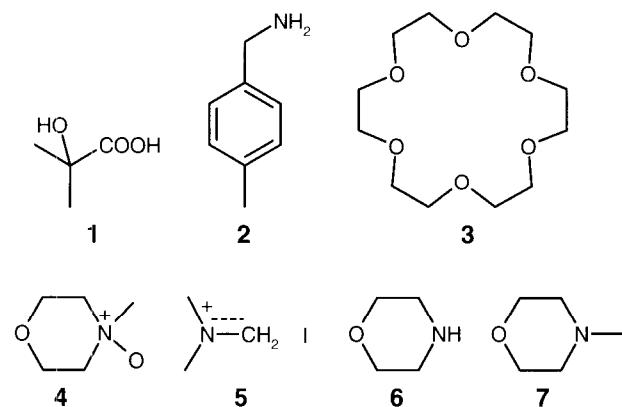


Figure 1. Components of the background electrolyte for CE measurements, amine compounds.

Autocatalytic decomposition of NMMO by carbenium-iminium ions. A typical experimental procedure is described in the following: To a 0.1 M solution of NMMO (**4**) in dry dichloromethane or dry chloroform Eschenmoser's salt (**5**, 1% relative to **4**) and, after 5 min, water (also 1% relative to **4**) were added. **5** and water can be replaced by adding morpholine (1% relative to **4**) and formalin (37%

aqueous HCHO, 1% relative to **4**). The mixture was stirred at r.t. while flushing with nitrogen to remove the forming HCHO. In intervals of 10 min, a 0.5 ml aliquot was taken, and analyzed by capillary electrophoresis after extraction into 3 mL of ultra-pure water. The reaction was finished when the electropherogram showed only morpholine (**6**), but no remaining starting material.

Results and Discussion

N-Methylmorpholine (**7**) and morpholine (**6**) have been recognized as the major byproducts during degradation reactions of NMMO (**4**) [3]. Previous attempts to solve the analytical problem of the quantification of NMMO, NMM and M in the corresponding reaction mixtures have been based on HPLC [4], capillary isotachopheresis [5] or capillary electrophoresis techniques [6]. However, none of these methods was a widely applicable standard operating procedure as they suffered from at least one of the following limitations:

- Only byproducts can be quantified, but cannot be detected together with NMMO and *vice versa*. Thus, a simultaneous determination and quantification of the three compounds is not possible.
- All three compounds can be separated, but quantification is impossible or restricted to roughly equal analyte concentrations.
- Tedious protocols, such as lengthy sample preparation or extremely high requirements as to solvent purity, are required for the measurement. The latter drawback mainly applies to HPLC as the quantification method where UV detection at 185 nm and corrosiveness of the analyte impose conditions too extreme for utilization as a general analytical approach, especially for applications in industrial process control or in kinetic investigations that require a quick and robust method.

To develop a general procedure for the separation and simultaneous quantification of *N*-methylmorpholine-*N*-oxide, *N*-methylmorpholine and morpholine, which is not limited by the above given drawbacks, capillary electrophoresis (CE) was chosen as the analytical method. In earlier attempts to apply this technique to the present task [6], the method was set up to

determine anions by indirect UV detection at 254 nm, with an electrolyte based on chromate or imidazole at a pH between 5 and 8. However, only the byproducts of NMMO, but not NMMO itself, could be detected and quantified in this pH range. In our approach, all nitrogen-containing compounds were analyzed in the electrophoretically mobile, protonated form, *i.e.*, as the respective ammonium compounds. Consequently, the cation mode was employed together with a rather low pH of the electrolyte. The conventionally used electrolytes were replaced by the system 2-hydroxy-2-methylpropanoic acid (**1**) / 4-methylbenzyl amine (**2**) / 18-crown-6 (**3**). This electrolyte enables indirect UV detection at 214 nm, and allows for a reliable performance at pH values between 2.5 and 5.

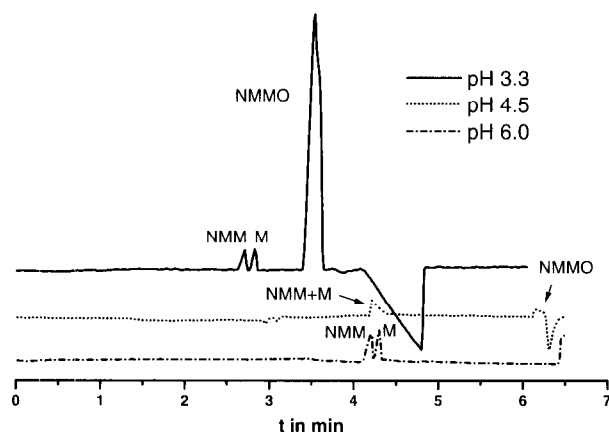


Figure 2. Separation of NMMO, NMM and M at different pH values of the electrolyte.

Reproducible CE results in the cation mode can be obtained only if all amine components are protonated and analyzed as the respective ammonium ions. Although a pH value of approx. 6.5 would suffice to convert *N*-methylmorpholine ($pK_a = 7.38$) or morpholine ($pK_a = 8.33$) into the corresponding ammonium ions, a pH of 4, or lower, is required to ensure almost complete protonation of NMMO ($pK_a = 4.75$), as demanded by the *Henderson-Hasselbalch* equation. With the initially used standard electrolyte with a pH of approx. 6, containing 50 mM 4-methylbenzyl amine and 30 mM hydroxy-isobutyric acid (HIBA) in ultra-pure water, a separation of **6** and **7** was feasible, but NMMO was undetectable (Figure 2, dashed line). At a pH of 4.5, NMMO was monitored, even though the conversion of the zwitterionic amine oxide into the positively charged

protonated species was evidently not complete. In addition, the separability of **6** and **7** seemed to be negatively affected at this pH (Figure 2, dotted line). Only at pH 3.3 the separation of all three analyte components was satisfactory (Figure 2, solid line).

Acidification of the standard electrolyte with a pH of 6 by diluted mineral acids (HCl, HNO₃), which are commonly used in CE analysis of amine compounds, gave very poor separations. Employing organic acids (acetic acid, trifluoroacetic acid, formic acid) to adjust the pH or changing electrolyte concentrations was similarly ineffective. The key solution to the problem was the use of **1**, both as a component of the background electrolyte and as a means to lower the pH. Thus, no additional component which might interfere with the electrolyte balance was introduced into the system, but merely the concentration of one component of the background electrolyte was increased.

The application of 30 kV run voltage, resulting in retention times of about 5 minutes produced electropherograms of sufficiently high quality and allowed for high-throughput analyses with high accuracy.

Another requirement set especially by industrial applications, determination and quantification of traces of degradation products in a NMMO matrix present in large excess, is also met: the byproducts NMM and M were reliably detected even in a 1000fold excess of NMMO, using the developed method. Figure 3 presents the electropherograms of four solutions containing the same amounts of *N*-methylmorpholine and morpholine in a molar ratio of 1, besides logarithmically increasing amounts of *N*-methylmorpholine-*N*-oxide. With concentrations of NMM and M being 0.01 mol·l⁻¹ throughout, the molar ratios NMM : M : NMMO were set to 1 : 1 : 1, 1 : 1 : 10, 1 : 1 : 100 and 1 : 1 : 1000. In the latter case, the analyte solution had to be diluted 1/10 by ultra-pure water to remain in the calibrated concentration range with linear system response.

If uncatalyzed oxidations or decomposition reactions involving NMMO are conducted at higher temperatures above 100°C, the reaction mixture is a complex mixture of intensively colored substances. Capillary electrophoresis of those mixtures with hydrostatic sampling gives totally irreproducible results. However, the

problems with conventional hydrostatic sampling of dark-colored samples due to disturbance of the UV detection by chromophores in the analyte can be almost completely overcome by electromigration in the present case. This is shown in Figure 4 for the oxidation of 10% xylose by NMMO at 100°C as an example.

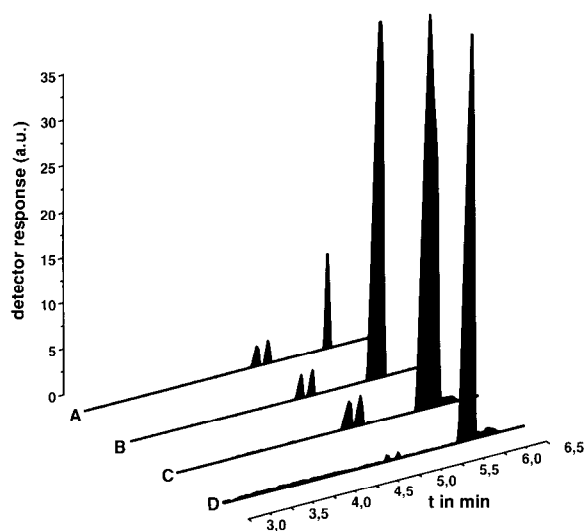


Figure 3. Separation of NMM, M and NMMO at different molar ratios: NMM / M / NMMO = 1:1:1 (A), 1:1:10 (B), 1:1:100 (C), and 1:1:1000, dil. 1:10 (D).

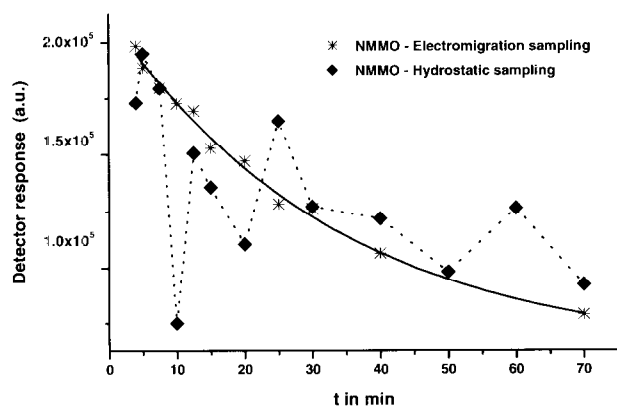


Figure 4. Kinetics of the oxidation of 10% xylose by NMMO monohydrate at 100°C monitored by CE with hydrostatic sampling (dotted line) and electromigration sampling (solid line).

As the colored species are probably irregularly composed electro-active compounds of higher molecular weight, the retention of different amounts of analyte by these colored decomposition products due to a matrix effect is probably the reason for the fact that electromigration proved to be superior to siphoning. Electromigration sampling does not interfere with the analysis parameters used, and gives the same reliable results as does

hydrostatic sampling in the absence of strong chromophores. For both sampling techniques, no other sample preparation than the dilution of the sample to a concentration within the calibrated range is necessary.

Applications of the analytical method. The reason for developing the presented analytical method was to follow the kinetics of decomposition reactions of NMMO, and oxidation reactions involving amine oxides. For example, solutions of cellulose in NMMO monohydrate produce both M (6) and NMM (7) according to mechanisms not yet completely understood. These byproducts, among others, are suspected to promote degradation of cellulose, cause discoloration of the resulting fibers [7], or even give rise to thermal [8] or autocatalytic [9] runaway reactions.

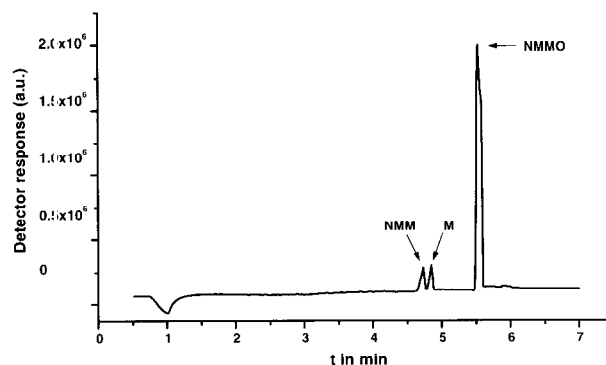


Figure 5. Example reaction: reaction of 5.5% cellulose with NMMO monohydrate at 120°C. Electropherogram of the reaction mixture after a reaction time of 8 mins.

As these processes are highly undesirable, NMMO solutions of cellulose used for fiber production are normally stabilized against decomposition and the detrimental effects of the byproducts generated. The continuous monitoring of the respective composition of the reaction mixture, or the testing of the effectiveness of stabilizers, by the presented method is feasible without any problems. The electropherogram of a reaction mixture of 5.5% cellulose in NMMO monohydrate after a reaction time of 8 minutes at 120°C is shown in Figure 5. The CE method developed was also used to investigate the kinetics of the autocatalytic decomposition of NMMO by carbenium-iminium ions. The mechanism of this reaction (Figure 6) has been investigated in detail as described elsewhere [9].

The carbenium-iminium ions which trigger the decomposition of **4** can be either introduced into the reaction mixture as a stable reagent, such as Eschenmoser's salt (**5**), cf. Figure 6, sequence A. In this case, **5** acts as an initiator causing production of the *N*-methylenemorpholinium cation (**8**) which is in turn the actual catalyst. Only 1% of this carbenium-iminium ion is able to completely decompose NMMO to morpholine and formaldehyde within minutes (Figure 7).

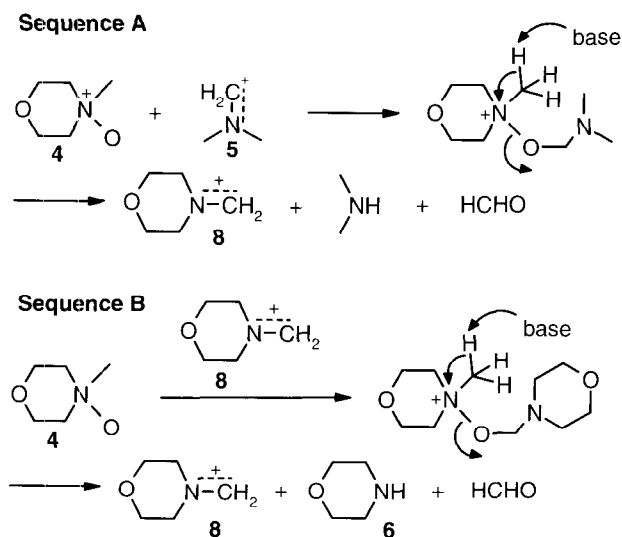


Figure 6. Reaction mechanism of the autocatalytic decomposition of NMMO induced by carbenium iminium ions (*Mannich* intermediates).

However, *Mannich* intermediate **8** can also be generated *in situ* by the reaction of morpholine and formaldehyde. In this case, which represents the typical decomposition of NMMO by its degradation products, the carbenium-iminium ion is both the initiator and the catalyst.

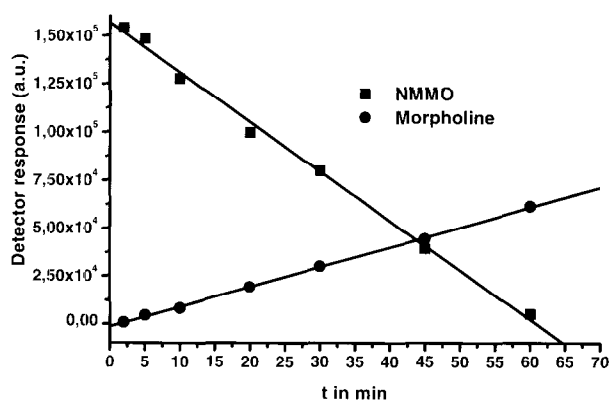


Figure 7. Kinetics of the decomposition of NMMO into morpholine and HCHO induced by the stable carbenium-iminium ion **5** (1% relative to **4**).

Morpholine (**6**) and formaldehyde form *N*-hydroxymethylmorpholine, which produces the *Mannich* intermediate **8** after protonation and dehydration. This carbenium-iminium ion causes the degradation of NMMO into morpholine and HCHO regenerating **8**, according to the mechanism in Figure 6, sequence B. Thus, the decomposition of **4** by the action of **8** is clearly an autocatalytic process. The kinetics of the complex mechanism are shown in Figure 8.

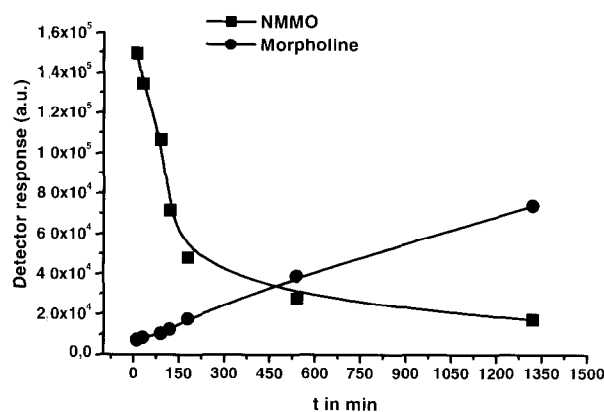


Figure 8. Kinetics of the autocatalytic decomposition of NMMO into morpholine and HCHO induced by a mixture of morpholine and HCHO (0.1% relative to **4**).

Through the autocatalytic nature of the reaction, only minute amounts of morpholine and HCHO are required to decompose large quantities of NMMO. This renders the prevention of the reaction seemingly rather difficult if both compounds are present at the same time. Since the *N*-methylenemorpholinium cation (**8**) has been shown to be present *in situ* in the system NMMO / cellulose / water by specific trapping reactions [10], the question might arise why solutions of cellulose in NMMO are stable at all. The reason is the much higher reaction rate of **8** with CH-acidic compounds present, such as carbohydrate structures, as compared to the sterically disfavored electrophilic attack at NMMO. Thus, the autocatalytic decomposition of NMMO becomes prominent only if the local *in situ*-concentration of **8** increases to a degree that its consumption in other reactions cannot compensate for its production.

Conclusion

A general method based on capillary electrophoresis (CE) with indirect UV detection has been described. The analytical procedure allows to separate and quantify *N*-methylmorpholine-*N*-oxide and its main reaction products *N*-methylmorpholine and morpholine, even if the former component is present in a large excess. A background electrolyte with a rather low pH of 3.3 is an essential for the separation performance. Hydroxy-isobutyric acid, an ingredient of the electrolyte itself, is used to adjust the pH.

The applicability of the method has been demonstrated by the analysis of reaction mixtures of NMMO with cellulose and xylose, respectively. In both cases, NMM and M are formed as byproducts, albeit at largely differing rates.

Similarly, the kinetics of the autocatalytic degradation of *N*-methylmorpholine-*N*-oxide induced by carbenium-iminium ions (*Mannich* intermediates) has been monitored. As the catalyst in the decomposition reaction, the *N*-methylenmorpholinium cation (**8**), can be formed *in situ* from morpholine and HCHO, the reaction might be a cause for hitherto unexplainable, „spontaneous” degradation reactions in reaction mixtures containing NMMO.

Acknowledgement

The support of the Department of Wood and Paper Science at North Carolina State University, Raleigh, USA, where parts of the experimental work were conducted, is gratefully acknowledged. We would like to thank Dr. A. Hofinger (Institute of Chemistry, University of Agricultural Sciences Vienna) for recording the NMR spectra. We are grateful to Doz. Dr. H. Sixta and Dr. H. Firgo for valuable comments. The financial support by the LENZING AG, Lenzing, Austria, is gratefully acknowledged.

References

- [1] a) Chanzy, H. *J. Polym. Sci., Polymer Phys. Ed.* **1980**, *18*, 1137. b) Chanzy, H.; Nawrot, S.; Peguy, A.; Smith, P. *J. Polymer Sci.* **1982**, *20*, 1909. c) Firgo, H.; Eibl, M.; Kalt, W.; Meister, G. Internationales Symposium „Alternative Cellulose - Herstellen, Verformen, Eigenschaften”, Thüringisches Institut für Textil- und Kunststofforschung (TITK), 7.-8. Sept. 1994, Rudolstadt/Schwarza, Thüringen.
- [2] a) Albini, A. *Synthesis* **1993**, 263. b) For transition metal catalyzed oxidations see following examples: Godfrey, A. G.; Ganem, B. *Tetrahedron Lett.* **1990**, *31*, 4825. Suzuki, S.; Onishi, T.; Fujita, Y.; Misawa, H.; Otera, J. *Bull. Chem. Soc. Jpn.* **1986**, *59*, 3287.
- [3] Taeger, E.; Michels, C.; Nechtawal, A. *Papier* **1991**, *12*, 784.
- [4] Sohn, O.S.; Fiala, E.S.; Conaway, C.C.; Weisburger, J.H. *J. Chromatogr.* **1982**, *242*, 347.
- [5] Widhalm, A.; Kenndler, E. *Anal. Chem.* **1991**, *63*, 645.
- [6] Jung, G.Y.; Kim, T.H.; Lim, H.B. *Analytical Sciences* **1996**, *12*, 367.
- [7] Taeger, E.; Franz, H.; Mertel, H. *Formeln, Faserstoffe, Fertigware* **1985**, *4*, 14.
- [8] Buijtenhuis, F.A.; Abbas, M.; Witteveen, A.J. *Papier* **1986**, *40*, 615.
- [9] Rosenau, T.; Potthast, A.; Kosma, P.; Chen, C.L.; Gratzl, J.S. *J. Org. Chem.* **1999**, *64*, 2166.
- [10] Potthast, A.; Rosenau, T.; Kosma, P.; Chen, C.L.; Gratzl, J.S. *Holzforschung* **2000**, in press.

DETERMINATION OF SMALL ANIONIC SULFUR SPECIES IN MAGNESIUM BASE BISULFITE COOKING LIQUOR BY CAPILLARY ELECTROPHORESIS (CE)

N. Schelosky, T. Baldinger

Lenzing AG, A-4860 Lenzing, Austria

Capillary electrophoresis was applied for quantitative determination of sulfite, sulfate and thiosulfate in magnesium base bisulfite cooking liquor in the course of digestion. Separation was achieved based on the results of Gutleben with a buffer consisting of 5 mmol/L potassium chromate, pH 11.0, and 0.001 % hexadimethrine bromide (HDB). For sampling under conditions of up to 150 °C and 8 bar a water cooled six port valve was inserted into a bypass of the process stream. The samples were purged out with a mixture of sodium hydroxide and formaldehyde. Furthermore 0.01 % hexadimethrine bromide was added to the samples. This method was properly validated in terms of calibration, limit of quantification, repeatability, linearity, accuracy and sample stability and was found

to be suitable for general research purposes. Quantification was done by relation of the migration time corrected peak areas to an internal standard (chloride). Application of this method to several laboratory magnesium bisulfite cooking experiments revealed sulfite concentrations of 80 to 15 mg/mL showing a decrease during the cooking process and sulfate concentrations between 4 and 7 mg/mL showing a comparatively slight increase. Thiosulfate, however, was below the limit of detection of 0.3 to 0.7 mg/mL under standard conditions.

Keywords: cooking liquor, analysis, capillary electrophoresis, sulfite, sulfate

Introduction

Generally, quantitative knowledge about the course of the concentration of compounds in a process can be assumed to be helpful for its understanding and optimization regarding yield, recovery or costs. In the case of the magnesium base bisulfite process - an industrially applied method for the production of pulp - sulfur dioxide, sulfite, respectively, and other small inorganic anionic sulfur species derived from it in the cooking liquor are interesting objects for observation. In this work sulfite, sulfate and thiosulfate were investigated.

In the early stages of magnesium base bisulfite cooking titrimetric methods for the determination of their concentration are feasible but in the course of the delignification this is not possible any more due to the complex matrix consisting

of degraded and solubilized organic compounds. To overcome this problem a separation step must be applied prior to quantification. From the analyst's pool of separation techniques capillary electrophoresis (CE) was chosen, because there is no expensive stationary phase prone to fouling, which has to be expected in the case of chromatography or electrochromatography on dirty samples without tedious sample clean-up. In addition, fast separations in the range of a few minutes and even seconds are possible.

Capillary electrophoresis has become a widely accepted separation technique in quantitative analysis [1, 2]. There are several publications in the field of pulping [3 - 7], and also about the separation of anions in magnesium base bisulfite cooking liquor [8]. Separations in capillary electrophoresis are based upon different electrophoretic mobilities of the analytes in an

electrical field, which in turn are determined by size and charge of the analytes and properties of the background electrolyte, such as viscosity and permittivity. Besides the ion's own mobility there exists also the so called electroosmotic flow (EOF), which originates from charges on the surface of the capillary, caused for instance by deprotonation of silanol groups, derivatization or coating, leading to oppositely charged layers in the buffer. Upon application of an external electrical field the mobile one of these layers moves along the capillary dragging the whole contents in the direction according to this layer's charge. With the aid of the above mentioned modifications the analyst can control the direction and size of the EOF, which contributes to the ion's observed mobility by vector addition of EOF and the ion's own mobility. Fast separations will be possible if these two vectors possess the same direction. For anions this demands a positively charged capillary surface, which can be managed by adsorption of polymeric quaternary ammonium ions on the mostly used fused silica capillaries.

Experimental

Based on the results of Gutleben [8] a capillary electrophoresis method was established for the quantitation of sulfite, sulfate and thiosulfate. A HP^{3D}CE instrument was used in the ce+p mode. The buffer consisted of 5 mmol/L potassium chromate adjusted to pH 11.0 with sodium hydroxide and 0.001 % hexadimethrine bromide (HDB) for the reversal of the EOF. The buffer was degassed by sonication and filtered through a 0.45 μm membrane filter. The separation occurred in a fused silica capillary of 60 cm length (51.5 cm effective length) and 50 μm diameter under the application of a voltage of -30 kV leading to a current of approximately 15 μA . Indirect UV detection was performed at 275 \pm 20 nm, the peak width was set < 0.01 min. Hydrodynamic injection was accomplished by 30 mbar and 10 s. The anions for calibration were used as their sodium salts. All substances were of p.a. grade, water was of HPLC grade.

Between runs, the capillary was purged by a multistep sequence applying 0.1 mol/L sodium hydroxide, buffer without HDB and running buffer, but lately it was found that purging with

running buffer at 2 bar and simultaneous application of a voltage of -30 kV for one minute was sufficient for repeatable results. The buffer (0.75 mL) was changed after six or less runs.

For sampling under conditions of up to 150 °C and 8 bar a water cooled six port valve was inserted into a bypass of the process stream. The samples were purged out into a 10 mL volumetric flask containing sodium chloride solution as an internal standard with a mixture of sodium hydroxide (final 0.2 mol/L) for sulfur dioxide absorbance and formaldehyde (final 0.037 %) for prevention of sulfite oxidation. This sampling device is shown in Figure 1.

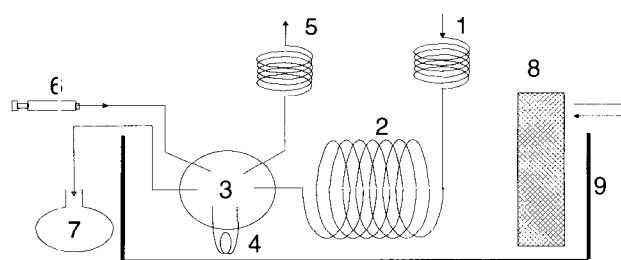


Figure 1. Experimental set up for sampling. 1 entrance from digester; 2 capillary coil (4 m) for thermostating; 3 six port valve; 4 sample loop; 5 exit to cooking liquor circulation system; 6 syringe for purging of the sample loop; 7 volumetric flask with internal standard; 8 thermostat; 9 water bath.

Furthermore, in a second dilution step with 0.037 % formaldehyde solution 0.01 % hexadimethrine bromide was added to the samples to avoid capillary fouling by matrix effects. Finally samples were filtered through a 0.45 μm membrane filter. Standards for calibration were prepared accordingly with the addition of sodium chloride, formaldehyde and HDB. A blank solution additionally contained sodium hydroxide. A synthetic sample was prepared by weighing the substances in one flask and treating them correspondingly. The volume of the sample loop of the six port valve was determined by filling with a furfural solution of known concentration, purging it out into a 10 mL and 25 mL volumetric flask and determining the final concentration by HPLC. By doing so, it could be also confirmed that a final volume of 10 mL is sufficient for complete purging of the sample loop.

Results and Discussion

Typical electropherograms obtained with this method are presented in figure 2.

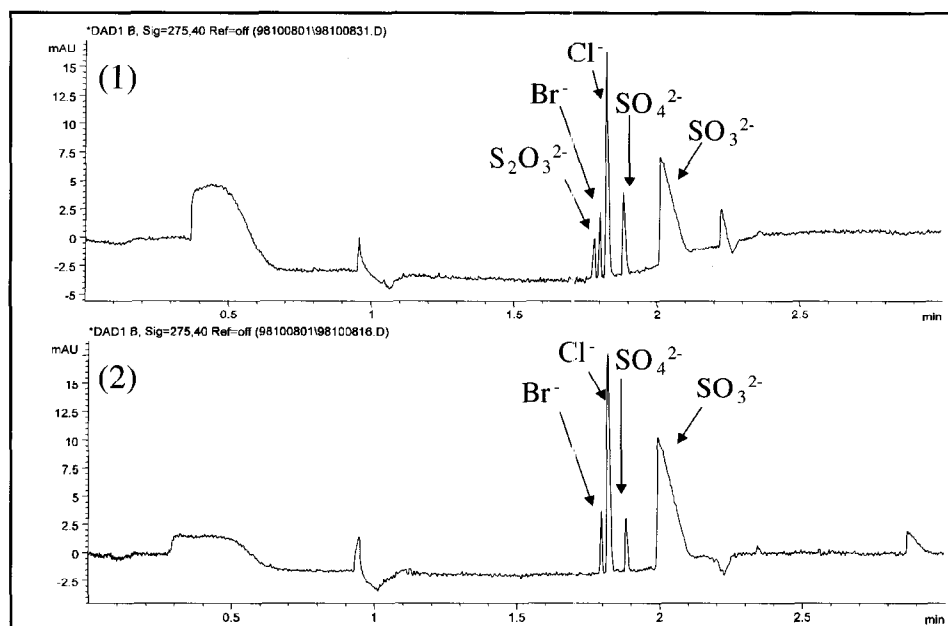


Figure 2. Electropherograms of standard (1) and sample (2).

Validation. Generally, quantification was done by relation of the migration time corrected peak areas to an internal standard (chloride).

Calibration was performed by triple injection of mixed standard solutions at four to six concentration levels and simple linear regression of the term $[\text{area (anion)} / \text{migration time (anion)}] / [\text{area (chloride)} / \text{migration time (chloride)}]$ versus concentration (anion) / concentration (chloride). During routine work calibration was done at three concentration levels by three or more injections throughout one batch. Linear calibration curves were obtained for sulfite (100 – 550 $\mu\text{g/mL}$, slope 0.9956, intercept -0.1735, r^2 0.998), sulfate (10 – 82 $\mu\text{g/mL}$, slope 0.7598, intercept 0.0034, r^2 0.999) and thiosulfate (10 – 100 $\mu\text{g/mL}$, slope 0.6029, intercept -0.0063, r^2 0.998). The linearity of the calibration curves was also successfully checked by plots of response factor versus concentration quotient, where no trends were visible and the response factors were all within 5 % of the average. The limit of quantification based on a peak height of nine times the noise was 55 $\mu\text{g/mL}$, 10 $\mu\text{g/mL}$ and 10 $\mu\text{g/mL}$ for sulfite, sulfate and thiosulfate, respectively. Thiosulfate was found to be absent at these concentrations under

standard dilution in laboratory cooking experiments. Measurements of less diluted samples pointed towards concentrations in the range of 0.2 mg/mL of thiosulfate in undiluted laboratory cooking acid. Thus, no values for some validation tests were obtained for thiosulfate. Concentrations, which were calculated from observed peak areas during calibration, deviated 0.2 to 5.4 %, 0.3 to 6.7 % and 0.1 to 12.8 % from the true values for sulfite, sulfate and thiosulfate, respectively. The comparatively high value of thiosulfate was due to a point at the limit of quantification, at higher concentrations the deviation was less than 5.4 %. The repeatability of the instrumental measurement expressed as the relative standard deviation of 12 successive injections of a sample was 1.6 % and 2.9 % for sulfite and sulfate, respectively. The repeatability including sampling and sample preparation determined by six samples and single injection was 2.0 % and 3.6 % for sulfite and sulfate.

Table 1. Summary of validation results.

| | SO ₃ ²⁻ | SO ₄ ²⁻ | S ₂ O ₃ ²⁻ | |
|--------------------|-------------------------------|--------------------------------|---------------------------------------------|--------------|
| calibration | range [µg/mL] | 100-550 | 10-82 | 10-100 |
| | r ² | 0.998 | 0.999 | 0.998 |
| | linearity check | ok | ok | ok |
| | loq* [µg/mL] | 55 | 10 | 10 |
| | max. error % | 5.4 | 6.7 | 12.8** / 5.4 |
| repeatability | instrument rsd% | 1.6 | 2.9 | < loq |
| | total rsd% | 2.0 | 3.6 | < loq |
| linearity (sample) | range | 50 - 250 % of routine dilution | | |
| | r ² | 0.999 | 0.998 | < loq |
| | linearity check | trend<5 % | ok | < loq |
| recovery | % of spiked samples | 96.2 | 105.9 | 104.4 |
| | % of titration | 100 | | |

* limit of quantification ** at the loq

The linearity of sulfite and sulfate in the sample matrix in the range of the calibration was proven by taking a sample containing two loop volumes and preparation of five dilutions thereof covering the range of 50 to 250 % of the standard dilution. A plot of measured concentration of the diluted

solutions versus dilution gave r² values of 0.999 and 0.998 for sulfite and sulfate, respectively. A plot of calculated concentration of the original sample versus dilution revealed a slight dependence of the result of sulfite on the dilution at low peak areas. However, all results were within 5 % of the overall average. In the case of sulfate no trends could be observed.

Accuracy was checked by spiking a sample before dilution up to twice the concentration of the untreated sample. Also thiosulfate, which was not detectable in the original sample, was added. Calculation of the recovery of these spiked samples yielded an average recovery of 96.2 %, 105.9 % and 104.4 % for sulfite, sulfate and thiosulfate, respectively. Comparison of capillary electrophoretic results and independent volumetric results of sulfite, which were routinely determined during the first stages of laboratory cooking experiments, showed an excellent correspondence of 100 % with a standard deviation of 4 %. A summary of these validation data is given in Table 1.

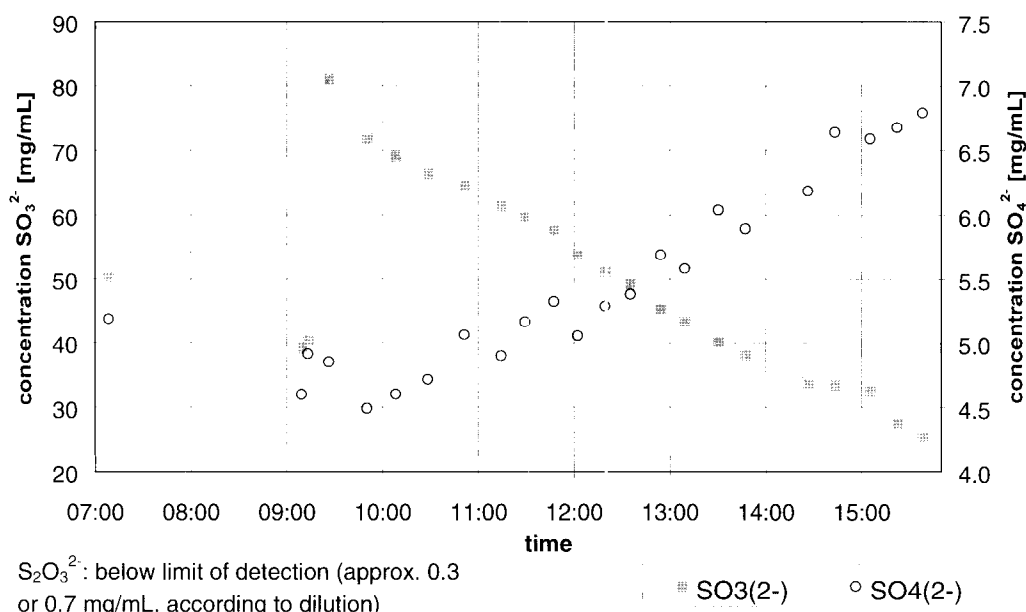


Figure 3. Concentration of sulfite and sulfate in cooking acid during a laboratory cooking experiment.

First experiments concerning the stability of untreated samples had revealed a 10 % increase of the sulfate and a corresponding decrease of the sulfite peak area after migration time and internal standard correction within six consecutive injections. Obviously some kind of protection against oxidation of sulfite had been required. Consequently, the suggested stabilization by

addition of formaldehyde was checked by sevenfold injection of a sample containing 0.037 % formaldehyde and also some added thiosulfate in the course of 13 hours. The results showed a random scattering without any obvious trend. The relative standard deviations of 1.3 to 2.1 % were within an acceptable range proving the efficiency of the proposed stabilization method

for the collection of one cooking experiment's diluted and stabilized samples and their batchwise analysis by CE afterwards. However, longterm storage, two weeks in a deepfreezer, was not successful.

Application. The above described and validated method was applied to several laboratory magnesium base bisulfite cooking experiments covering different kinds of wood, such as beech, eucalyptus and aspen, and several cooking conditions. Sulfite concentrations of 80 to 15 mg/mL showing a decrease during the cooking process and sulfate concentrations between 4 and 7 mg/mL showing a comparatively slight increase were found. Thiosulfate, however, was below the limit of detection of 0.3 to 0.7 mg/mL under standard conditions. Under less dilute conditions it was found to be present at about 0.2 mg/mL at the starting point of cooking and to decrease during the process. Figure 3 shows the course of concentrations of sulfite and sulfate during a typical magnesium base bisulfite cooking experiment.

Conclusion

A CE method for the quantitative determination of sulfite, sulfate and, with limitations, of thiosulfate in magnesium base bisulfite cooking liquor was validated and found suitable for general research purposes. However, precision could be improved and the linear range be extended. Nevertheless, the practical application to various laboratory cooking experiments was satisfactory.

Acknowledgements

The authors would like to express their thanks to the FEL group, Lenzing AG, for access to the CE instrument, to Mag. Gutleben and Prof. Zemann for information concerning the CE method, as well as to Mr. Moosbauer and Mr. Scheinecker for their practical assistance.

References

- [1] Engelhardt, H.; Beck, W.; Schmitt, T. *Kapillarelektrophorese*, Vieweg, 1994.
- [2] Jandik, P.; Bonn, G. *Capillary Electrophoresis of Small Ions and Molecules*, VCH, 1993.
- [3] Romano, J.; Jandik, P.; Jones, W.R.; Jackson, P.E. *J. Chromatogr.* **1991**, *546*, 411.
- [4] Salomon, D.R., Romano, J.P. *Process Control Qual.* **1992**, *3*, 219.
- [5] Jones, W.R. *J. Chromatogr.* **1993**, *640*, 387.
- [6] Masselter, S.M.; Zemann, A.J.; Bonn, G.K. *J. High Resol. Chromatogr.* **1996**, *19*, 131.
- [7] Volgger, D.; Zemann, A.; Bonn, G.K. *J. High Resol. Chromatogr.* **1998**, *21*, 3.
- [8] Gutleben, W. diploma thesis, University of Innsbruck, 1998.

SOME FEATURES OF THE INTERMOLECULAR INTERACTION OF ANIONACTIVE LIGNIN WITH SYNTHETIC OLIGOMERS IN AQUEOUS SOLUTIONS

G. Shulga,^a E. Lagzdin,^b A. Treimanis^c

^a Latvian State Institute of Wood Chemistry, 27 Dzerbenes Str., LV-1006 Riga, Latvia

^b Institute of Inorganic Chemistry, Technical University, 1 Kalku St., LV-1050 Riga, Latvia

The interaction between sodium lignosulphonate and synthetic amphiphilic oligomers - sodium alumoalkylsilixonalate in diluted reaction mixtures in the 3-7 pH range has been investigated. Methods of potentiometric and conductometric titration as well as turbidimetry and liquid chromatography were used for the study. The interaction between lignosulphonate and oligomers is of electrostatic nature and leads to the formation of intermolecular complexes. Their concentration in the mixture is determined by the composition of mixture and its pH value. From the viewpoint of the DLFO theory, such an interaction may be characterized as the compensation of the "effective" charge. The presence of low-molecular weight electrolytes in the reaction

mixture impairs the conditions of the interaction between the components due to the competition in binding a positively charged molecule of oligomeric heteroxyloxanolate with chloride-anions. A gain in the degree of association between the oppositely charged molecules in water-ethanol mixtures is conditioned by a lower degree of solvation of the interacting poly- and oligoelectrolytes. The formation of donor-acceptor bonds in intermolecular complexes has been revealed. The structural features of the intermolecular complexes determine their surface-active and adhesive properties.

Key words: alumoalkylsilixonalate, intermolecular complexes, lignosulphonate, surface tension

Introduction

Investigation of pulping processes as well as development of methods for the synthesis of new polymeric products from lignin-based products are underway at the Latvian State Institute of Wood Chemistry [1].

It is known that almost 95% of all lignin-derived products are generated from sulphite spent liquor, and only 5% are related to kraft pulping. In spite of the fact that kraft pulping is of considerable priority world-wide, the competitiveness of the sulphite pulping process could be increased by development of rational methods for modifying its by-products.

Much attention has been paid recently to studies on the interpolyelectrolyte interactions of lignosulphonate with polymeric cations [2-4] that are of considerable importance in papermaking and waste water treatment [5,6]. The polymeric

products of interpolyelectrolyte reactions have found applications as surfactants, binders, glues, fillers, emulgators, reinforcing agents, etc. [7,8]. At the same time, the interpolymer interactions of lignins with oligomeric ampholytes in aqueous media have not been adequately investigated.

The aim of the present study was to establish the features of the interaction of lignosulphonates with synthetic oligomers in aqueous media, and to study the properties of the polymeric products formed.

Experimental

Purified commercial sodium lignosulphonate from spruce wood had the following formula: $C_9H_{6.54}O_{2.57}(OCH_3)_{0.71}(SO_3Na)_{0.35}(OH)_{0.68}(CO)_{0.36}$. Its molecular weight was determined by size-exclusion chromatography

using polystyrene calibration standards and it was found to be approx. 41 000 Dalton.

As synthetic oligomers, sodium aluminosiloxanolate oligomers (ASO) with the Si/Al mass ratio equal to 2.91 were used. ASO were obtained under laboratory conditions by adding aluminium to alkaline solution of sodium alkylsiloxanolate at room temperature [9]. The investigation of the behaviour of ASO in aqueous media, which was carried out by potentiometric and conductometric titration, viscosimetry, liquid chromatography, IR and UV spectroscopy, has shown a considerable change of the molecular structure of ASO upon variation of the pH value, caused by a different coordination of silicon atoms with aluminium. The presence of multi-charged positive Al ions in acidic media and negatively charged aluminate- and siloxanolate ions in alkaline media imparted amphiphilic properties to siliconorganic oligomers. The amphiphilic nature of ASO manifested itself clearly in reactions with polyacrylic acid in acidic media and with polydimethyldiallylammonium chloride in neutral and alkaline media [10].

Reaction mixtures prepared by mixing aqueous solutions of LS and ASO at $20 \pm 1^\circ\text{C}$ were characterized by the composition Z (mass ratio oligomers / LS) and varied from 0.1 to 7. The concentration of ASO in reactions with LS was considerably lower than CCM (critical concentration of micelle formation) and did not exceed 0.1 g/dl. pH regulation of the mixture was done by adding HCl or NaOH. Potentiometric titration was performed using a Radiometer pH-meter within the pH range 3 – 7, conductometric titration with an OK-102/1 conductometer. The specific conductivity of distilled water used was equal to $4.5 \cdot 10^{-6}$ S/cm. Turbidity of reaction mixtures was determined by a KFK-2 photocolorimeter and characterized by light transmittance (T_c) measured at a wavelength of 540 nm and expressed on a percentage basis. Molecular weight distribution of the formed polymer products was determined by means of size-exclusion chromatography with a SFERON P-1000 column, refractive index detector, and 0.01 N acidic buffer as the eluant with a flow rate of 20 ml/h. Surface tension of reaction mixtures was determined by the Wilhelmy plate method in the temperature range $20\text{--}60^\circ\text{C}$.

Results and Discussion

The mechanism of the interaction between Na-LS and ASO molecules was studied by the method earlier used for studies of intermolecular interactions between oppositely charged polyelectrolytes [11]. Potentiometric titration curves of both LS and ASO in acidic media, as well as their aqueous reaction mixtures at different component ratios are represented in Figure 1. The curve corresponding to the reaction mixtures (curve 3) is shifted to the lower pH range and reveals two steps of titration, characterised by smaller pK_a values than the initial ASO. A comparison of the titration curves displays that the mixing of components is accompanied by a release of protons. This is indicative of the electrostatic nature of the interaction between LS and ASO. An interaction of this type may be represented by Scheme 1.

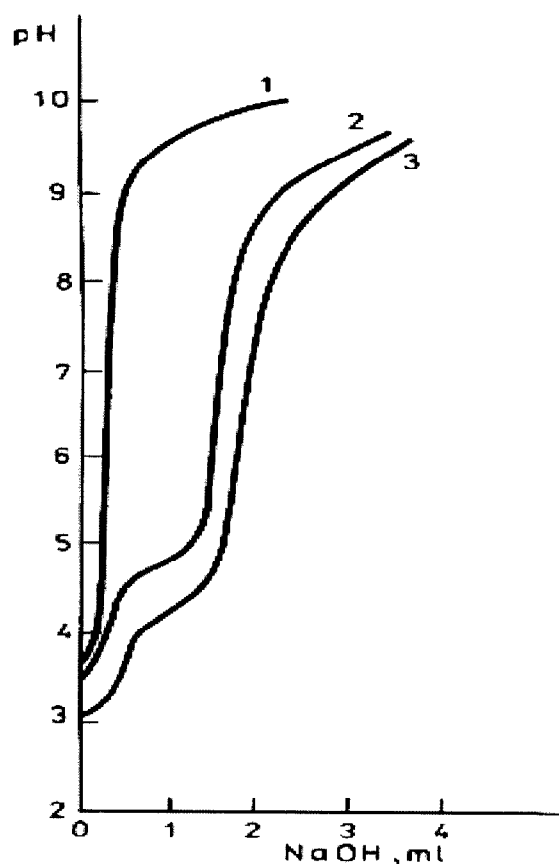
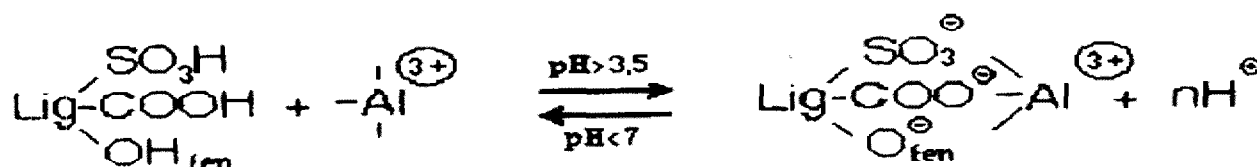


Figure 1. Potentiometric titration curves of acidic aqueous solutions: 0.01 g/dl LS (1); 0.01 g/dl ASO (2) and their reaction mixture with composition $Z=1$; concentration of NaOH: 0.04 mole/l; 20°C ; titration rate: 0.1 ml/min; volume of solutions: 50 ml.



Scheme 1. Interaction between LS and ASO.

The concentration of released protons calculated as a difference between pH values of acidic LS and reaction mixture solutions (ΔpH) increases when the oligomers content is higher and decreases when there is an excess of the LS content in the mixture. At the same time, the dependence of ΔpH on the ASO concentration in the reaction mixture is nonlinear. A maximum pH is observed at a threefold oligomers excess in the reaction mixture (Figure 2). Obviously, this mass ratio of the components corresponds to the stoichiometry of the intermolecular reaction.

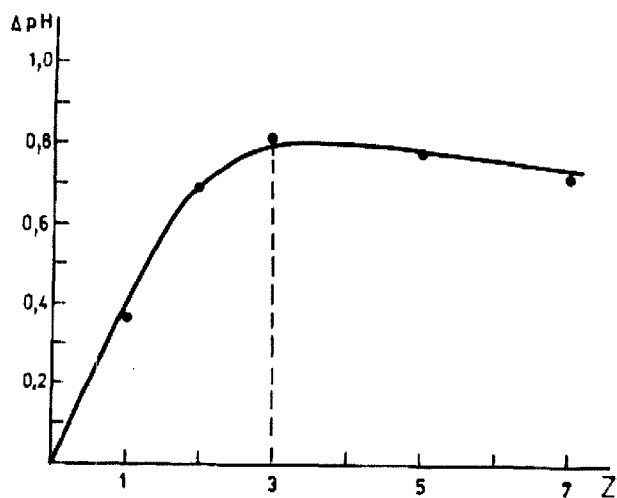


Figure 2. Dependence of released protons concentration on LS-ASO reaction mixture composition Z ; LS concentration: 0.01 g/dl.

As follows from the analysis of normalized chromatograms (Figure 3), the introduction of oligomers into aqueous solutions of LS is accompanied by the increase of the first peak area and its shift to higher molecular weight values. If the LS to ASO ratio is decreased, the growth of the area of the first peak and its shift are more evident (curves 2, 3). The changes in the molecular mass distribution of the LS-ASO mixture and its dependence on the composition of the reaction mixture indicates the formation of LS-ASO associates - intermolecular complexes.

The polymeric product formation is confirmed also by alterations in the mobility of interacting molecules. It is manifested as a decrease of the specific conductivity from $590 \cdot 10^{-6}$ S/cm at pH 3 to $309\text{-}408 \cdot 10^{-6}$ S/cm within the pH range 4-6 (Figure 4).

The water-solubility of the formed intermolecular complexes depends on the composition of the reaction mixture. In the 4-6 pH range at mixture compositions $Z \geq 1$, phase phenomena are observed, accompanied by the formation of colloidal dispersions. It is characteristic that at a considerable excess of ASO in the reaction mixture ($Z > 3$), only water-soluble products are formed.

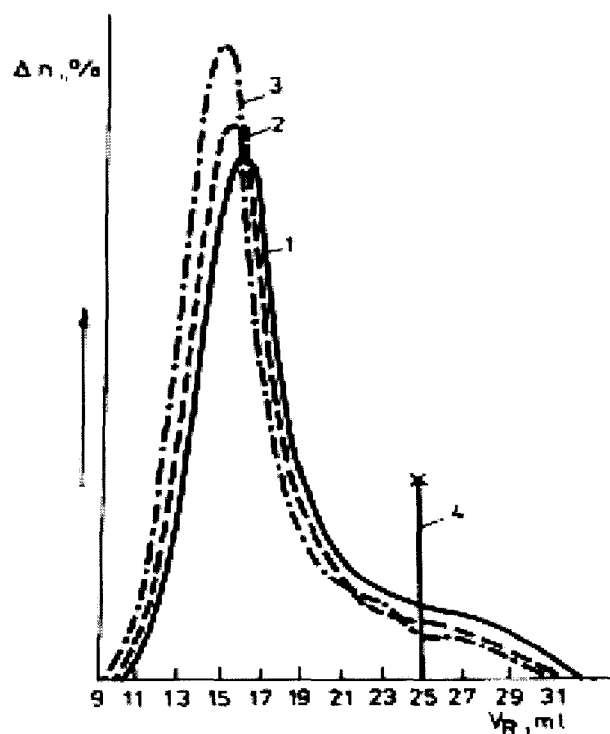


Figure 3. Normalized chromatograms LS (1) and LS-ASO reaction mixtures with following composition Z : 0.5 (2); 0.8 (3); elution volume of ASO (4); pH 4.5; flow rate: 20 ml/h.

According to the analysis of the dependencies of ΔpH and light transmittance coefficient on the pH of the mixture (Figure 4), the intermolecular interaction in the reaction mixture is enhanced as

the pH increases from 3 to 6. This may be assumed to be connected with the diminishing of the hydrate shell thickness around the ASO molecule as a result of decreasing its ionisation degree. It was found that the highest turbidity of reaction mixtures ($1 \leq Z < 3$) is observed at pH values close to the isoelectric point of oligomeric molecules.

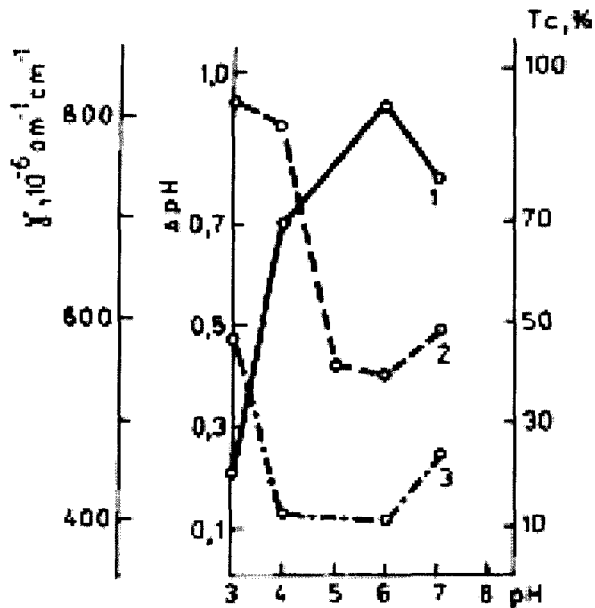


Figure 4. Dependence of released protons concentration (ΔpH) (1), light transmittance coefficient (T) (2) and specific conductivity (γ) (3) on the pH value of LS-ASO reaction mixtures; $Z=1$; LS concentration: 0.01 g/dl.

The stability of the formed products is determined by the pH range in which the metal atoms of oligoelectrolytes are positively charged. In neutral medium, the dissociation of the

intermolecular associates proceeds, which is testified by the decrease of turbidity and the increase of conductivity of the LS-ASO reaction mixtures. Such a behaviour of LS and synthetic oligomers in acidic aqueous mixtures confirm LS-ASO intermolecular associates owing to salt (ionic) bonds. The interaction between electrolytes can be explained from the viewpoint of the DLFO theory as neutralizing of the "effective" charge [12].

The quality of the solvent is known to exert a definite effect on the conversion of electrolyte systems and may be varied by adding a low-molecular weight electrolytes or an organic solvent to the aqueous reaction mixture. The increase of the ionic strength of reaction mixtures due to the introduction of NaCl causes a shift of the titration curves to the region corresponding to the neutral medium. Simultaneously, the quantity of released protons and the turbidity of reaction mixtures are decreased (Figure 5A).

Such a behaviour of poly- and oligoelectrolytes in the presence of low-molecular weight electrolytes points out the deterioration of reaction conditions for electrostatic interactions due to the screening of ASO molecules by chloride anions. At the same time, the turbidity of reaction mixtures is increased in water-ethanol solutions (Figure 5B). The gain in chemical affinity between LS and ASO molecules in water-ethanol solutions is supposed to be related to the smaller extent of solvation of both components.

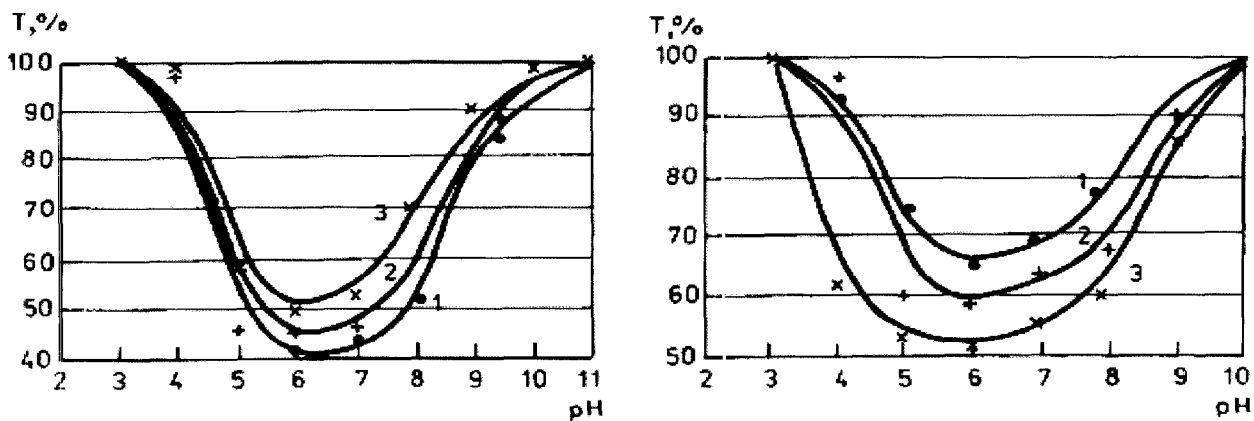


Figure 5. A) Effect of NaCl concentration on the turbidity of reaction mixture with composition $Z = 1$; in bidistilled water (1); in 0.03 mole/l NaCl solution (2); in 0.05 mole/l NaCl solution (3); LS concentration: 0.01 g/dl. B) Effect of ethyl alcohol concentration in bidistilled water on the turbidity of reaction mixtures with composition $Z = 1$; in bidistilled water (1); in water with 17.5 g/dl alcohol concentration (2); in water with 35.0 g/dl alcohol (3); LS concentration: 0.0075 g/dl.

The analysis of the ESR spectra of the initial components of reaction mixtures and products of their interaction has shown that, in acidic media, along with salt bonds, a definite contribution to the stability of complex compounds is provided by bonds of electron donor / electron acceptor type. The donor-acceptor interaction between aluminium ions and LS phenolic hydroxyl and carbonyl groups as well as with the π -electrons of aromatic ring results in a considerable rearrangement of electron density, both of the donor and acceptor, and is accompanied by the formation of stable paramagnetic centres [13].

Modification of anionactive lignin by interaction with synthetic oligomers in reaction mixtures with $Z \leq 3$ results in a considerable hydrophobicity of its molecules. This is shown by the essential increase of the distribution constant values of LS-ASO intermolecular complexes relative to the initial LS in the system n-heptane / water determined according to [14]. The structural peculiarities of LS-ASO intermolecular complexes cause their surface activity at different interfaces that may be varied by changing the composition and the concentration of the reaction mixtures.

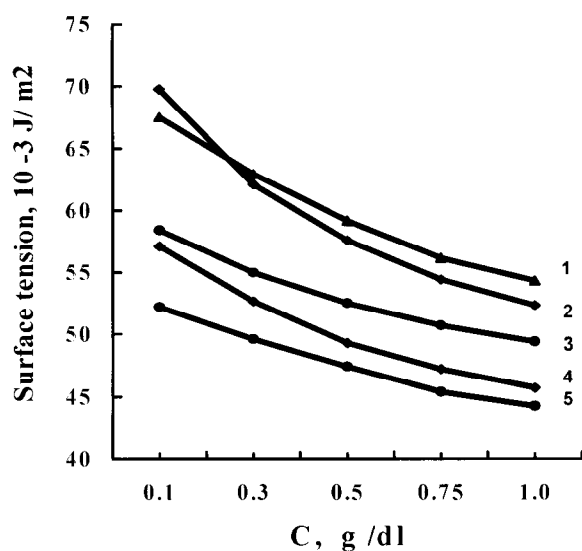


Figure 6. Surface tension isotherms of LS (1), ASO (2) and their reaction mixture with $Z=0.5$ at different temperatures: 20°C (3), 40°C (4), 60°C (5); pH 5.2. Adsorption isotherms for LS and ASO solutions were determined at 20°C.

The intermolecular complexes formed in semidilute solutions of the reaction mixtures with $Z < 1$ are water-soluble. In acidic media they are

characterized by lower values of the surface tension at the water-air interface relative to the initial components with the same concentration (Figure 6). It is shown that an increase in temperature of the LS-ASO reaction mixture in the range 20-60°C results in a noticeable decrease in surface tension (Figure 6, curves 3, 4, 5). Negative values of the temperature coefficient of the surface tension indicate perhaps the enhancement of the polymer-oligomer association processes in interface layers as a result of increased hydrophobic interactions.

The polymeric products of the interaction between LS and amphiphilic oligomers, formed in moderately concentrated and concentrated mixtures (> 10 g/dl) with composition Z close to the stoichiometric one in the pH range 5-6, are characterized by adhesive properties. The studies carried out have shown that such products are capable of cementing the particles of sand and forming the sand-polymer layers with a thickness of 4-14 mm and a penetration resistance of 0.49-2.90 MPa. The composite layers formed protect the soil surface from erosion processes and are characterised by a good atmospheric durability [15].

Conclusions

1. In acidic media, the interaction between lignosulphonate and water-soluble synthetic oligomers is of electrostatic nature and leads to the formation of intermolecular complexes. Their content in reaction mixtures depends on composition and pH of the reaction mixture. Donor-acceptor bonds make a definite contribution to the formation of reaction products.
2. The addition of low-molecular weight electrolytes to the LS-ASO reaction mixture deteriorates the interaction due to binding of low-molecular anions by oligomer molecules.
3. The increase of the association degree between LS and ASO molecules in the presence of ethanol may be related to the lower extent of solvation.
4. The structural peculiarities of the intermolecular complexes determine their surface activity at the different interfaces.

References

1. Alksnis, A.; Jakobsons, M.; Treimanis, A.; Viesturs, U. Wood and pulping chemistry in Latvia today. *TAPPI Journ.* **1992**, *11*, 69.
2. Ström, G.; Stenius, P. Formation of complexes, colloids and precipitates in aqueous mixture of lignin sulfonate and some cationic polymers. *Colloids and Surfaces*, **1981**, *2*, 357.
3. Shulga, G.M.; Kalyuzhnaya, R.I.; Zezin, A.B.; Kabanov, V.A.; Mozheiko, L.N.; Rekner, F.V. Specific features of the reactions between lignosulfonates and polymeric bases in aqueous solutions. *Polymer Science* **1984**, *26*, 291.
4. Shulga, G.; Zakis, G.; Neiberte, B.; Gravitis, J. Synthesis and properties of novel polyelectrolytes on the basis of wood polymers. In: *Recent Advances in Environmentally Compatible Polymers*, eds. Kennedy, J.; Phillips, G.; Williams, P.; Hourwood Ltd., 1999.
5. Ström, G.; Stenius, P. Wechselwirkung zwischen kationischen Polymeren und anionischen Holzpolymeren sowie deren Einfluß auf die Papierstoff-Entwässerung. *Wochenbl. Papierfabr.* **1987**, *115*, 386.
6. Ganjidoust, H.; Tatsumi, K.; Yamagishi, T.; Gholian, R.N. Effect of synthetic and natural coagulant on lignin removal from pulp and paper waste-water. *Water Science and Technology* **1997**, *35*, 291.
7. Shulga, G.; Rekner, F. Erosion control and improvement of soil using interpolymer lignin-polyamine complexes. *Proceedings, UIFRO International Conference, Zvolen, Slovakia, 1997*, pp. 129.
8. Lapsa, V.; Betkers, T.; Shulga, G.; Pulp and Papermaking Fibre Wastes for Obtaining of Composite Materials. In: *Pulp for Papermaking - Fibre and Surface Properties*, eds. Kennedy, J.; Phillips, G.; Williams, P.; Horwood Ltd., 1999.
9. Lagzdin E. The study of sodium methylsiliconate solutions containing various metallic ions, and their possible application. *Proceedings LAS* **1979**, *11* (388), 80.
10. Havkina, B.L.; Shulga, G.M.; Telysheva, G.M.; Kuznetcova, M.E.; Lagzdin, E.A.; Soms, A.V. Interpolymer complexes based on metallosiliconorganic compounds. *Proceedings, 2nd All-Union Conference on Interpolymer complexes, Riga, Latvia, 1989*, pp. 440.
11. Shulga, G.M.; Kalyuzhnaya, R.I.; Mozheiko, L.N.; Rekner, F.V.; Zezin, A.B.; Kabanov, V.A. Cooperative intermacromolecular reactions with the participation of lignosulfonates. *Polymer Science* **1982**, *24*, 1516.
12. Ruthen D. Principles of Adsorption and Adsorption Processes. John Wiley & Sons: New York, 1984.
13. Dizbit, T.; Telysheva, G.; Shulga, G. ESR as a monitoring method of lignin activity at their interaction with monomer-oligomer systems. In: *The Chemistry and Processing of Wood and Plant Fibrous Materials*, eds. Kennedy, J.; Phillips, G.; Williams, P., Woodhead Ltd.: Cambridge, 1996, pp.393.
14. Afanas'ev, N.I.; Ph.D. thesis, Institute of Wood Chemistry, Latvian Academy of Science, Riga, 1988.
15. Telysheva, G.; Shulga, G. Silicon-containing polycomplexes on the base of natural polymer for environment protection. *Journ. of Agricultural Engineering Research*, **1995**, *62*, 2217.

COMPARATIVE EVALUATION OF TCF BLEACHED HARDWOOD DISSOLVING PULPS

H. Sixta

Lenzing AG, A - 4860 Lenzing, Austria

With an annual production of some 3.5 million tons between 1990 and 1995, dissolving wood pulp accounts for only 2% of the total wood pulp production. However, the high demands for cellulose purity and reactivity as well as its manifold routes of utilization are the reason for the advanced state of technology within the pulp industry.

For dissolving pulp production, only acid sulfite and prehydrolysis kraft processes (PHK) are of major practical importance. Unlike paper grade pulping the acid sulfite process is the dominant process for the production of dissolving pulps and accounts for approximately 60% of the total production.

The quality profile of both types of dissolving pulps made from eucalyptus species was studied with respect to their chemical composition, cellulose structure at molecular, supramolecular and morphological level, alkaline oxidative degradation kinetics and the course of heterogeneous derivatization reactions.

In comparison to PHK, acid sulfite pulps generally showed a higher level of viscosity in combination with a higher fraction of low molecular weight cellulose indicated by the low R10 content, the high difference between R18 and R10, the high copper number and the broad molecular weight distribution (GPC).

Supramolecular structure (cellulose I to Na-cellulose I lattice transition) and cellulose morphology (electron micrograph) of both categories of pulps approach one another with increasing prehydrolysis intensity in case of PHK pulps.

Aging experiments revealed that pulps of high polydispersity (sulfite pulps) are characterized by a rapid viscosity degradation down to a level of 320-350 ml/g resulting in a sharp decline in polydispersity. Consequently, the aging degradation mechanism based on number-average degree of polymerization seems to be rather independent from the origin of pulp and strictly follows a zero-order rate equation.

In general, viscose made from PHK pulps showed a lower content of undissolved particles compared to viscose made from sulfite pulps probably due to higher alkali resistance.

Acetylation efficiency was characterized by the coefficient of yellowness of cellulose triacetate solution. Color intensity was found to correlate linearly with pentosan content, more or less independent of pulp origin.

Keywords: Dissolving pulps, acid sulfite, prehydrolysis kraft, ageing, viscose, cellulose acetate

Introduction

For wood dissolving pulp production, only acid sulfite cooking and the prehydrolysis kraft process are of major importance. A comprehensive comparison of both process technologies has been recently published by Sixta and Borgards [1]. Unlike paper grade pulping, the acid sulfite process is the dominant process for the production of dissolving pulps and accounts for approximately 60% of the total

production. During the past thirteen years a major part of the softwood has been replaced by hardwood species with the proportion of softwood shifting from 80% (in 1985) to only 46% (in 1998). It is expected that this trend will continue provided that hardwood high-purity pulps will meet the specifications required for the production of *e.g.* cellulose esters and ethers. The differences in pulp properties between acid sulfite and kraft pulps have been the subject of numerous studies. Jayme and Korten advanced a

hypothesis that for a given degree of delignification, sulfite pulps were more degraded on the outside of the fiber than were kraft pulps [2]. This hypothesis was supported by Luce who developed the method of „chemical peeling“ to study the radial distribution of different properties across the fibre wall [3]. According to his results, the DP of the kraft pulp was uniform throughout the fiber wall while in the sulfite pulp the DP of the outer layers was low, and of the inner layers high. It can be concluded that acid sulfite cooking liquor penetrates through the pits into the porous middle lamella where delignification proceeds from the primary wall. On the other hand alkaline cooking conditions promote rather uniform pulping reactions due to the high swelling properties. Hamilton and Thompson have studied the main differences in the carbohydrate constituents of wood celluloses prepared by the sulfite and kraft pulping processes [4]. According to their findings, xylan from hardwoods is converted to a short chain 4-*O*-methylglucurono-xylan by the acid sulfite pulping procedure and to high-molecular weight xylan without side chains by the PHK pulping process. The glycosidic bond between uronic acid and the xylan backbone is particularly sensitive to alkaline cleavage. The significantly lower molecular weight of the residual hemicellulose fraction in sulfite pulps compared to kraft or PHK pulps has also been pointed out by Jayme and Köppen [5]. Page proposed a concept based on supramolecular properties to explain the differences between sulfite and kraft pulps [6]. Sulfite pulp is seen as containing largely crystalline and paracrystalline cellulose, whereas in kraft pulp substantial transformation of the paracrystalline regions to the amorphous state has occurred. The high LODP, the high modulus in the stress-strain curve, the excellent swelling properties, the low tear strength and the high beating rate of sulfite pulps were attributed to the higher amount of crystalline and paracrystalline regions compared to kraft pulps. In addition, sulfite pulps were found to be far more reactive towards xanthation compared to kraft pulps [7].

The influence of prehydrolysis on the properties of kraft pulps (PHK pulps) was not the subject of most of the studies mentioned above. This paper is therefore concerned with some of the main differences in the quality profile of acid sulfite

and prehydrolysis kraft pulps using hardwood as the raw material.

Materials and Methods

Substrates. Three different Mg based acid sulfite pulps and four different prehydrolysis kraft pulps (PHK) were selected as the main substrates for the comparative evaluation (Table 1). For both types of pulps eucalyptus was used as a wood source, in case of the acid sulfite pulps the *globulus Labill* species (46% cellulose, 13.9% pentosan, 21% Klason lignin, 0.21% DCM extractives) from the north eastern part of Spain, and in case of the PHK pulps a mixture of eucalypt *urophylla* and *cloeziana* (44% cellulose, 13% pentosan, 26% Klason lignin, 0.25% DCM extractives) originating from the state of Bahia, Brazil. With the exception of the Klason lignin content, the chemical composition of the wood species were quite comparable. Each category of pulp was represented by different levels of cellulose purity. Low and high purity dissolving pulps using the same technology of purification were designated as viscose and acetate grades (hot caustic extraction in case of sulfite pulps, vapor phase prehydrolysis in case of PHK pulps). The cold caustic extraction technology (CCE) was applied to achieve the highest possible level of cellulose purity for each type of pulp.

Table 1. Selection of eucalypt dissolving pulps used for the comparison of sulfite and PHK pulps.

| Category of Pulps | Grades | Abbrev. | Origin |
|-------------------|-----------|--------------------|--------|
| Acid Mg Sulfite | Viscose | Mg-V | lab |
| Acid Mg Sulfite | Acetate | Mg-Ac | lab |
| Acid Mg Sulfite | Acetate | Mg-AcE | lab |
| | CCE | | |
| PHK | Viscose-1 | PHK-V _m | mill |
| PHK | Viscose-2 | PHK-V-l | lab |
| PHK | Acetate | PHK-Ac | mill |
| PHK | Acetate | PHK-AcE | lab |
| | CCE | | |

Acid Mg sulfite pulping was carried out with a liquor-to-wood ratio of 2.7:1, a total SO₂ charge of 179-184 g/kg o.d. wood of which 65% was (true) free SO₂. Cooking time was controlled by H-factor necessary to achieve the target

viscosity. The cooking phase was terminated by releasing the pressure to 4.5 bar within a period of 60 min. In case of the sulfite pulps an (EO)ZP bleaching sequence was chosen for all grades. The additional CCE treatment was included between ozone and peroxide bleaching. Purity levels for standard viscose and acetate grades were achieved by choosing the appropriate alkali charges in the E-stage. The (EO) pretreated pulps were subjected to medium consistency ozone (Z) bleaching. The amount of ozone charge necessary to adjust the viscosity was determined in a set of pre-trials. Peroxide (P) bleaching conditions were selected according to the required brightness targets (viscose grade $\geq 90\%$ ISO; acetate grade $\geq 92\%$ ISO). The PHK pulps were manufactured at the Bacell S.A. mill (mill pulps) or in the laboratory according to the technology applied at the Bacell mill (lab pulps) [8]. A detailed description of the cooking and bleaching technology and conditions can be found elsewhere [1]. For the evaluation of the acetylation and xanthation performance additional market dissolving pulps were considered to study also the influence of different hardwood species. The selection of pulps included beech and eucalyptus sulfite pulps as well as mixed American hardwood PHK pulps with and without CCE treatment.

Analytical methods. Kappa number according to T236 cm-85 mod., viscosity according to SCAN-CM 15:88, brightness according to ISO 3688/2470, alkali resistancies according to ISO 699 / ZM IV/39/67, carbohydrate composition following total hydrolysis and HPLC separation and AX/EC-PAD detection, copper number according to ZM IV/8/70, carboxylic groups according to Das Papier 1965, 19, No 1, DCM extractives according to ISO 624, cations by means of ICP after microwave digestion, molecular weight distribution after dissolving in LiCl/DMAc and GPC separation [9], WRV according to ZM IV/33/57, LODP according to the method of Sarkov, ageing kinetics according to ZMIII/19/69 mod. and acetylation according to a method of Rhodia adapted by Lenzing [10].

Special methods:

Lattice transition from cellulose I to that of Na-Cellulose I as a function of NaOH-concentration was determined according to the method of Kunze and Fink [11] using ^{13}C cross-polarization/magic angle spinning (CP/MAS)

NMR technology (Varian 400 MHz spectrometer, 5.7 kHz rotation frequency, cross-polarization time 1ms, time of repetition 3 s).

TEM-investigations to study the fibrillar architecture were carried out by the group of Fink at Fraunhofer IAP, Teltow, Germany.

Filterability of viscose was determined according to Treiber [12].

Results and Discussion

The characterization of dissolving pulps with respect to further processing properties still requires time consuming performance and testing of the corresponding derivatization or dissolving reactions on a lab-scale basis. That means, for example, that the suitability as viscose pulps can only be tested in a bench-scale viscose plant under controlled conditions. Sometimes even pilot plant or mill-scale tests are needed to prove the aptitude of the dissolving pulp. Unfortunately, a simple chemical characterization according to today's standard methods is not sufficient to give a full picture of the dissolving pulps' properties. The relations between structure, chemical composition and behavior with regard to topochemical reactions are too complex. A reliable analysis of the property profile of dissolving pulps demands the extensive characterization of the cellulose structure at different levels including the performance of appropriate application tests.

The quality profile of both types of dissolving pulps, acid sulfite and prehydrolysis kraft, is comparatively evaluated in the following with respect to chemical composition, cellulose structure at molecular, supramolecular and morphological level, alkaline oxidative degradation (aging) kinetics, and the course of heterogeneous derivatization reactions under alkaline (viscose) and acidic conditions (cellulose triacetate).

Chemical Composition. Standard dissolving pulp specification provides a rough estimate on the chemical and physical properties. The average molecular weight (intrinsic viscosity) is a measure for solution rheology and final product properties. Alkali resistancies (R18, R10) are important to predict product yield and the proportion of high molecular cellulose fraction.

Reducing end groups (copper number) and carboxylic groups are characteristic for the degradation behavior and the state of solution of derivatives or direct solution systems. In addition, non-cellulosic inorganic (metal ions) and organic contaminations (hemicelluloses, resins) can be ascribed to process instabilities (precipitation, high solution viscosity, limited filterability) and deteriorated product quality

(broad molecular weight distribution, reduced chemical stability). Moreover, the optical properties of fresh and aged samples reveal the amount and the structure of chromophores as well as the surface structure of the pulp. Table 2 offers a preliminary comparison of the two types of dissolving pulps on the basis of standard specification.

Table 2. Standard specification of a selection of eucalyptus acid Mg sulfit and eucalyptus prehydrolysis kraft pulps.

| Parameter | Unit | Acid Mg Sulfit Pulps | | | Prehydrolysis Kraft Pulps | | | |
|-------------------|---------|----------------------|-------|--------|---------------------------|--------------------|--------|---------|
| | | Mg-V | Mg-Ac | Mg-AcE | PHK-V _m | PHK-V _l | PHK-Ac | PHK-AcE |
| Brightness | % ISO | 91.5 | 92.5 | 92.9 | 90.6 | 91.3 | 90.9 | 92.0 |
| Viscosity | ml/g | 536 | 599 | 609 | 430 | 438 | 504 | 498 |
| R18 | % | 94.8 | 96.9 | 97.8 | 97.1 | 96.8 | 98.0 | 98.2 |
| R10 | % | 86.8 | 91.3 | 91.4 | 92.9 | 93.2 | 94.0 | 95.1 |
| Pentosan | % | 2.0 | 1.8 | 1.1 | 3.3 | 3.6 | 1.4 | 1.0 |
| Copper number | % | 1.70 | 0.70 | 0.80 | 0.34 | 0.56 | 0.18 | 0.30 |
| Carboxylic groups | mmol/kg | 22 | 23 | 19 | 27 | 34 | 26 | 22 |
| DCM extractives | % | 0.13 | 0.05 | 0.06 | 0.15 | 0.05 | 0.21# | 0.07 |
| Calcium | ppm | 10 | 7 | 8 | 21 | | 14 | 10 |
| Silicium | ppm | 14 | 10 | 6 | 8 | | 12 | 14 |
| Iron | ppm | 6 | 6 | 5 | 2 | | 3 | 6 |

including Viscocell

In comparison to PHK pulps, acid sulfite pulps generally show a higher level of viscosity and a significantly higher fraction of low molecular weight cellulose indicated by the low R10 content, the high difference between R18 and R10 and the high copper number. The former is mainly related to the comparatively lower selectivity and efficiency of TCF bleaching of PHK pulps due to both a lower reactivity of the residual lignin structures and the higher specific extinction coefficient of the chromophores. The high alkali resistancies, the low difference between R18 and R10 3.1-4.2 as compared to 5.6-8.0 in case of sulfite and the low copper numbers are an intrinsic property of PHK pulps being related to the chemistry of the acidic prehydrolysis and the subsequent alkaline cooking process [1]. The surprisingly low R18 to pentosan ratio is also typical for PHK pulps and signals a xylan fraction which is of high molecular weight and not readily accessible. Significant differences between sulfite and PHK pulps can also be observed by following the changes of the quality parameters in the course of reinforced purification reactions necessary for

the production of acetate grades with and without additional cold caustic extraction. Pentosan removal is more efficient for PHK pulps ($\Delta P = 2.2-2.6$ vs. $0.2-0.9$) whereas a higher increase in alkali resistance is observed for sulfite pulps ($\Delta R10 = 4.5$ vs. $0.8-1.9$).

The concentration of carboxylic groups is not influenced by means of standard purification for both types of pulps. The removal of carboxylic groups during hot caustic extraction equals the new formation of aldonic acid groups. Cold caustic extraction partly dissolves carbonic acid moieties resulting in a slightly overall reduction of carboxylic groups (approx. -15%). The content of aldonic acid groups in acid sulfite pulps can be influenced by controlling the viscosities of the unbleached and bleached pulps. The reduction of viscosity by means of prolonged cooking (increased H-factor) causes an almost linear decrease of carboxylic acids, obviously due to the removal of xylan (-3 mmol COOH/kg per 100ml/g viscosity reduction). Other pulping conditions, like the amount of excess SO₂, reveal no influence on the formation of aldonic acids. Carboxylic groups are

generated during bleaching in the course of degradation reactions by means of a reinforced ozone treatment (+ 1.5 mmol COOH/kg per 100 ml/g viscosity reduction).

The copper number is proportional to the amount of reducing end groups. A gradual reduction in viscosity during acid sulfite pulping causes an increase in copper number because of significant cellulose degradation proceeding parallel to xylan removal (net increase of copper # equals 0.1 % per 100 ml/g viscosity reduction). A shift to a higher proportion of excess SO₂ in the cooking acid results in a slight increase of copper number presumably due to a change of the hydrolysis-to-sulfonation ratio towards hydrolysis. The removal of low molecular weight polysaccharides during hot caustic extraction leads to a drastic decrease in copper # (-0.3 to -0.4% per increase of 1% R18) whereas cellulose degradation during ozone treatment slightly raises copper number again (+0.1% per 200 ml/g viscosity reduction).

Since celluloses from natural sources and after chemical treatment are always polydisperse, the determination of the average MW is insufficient to predict specific product properties. Additional information is provided by measuring molecular weight distribution of dissolving pulps. The results of GPC measurements of cellulose solutions in LiCl/DMAc with MALLS/ RI detection are given in Table 3 and Figure 1.

Table 3. Numerical evaluation of molecular weight distribution of selected sulfite and PHK dissolving pulps.

| Parameter | Acid Mg Sulfite Pulps | | | Prehydrolysis Kraft Pulps | | |
|-----------------|-----------------------|-------|--------|---------------------------|---------|----------|
| | Mg-V | Mg-Ac | Mg-AcE | PHK -V _m | PHK -Ac | PHK -AcE |
| DP _w | 1623 | 1560 | 1480 | 970 | 1140 | 1090 |
| DP _n | 203 | 365 | 350 | 285 | 350 | 381 |
| PDI | 8.0 | 4.3 | 4.2 | 3.4 | 3.2 | 2.9 |
| wt% < DP50 | 5.8 | 2.0 | 1.7 | 2.7 | 1.6 | 1.4 |
| wt% < DP100 | 11.0 | 5.3 | 5.0 | 6.8 | 4.8 | 4.3 |

The numerical evaluation of the MW distributions confirms the broader distribution and the higher amount of low molecular weight carbohydrate fractions of the sulfite pulps. Figure 1 compares sulfite and PHK pulps at different levels of purity. The low molecular weight fraction can be reduced to a comparable level as in the corresponding PHK pulp (PHK-Ac) by means of reinforced hot caustic extraction (Mg-Ac). Cold caustic extraction causes the extraction of degraded cellulose (predominantly β-cellulose) which results in a further narrowing of molar mass distributions. Even after the most efficient purification treatment, sulfite pulps show a higher polydispersity mainly due to a higher fraction of medium and very high molecular weight cellulose (Figure 1).

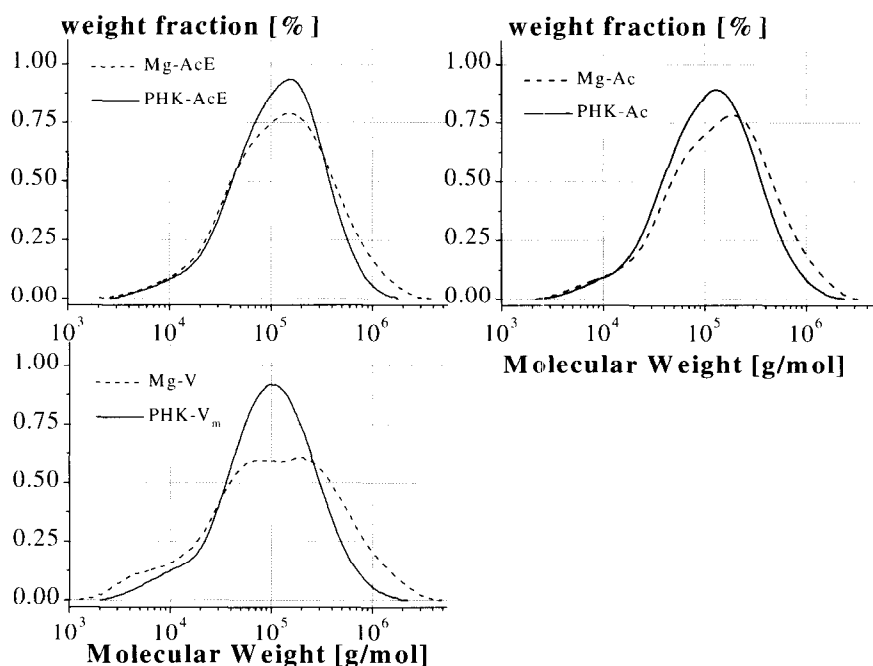


Figure 1. Molar mass distribution of different grades of sulfite and PHK pulps.

Supramolecular structure. In accordance with the widely accepted two-phase model for cellulose (fringed fibril model) regions of low (amorphous) and high degree of order (crystalline) can be assumed. The degree of order was determined by means of FTIR spectroscopy using the ratio of the absorption intensities at 1370 cm^{-1} and 2900 cm^{-1} [13]. The results have been expressed as X-ray crystallinity X_C , because of the close correlation to X-ray crystallinity. The crystalline dimensions were characterized by determining the level-off DP (LODP) of the dissolving pulps. The results are listed in the Table 4.

Table 4. Degrees of crystallinity, X_C , and LODP's of selected sulfite and PHK dissolving pulps.

| Parameter (Unit) | Acid Mg Sulfite Pulps | | | Prehydrolysis Kraft Pulps | | | |
|------------------|-----------------------|-------|--------|---------------------------|--------------------|--------|---------|
| | Mg-V | Mg-Ac | Mg-AcE | PHK-V _m | PHK-V ₁ | PHK-Ac | PHK-AcE |
| X_C (%) | 56 | 54 | 53 | 57 | 53 | 53 | |
| LODP (ml/g) | 105 | 92 | 90 | 84 | 85 | 80 | |

The degrees of order differ only slightly, thus indicating a low sensitivity towards different types of pulps and purity levels. The level-off DPs, however, show a clear dependency on alkali resistance (R18) which had also been reported by Steege and Philipp [14]. The size of crystalline regions decreases parallel to the removal of non-cellulosic impurities in different levels for sulfite and PHK pulps. The lower LODP values of the PHK pulps might be explained by their lower polydispersity.

The alkali concentration necessary for the lattice transition from cellulose I to Na-cellulose I (and after neutralization to cellulose II) is an important criterion for characterizing pulp reactivity towards alkali cellulose formation as an intermediate for the production of viscose fibers or cellulose ethers. The transformation to Na-cellulose modification I begins at lye concentration of about 6 % and is completed at about 14% NaOH (Figure 2). It is well known that the transition curve from cellulose I to Na-cellulose I depends on the supramolecular structure of the dissolving pulp. Sulfite pulps generally require a lower lye concentration for this lattice conversion than prehydrolysis kraft pulps [1] which has been fully confirmed in this

study. The difference in lye concentration between the two categories of pulp necessary to transform 50% to Na-cellulose I is about 0.9% (9.4% for sulfite vs. 10.4% for PHK pulp). Compared to cotton linters, the difference to sulfite pulps is small and can further be reduced by reinforcing prehydrolysis conditions (Figure 2: PHK-Ac). The more complete removal of pentosan (by increasing the P-factor) in case of acetate grade PHK pulp obviously changes the supramolecular structure and results in a definite shift of the transition curve to lower alkali concentration. Above 11% NaOH the curve of the PHK-Ac pulp proceeds similar to that of the sulfite pulps.

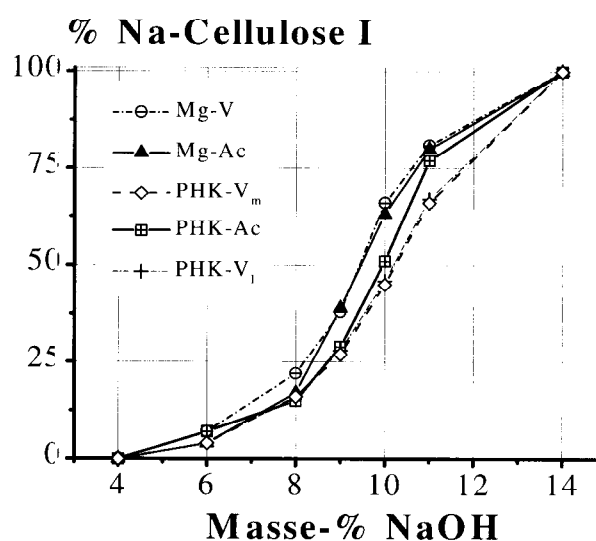


Figure 2. Lattice transition from cellulose I to Na-cellulose-I of selected sulfite and PHK pulps.

Architecture of fibrillar elements (cellulose morphology). Fibrillar morphology of pulps is highly dependent on pulping process and pulping conditions. It is assumed that the hydrogen sulfite / sulfurous acid solution penetrates through the pits into the middle lamella where the pulping reaction starts from the primary wall across the cell wall. As a consequence, the primary wall is sometimes completely removed after acid sulfite pulping. Pulping under alkaline conditions (kraft process), however, enables rather uniform pulping reactions across the cell wall layers due to the high swelling properties of white liquor. The electron micrograph of the sulfite pulps indeed confirms that the primary wall has been removed. The morphological architecture of the sulfite acetate grade pulp is clearly dominated by the S1 layer (Figure 3a).

On the other hand residues of the primary wall can be detected for the PHK viscose pulp (Figure 3b at the top). As expected from previous results (see lattice transition as a function of NaOH concentration) the primary wall is further removed as soon as prehydrolysis conditions are intensified. Therefore, the microfibrillar structure of the PHK acetate pulp (PHK-AcE) is almost comparable to that of the sulfite pulps (Fig. 3c).



Figure 3a. Electron micrograph of the sulfite acetate pulp (Mg-Ac).



Figure 3b. Electron micrograph of the PHK viscose pulp.



Figure 3c. Electron micrograph of the PHK acetate pulp.

Oxidative alkaline degradation kinetics (aging).

The average molar mass of dissolving pulps is adjusted by oxidative alkaline degradation to the degree of polymerization necessary for the production of viscose fibers or cellulose ethers. It is a general observation that the aging of alkali cellulose prepared from different pulps differs remarkably. [2, 9] Aging experiments have therefore been carried out at two temperature levels (30°C, 50°C) to investigate possible relationships between aging rates and other pulp properties. The results were evaluated according to the following zero order kinetic equation:

$$\left[\frac{10^4}{P_j} - \frac{10^4}{P_o} \right] = A \cdot \exp\left(\frac{E_a}{R} \cdot \frac{1}{T} \right) \cdot t^n \quad (1)$$

As P_j and P_o are calculated from intrinsic viscosity, the exponent n reflects the changes of polydispersity during the degradation reaction. In case of Mg-V dissolving pulp ageing kinetics has been calculated also on the basis of the number average degree of polymerization values derived from GPC measurements. The results of the non-linear regression analysis are summarized in Table 5.

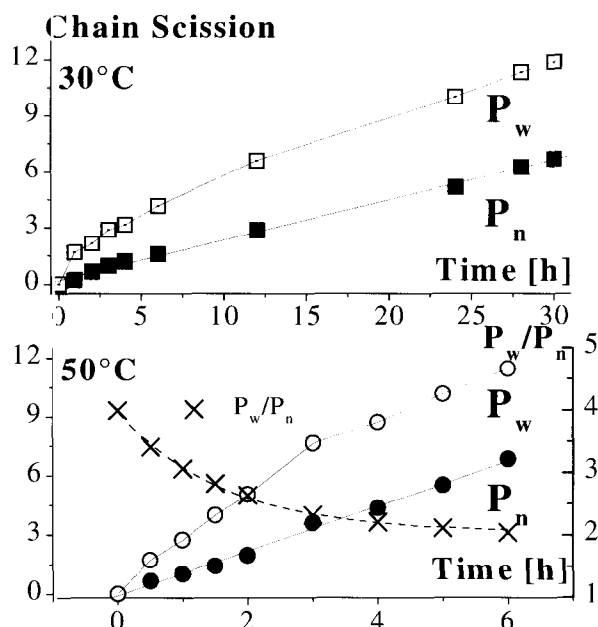
Table 5. Results of kinetic measurements of alkaline aging of the selected sulfite and PHK dissolving pulps.

| | Acid Mg Sulfite Pulps | | | | Prehydrolysis Kraft Pulps | | |
|----------------|-----------------------|---------|----------|-----------|---------------------------|-----------------------|-----------|
| | Mg-V Pw | Mg-V Pn | Mg-Ac Pw | MgA cE Pw | PHK-V _m Pw | PHK-V _l Pw | PHK-Ac Pw |
| ln A | 17.9 | 24.4 | 21.35 | 20.6 | 27.65 | 24.61 | 25.1 |
| E _a | 44.9 | 65.3 | 54.6 | 52.5 | 72.1 | 64.4 | 65.9 |
| n | 0.68 | 0.96 | 0.77 | 0.74 | 0.85 | 0.88 | 0.87 |
| Cu# | 1.69 | | 0.70 | 0.77 | 0.34 | 0.56 | 0.18 |
| PDI | 8.0 | | 4.3 | 4.2 | 3.4 | | 3.2 |

Table 5 reveals the aging kinetic coefficients based on viscosity measurements to be strongly dependent on the change of polydispersity throughout the degradation reaction which is characterized by a deviation of the exponent n from 1. The high polydispersity of sulfite dissolving pulps gives evidence of a high content of reducing end groups which in turn initiates a high reaction rate following the mechanism proposed by Mattor [16]. It has been shown that the rapid degradation of viscosity down to a level of around 320 – 350 ml/g is accompanied by a decrease of copper number from 0.6% to a level of around 0.2% and remains rather stable in the course of further viscosity reduction. At the same time the concentration of carboxylic groups increases from appr. 15 mmol/kg (regenerated alkali cellulose at $t=0$) to appr. 30 mmol/kg at 350 ml/g up to 40 mmol/kg at a viscosity of 200 ml/g. In case of Mg-V pulp both the weight- and the number-average molecular mass have been investigated by means of GPC to study depolymerization kinetics. The results indicated in Figure 6 confirm the sharp decline in polydispersity (of sulfite pulps) during the first depolymerization phase. Consequently, ageing kinetics based on number-average degree of polymerization strictly follows a zero-order rate equation (equation 2). Within the viscosity ranges typical for the production of viscose fibres the experimental data fit very well to a one-stage zero-order rate law. However, it can be expected that the degradation process becomes slower at very low degrees of polymerization due to limited access to highly crystalline regions or a reduced reactivity of the residual cellulose because of the increasing oxidation of reducing end groups.

$$\left[\frac{1}{P_{n,t}} - \frac{1}{P_{n,0}} \right] = k \cdot t \quad (2)$$

Since the rate constants approximate to values typical for the narrowly distributed PHK pulps, the basic mechanism of oxidative alkaline depolymerization seems to be rather independent from the origin of pulp (see Table 5). The influence of supramolecular structure on aging kinetics cannot be excluded on the basis of today's knowledge. More detailed investigations are certainly necessary to answer this question.

**Figure 4.** Course of ageing depolymerization of alkali-cellulose of the Mg-V pulp using both number- and weight-average degree of polymerization.

Viscose Filterability. The decisive test methods for the evaluation of the suitability of dissolving pulps for viscose application are the determination of filterability performance and number of undissolved particles of viscose produced under constant conditions. A selection of different hardwood sulfite and PHK pulps were converted to viscose to investigate the corresponding quality parameters. The results are summarized in Table 6.

The main pulp purity parameters are not very sensitive to viscose quality within a certain range. Of all the hardwood pulps examined eucalypt *urograndis* PHK pulp, showing the highest level of pentosan content, reveals the best viscose quality with respect to filterability and number of undissolved particles. From both

purity parameters the R18 content is more relevant to viscose quality obviously because it characterizes the alkali-soluble carbohydrate fractions under steeping conditions. Wood species and wood provenance show an important influence on viscose filterability, especially using sulfite pulping technology. The change from *Eucalypt globulus* (Spanish provenance) to *Eucalypt grandis* (South American provenance) causes a significant improvement of cellulose reactivity towards xanthation. The reasons are mainly a better and more homogeneous accessibility, a lower content of critical inorganic contaminants, such as calcium and silicon, as well as certain resin compounds preventing or impeding the derivatization reaction. In general, viscose made from PHK pulps shows a lower content of undissolved particles in the range of 3 - 150 μ m compared to the viscose made from sulfite pulps despite a similar level of filterability.

Table 6. Quality of test viscose samples made from hardwood sulfite and PHK pulps.

| Wood Species | Process | Pulp Parameters | | | Viscose Quality | |
|----------------------------|---------|-----------------|---------|----|-----------------|------|
| | | Pentosan, % | R18 [%] | n | FV # | P ## |
| Beech | Mg | 3.1 | 93.0 | 40 | 362 | 23 |
| <i>Eucalypt globulus</i> | Mg | 2.0 | 94.8 | 4 | 328 | 36 |
| <i>Eucalypt grandis</i> | Mg | 2.6 | 95.4 | 4 | 437 | 8 |
| <i>Eucalypt urograndis</i> | PHK | 3.5 | 97.0 | 32 | 492 | 6 |
| Mixed Am. Hardwood | PHK | 2.8 | 95.9 | 4 | 419 | 13 |
| Mixed Am. Hardwood | PHK | 1.0 | 98.5 | 4 | 354 | 14 |
| | CCE | | | | | |

filter value

particles [ppm]

Evaluation of Cellulose Triacetate Solution. It is well established that hemicelluloses exert major deleterious influences on the high-catalyst processing of dissolving wood pulp into cellulose acetate [17]. The experiences are based on softwood hemicelluloses as most of the acetate grade dissolving pulps are made from softwood species (*e.g.*, southern pine). It has been reported that glucomannan is a major contributor to diacetate haze, high false viscosity and poor filtration. Xylan on the other hand is mainly responsible for di- and triacetate color and thermal instability. In our studies the hardwood dissolving pulps were subjected to the low-

catalyst acetic acid acetylation process to measure the coefficient of yellowness of the triacetate solution in acetic acid. The results are shown in Figure 5 as a function of the pentosan content of the dissolving pulps.

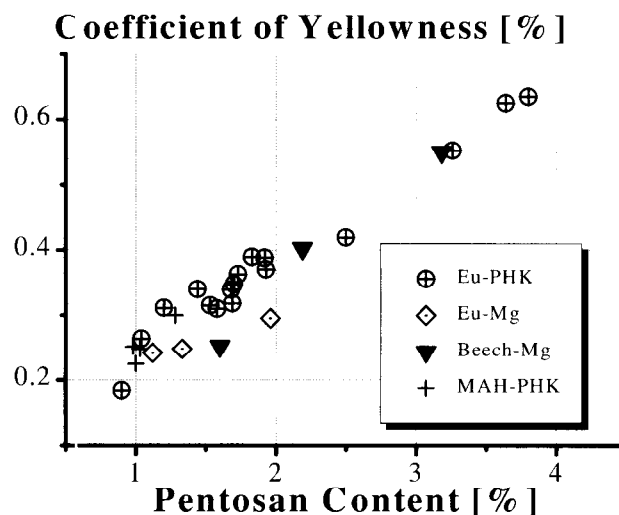


Figure 5. Coefficient of yellowness as a function of the pentosan content of the selected sulfite and PHK pulps.

The coefficient of yellowness increased linearly with the content of pentosan (xylan) in the pulps that were converted to a cellulose triacetate solution. In the range of low pentosan concentration there seems to be a tendency to lower color intensity for sulfite as compared to PHK pulps. However, taking all results into account, the influence of the pentosans largely the same regardless of the pulp source. These results are in good agreement with published values obtained from studies with softwood dissolving pulps using the high-catalyst acetic acid acetylation process and show that both process performance and quality of final cellulose acetate products are mainly influenced by the content of non-cellulosic impurities of the raw material.

Acknowledgement

The author thanks the pulp research team of the Lenzing AG, Lenzing, Austria, which has performed most of the experimental work, and the management of Lenzing AG, which has kindly consented to the publication of this paper. The work on the electron micrographs by the team of H.-P. Fink at Fraunhofer IAP, Teltow, Germany, is gratefully acknowledged.

References

- [1] Sixta, H.; Borgards, A. New technology for the production of high-purity dissolving pulps. *Das Papier* **1999**, *53* (4), 21-34.
- [2] Jayme, G.; von Köppen, A. Strukturelle und chemische Unterschiede zwischen Sulfit- und Sulfatzellstoffen. *Das Papier* **1950**, *4* (23/24), 455-462.
- [3] Luce, J.E. Radial distribution of properties through cell wall. *Pulp and Paper Magazine of Canada* **1964**, T-419-T423.
- [4] Hamilton, J.K.; Thompson, N.S. A chemical comparison of kraft and sulfite pulps. *Pulp and Paper Magazine of Canada* **1960**, T-263-T-272.
- [5] Jayme, G.; von Köppen, A. Strukturelle und chemische Unterschiede zwischen Sulfit- und Sulfatzellstoffen. *Das Papier* **1950**, *4* (21/22), 415-420.
- [6] Page, D.H. The origin of the differences between sulphite and kraft pulps. *Journal of Pulp and Paper Science* **1983**, TR15 – TR20.
- [7] Jayme, G.; von Köppen, A. Strukturelle und chemische Unterschiede zwischen Sulfit- und Sulfatzellstoffen. *Das Papier* **1950**, *4* (19/20), 373-378.
- [8] Wizani, W.; Krotscheck, A.W.; Schuster, J.; Lackner, K. Processes for the production of viscose pulps. Austrian patent A 2382/92, 1992.
- [9] Schelosky, N.; Röder, R.; Sixta, H.; Baldinger, T.; Milacher, W.; Morgenstern, B. Molecular mass distribution of cellulosic products by size exclusion chromatography in DMAc / LiCl. *Das Papier* **1999**, *53* (12), in press.
- [10] Schelosky, N. Evaluation of the Acetylation Test Method, FEZ-Bericht, Lenzing AG, 1998, 25/98.
- [11] Kunze, J.; Fink, H.P. Charakterisierung von Cellulose und Cellulosederivaten mittels hochauflösender Festkörper-¹³C-NMR-Spektroskopie. *Das Papier* **1999**, *53* (12), in press.
- [12] Treiber, E.; Rehnström, J.; Ameen, C.; Kolos, F. Using a laboratory viscose small-scale plant to test chemical conversion pulps. *Paper* **1962**, *16* (3), 85-94.
- [13] Lenzing AG, Internal Test Report. FEZ 1997, 6/97.
- [14] Steege, H.H.; Philipp, B. *Zellst. Pap.* **1974**, *23*, 68-73.
- [15] Koutu, B.B.; Bhagwat, V.W. Effect of copper number of pulp on ageing of alkali-cellulose. *J. of Polym. Materials* **1997**, Dec., 325-331.
- [16] Mattor, A.J. A study of the mechanism of alkali cellulose autoxidation. *Tappi* **1963**, *46* (10), 586-591.
- [17] Wilson, J.D.; Tabke, R.S. Influences of hemicelluloses on acetate processing in high-catalyst systems. *Proceedings, TAPPI Dissolving Pulps Conf.* (Atlanta, Ga), 1973, Oct. 24-26, 55-68. *Tappi* **1973**, *57* (8), 77-80.

PEROXIDE APPLICATION IN ECF SEQUENCES - A DESCRIPTION OF THE STATE-OF-THE-ART

H.U. Süß, K. Schmidt, H. Jakob

Degussa-Hüls AG, D-63403 Hanau, Germany

In ECF bleaching the delignification effect in the extraction stages is intensified with other chemicals in order to decrease the demand for chlorine dioxide. The typical approach is to add oxygen and hydrogen peroxide to the first E stage and to reinforce the second E stage with H₂O₂ only. A final P stage can be very favorable to lower the ClO₂-demand, because much less than the stoichiometrically calculated amount of H₂O₂ is required. Brightness stability in accelerated heat aging is better after a final P stage compared with a final D stage. Very high temperature and pressurized conditions do not result in an advantage for peroxide bleaching as thermal decomposition reduces viscosity and yield.

The effects are best if moderate amounts of hydrogen peroxide are applied at a temperature level not above 90°C. Higher temperature results in lower viscosity and higher effluent COD loads. Pulps can be bleached with very low chlorine dioxide amounts and higher peroxide input to yield "ECF light" pulp grades with very low OX levels. Final bleaching with high peroxide addition decreases the OX level as a result of the saponification and extraction down to the range accepted for TCF pulp.

Keywords: chlorine dioxide, hydrogen peroxide, yield, OX

1. Materials and Methods

All bleaching experiments were conducted with oxygen delignified softwood or hardwood kraft pulps from commercial operations. Yield of oxygen delignification was determined using a high Kappa commercial softwood pulp in a rotating autoclave with 0.5 MPa O₂ pressure. The reinforced extraction stages were run in a proprietary high shear mixer applying 0,3 MPa O₂. Chlorine dioxide stages were made in PE bags. All stages were conducted at 10% consistency. Ozone was applied in a proprietary fluidized bed reactor at 30% consistency.

Standard procedures were applied for Kappa number (T 236), viscosity (T 230), OX (DIN 38409), heat aging (T260), COD (Zellchem X/2/76) and brightness (ISO 2470).

2. Introduction

ECF bleaching, the substitution of chlorine bleaching with chlorine dioxide, has become the

most attractive method to bleach chemical pulp. It allows high pulp quality and acceptable yield, while at the same time only a low level of halogenated compounds is produced. ECF bleaching normally follows an oxygen delignification stage, therefore the demand for active chlorine can be very low compared to conventional bleaching. The AOX level in the effluent and the OX level in the pulp become low and government standards are typically met without difficulties. However, the total cost of bleaching is higher compared with conventional chlorine bleaching. One reason is the higher cost of chlorine dioxide compared with chlorine, even with less active chlorine needed after the oxygen treatment. Another important point is the lower yield upon oxygen delignification.

The intensity of an oxygen stage is increased by the application of higher temperature and higher alkalinity. This results in an intensified delignification as well as in an increased extraction, thus producing a higher loss of material. In order to keep the wood requirement acceptable, the intensity of an oxygen stage has

to stay within limits. The total yield on wood is about 43.5% in ECF bleaching without an O stage, it decreases to 42.5% with an oxygen stage [1]. In consequence, the demand for bleaching chemicals cannot be lowered by simply intensifying the oxygen stage. Oxygen delignification is more selective compared with extended pulping, it is however, less selective than chlorine dioxide bleaching. In Figure 1 the yield of an oxygen treatment is plotted against delignification. The higher the delignification rate becomes, the more pulp is dissolved. The curves become visibly flat, a higher delignification is accompanied by growing losses.

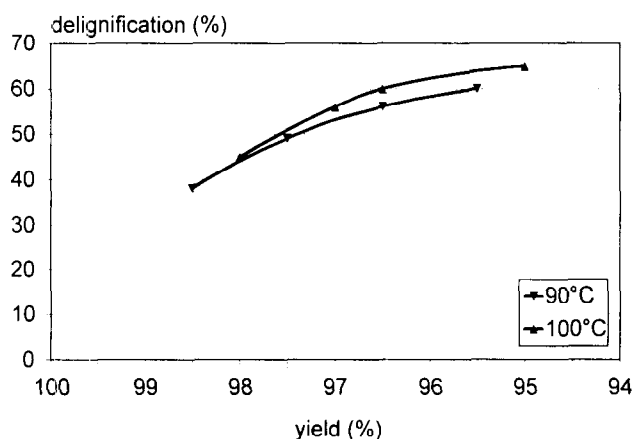


Figure 1. Delignification of a softwood kraft pulp (Kappa 51) with increasing caustic soda charges, reaction at 90°C or 100°C, 0.4 MPa O₂, 1.5 h; NaOH charge variable from 1% to 5%.

In order to effectively control the costs of bleaching, it is required to carefully balance the lower yield achieved with oxygen and the decreasing demand for bleaching chemicals. It is desirable to lower the residual lignin level to consume less chlorine dioxide, however, it does not make sense to shrink the yield more than necessary. It does also not make sense to keep the yield high by controlling the oxygen stage effects and to cut the yield later in the sequence through inadequate bleaching conditions. Therefore, in the trials described below, the oxygen stages were run with moderate conditions, reaching delignification rates of close to 50% with softwood pulps and only up to 40% with hardwood pulps. An O stage delignification of 40% is already high. Because of the high level of hexenuronic acids in hardwood pulps their contribution to the Kappa number has to be taken

into account. The real lignin amounts only for about 60% to 70% of the Kappa number. Thus, a drop in Kappa number by 40% is equivalent to a drop by 75% calculated on lignin [2].

Chlorine dioxide was used in our trials as the workhorse for delignification, hydrogen peroxide was applied with the target to assist in the oxidation of residual lignin and to substitute as much ClO₂ as possible without affecting the pulp quality and the effluent load. The brightness target for hardwood pulps was typically 90+ (%ISO) and 89 (%ISO) for softwood pulps. The sequences compared in this study are O-D₀-Eop-D₁-E(p)-D₂ or O-D₀-Eop-D₁-D₂ respectively O-D₀-Eop-D₁-P.

3. Results and Discussion

First extraction stage application of H₂O₂
Chlorine dioxide oxidizes the phenolic groups in the residual lignin to compounds with carboxylic acid groups which become water soluble in a subsequent extraction stage. The amount of alkali required for this extraction correlates with the number of acidic groups that need neutralization and with the improved solubility of the oxidized lignin under alkaline conditions. Figure 2 shows the effect of the caustic soda amount on the Kappa number after extraction in the absence of additional oxidizing compounds. There is a moderate influence of the alkalinity on the degree of lignin extraction. However, the differences remain small as long as the pH is above 10 at the end of the treatment. It is therefore not attractive to add caustic soda amounts above 1.8%.

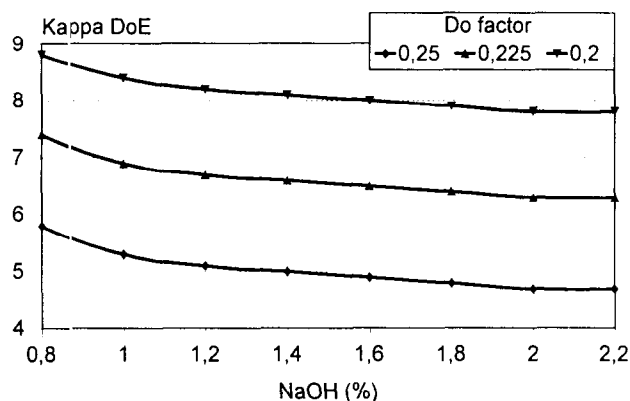


Figure 2. Delignification of softwood kraft pulp (MCC pulp, Kappa 25) with the stages DE using different levels of ClO₂ and NaOH. D₀ stage 50°C, 1h, pH 3; E stage 75°C, 1.5h; 10% cons.

In contrast to chlorine, chlorine dioxide is not primarily demethoxylating phenol ethers. Only under stronger acidic conditions intermediate hypochlorous acid, ClOH, is generated in higher amounts and degrades phenol ether structures. Since the number of free phenolic groups was already decreased during the oxygen treatment, ClO₂ cannot be as effective as chlorine. It becomes favorable to support the lignin oxidation reaction with the addition of oxygen and hydrogen peroxide in the extraction stage. The addition of hydrogen peroxide decreases the lignin content further by nearly two Kappa units with the addition of 0.5% H₂O₂ as a result of additional oxidation. Figure 3 compares the Kappa numbers achieved with a constant caustic soda charge of 1.8% and different peroxide amounts. The application of hydrogen peroxide allows to lower the Kappa factor for a given Kappa number target. Typically hydrogen peroxide and oxygen are added in combination, with amounts of about 5kg/t each. Thorough mixing is essential to see a positive effect of the oxygen gas addition.

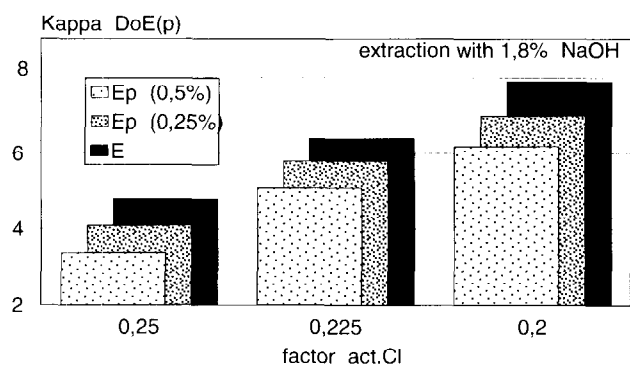


Figure 3. Effect of an oxidative supported extraction bleaching softwood kraft pulp with D₀Ep. Peroxide addition 0.25% and 0.5%. Conditions: cf. Figure 2.

The addition of both chemicals decreases the demand for chlorine dioxide. There are additional positive side effects: the brightness of the pulp increases already in the E stage to a level between 75 %ISO and 80 %ISO, depending on the amount of hydrogen peroxide added. The effluent color is improved, the Ep stage effluent color becomes light brown instead of dark brown. The addition of larger amounts of H₂O₂ increases the delignification and the brightness. It is, however, necessary to increase the temperature simultaneously, because increased

amounts of hydrogen peroxide are not consumed under moderate conditions. An oxygen predelignified pulp can be bleached to a significantly lower lignin residue and a higher brightness if the temperature in the Eop stage is increased from 80°C to 95°C. Figures 4 and 5 give the results of such a treatment with higher intensity.

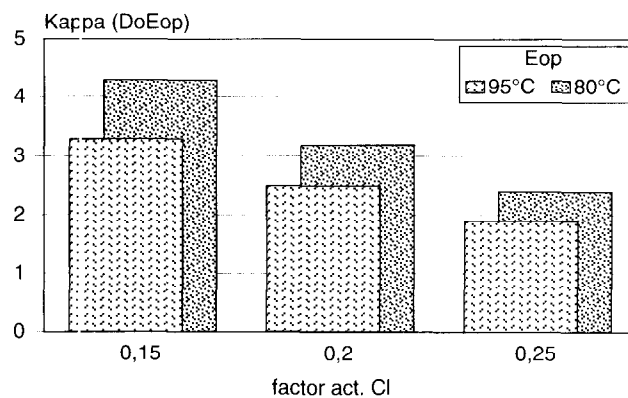


Figure 4. Delignification of Kappa 15 oxygen delignified softwood pulp with different active chlorine amounts and Eop conditions. D₀ stages at pH<3, 1 h, 50°C; Eop with 1.8% NaOH, 0.1% MgSO₄, 0.5% H₂O₂ at 80°C or 1% H₂O₂ at 95°C, 1.5h.

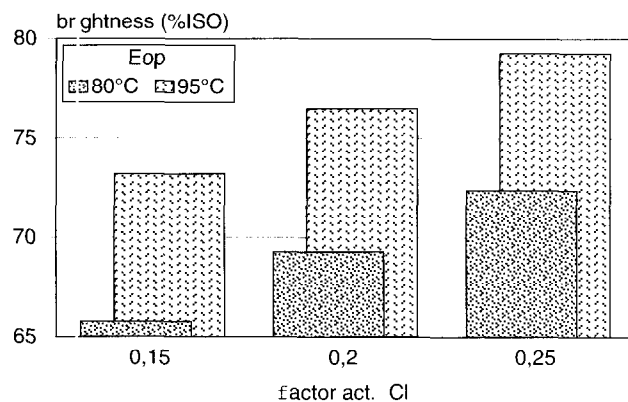


Figure 5. Brightness increase with OD₀Eop treatment and different ClO₂ amounts and peroxide addition. Conditions: cf. Figure 4.

Unfortunately, not everything turns out positive at higher temperature: the COD increases and the viscosity drops. In Figure 6, a comparison of the viscosity levels is made after final brightening with different Kappa factors for active chlorine in D₀ and D₁ with the sequence OD₀EopD₁P. The negative impact of the higher Eop temperature on the pulp quality becomes visible. Independent of the amounts of chlorine dioxide applied in the

final bleaching sequence, all pulps produced with the higher Eop stage temperature do have a lower final viscosity. It is therefore necessary not to push the temperature in the Eop stage above limits.

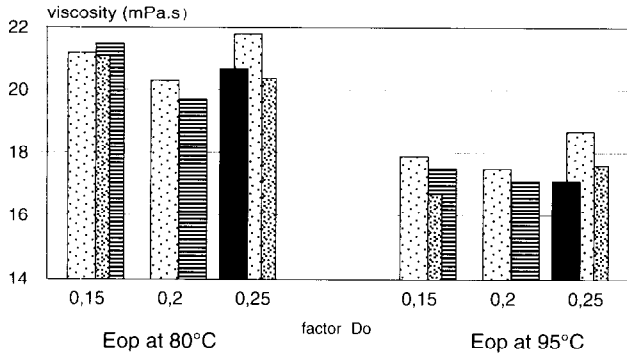


Figure 6. Viscosity drop with higher temperature in Eop after final brightening with different amounts of ClO₂ in D₀ and D₁ and a final P stage (0.3% H₂O₂, 80°C).

The effect of more peroxide added to an Eop stage is given for the Kappa number and the brightness in Figure 7. Simultaneously, the temperature was increased in order to achieve a sufficient consumption of the peroxide added. The graph shows that the positive effect of the peroxide addition levels off at about 90°C. This temperature seems to be the highest that should be applied in an Eop stage. Figure 8 has the effect on the combined COD from the D₀ and the Eop stages. Because an increasing COD indicates a loss in yield [3], it is definitively not advantageous to run Eop stages at very high temperature.

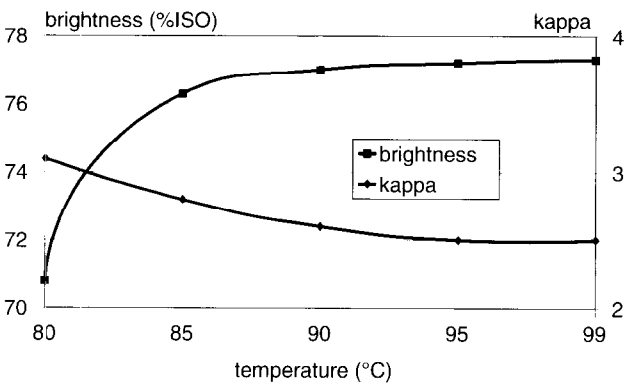


Figure 7. Brightness increase and Kappa drop with temperature in D₀Eop bleaching of oxygen delignified softwood kraft pulp. Do stage with 3 % ClO₂ (kappa factor 0.2) at 50°C, 1h. Eop stage with 0.5% (80°C), 0.75% (85°C and 90°C), and 1% H₂O₂ (95°C and 99°C).

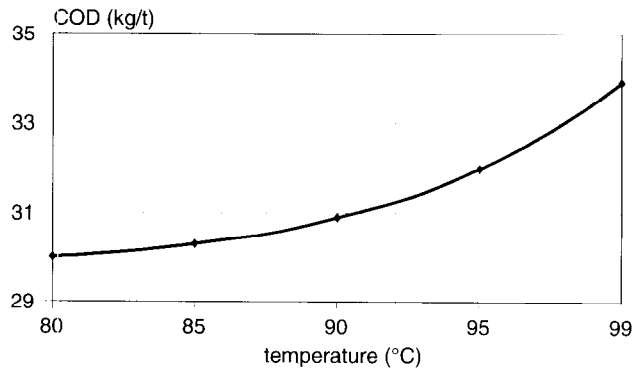


Figure 8. Increase of COD from the D₀Eop stages with increasing temperature bleaching of oxygen delignified softwood kraft pulp. Conditions for Eop stage: cf. Figure 7.

With hardwood pulps the results are very similar. Because of the typically higher initial brightness and the good bleachability the brightness level after an Eop stage can well be above 80% ISO.

It is an advantage to increase brightness in the Eop stage. It might seem more appropriate to focus on delignification that early in the sequence, however, the brightness gain of the Eop stage remains visible even after the final bleaching stage. The results for a softwood kraft pulp are given in figure 9. The pulp was delignified to the same Kappa level using different amounts of ClO₂, either with a D₀E or a D₀Eop treatment. Final bleaching was made with identical amounts of active chlorine. The higher brightness after the Eop stage is still visible at the end of the whole sequence.

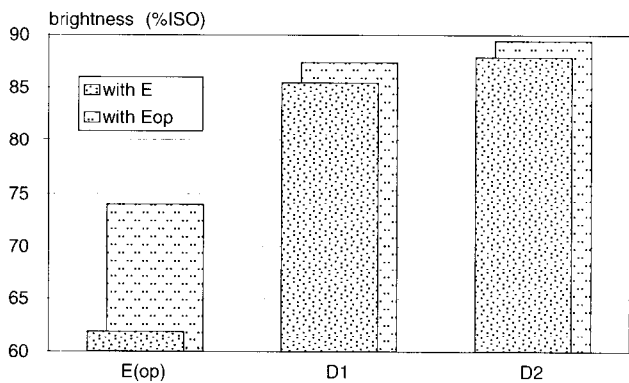


Figure 9. Comparison of brightness increase with D₀ED₁D₂ and D₀EopD₁D₂ bleaching; D₀ with factor 0.28 (E) resp. 0.22 (Eop) to Kappa 3.0 and constant active Cl addition in D₁D₂.

Second extraction stage application of H₂O₂. In the second extraction stage the application of hydrogen peroxide can be very effective either in decreasing the total amount of ClO₂ in final bleaching or even in replacing the last D stage completely. This addition of H₂O₂ to cut the demand for ClO₂ is not new. It was described already as early as 1980 [4]. The addition of 0.225% H₂O₂ in the second E stage resulted in a replacement of 1.3% ClO₂ (active Cl). The savings resulted from a lower demand in the D₁ stage as well as from the D₂ stage. There was a long list of other advantages: lower cost for bleaching chemicals, less steam required, higher final brightness, improved viscosity, and better strength.

However, a long bleaching sequence with D₁ED₂ final bleaching stages is not very typical any more. Quite a number of bleach plants have been rebuilt with the elimination of the second E stage. Sometimes the pulp is neutralized between the final D₁D₂ treatment, very often even this step was eliminated. In these cases the application of hydrogen peroxide targets for the replacement of the last D stage and, in order to become cost-effective, has in addition to replace some of the amounts of ClO₂ added to the D₁ stage.

The substitution of the final D stage with a P stage in a short OD₀EopD₁D₂ sequence can be very effective. Figure 9 shows the overstoichiometric replacement of ClO₂ with a small amount of H₂O₂. The pulp was prebleached with the sequence O-D₀-Eop to a brightness level of 82.1 %ISO and had a Kappa number of 3.5. The demand for chlorine dioxide in final bleaching with two subsequent D stages was as

high as 1.25% (active Cl). Two stages with chlorine dioxide are necessary as the curve for the brightness after the first D stage illustrates. Even with very high ClO₂-amounts the brightness increases only to 89 %ISO, below the target brightness for market pulp. Only after washing and the addition of more ClO₂ in the second D stage this brightness level is reached. The substitution of the last D stage with a peroxide treatment has the potential to replace much more ClO₂ than just the amount added to the D₂ stage. It is neither necessary to apply high amounts of H₂O₂ nor to use aggressive conditions, with rather moderate amounts of H₂O₂ at about 80°C a significant brightness increase results. In the example the substitution rate for H₂O₂ to active chlorine is 1 to 4. It can be significantly higher on mill scale. Trials at Bahia Sul Celulose have found substitution rates of up to 1 to 9 [5], mainly as the result of much less peroxide needed compared to the amount applied in the example.

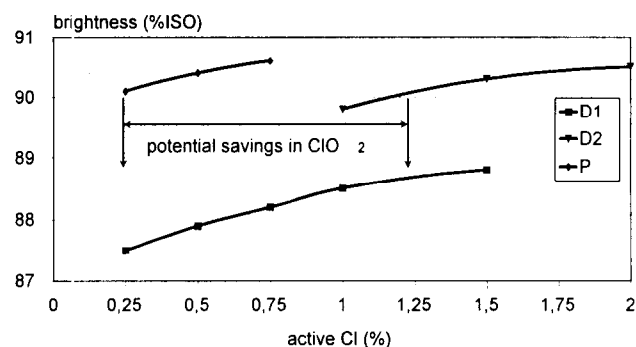


Figure 10. Final bleaching of eucalyptus kraft pulp with hydrogen peroxide. Predelignification with O-D₀-Eop to brightness 82.1 %ISO and Kappa 3.5. P stage: 0.25 % H₂O₂, 0.4 % NaOH, 80°C, 3 h.

Table 1. Final bleaching of eucalyptus kraft pulp after O-D₀-Eop-D₁ prebleaching with H₂O₂; brightness 87.7 %ISO, P stage at 75°C, 2 h.

| H ₂ O ₂ (%) | NaOH (%) | MgSO ₄ (%) | sodium silicate (%) | H ₂ O ₂ resid. (%) | Brightness %ISO | Viscosity (mPa.s) | heat aging (points) |
|-------------------------------------------|----------|-----------------------|---------------------|------------------------------------------|-----------------|-------------------|---------------------|
| 0,25 | | | | 0,02 | 87,6 | 8,5 | 7,2 |
| 0,25 | 0,4 | | | 0,01 | 90,2 | 10,8 | 2 |
| 0,5 | 0,4 | | | 0,1 | 90,8 | 10,1 | 2,8 |
| 0,25 | 0,4 | 0,1 | | 0,04 | 90,5 | 11,2 | 2,6 |
| 0,25 | 0,3 | 0,1 | 0,25 | 0,04 | 90,7 | 13,4 | 2,6 |
| 0,25 | 0,3 | 0,1 | 0,5 | 0,05 | 90,8 | 13,8 | 2,4 |
| D ₁ -D ₂ reference: | | | | | 90,4 | 13,2 | 4,6 |

The presence of a small amount of sodium silicate to buffer the reaction during the peroxide treatment improves the viscosity level. Brightness stability in accelerated heat aging (Tappi standard T 260) is improved compared to the reference with two final D stages. Table 1 shows data for different amounts of additives and their effect on the bleaching result. In the absence of caustic soda, the viscosity dropped and the brightness stability was poor. The addition of magnesium sulfate and especially sodium silicate improved the viscosity and had a positive impact on the brightness increase.

For softwood pulps the economy of a D₁P combination compared to a D₁D₂ treatment is more difficult to meet. However, savings in the demand for chlorine dioxide become visible if the final D stage is exchanged for a P stage. Figure 11 has the results achieved in bleaching a New Zealand softwood pulp with either final DD or DP stages. In both cases prebleaching was conducted applying ClO₂ in D₀ with Kappa factor 0.25 and an Eop stage with 0.4% H₂O₂. The standard sequence with two final D stages reached brightness 88 with an input of about 2% of active chlorine applied in both stages. This brightness was already achieved with less than 1% of active chlorine applied in D₁ and a P stage with only 0.25% H₂O₂. With more ClO₂ applied in D₁ the brightness ceiling could be pushed up to nearly 90% ISO. The exchange of the final D for a P stage offers a higher brightness range compared with only D bleaching.

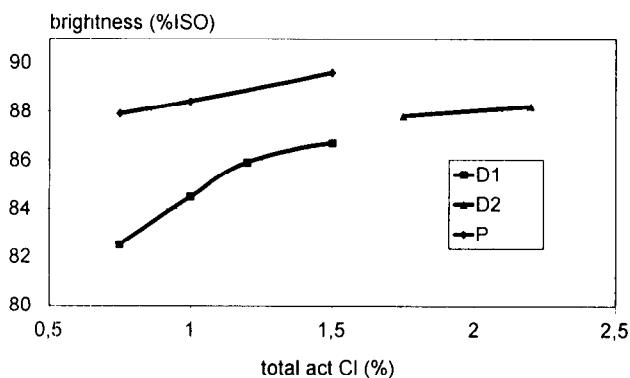


Figure 11. Final bleaching with DD or DP of softwood kraft pulp. Peroxide charge 0.25%, 80°C; pretreatment with sequence OD₀Eop; D₀: Kappa factor 0.25, 50°C, 1h, 10% cons.; Eop: 1.8 % NaOH, 0.4% H₂O₂, 0.3 MPa O₂, 1.5h, 10% cons.

On top of this, brightness stability is improved with a final P stage. Figure 12 shows the data for the accelerated aging test using high humidity and high temperature (Tappi T 260). Reversion is lower for the peroxide bleached pulps.

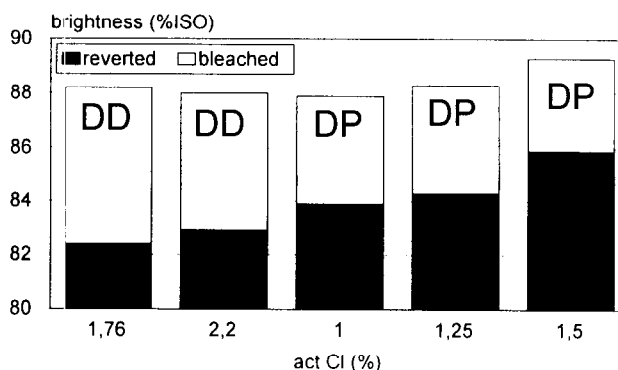


Figure 12. Heat aging of softwood pulp bleached with the sequences OD₀EopD₁D₂, resp. OD₀EopD₁P. (Tappi test method T 260).

In final bleaching with hydrogen peroxide, rules found for the Eop stage application of H₂O₂ apply again. It is not attractive to increase the temperature above the limits already described for the Eop stage application. Because higher amounts of H₂O₂ are only consumed at higher temperature it has been recommended to run these stages at a temperature above 100°C, and also pressurized conditions have been labeled to be attractive [6, 7]. With the target to cut the chlorine dioxide demand in an O-D₀-Eop-D₁-P sequence, the amounts of ClO₂ applied in the D₁ stage were altered. The lower brightness resulting from smaller amounts of chlorine dioxide were compensated with higher amounts of H₂O₂.

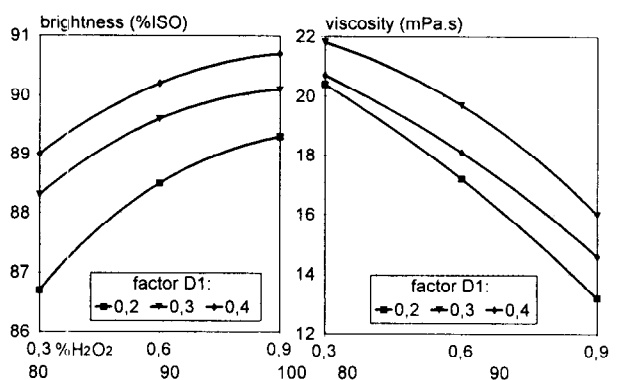


Figure 13. Bleaching of softwood kraft pulp with the sequence O-D₀-Eop-D₁-P; factor D₀ 0.25; Eop at 80°C; D₁ stage with increasing ClO₂ charges at 70°C; final P stage at 80, 90 and 100°C with increasing amounts of H₂O₂.

Again, because the turnover of hydrogen peroxide was poor, the temperature needed to become higher with higher input of peroxide. Figure 13 has the resulting brightness curves and the viscosities. The example was selected from a set of trials with different temperature in the first and second extraction stage. It is possible to compensate the lower input of ClO_2 in the D_1 stage with an increasing amount of H_2O_2 . Brightness levels of 89 or 90 %ISO are achieved. The temperature increase results on the other hand in significantly lower viscosities. This limits the applicability of very high temperature in peroxide stages. It goes without saying that a temperature above the boiling point of water as it is applied in pressurized P stages yields even poorer viscosities. Yield suffers from aggressive treatment. A comparison of moderate and hot temperatures in the E stages was made for an oxygen delignified softwood kraft pulp using the sequence $\text{D}_0\text{EopD}_1\text{P}$. The decrease in yield shows up as an increase in COD. In order to keep the effluent COD low and the yield high it is

therefore essential to avoid drastic E or P stage conditions.

"ECF light" bleaching conditions. Pulps with very good bleachability are an ideal raw material for short bleaching sequences. While in general the application of short sequences is uneconomical if high brightness levels are the target, they become attractive if a "new" pulp quality can be generated. This is the case for bleaching with very little chlorine dioxide. Oxygen delignified pulps are treated with chlorine dioxide or ozone and ClO_2 subsequently in one stage followed by one or two P stages. Rather low amounts of chlorine dioxide are applied and the brightness is achieved with a higher input of hydrogen peroxide. The resulting pulps do have a very low residue of halogenated compounds (OX). These pulps compete in the market with TCF bleached pulps. Compared with the latter, they are superior in brightness and strength. In Brazil the term "ECF light" is used for those pulps.

Table 2. Comparison of yield in ECF bleaching of a softwood kraft pulp using moderate or aggressive conditions in the oxidative reinforced E stages.

| sequence | ClO_2 (% act. Cl) | H_2O_2 (%) | temp. in Eop and P ($^\circ\text{C}$) | COD, kg/t | Yield, % |
|------------------------------------------------------------------------|----------------------------|----------------------------|-----------------------------------------|-----------|----------|
| $\text{D}_0\text{EopD}_1\text{P}$ | 5,52 | 0,65 | 75 | 37,5 | 96,00 |
| $\text{D}_0\text{Eop}_{(\text{hot})}\text{D}_1\text{P}_{(\text{hot})}$ | 3,44 | 1,55 | 98 | 44,3 | 95,15 |

Table 3. Final bleaching with hydrogen peroxide following an O-Z/D predelignification, eucalyptus kraft pulp, O_2 del. to Kappa 8,6; 0,45% O_3 , 1% ClO_2 (active Cl).

| H_2O_2 (%) | NaOH (%) | Sodium silicate (%) | temp. ($^\circ\text{C}$) | time (h) | H_2O_2 -residual (%) | COD (kg/t) | brightness (%ISO) | viscosity (mPa.s) |
|----------------------------|----------|---------------------|----------------------------|----------|--------------------------------------|------------|-------------------|-------------------|
| 1,5 | 0,8 | -- | 90 | 2 | 0,54 | 8,4 | 90,8 | 12,1 |
| 1,5 | 0,8 | 0,5 | 90 | 2 | 0,78 | 7,9 | 90,6 | 13,1 |
| 1,5 | 0,8 | -- | 105 | 1 | 0,37 | 11,8 | 90,8 | 10,8 |

Table 4. Bleaching of eucalyptus kraft pulps with low amounts of ClO_2 and/or O_3/ClO_2 and high peroxide charges in Eop, resp. P.

| Sequence | active Cl (%) | H_2O_2 (%) | brightness (%ISO) | OX (g/t) |
|--------------------------------------|---------------|----------------------------|-------------------|----------------|
| D_0EopP | 1,4 | 0,5 + 1,5 | 89,3 | 69,4 \pm 5,1 |
| Z/ $\text{D}_0\text{EopD}_1\text{P}$ | 1,4 + 0,6 | 0,3 + 0,25 | 92,3 | 39,4 \pm 1,2 |
| Z/ D_0EopP | 1,4 | 0,3 + 1 | 90,4 | 24,3 \pm 0,5 |

Again there is no advantage of high temperature and pressurized conditions in the P stage, despite of its recommendation in some papers. Table 3 provides data describing the results of final

bleaching with H_2O_2 at different temperature levels. Pressurized conditions do not result in a better brightness, they yield a faster consumption of the peroxide and a lower viscosity together

with a higher COD. Thus they are significantly less selective. More important is the buffering action of the small amount of sodium silicate, it results in the lowest consumption of H_2O_2 despite of an identical brightness. These conditions also give the lowest COD and the highest viscosity.

The amount of halogenated residue is slightly higher in cases where only ClO_2 is used in the D_0 stage. There is a pronounced effect on the application of one or two D stages. The OX level is higher if two D stages are applied. Table 4 has data for trials using sequences with D_0EopP or Z/D_0EopP stages, and alternatively D_0EopD_1P resp. Z/D_0EopD_1P stages. The amount of active chlorine in D_0 has a limited effect, because two subsequent alkaline P stages saponify, extract and decompose the halogenated material. The effect is very pronounced for the pulps treated with chlorine dioxide and ozone. Obviously, the aggressive reactions of ozone yield a more degraded lignin which is more easily extractable. Therefore, the level of OX remaining in the pulp becomes very low. It is so low, that it is within the range that is accepted to describe TCF pulps, *i.e.*, below 30 g/t. Thus such a pulp cannot be identified any more by its OX as an ECF pulp, it could as well be a TCF pulp.

4. Conclusions

First E stage application of H_2O_2 :

- * Peroxide and oxygen addition result in:
 - * better delignification
 - * higher brightness
 - * lower demand for chlorine dioxide

Second E stage application of H_2O_2 :

- * Moderate amounts of peroxide yield:
 - * cost effective substitution of ClO_2
 - * higher brightness stability
 - * lower level of halogenated compounds (OX)

In both cases it is important to avoid extreme temperatures, they would cause a higher COD and a lower yield.

5. References

- [1] Gullichsen, J. Bleaching, the Scandinavian situation. International Pulp Bleaching Conference, Helsinki, 1998, opening session.
- [2] Süss, H.U.; Filho, C.L. Chemicals demand in ECF bleaching of eucalyptus pulp with extended prebleaching. ABTCP Conference São Paulo, May 1998.
- [3] Süss, H.U.; Kronis, J.D. The Correlation of COD and Yield in Chemical Pulp Bleaching. *Proceedings*, Tappi Breaking the Pulp Yield Barrier Symposium, Atlanta, GA, 1998, 153 - 162.
- [4] Loutfi, H. The use of hydrogen peroxide in bleaching Kraft softwood pulp. *Proceedings*, CPPA annual meeting, Montreal, 1980, B71-77.
- [5] Dos Santos, C.A.; Süss, H.U.; Mambrim, O. Filho, Flexibilização da sequência de branqueamento ECF da Bahia Sul Celulose s. a. 28° Congresso anual de celulose e papel, São Paulo, 1995.
- [6] Devenyns, J.; Renders, A.; Carlier, J.; Walsh, P. Optimal use of hydrogen peroxide to design low AOX ECF sequences. *Proceedings*, Tappi Pulping Conference 1995, 281 - 288.
- [7] Reeves, R.; Boman, R.; Nordén, S. Impact of sequence position for pressurized (PO) stage in ECF bleaching. *Proceedings*, Tappi Pulping Conference 1995, 263 - 267.

THE SWELLING BEHAVIOUR OF SPRUCE WOOD CELL WALLS DURING KRAFT PULPING

A. Treimanis,^a T. Maloney,^b V. Klevinska,^a M. Eisimonte,^a H. Paulapuro^b

^a State Institute of Wood Chemistry, 27 Dzerbenes St., Riga, LV 1006, Latvia

^b Helsinki University of Technology, P.O. Box 6300, FIN-02015 Hut, Finland

The swelling of spruce wood cell walls during kraft and extended kraft pulping was evaluated by fiber saturation point (FSP) measurements and direct light microscopy. The pulping processes were characterized by a gradual growth in FSP from 0.62 ml/g to a maximum 1.25-1.37 ml/g at pulp yield of 65-48%. After this a slight decrease of FSP was observed. When the total cell wall volume was calculated on the basis of one gram of the original unpulped wood a distinct contraction of the cell wall was observed at lower yields. Direct measurements of cell wall thickness showed a characteristic bimodal distribution consisting of both thin-walled springwood and thick-walled summerwood fibres. The

thickness of the cell wall of springwood fibers was found to increase to a maximum (about 5 μm) at approximately 90% yield and then decreased to 4.4-4.5 μm . The pattern of spruce springwood fiber wall thickness as a function of pulp yield resembled the swelling behavior of birch wood fiber walls measured with solute exclusion. Solute exclusion measurements indicated a larger contraction of the cell wall at the end of cooking than was observed by microscopy.

Keywords: spruce, fibre wall, swelling, fibre saturation point, kraft pulping

Introduction

Quantification of the pulp fibre degree of swelling is important for the evaluation of fibre wall's accessibility to bleaching chemicals (especially gaseous), for the appraisal of pulp's papermaking properties and with respect to the behaviour of fibres during enzymatic hydrolysis. The development of fiber swelling is also very important for the transport of lignin fragments out of the cell wall in delignification.

One of the most widely known methods for the measurement of pulp fibre swelling is the solute exclusion technique which determines the so-called fibre saturation point (FSP). The FSP is the volume of water imbibed in cell wall in pores less than 50 nm.

The most important research directly related to the present study was published by Stone and Scallan in the 1960's [1, 2]. In these studies the solute exclusion technique was used to measure fibre swelling and pore volume. It was

demonstrated that kraft delignification proceeds in three stages: a slight expansion of the cell wall in early delignification, replacement of dissolved material by an equal amount of water down to about 60% yield, and contraction of the cell wall thereafter.

While these earlier studies have been generally well accepted it is worthwhile to consider kraft delignification in further detail and from a different point of view. The aim of the present study was to investigate by direct microscopic observations the changes of cell wall dimensions calculated from solute exclusion data for spruce kraft pulp fibres at different yields.

Materials and Methods

Latvian spruce (*Picea abies*) wood chips with dimensions of 20x20x2 mm were used for pulping experiments. Kraft and extended kraft cooks were carried out in 24 rotating stainless

steel autoclaves in a glycerol bath. To ensure the comparison of the pulping processes the total effective alkali during the two processes was equal. The active alkali content and liquor-to-wood ratio were varied according to [3].

At the 1st stage of the extended kraft cooking wood chips were treated with 28 g/l Na₂S solution at room temperature. After this treatment the liquor was removed. At the 2nd stage cooking liquor with sulphidity of 30% and active alkali of 51 g/l was added. The autoclaves were heated to 175°C at 1.5°C/min. Delignification time in the second stage was 60 min at 175°C. Only NaOH solution (20 g/l) was used at the 3rd stage of the process. This stage lasted for 30 min at 175°C. The conventional kraft pulping was carried out at liquor sulphidity of 31.5% and active alkali concentration of 60.5 g/l in Na₂O units. The first sampling was performed after the chip impregnation, then after heating to 90, 110, 135, 150, 160, 175°C as well as after delignification at the final temperature for 30, 60 and 90 min. The yield and Klason lignin content for each sample was measured.

Prior to the FSP measurements the samples were exchanged to the sodium form by soaking in sodium acetate overnight and then thoroughly washed with distilled water. Samples at high yield were defiberized in a blender. The fines (<200 mesh) were removed with a Dynamic Drainage Jar. The FSP was calculated as the amount of water per gram of oven dry pulp (or per gram of initial wood) inaccessible to a 2,000,000 Dalton dextran polymer (T2000 from Pharmacia). The solute exclusion method of Stone and Scallan was used [1]. The concentration of dextran in the solute exclusion measurements was measured with an Autopol IV polarimeter (Rudolph Research Analytical). The cell wall volume was calculated as the sum of the water and solid material's volume on the basis of 1 gram of original wood before pulping. For this calculation it was assumed that the density of the cell wall's solid material was 1.5 g/ml.

The apparent cell wall thickness was determined with direct microscopic measurements. The measurements were done by preparing a slide of wet pulp fibres, adding Graff-C stain and viewing the fibers through a monitor connected to a Leitz Labolux S microscope. The cell wall thickness was calculated as ½ the difference of

the fiber and lumen diameter. 200 fibres were measured per test point.

Results and Discussion

In Table 1 the characteristics of the spruce wood residues pulped to different yields are shown. The table shows that the FSP grows from about 0.6 ml/g (initial wood) to a maximum 1.36-1.44 ml/g at 52-63% yield for both the kraft and extended kraft processes. The FSP for several of the extended kraft samples are lower than those of the corresponding conventional kraft samples.

Table 1. Residual lignin content and FSP values of spruce wood pulped to different yields in conventional and extended kraft cooking.

| Sample | Yield, % | Lignin, % | FSP, ml/g |
|------------------------------------|----------|-----------|-----------|
| 0 | 100 | 29.6 | 0.62 |
| Conventional kraft delignification | | | |
| 1 | 98.1 | 28.7 | 0.86 |
| 2 | 95.4 | 28.5 | 0.85 |
| 3 | 91.4 | 29.6 | 0.87 |
| 4 | 80.6 | 29.8 | 1.09 |
| 5 | 75.8 | 27.6 | 1.25 |
| 6 | 72.1 | 25.9 | 1.22 |
| 7 | 63.4 | 19.6 | 1.44 |
| 8 | 50.6 | 7.1 | 1.36 |
| 9 | 47.8 | 4.4 | 1.37 |
| 10 | 46.5 | 3.4 | 1.35 |
| Extended kraft delignification | | | |
| 11 | 99.0 | 29.1 | 0.75 |
| 12 | 94.6 | 28.9 | 0.85 |
| 13 | 88.0 | 29.8 | 0.89 |
| 14 | 80.0 | 29.5 | 1.13 |
| 15 | 74.0 | 26.7 | 1.20 |
| 16 | 66.6 | 21.7 | 1.27 |
| 17 | 52.5 | 8.7 | 1.34 |
| 18 | 48.5 | 4.7 | 1.36 |
| 19 | 47.0 | 4.0 | 1.29 |
| 20 | 44.9 | 2.9 | 1.33 |

Figures 1 and 2 illustrate the changes in fiber pore volume calculated in milliliters per gram of initial wood, *i.e.*, on the basis of the same fiber number (curve 2 in the figures). The results agree

in general with those previously reported [1]. Three phases of cell wall swelling are evident: increase of water filled pore volume during the loss of the first 10-15% of solids, constant pore volume from 65-70% yield and finally a decrease in pore volume in the end of pulping. The final pore volume is quite close to the initial wood

pore volume, about 0.6-0.7 ml/g. At the beginning of delignification there is a slightly more pronounced swelling in the case of conventional kraft cooking. This is probably due to a relatively higher concentration of active alkali.

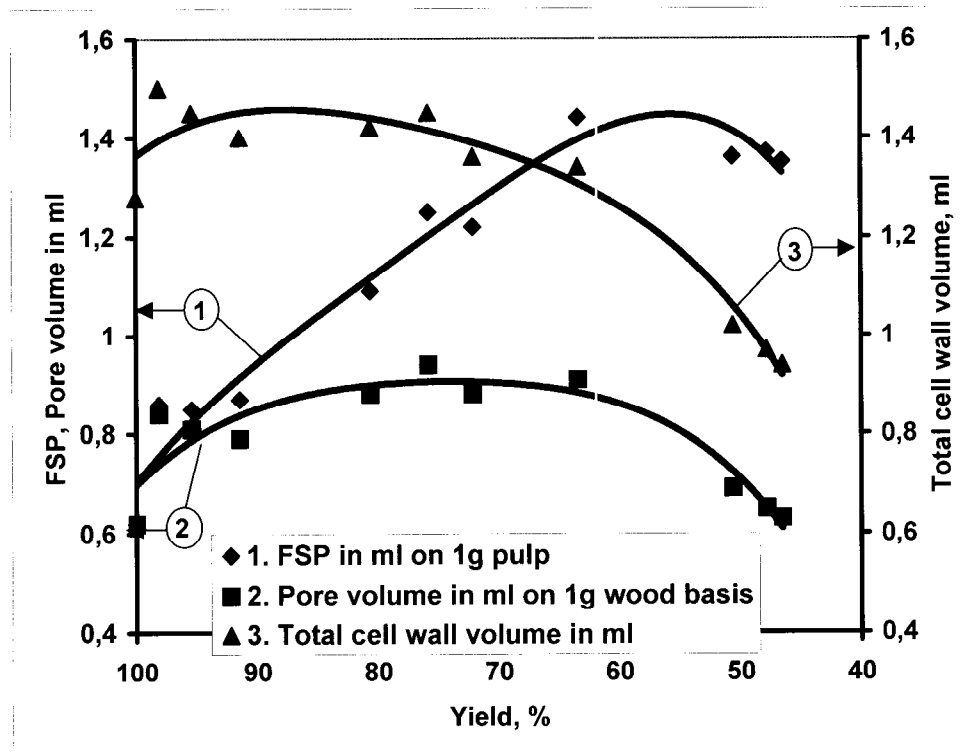


Figure 1. Fiber saturation point, fiber pore volume and total cell wall volume vs. yield in conventional kraft pulping.

Curve 3 in Figures 1 and 2 shows the total volume of the cell wall as a function of yield. These curves show that the cell wall contracts about 37-38% in the end of pulping compared to the original unpulped wood fibre. The amount of contraction is about the same for both the conventional and extended kraft cooking.

It seems likely that the volumetric contraction of the cell wall should be reflected in the cell wall thickness. Cell wall thickness was determined by direct microscopic measurements after staining the fibres. We confirmed our measurements by assessment of several samples at the Finnish Pulp and Paper Research Institute (KCL) where a more sophisticated version of the technique was available. The cell wall thickness values at both laboratories agreed within the confidence of the measurements.

A plot of the average cell wall thickness as a function of yield is shown in Figure 3. A

characteristic bimodal distribution was obtained consisting of both thin-walled springwood and thick-walled summerwood fibres. Because the distribution was so wide it was difficult to statistically differentiate the samples, *i.e.*, the average depended too heavily on the fraction of springwood and summerwood which was counted. A considerable reduction in scattering could be made if only springwood or summerwood was considered. This was done by counting 200 fibres at random and classifying all fibres with cross-sectional dimensions greater than 8 μm as summerwood and all fibres less than or equal to 8 μm as springwood. This division was based on the individual sample distributions which showed separation of the nodes at 8 μm . The average cell wall thickness for springwood gave the most favourable scatter since it includes about 79% of the fibres.

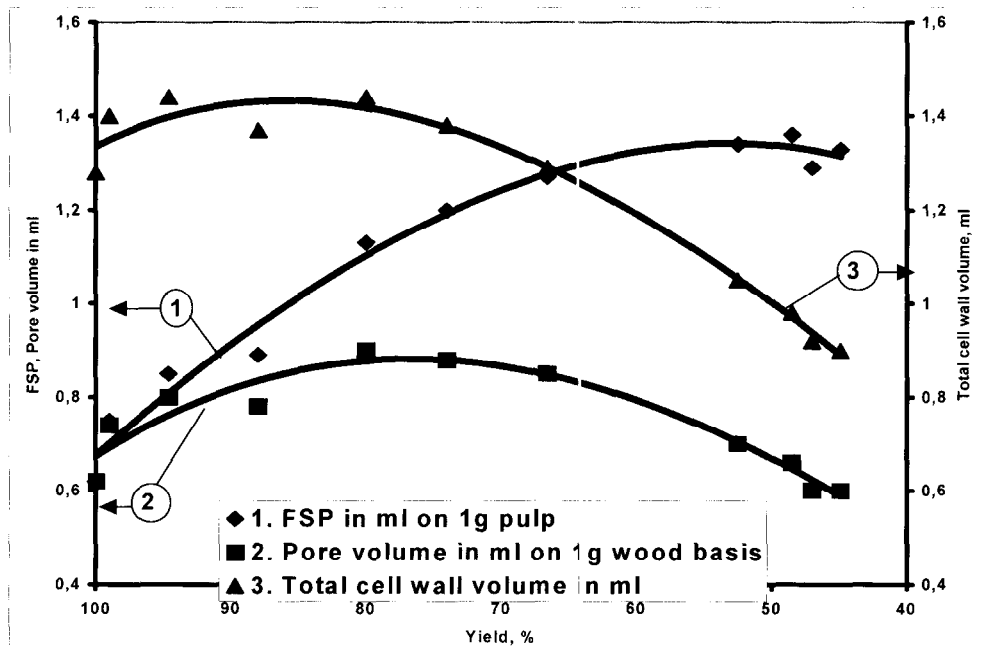


Figure 2. Fiber saturation point, fiber pore volume and total cell wall volume vs. yield in extended kraft pulping.

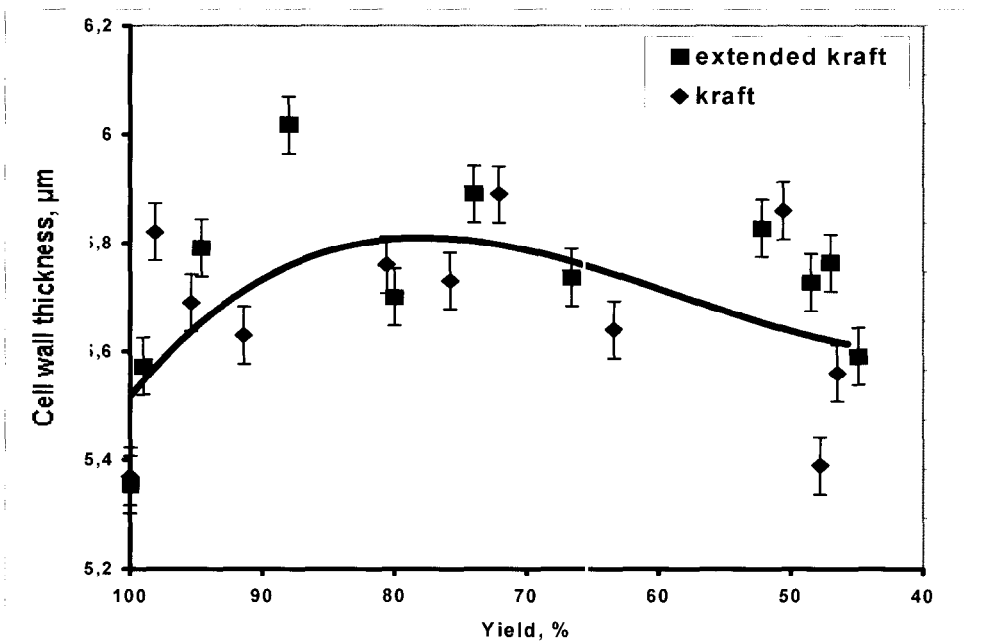


Figure 3. Cell wall thickness vs. yield for kraft and extended kraft delignification (all fibers).

The results of direct fibre wall thickness measurements for all samples are shown in Figure 3. They show the same three phases of fibre wall transformation during kraft pulping: expansion of cell wall width from 5.4 to 5.6-5.7 μm at about 94-95% yield, a near constant thickness to about 53-55% yield and a slight contraction in thickness in the end of pulping. Thus, the results in Figure 3 show an expansion and contraction of the cell wall but the extent of contraction, and the yield when it begins, do not

correspond to what is predicted from solute exclusion. Based on the 37-38% contraction (Fig. 1 and 2) predicted from solute exclusion the cell wall thickness should drop to about 3.5 μm . It seems that the cell wall thickness measurements do not reflect precisely the change in fiber wall volume. One possible explanation for this is that pulping distorts the cell wall in a way that makes accurate determination of the cell wall thickness difficult. For example, the delignified fibers may tend to flatten and become

oval causing the apparent thickness to increase. Another possibility is that there is some delamination or other process which forms very large pores. The pores with dimensions greater than 50-60 nm are not measured by solute exclusion, but contribute to the cell wall

thickness viewed with a microscope. The discrepancy between solute exclusion data and light microscopic measurements of the fiber wall has been noted by Page [4] in connection with beating.

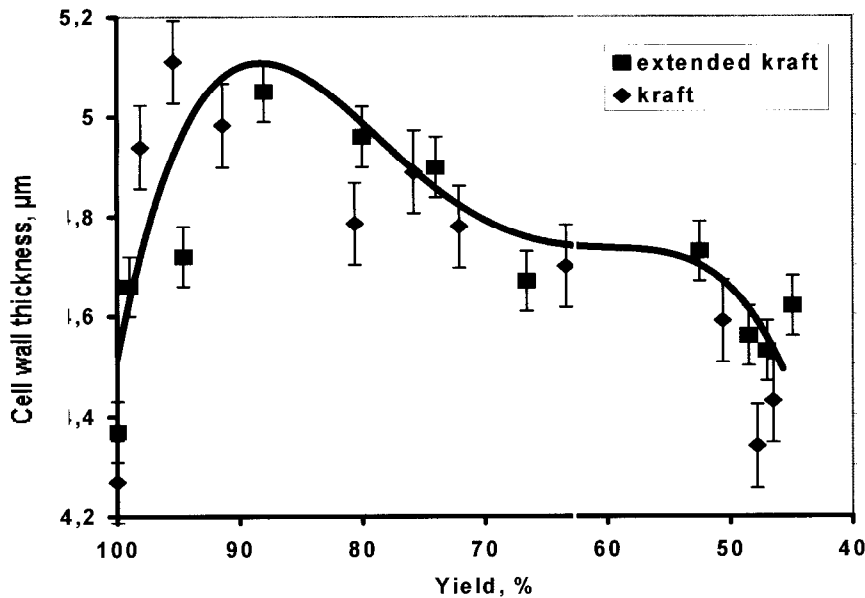


Figure 4. Cell wall thickness vs. yield for kraft and extended kraft delignification (spring wood fibers).

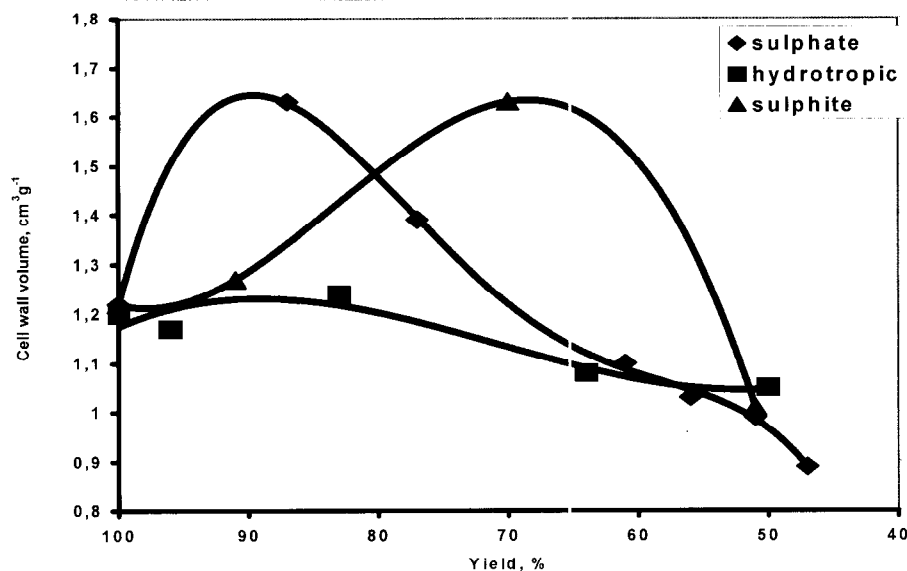


Figure 5. Birch wood total cell wall volume as function of pulp yield for kraft, sulphite and hydrotropic pulping processes.

Figure 4 illustrates the changes in springwood cell wall thickness during kraft and extended kraft processes. After an initial increase in cell wall thickness from 4.3 to 5 μm the cell wall steadily contracts throughout the remainder of pulping. The two pulping processes do not show

very much difference. However, the conventional kraft samples do show a steeper increase in the initial swelling and a more pronounced final contraction than the extended delignification samples.

The curves in Figure 4 resemble the pattern of swelling changes for birch wood in kraft pulping (Figure 5). Birch cell walls exhibit substantial swelling during the initial phase of cooking [5 - 6], then the cell wall volume decreases steadily thereafter. Possibly these similarities could be explained by a lower density of lignin-carbohydrate cross-links (and, probably, lower lignin content) in both the spruce springwood and birch wood compared to spruce summerwood.

Conclusions

The solute exclusion results from kraft and extended kraft delignification confirm that there are three phases of spruce cell wall volume alteration: initial swelling, near constant cell wall volume and contraction at lower yields. Only small differences were found between conventional and extended kraft cooking.

Direct microscopic measurements of cell wall thickness generally confirmed the swelling pattern of kraft delignification except for some important details. The yield at which the swelling behavior changed was not the same for microscopy and for solute exclusion. Additionally, the extent of the contraction was much less for microscopy than for solute exclusion. One possible explanation for this disagreement is that the cell wall distorts in such a way as to impede accurate measurement of the cell wall thickness. Another possible cause is that cell wall delaminations were formed in pulping or sample handling which were outside the range of solute exclusion measurements.

Acknowledgement

The authors are grateful to the Finnish Academy for financing part of this research project. Pulping experiments and determination of lignin were performed by Marite Škute in Riga. Her efforts are gratefully acknowledged.

References

1. Stone, J.E.; Scallan, A.M. The effect of component removal upon the porous structure of the cell wall of wood. II. Swelling and the fiber saturation point. *TAPPI Journal* **1967**, *50* (10), 496.
2. Stone, J.E.; Scallan, A.M. The effect of component removal upon the porous structure of the cell wall. Part III. A comparison between the sulfite and kraft processes. *Pulp and paper Magazine of Canada* **1968**, *69* (6), 69.
3. Klevinska, V.; Treimanis, A. Pre-treatment of wood chips with green liquor and its effect upon kraft delignification. *Cellulose Chemistry and Technology* **1997**, *31*, 253.
4. Page, D.H. The beating of chemical pulps – the action and the effects. Fundamentals of papermaking. In: Transactions of the 9th Fundamental Research Symposium held at Cambridge, September 1989. Mechanical Publications Ltd.: London, 1989, pp. 1.
5. Treimanis, A. Struktur der Zellstoffasern und ihr Einfluss auf die Verarbeitbarkeit. *Zellstoff und Papier* **1989**, *38* (3), 82.
6. Treimanis A. Wood pulp fibre structure and chemical composition, their influence on technological processes. *Nordic Pulp and Paper Research J.* **1996**, *3*, 146.

FRACTIONATION OF BEECH DISSOLVING PULP

R. Yaldez

Lenzing AG, Werkstr. 1, A - 4860 Lenzing, Austria

Due the complex cell morphology of beech wood the use of beech magnesium sulfite dissolving pulp causes several problems in the subsequent rayon process. The target of this work was to investigate the possibilities of commercial available equipment for fiber fractionation of dissolving magnesium sulfite pulp of beech. Bleached and unbleached beech pulp was fractionated with three different pilot plant fractionators. For reference a Bauer-McNett classifier was used as the most common lab-scale fractionator. The fiber length distribution was estimated by a Kajaani 200. More than 65% of the short fiber fraction of the pilot fractionator are fibers shorter than 0.2 mm. It was confirmed that the residual lignin, ash and resin content of the short fiber fractions is essentially higher, the alkali solubility and brightness

lower as compared to the long fiber fraction. Surprisingly, on one hand the fines had a poor reactivity, on the other hand an extremely clean long fiber fraction had a similar reactivity expressed as *Treiber* filterability and a similar content of gel particles in the viscose compared to the unfractionated pulp. Further experiments were performed on a pilot viscose fiber. Due the lower alkali solubility of the long fiber fraction the hemicellulose content of the press lye was lower. The optical properties of viscose fibers can be improved by using a fractionated pulp for viscose preparation.

Keywords: beech acid magnesium sulfite pulp, fractionation, parenchyma cells, fiber length distribution, viscose

Introduction

Producers of chemical pulp have always wished to optimize the pulp quality with regard to the properties of the final product at lowest costs. Due the complex cell morphology of beech wood the use of beech Mg sulfite dissolving pulp causes specific problems in the subsequent rayon process. Compared to high purity softwood dissolving pulps, the behavior in the steeping step, the reactivity and the filterability of the viscose, and the resulting optical properties of the viscose fiber are limited. The content of low molecular weight hemicellulose is relatively high and the DP distribution is broad. The most common figures to determine the pulp quality for the viscose process are the content of gel particles and the filterability of the viscose [1], the behavior in the steeping press, the optical properties, the content of inorganic substances and extractives, the viscosity, the molecular weight distribution [2] and the alkali solubility. It is well-known that different cell types of pulped wood have different characteristics [3].

Therefore it is an old target to overcome the given disadvantages in the following process by fractionating the pulp into more homogeneous fractions [4]. Economic considerations and the necessarily difficult machinery stopped the activities in this field up to the eighties. Just the inventions in the field of screening, dewatering and fiber recovery within the last years and the improved usage of waste paper promoted the old idea of separating the pulp into fractions of different specific properties.

The Lenzing AG produces beech Mg sulfite dissolving pulp and has therefore a limited pulp quality. The aim of this investigation was to investigate the possibilities of fractionation under these new circumstances.

Materials and Methods

Raw material. For the experiments different grades of a conventionally cooked beech Mg sulfite dissolving pulp were used. The low-grade pulp, KZO3, is bleached to an R18 content of

93.0 - 94.2 % and a brightness of 88.3 - 89% ISO; the medium-grade pulp, KZE, has an R18 content of 95.7% and a brightness of 91.2% ISO. Further properties of the raw material are shown in Table 3.

The Bleached and unbleached beech pulp was fractionated by three different pilot plant fractionators. Two of them use a woven fabric for separating the fibers, the third was a specially designed pressure screen with drilled screening plates. The rate of separation was controlled by adapting the consistency of the feed, the relative velocity between the pulp suspension and the fabric or the split of the reject and accept flow. For reference a Bauer McNett classifier was used as the most common lab-scale fractionator.

The fiber length was also measured by a Kajaani 200 to get more information about the fiber length distribution of single fractions [5, 6].

Standard methods. Bauer-McNett classification (modification of T233 cm 82); Kajaani 200 measurement [7]; Kappa number (modification of T236 cm 85); Viscosity (SCAN-CM 15:88); brightness (ISO 3688/2470); alkali resistances (ISO 699/ZMIV39/67); carbohydrate composition following total hydrolysis and HPLC separation with AX/EC-PAD detection; copper number (ZM IV/8/70); carboxylic groups according to Papier 1965, 19 (1); DCM extractives (ISO 624); molecular weight distribution after dissolving in LiCl/DMAc and GPC separation [8]; filterability of viscose according to Treiber [9].

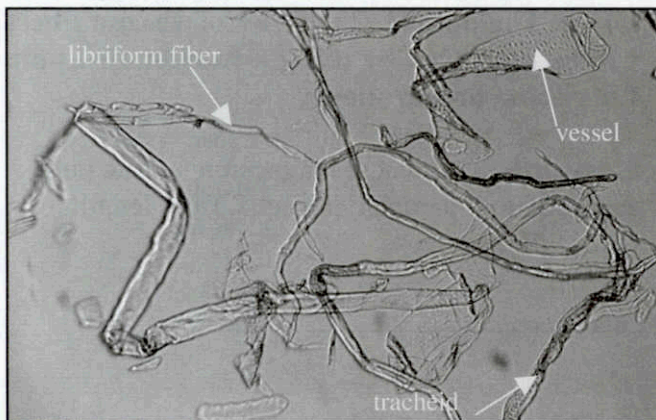


Figure 1. Long fiber fraction of beech sulfite pulp.

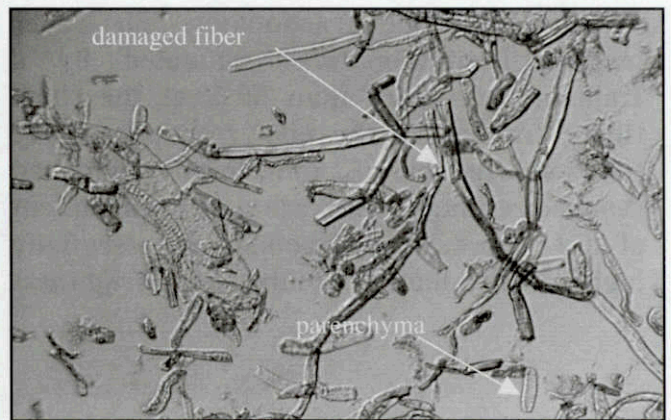


Figure 2. Short fiber fraction of beech sulfite pulp.

Results and Discussion

The target of the pilot runs was to improve the pulp quality by separating the parenchyma cells. Every separating technology uses specific physical properties of the particles to segregate the components. In the case of pulp fibers, these are usually fiber length, thickness, specific weight, stiffness or even the hydraulic behavior of different cell types. Figures 1 and 2 show the major cell types composing beech hardwood. The fiber length seems to be the most important difference between the parenchyma cells and libriform fibers. The screening technology is the most frequent way to separate sheaves or fines from the long fiber fraction. The screen can be a fabric or a drilled or slotted plate. However, by this approach it is impossible to separate the parenchyma cells from the broken fibers. The hydraulic behavior of the vessel elements is still hard to estimate. Even the quick quantitative

measurement of the vessel elements is still an unsolved problem.

Kumar et al. [10], who investigated the behavior of a pulp suspension in a screen, were able to show that fiber passage increases with increase slot width, increased fiber flexibility, reduced fiber length and reduced upstream velocity. The ability of screens to segregate one type of fiber from another was found to be the greatest at low slot velocities.

Acid cooked beech sulfite pulp has a very broad fiber length distribution. The two lines in Figure 3 representing laboratory cooks (filled and unfilled squares) show the influence of the cooking conditions and the final pulp viscosity as a reference for a gentle handed pulp. As a general rule it can be pointed out, that the fiber length decreases with decreasing pulp viscosity and with slower cooking conditions. During the following washing and screening the damaged fiber are shorted and therefore the unbleached

pulp shows a higher share of fines. Further shorting happens during the following bleaching steps.

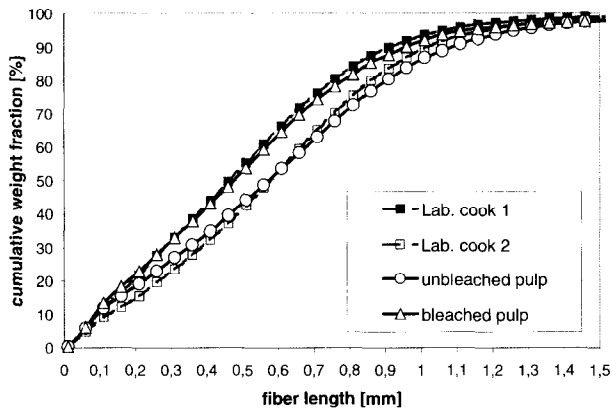


Figure 3. Influence of cooking, screening and bleaching on the fiber length distribution.

The target of this investigation was also to check different commercial available fractionators. The two equipment types A and B use a woven fabric for separating the fines. The third equipment tested works like a special designed pressure screen with drilled screening plates. Table 1 contains the most important operating conditions and the used controlling parameters.

Table 1. Experimental setups for equipment A, B and C.

| Parameter | A | B | C |
|------------------------------|----------------------------------|------------------------------------------|------------------------------------------|
| screen | fabric | fabric | drilled, Ø0.8 mm |
| consistency feed, % | 0.7 | 0.5 | 0.5 |
| Consistency long fiber, % | 8 | 1.1 | 0.65 |
| Consistency fines, % | 0.15 | 0.1 | 0.2 |
| controlled parameters | feed flow, fabric speed | feed & accept flow, rotor speed | feed & accept flow, rotor speed |

Figure 4 shows the results of the test runs. All curves correspond to trials with a 15% reduction of fines. Both types of equipment which separate the fines through a fabric gave a similar distribution of the short fiber fraction. More than 65% of the short fibers are shorter than 0.2 mm. Remarkably, variations of the operating

conditions within a wide range did not significantly the fiber length distribution of these short fiber fractions.

It was even possible to fractionate with the pressure screen. Compared to the fiber length distribution of the feed, the long fiber fractions of equipment B and C changed little. The results of the runs with equipment A showed a significant reduction of the fines also in the long fiber fraction.

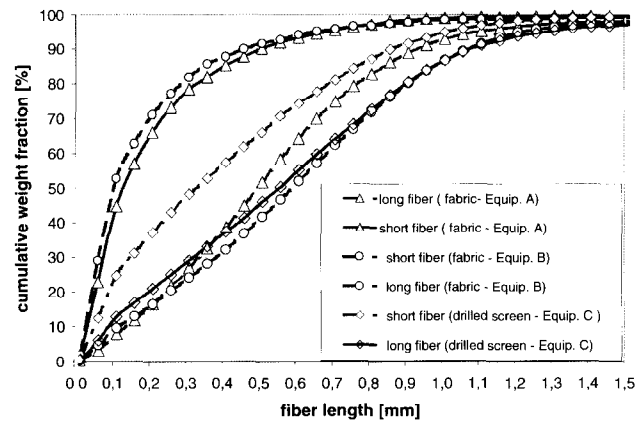


Figure 4. Fiber length of short and long fiber fractions from different fractionators (splitting rate: short fiber 15%; long fiber 85%).

Figure 5 shows the effect of the mass flow splitting. Remarkable is the peak at short fiber length which is typical for a beech sulfite pulp.

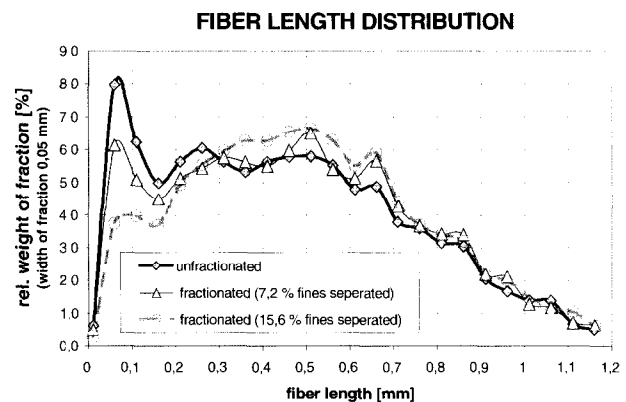


Figure 5. Influence of splitting rate in regard to the fiber length distribution.

To compare the results of the pilot equipment with results of a Bauer McNett fractionator the unfractionated pulp was fractionated by a Bauer McNett and the fiber length of the fractions was estimated by a Kajaani200. Figure 6 and Table 2

show the fiber length distributions with this experiment. The short fiber fraction of equipment A has a similar distribution as the passage of screen DIN 200.

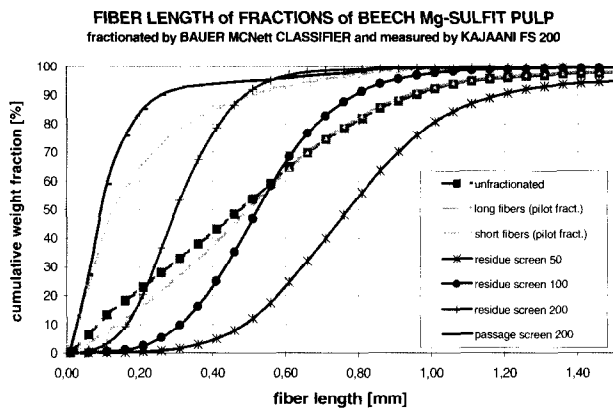


Figure 6. Bauer McNett fractions compared with the results of equipment A.

Table 2. Bauer McNett fractions of short and long fiber fractions from different fractinators (splitting rate: short fiber 15%; long fiber 85%).

| Screen | feed | long fiber | fines |
|--------------------|------|------------|-------|
| <i>Equipment A</i> | | | |
| R50 | 29 | 35 | 0.8 |
| R100 | 27 | 28 | 5.5 |
| R200 | 14 | 14 | 11 |
| D200 | 30 | 23 | 82.7 |
| <i>Equipment B</i> | | | |
| R50 | 23 | 31 | 0.5 |
| R100 | 28 | 31 | 5.5 |
| R200 | 16 | 16 | 9 |
| D200 | 33 | 22 | 85.0 |
| <i>Equipment C</i> | | | |
| R50 | 23 | 27 | 5.5 |
| R100 | 28 | 28 | 14.5 |
| R200 | 16 | 15 | 9 |
| D200 | 33 | 30 | 71 |

These results indicate the formation of additional fines during fractionation. Figure 7 shows the correlation between the fiber length and the coarseness. The different points represent the results of Kajaani measurements of different fiber fractions of beech sulfite pulp. The fractions were prepared with a Bauer McNett or the tested equipment A. The coarseness of beech pulp seems to increase with low fiber length.

COARSENESS of BEECH Mg-SULFIT PULP

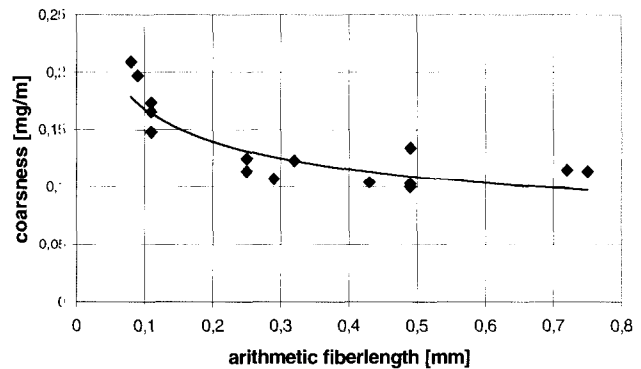


Figure 7. Coarseness of beech pulp.

The explanation for this effect is the fact that the fines are just partly accounted for by the Kajaani measurement.[7]

Pulp quality. It was confirmed that the residual lignin, ash and resin content of the short fiber fractions is higher, the alkali solubility and brightness is lower as compared to the long fiber fraction [11, 12, 13] as shown in Table 3.

Surprisingly, the fines had a poor reactivity on one hand. On the other hand an extremely clean long fiber fraction had a similar reactivity expressed as Treiber filterability and content of gel particles in viscose compared to the unfractionated pulp.

Even the distribution of the molecular weight shows that the single fractions have different characteristics. The long fiber fraction has a closer distribution compared to the feed.

Figure 8 contains the reflectance spectra in visible light of different fractions. The long fiber fractions have a higher reflectance than the feed. This effect is nearly independent of the rate of separation. The separated fines have a lower reflectance, and the more gentle separated fractions (e.g. 7.2% fines) result in an even lower reflectance. This result confirms the figures of Gruber *et al.* [3] who estimated the content of optical active compounds in different fiber fractions of spruce sulfite pulp.

Suitability for the viscose process. Further experiments were performed in a pilot viscose fiber plant to get a better correlation to the final product. Due the lower alkali solubility of the long fiber fraction, the hemicellulose content of the press lye is lower. The draining of the pulp slurry is improved.

Table 3. Pulp quality (beech pulp KZO3).

| Fractionator Parameter | Bauer McNett | | | Equipment A | | | |
|---------------------------|--------------|--------------------|-------|-------------|-------------|-------------|---------------------|
| | feed | long fiber | feed | long fiber | long fiber | short fiber | |
| | | fraction, sieve 50 | | (7% fines) | (15% fines) | | |
| Kappa Number | - | 0.76 | 0.54 | 0.63 | 0.53 | 0.47 | 0.95 |
| Brightness | %ISO | 88.3 | 88.8 | 89 | 89.5 | 89.8 | 82.5 |
| Viscosity | ml/g | 531 | 606 | 585 | 585 | 606 | 463 |
| R ₁₀ | % | 87.1 | 91.4 | 88.84 | 88.9 | 89.9 | n.d. |
| R ₁₈ | % | 93.0 | 94.4 | 94.2 | 94.2 | 94.3 | 91.5 |
| DCM extractive | % | 0.15 | 0.06 | 0.15 | 0.10 | 0.08 | 0.41 |
| Ash | % | 0.02 | 0.04 | | | | |
| Pentosan | % | 3.18 | 3.07 | 2.88 | 2.9 | 2.82 | 2.87 |
| Glucan | % | 94.0 | 94.40 | 94.7 | 94.6 | 91.4 | 92.9 |
| Xylan | % | 3.30 | 3.20 | 2.4 | 2.5 | 2.4 | 2.5 |
| Mannan | % | 1.10 | 1.10 | < 0.5 | < 0.5 | < 0.5 | < 0.5 |
| Filterability | | 434 | 426 | 301 | 428 | 370 | 17 |
| Gel particle | ppm | 24 | 26 | 42.9 | 37.3 | 35.5 | >>> |

Shaded fields: old laboratory method.

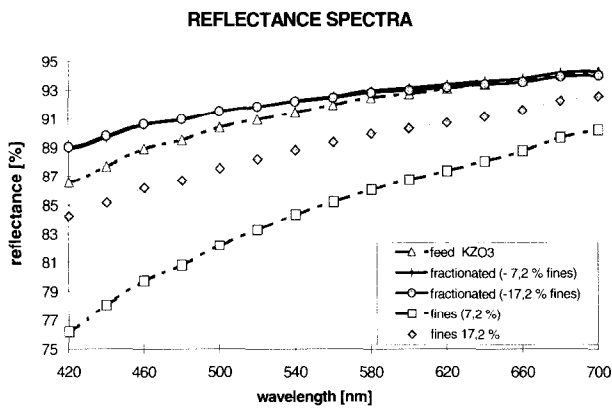


Figure 8. Influence of fractionation on the reflectance in visible light.

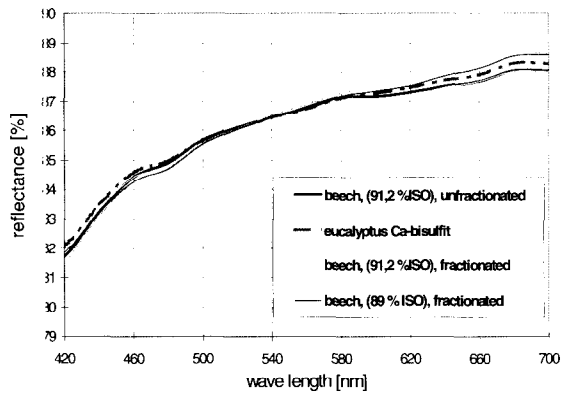


Figure 10. Reflectance spectra of viscose fibers bleached with H₂O₂.

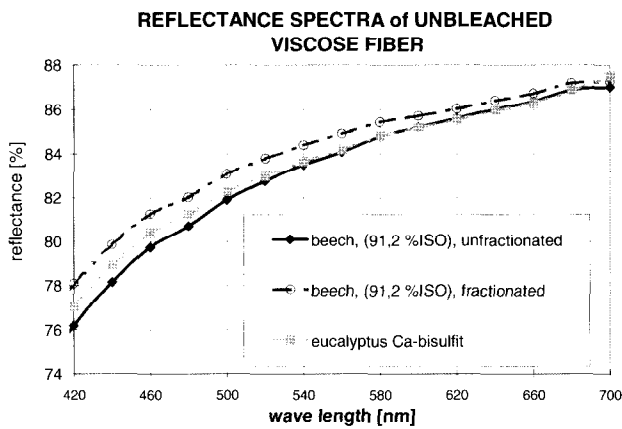


Figure 9. Reflectance spectra of unbleached viscose fibers.

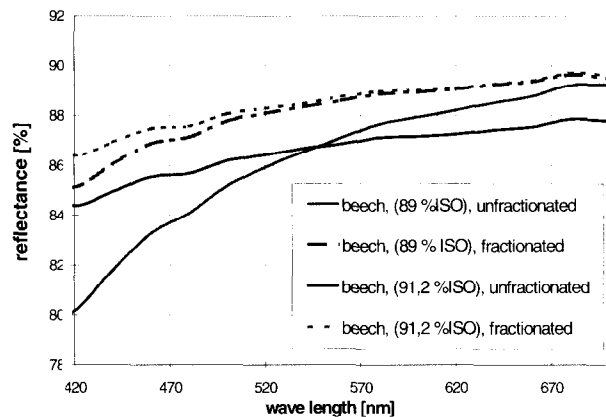


Figure 11. Reflectance spectra of viscose fibers bleached with 0.4 kg/m³ sodium hypochlorite.

The change of the optical pulp properties can be even noticed in the viscose fiber. The reflectance of viscose fiber produced from fractionated beech sulfite pulp has essentially improved especially for low wavelengths (Figures 8 and 9). A further bleaching of the viscose fiber with H_2O_2 improves the brightness a little, the differences of the unbleached fibers are levelled out (Figure 10).

In contrast to bleaching with peroxide, bleaching of viscose fiber made from fractionated pulp with hypochlorite results in an essentially improved reflectance compared to fibers from unfractionated beech sulfite pulp (Figure 11).

Conclusions

It was possible with the tested pilot equipment to fractionate acid cooked beech Mg sulfite pulp. It is remarkable that variations of the operating conditions within a wide range do not significantly change the fiber length distribution of the short fiber fraction, but at the same time the content of fines of the long fiber fractions is not reduced to the same extent. Therefore, it must be assumed that the tested commercial equipment leads to a further shorting of the fiber. The known characteristics of the different fractions were confirmed.

References

- [1] Zubakhina, N.L.; Serkov, A.T.; Virezub, A.I. 1972. *Khim. Volokna* **1972**, 14, 33.
- [2] Silvia A.A.; Laver, M.L. *Tappi J.* **1997**, 80, 173.
- [3] Gruber, E.; Ezzat, S.; Schurz, J. *Papier* **1974**, 28, V8.
- [4] Dubach, M.; Rutishauser, M. *Papier* **1957**, 11, 37.
- [5] Graff, S.; Paris, J. *Inv. Tec. Papel.* **1992**, 113, 555.
- [6] Tasman, J. E. *Tappi* **1972**, 55, 136.
- [7] Graff, S.; Paris, J. *Inv. Tec. Papel.* **1992**, 113, 555.
- [8] Schelosky, N.; Röder T.; Sixta, H.; Baldinger, T.; Milacher, W.; Morgenstern B. *Papier* **1999**, 53, in press.
- [9] Treiber, E.; Rehnström, J.; Ameen, C.; Kolos, F. *Papier* **1992**, 16, 85.
- [10] Kumar, A.; Gooding, R.W.; Kerekes, R.J. *Tappi J.* **1998**, 81, 247.
- [11] Bandel, W. *Papier* **1957**, 11, 238.
- [12] Nagrodskii, I.; Naumova, Z.N.; Zarudskaya, O.L.; Fedorova, Z.A. *Bumazh. prom.* **1971**, 7, 20.
- [13] Treiber, E.; Stenius, S.A.; Rehnström, J. *Svensk Papperstid.* **1958**, 61, 55.